Paleocene to Lower Eocene sediments of the eastern Neo-Tethyan Ocean: sedimentary and geodynamic evolution as well as biostratigraphy of the larger benthic foraminifera *Lockhartia* and the genesis of nodular limestones

Dissertation zur Erlangung des
Doktorgrades der Naturwissenschaften (Dr. rer. nat.)
im Fachbereich Geowissenschaften der
Universität Bremen

vorgelegt von

Michaela Kahsnitz

Bremen, 2017

Universität Bremen

Gutachter / Reviewer:

Prof. Dr. Helmut Willems

PD Dr. Jens Lehmann

Tag des Kolloquiums / Day of colloquium:

29.08.2017

Mitglieder des Prüfungsausschusses / Member of thesis committee:

Prof. Dr. Heiko Pälike

Prof. Dr. Dr. Gerold Wefer

Dr. Karl-Heinz Baumann

Herr Dominik Nommensen

Erklärung

Name: Michaela M. Kahsnitz
Anschrift: Altenburger Str. 20, 28205 Bremen

Hiermit versichere ich, dass ich

1. die Arbeit ohne unerlaubte fremde Hilfe angefertigt habe,
2. keine anderen als die von mir angegebenen Quellen und Hilfsmittel benutzt habe und
3. die den benutzten Werken wörtlich oder inhaltlich entnommenen Stellen als solche kenntlich gemacht habe.

Bremen, Juni 2017

Michaela Kahsnitz
(Unterschrift)

Preface

This PhD project was part of the priority program 1372 Tibetan Plateau: Formation – Climate – Ecosystem (TiP) and the Strategy Priority Research Program (B) of the Chinese Academy of Sciences (CAS, Grant No. XDB03010102) and funded by the German Science Foundation (DFG Wi725/26 and DFG Wi725/29) as well as the University of Bremen (01/2013 to 11/2015).
The results of this research are compiled in three first-authorship manuscripts (cumulative dissertation) which are published, accepted, or submitted in peer-reviewed international scientific journals. My own contributions of these manuscripts are as followed:

1) **Paleocene and Lower Eocene shallow-water limestones of Tibet: microfacies analysis and correlation of the eastern Neo-Tethyan Ocean.**
Authors: Michaela M. Kahsnitz, Helmut Willems, Luo Hui, Zhou Zhicheng
Status: Submitted to Palaeoworld.
Own contributions: Microfacial analysis (relative abundances of organisms in thin sections) and correlation of five sections from the passive and active continental margin of the eastern Neo-Tethyan Ocean; preparation of samples from Cuojiangding for carbon isotope measurements from bulk sediment and total organic carbon; text and figures.

2) **Stratigraphic distribution of the larger benthic foraminifera *Lockhartia* in South Tibet (China).**
Authors: Michaela M. Kahsnitz, Qinghai Zhang, Helmut Willems
Status: Published, Journal of Foraminiferal Research (2016), 46:34-47.
Own contributions: Thin section analysis (biostratigraphy, taxonomy and relative abundances of *Lockhartia*); regional correlation of stratigraphic ranges of *Lockhartia*; integration of data with published results on *Lockhartia* of the entire Neo-Tethyan Ocean; text and figures.

3) **Genesis of Paleocene and Lower Eocene shallow-water nodular limestones of South Tibet (China).**
Authors: Michaela M. Kahsnitz, Helmut Willems
Status: Accepted for publication in Carbonates and Evaporites.
Own contributions: Collecting samples of limestone nodules and surrounding marls in Tibet; documenting field observations; thin section analysis (microfacies analysis, analysis of sedimentary and diagenetic features); reconstruction of depositional environment; preparation of samples for stable isotope, total organic carbon and carbonate measurements; reconstruction of the genesis of different nodular limestone types; text and figures.

Acknowledgements

First of all, I would like to express my sincere gratitude to my mentor and supervisor Prof. Dr. Helmut Willems. He gave me the opportunity to travel to and work on ”the roof of the world”. It was a great privilege to continue my work within his research group and to enhance and deepen my knowledge on the sedimentary evolution in the eastern Neo-Tethyan Ocean, after finishing my master thesis. Before that I had no connection to the far away Tibet. Based on his experience, dedication and great knowledge, he gave me a comprehensible understanding of the charm and uniqueness of the country. Even today I sometimes have an ”*I want to go to Tibet*” sort of feeling, which I try to restrain by reading the adventures and experiences of Alexandra David-Néel or Heinrich Harrer. Continuous professional support, constructive criticism, motivation, patience, inspiration and suggestions of Helmut Willems were invaluable for completing this work.

Secondly, I want to thank PD Dr. Jens Lehmann for accepting to be my second reviewer, for taking the time and the effort to read my thesis, for his kind support as well as for his constructive comments and last but not least some lively roundtable discussions (sometimes also far away from Science) at the Geosciences Collection.

I also want to thank my colleagues at the ”Historical Geology - Palaeontology” research group (in alphabetic order) - Anne, Britta, Christiane, Elke, Ines, Jens, Maria, Monika, Petra, Qinghai and Xiaoxia - they have been a great source for friendship and tea-time chats as well as helpful advices and collaboration. Thank you for the pleasant working atmosphere, sharing the office, solving several computer problems, as well as for laboratory, technical and English assistance. In particular I wish to thank Qinghai Zhang, who took me to Tibet twice for carrying out field-work, getting a deep insight into the Chinese and Tibetan culture and traditions. Especially the very delicious food (even though the food is very meat-based, always leading to detailed but pleasant conversations with a vegetarian like me) and the learning of some Chinese words: Xiè Xiè! (Thank you!)

Dieter von Bargen and Martin Krogmann, colleagues from the Geosciences Collection at the University Bremen, owe thankes for their support and constructive discussions, they helped navigating my work onto the right path.

I would like to thank Susanne Steinfeld for answering all administrational questions. I will always remember her kind-hearted and open nature, even if I knocked at her door for the same request twice.

I would like to thank Brit Kokisch, Dr. Henning Kuhnert and Jenny Wendt for the preparation and processing of carbonate and isotope samples and for always taking the time answering my questions. Jenny especially owe thanks, for the introduction into the preparation of samples for isotope measurements from the organic material of my samples.

A special thanks goes to Prof. Dr. Rüdiger Henrich of the research group ”Sedimentology - Palaeoceanography” for giving me the opportunity to finish my thesis at an appropriate workplace and his very kindhearted Ph.D. students Grit and Deborah for sharing their office for the last few month of my Ph.D.

Besides this, I also want to thank those people, who helped making my daily life enjoyable. I want to thank my friends from my hometown, who managed a trip to Bremen for a weekend (or two), especially Tina and Thomas, for retaining our tradition of having Mexican food at El Mariachi. Julia and Carina are thanked to manage some trips to Dresden, fatefully always on the hottest day of the year. I want to thank the most valuable persons of my life: Julia and Jasmin - thank you both for your moral and emotional support, for your cordiality and your sometimes slightly crazy manner, for some comfortable, funny and/or memorable days and for a strong friendship, that helps through all ups and downs that life provides.

Finally, I want to thank my family - who raised me with all the patience they had, for all the unconditional love and care. Thank you for the never-ending support, even over long distances.

Abstract

Larger benthic and symbiont-bearing foraminifera are known as important producers of shallow-water carbonate sediments. Their depth distributions are influenced by the type of symbiont they inhabit and controlled by parameters like temperature, hydrodynamic energy, topographic conditions or substrate type. That is why larger benthic foraminifera and their association with other organisms are used to reconstruct paleoenvironmental as well as paleobathymetrical conditions. Paleocene to Lower Eocene sediments of the eastern Neo-Tethyan Ocean are used to compare differences and similarities of the passive and active continental margin and to determine the sedimentary and geodynamic evolution of the sedimentary basin. The observation of larger benthic foraminifera and their association showed the distribution of eleven microfacies in four sections of the passive Indian (Tethys-Himalaya) and four microfacies in one section of the active Asian (Xigaze forearc basin) continental margin of the eastern Neo-Tethyan Ocean. Based on the distribution of the observed microfacies, depositional environment ranges from very shallow tidal flat and restricted lagoonal part of the inner carbonate ramp to the outer carbonate ramp, showing a two-stepped deepening event from Lower Paleocene to Lower Eocene within the entire eastern Neo-Tethyan Ocean.
Besides paleoenvironmental and paleobathymetrical reconstructions, larger benthic foraminifera are an important biostratigraphic tool due to their rapid diversification and abrupt extinctions. In India the Paleocene Ranikot Formation is characterized by the high diversity of the larger benthic foraminifera *Lockhartia*, therefore the eastern Neo-Tethyan Ocean is also called ”Ranikot Sea” or ”Lockhartia Sea”. Shallow-water sediments of three profiles from the Tethyan Himalaya reveal the stratigraphic ranges of seven *Lockhartia* species. Based on the stratigraphic distribution of these species five interval biozones (called ”*Lockhartia* biozones”) are established showing a stratigraphic conformity of sediments from the Tethyan Himalaya. Correlation of established biozones with the well-established shallow benthic zones used for biostratigraphy of shallow-water environments suggest an earlier evolution of some *Lockhartia* species in the eastern Neo-Tethys compared to the western Tethyan Ocean. Additionally, *Lockhartia* shows an increasing diversity from Middle to Late Paleocene and a reduction of diversity within the Lower Eocene of the Tethys-Himalaya. In literature changes in foraminiferal diversity and assemblage at the Paleocene-Eocene boundary are interpreted as being the result of climatic and geochemical changes called Paleocene-Eocene Thermal Maximum and carbon isotope excursion. In the south of Tibet, the sharp negative shift of the carbon isotope excursion representative for the Paleocene-Eocene boundary is located in a nodular limestone bed of the Zhepure Shan Formation in Tingri. Based on field appearances five categories of nodular limestones and some transitional members can be classified. Processes responsible for the genesis of nodular limestones in Tingri are differential diagenesis followed by chemical and mechanical compaction. Differences in clay content are assumed to be responsible for the various types of nodular limestones.

Zusammenfassung

Symbionten-tragende Großforaminiferen sind weltweit bekannt als bedeutende Produzenten von Flachwasser-Karbonaten. Die Tiefenverteilung der Großforaminiferen wird durch die Art des Symbionten, aber auch durch andere Parameter wie die Temperatur, die hydrodynamische Energie, die topographische Bedingungen sowie die Art des Substrates bestimmt. Aus diesem Grund können Großforaminiferen und ihre begleitenden Assoziationen genutzt werden, um die Paläoumwelt sowie die vorherrschenden Paläowassertiefen zu rekonstruieren. In dieser Arbeit wurden Sedimente aus dem Paleozän und dem Unteren Eozän des östlichen Tethys-Ozeans genutzt, um Unterschiede und Gemeinsamkeiten des passiven und aktiven Kontinentalrandes zu bestimmen und die sedimentäre sowie geodynamische Entwicklung des Sedimentbeckens zu erfassen. Großforaminiferen und ihre begleitenden Assoziationen zeigen die Verteilung von elf Mikrofazies in vier Profilen des passiven indischen (Tethys-Himalaya) und vier Mikrofazies in einem Profil des aktiven asiatischen (Xigaze forearc Becken) Kontinentalrandes des östlichen Tethys-Ozeans, repräsentativ für einen Ablagerungsraum von einem tidalen oder teilweise geschützten lagunären Flachwasserbereich bis hin zur äußeren Karbonatrampe. Im gesamten östlichen Neo-Tethys Ozean konnte in den Paleozänen bis Eozänen Sedimenten ein Vertiefungsereignis in zwei Stufen ausgemacht werden.
Neben der Rekonstruktion der vergangenen Umweltbedingungen sind Großforaminiferen durch ihre schnelle Ausbreitung und das Vorkommen von kurzlebigen Arten wichtige Werkzeuge zur Biostratigraphie von Sedimenten. Die in Indien vorkommende Ranikot Formation des Paleozäns wird charakterisiert durch das Auftreten der Großforaminifere *Lockhartia* mit einer hohen Artenvielfalt. Aus diesem Grund wird der östliche Neo-Tethys Ozean auch ”Ranikot Sea” oder ”Lockhartia Sea” genannt. In den Flachwasser-Sedimenten aus drei Profilen des Tethys-Himalayas konnten die stratigraphischen Reichweiten von sieben *Lockhartia*-Arten ausgemacht werden. Basierend auf diesen stratigraphischen Reichweiten wurden fünf Intervall-Zonen (sogenannte ”*Lockhartia* Biozonen”) etabliert, die eine stratigraphische Übereinstimmung der Sedimente des Tethys-Himalayas aufweisen. Korrelationen der *Lockhartia* Biozonen mit den in der Literatur bekannten und gängigen benthischen Flachwasserzonen legen nahe, dass die Evolution einiger *Lockhartia*-Arten im östlichen Neo-Tethys, verglichen mit dem westlichen Tethys-Ozean, früher eingesetzt hat. Zudem zeigt die Verteilung von *Lockhartia* im Tethys-Himalaya eine zunehmende Diversifizierung vom mittleren bis späten Paleozän und eine Abnahme der Diversifizierung im Unteren Eozän.
Umbrüche in der Diversität und der Vergesellschaftung von Foraminiferen an der Paleozän-Eozän Grenze werden in der Literatur durch die vorherrschenden klimatischen und geochemischen Änderungen interpretiert, bekannt als Paleozän-Eozän Temperaturmaximum und Kohlenstoff-Isotopen Exkursion. In Süd-Tibet konnte der stark negative Ausschlag in der Kohlenstoff-Isotopie, der die Paleozän-Eozän Grenze repräsentiert, in den Knollenkalken der Zhepure Shan Formation in Tingri ausgemacht werden. Basierend auf den Felduntersuchungen konnten verschiedene Ausprägungen der Knollenkalke sowie einige Übergangssedimente

klassifiziert werden. Die Genese der Knollenkalke in Tingri geht mit einer differentiellen Diagenese, gefolgt von einer chemischen und mechanischen Kompaktion einher. Unterschiede in den Tongehalten innerhalb der Formation sind vermutlich verantwortlich für die unterschiedlichen Ausprägungen der Knollenkalke.

Contents

1 Introduction

The present study will help to understand the general biostratigraphic and sedimentary development, as well as the evolution of carbonate ramp and forearc basin depositions in the eastern Neo-Tethyan Ocean. Therefore samples were taken from Paleocene to Lower Eocene shallow-water carbonates of the passive Indian and predominantly siliciclastic material of the active Asian continental margin of the Neo-Tethys Ocean.

In the focus of this study are (1) the general sedimentary development of the Indian passive continental margin (Tethys Himalaya) and the Asian active continental margin (Xigaze forearc basin) of the eastern Neo-Tethyan Ocean based on microfacies analysis, (2) the evolution and regional correlation of the larger benthic foraminifera (LBF) *Lockhartia* within the eastern Neo-Tethyan Ocean (also called Lockhartia Sea) and the comparison of the results with the western Neo-Tethys Ocean, (3) as well as the genesis of the Upper Paleocene to Lower Eocene nodular limestones in Tingri (South Tibet) based on microfacies analysis and in respect to the climatic and geochemical changes characteristic for the Paleocene-Eocene boundary.

1.1 Geologic setting

After break-up of the African continent during Jurassic and Lower Cretaceous, the Indian continent moved north in counterclockwise rotation (Ali and Aitchison, 2005), leaving a wide range for the Neo-Tethyan Ocean flanked by Europe and Asia to the north and Africa and India to the south. Sediments observed within this work were deposited within the eastern Neo-Tethyan Ocean (Fig. 1.1). Paleocene and Lower Eocene sediments of Zanskar, Tingri, Gamba and Guru were deposited on a carbonate ramp within a shallow-marine environment at the northern passive margin of the Indian continent (Gaetani et al., 1986; Fuchs and Willems, 1990; Willems, 1993; Zhang et al., 2012) close to the equator, while sediments of Cuojiangding were deposited within a forearc basin at the southern active margin of the Asian continent at lower to middle latitudes (Qian et al., 1982; Liu et al., 1988; Ding et al., 2005). The exact moment of collision between the Indian and Asian continent and therefore "the time of disappearance of the Neo-Tethys oceanic lithosphere" (Ding et al., 2005, p. 1) is still debated, with views ranging from ~70 Ma (Yin and Harrison, 2000), via 65 Ma (Wan et al., 2002; Ding et al., 2005), 56 Ma (Zhang et al., 2012) and 55 Ma (Garzanti et al., 1987) right up to 34 Ma (Aitchison et al., 2007) and 25 Ma (van Hinsbergen et al., 2012). The collision of India and Africa resulted in the closure of the Tethyan Ocean, the formation of the Himalaya, as well as the formation of the Tibetan Plateau.

Today, the investigated sections belong to the Himalayan orogenic belt covering an area from western Zanskar (Chulung Chu) in northern India to South-Tibet (Cuojiangding, Tingri, Gamba and Guru) in China (Fig. 1.2a), which can be divided into different east to west trending structural units (Gansser, 1964), described from north to south (after Hu et al., 2016):

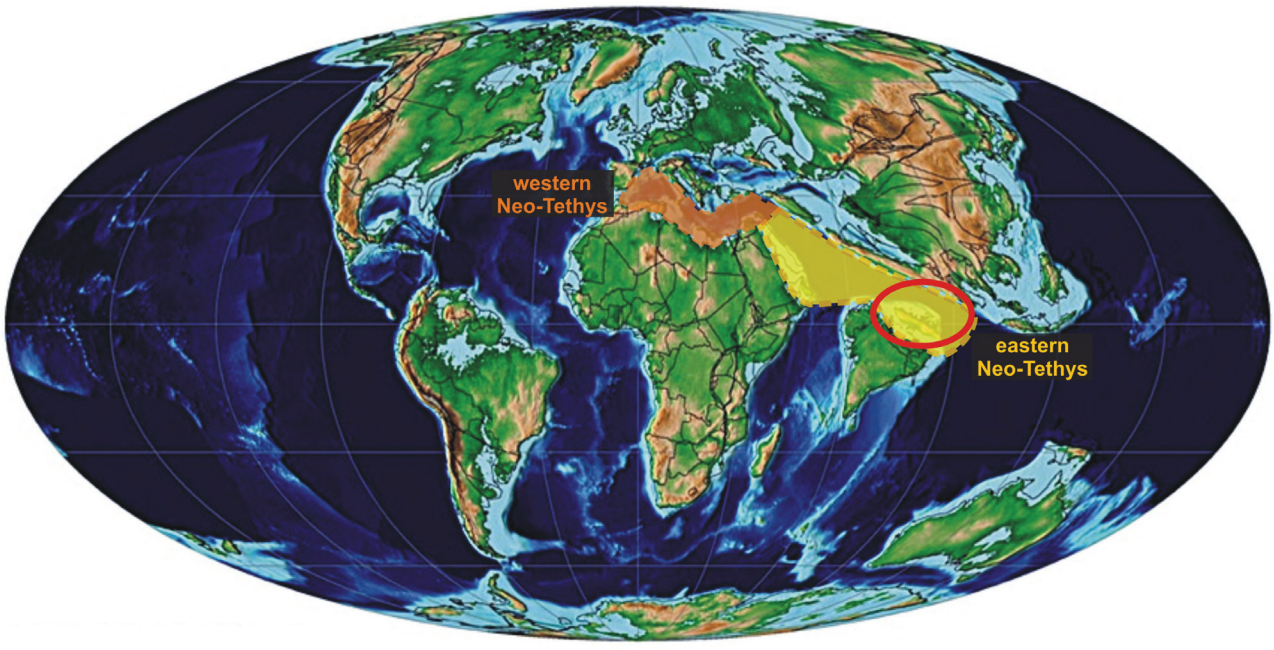

Figure 1.1: Global paleogeographic map at the Paleocene-Eocene boundary showing the distribution of the Neo-Tethyan Ocean (after Scotese, 2011. Sediments observed within this work were deposited within the eastern Neo-Tethyan Ocean.

1. Lhasa Block: The southern Lhasa block is represented by Triassic to Paleogene granitoids of the Gangdese batholith (e.g., Chung et al., 2005; Ji et al., 2009; Zhu et al., 2011) and Paleogene non-marine volcanic sequences of the Linzizong volcanic succession (e.g., Mo et al., 2008; Zhu et al., 2013; Zhang et al., 2014).

2. Xigaze forearc strata: Cretaceous turbidite sandstones, interbedded mud rocks, as well as shelfal to deltaic deposits. Paleocene to Lower Eocene alternating sequence of limestone, sandstone, conglomerate and volcanic tuff (Liu et al., 1988; Ding et al., 2005; Hu et al., 2016).

3. Yarlung Zangbo suture zone (YZSZ): Ophiolites and tectonic mélange with serpentinite or shale matrix marking the contact between the Asian continent to the north and the Indian continent to the south (e.g., Cai et al., 2012; Xu et al., 2015).

4. Tethyan Himalaya: Cretaceous to Lower Paleogene marine sedimentary sequences deposited at the northern passive margin of the Indian continent. Separated by the Gyirong-Kangmar thrust (Ratschbacher et al., 1994) the Tethyan Himalaya is divided into a northern zone, dominated by deep-water outer shelf, continental slope and rise deposits (Li et al., 2005) and a southern zone, characterized by shallow-water carbonates and terrigenous sediments (e.g., Willems, 1993; Liu and Einsele, 1994; Jadoul et al., 1998).

5. Himalaya: Subdivided into Higher, Lesser and Sub-Himalaya.

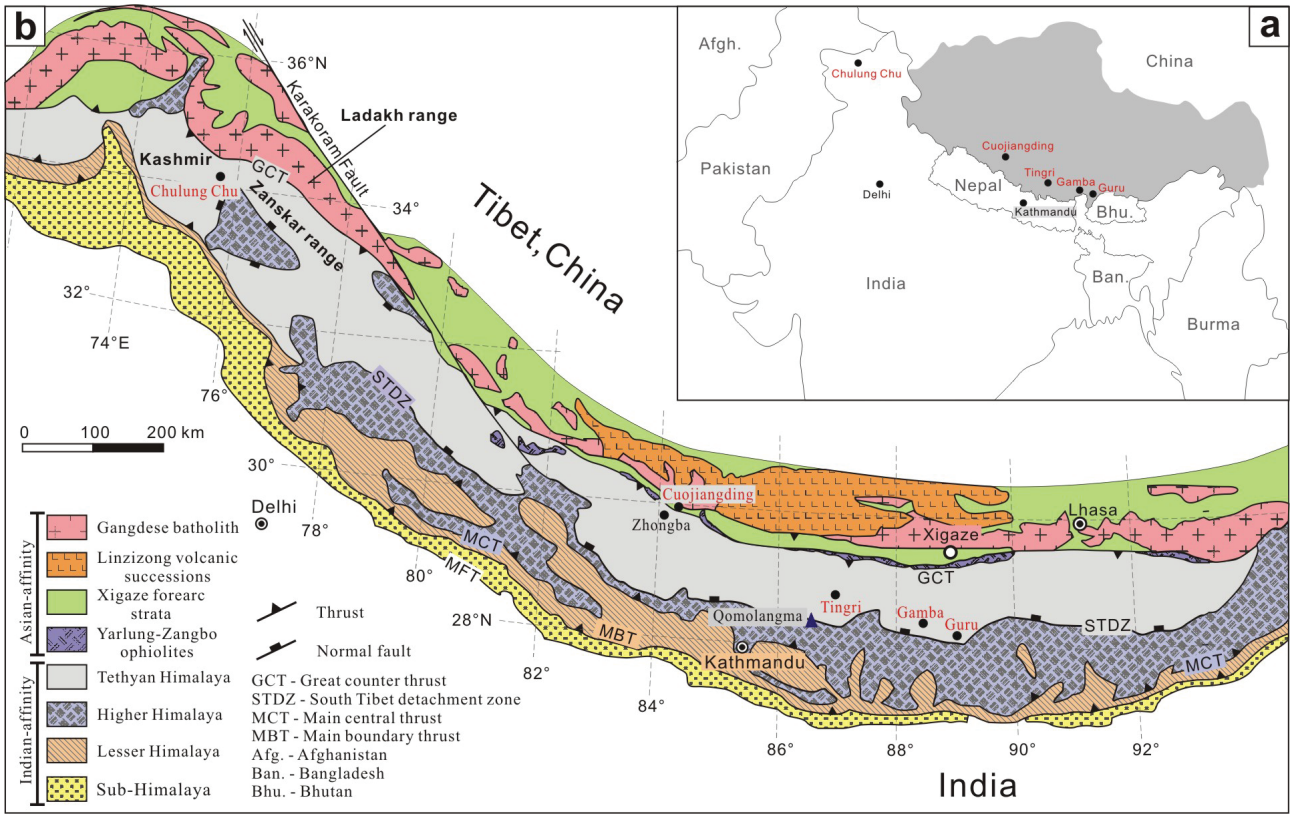

Figure 1.2: Geographic and geologic overview of the studied section. **A** Location of the investigated sections, covering an area from western Zanskar (Chulung Chu) in India to South Tibet (Cuojiangding, Tingri, Gamba and Guru). **B** Geological map of the Himalaya (after Hu et al., 2016). The Himalayan orogenic belt can be divided in different east to west trending structural units (Gansser, 1964), described from north to south: Lhasa Block, Xigaze forearc basin, Yarlung Zangbo suture zone, Tethyan Himalaya and Himalaya. Sediments from Zanskar, Tingri, Gamba and Guru are part of the Tethyan Himalaya, while sediments of Cuojiangding belong to the Xigaze forearc basin.

The investigated area Cuojiangding of this study is part of the Xigaze forearc basin, while Zanskar, Tingri, Gamba and Guru are part of the southern Tethyan Himalaya (Fig. 1.2b).

1.2 Stratigraphic system

Two stratigraphic systems were established for the Lower Paleogene sediments of Tingri and Gamba in south Tibet by Willems in 1993 (Fig. 1.3). At Tingri the shallow-water marine strata are presented in the Zhepure Shan Formation, underlain by the Jidula Formation and overlain by the Youxia Formation showing the end of the marine sedimentation (Willems, 1993; Zhu et al., 2005). The time equivalent sedimentary series at Gamba is represented by the Zongpu Formation, also underlain by the Jidula Formation and overlain by the Zongpubei Formation. Both, Zhepure Shan and Zongpu Formations can be subdivided into four lithological units, described from bottom to top: cyclic limestone (Member A), massive limestone (Member B), nodular limestone (Member C), massive limestone (Member D). Based on the stratigraphic distribution of larger benthic foraminifera those sediments are of Paleocene to Lower Eocene age (Willems, 1993; Zhang et al., 2013).

Wan et al. (2010, p. 71) used a ”single stratigraphic system as both Gamba and Tingri areas are part of the same sedimentary basin and have similar stratigraphic patterns” and therefore described differences in stratigraphic classification as unnecessary. Hu et al. (2012) also suggested to use a single stratigraphic system. Hence in some literature sedimentary sequences at Tingri and Gamba are composed of Jidula, Zongpu and Zhepure/Enba Formations from bottom to top (Wan et al., 2002, 2010, 2014; Li et al., 2015; Jiang et al., 2016).

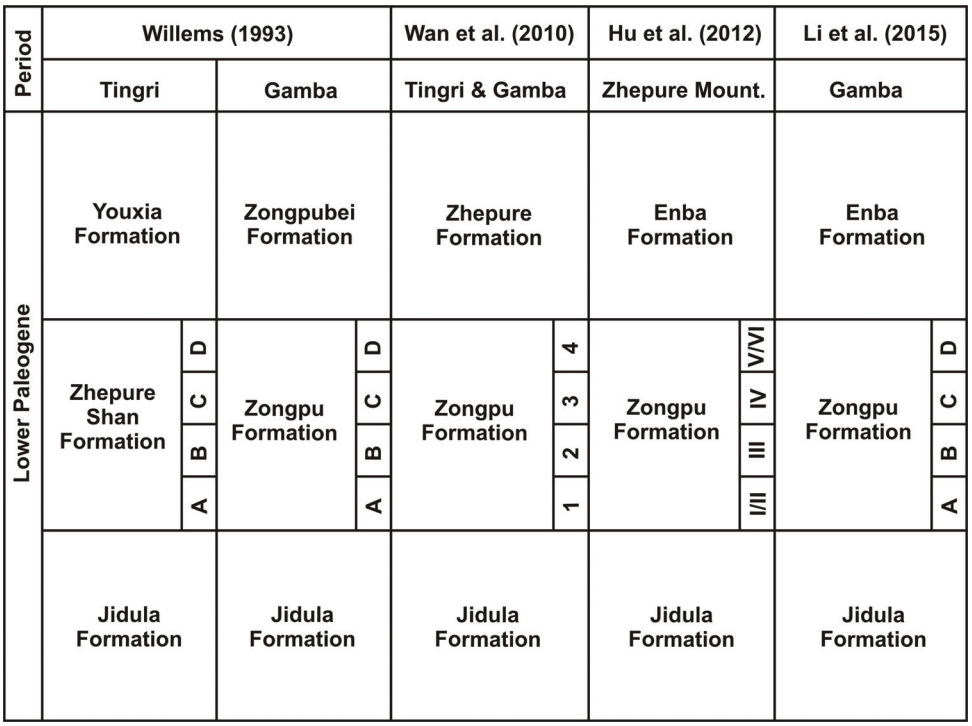

Figure 1.3: Correlation of Lower Paleogene stratigraphic systems for South Tibet. Willems (1993) established two stratigraphic systems with Members A to D, while Wan et al. (2010) and Hu et al. (2012) used a single stratigraphic system for Tingri and Gamba. Abbreviation: Mount. = Mountain.

In this work both established stratigraphic systems are used based on the requirements and expectations the Journal and/or the reviewer of the manuscripts had. Nevertheless, the system established by Willems (1993) is used in most cases to keep it constant for all publications of the working group.

1.3 Larger benthic foraminifera (LBF)

Foraminifera are important marine single-celled protozoa, which can be divided into two different groups based on their living strategy: planktonic (living in the water-column) and benthic (living in or on the sediment surface). Larger benthic foraminifera (LBF) are an informal group of benthic foraminifera with large test sizes and complicated internal structures (Ross, 1974), providing housing for algal symbionts (Haynes, 1965; Lee, 1998; Hallock, 1999). Due to the relationship with photosynthetic symbionts, LBF are living in tropical, shallow-water, oligotrophic and well-lighted environments with water depth less than 130 m (Hottinger, 1983; Hallock, 1984, 1999). Light quality influences the depth distribution of LBF based on the type of symbiont they inhabit: chlorophycean (0 m to 15 m), rhodophycean and dinophycean (0 m to 70 m) or diatoms (0 m to 130 m). Additional parameters influencing the depth distribution of LBF are temperature, hydrodynamic energy, topographic conditions or substrate type (e.g., Hottinger, 1981, 1983; Leutenegger, 1984; Renema, 2002). Therefore LBF and LBF associations are described as sensitive tool to reconstruct paleoenvironmental and paleobathymetrical conditions (Hallock and Glenn, 1986; Hottinger, 1997; Beavington-Penney and Racey, 2004).

In the eastern Neo-Tethyan Ocean, Paleocene to Lower Eocene LBF and their association with other organisms (e.g., green algae, corals) show the distribution of eleven microfacies in four sections from the passive Indian (Tethyan Himalaya) and four microfacies in one section from the active Asian (Xigaze forearc basin) continental margin. The correlation of the observed microfacies are used to reconstruct the paleoenvironmental development and the sedimentary history of the eastern Neo-Tethyan Ocean, showing a two-stepped deepening event from Lower Paleocene to Lower Eocene (see chapter 2 ”Paleocene and Lower Eocene shallow-water limestones of Tibet: microfacies analysis and correlation of the eastern Neo-Tethyan Ocean”, p. 19).

Besides paleoenvironmental and paleobathymetrical evidence, LBF determination to the species level is ”biostratigraphically important because of their episodes of rapid diversification and abrupt extinctions” (Hallock, 1985, p. 195). Taxonomic differentiation of LBF species is highly difficult because most fossils occur within cemented limestones and have to be studied in random thin sections to determine morphological characteristics like size, number and proportions of structural elements (Hottinger, 2007, 2009). Based on detailed biostratigraphic studies of the LBF *Alveolina*, *Assilina* and *Nummulites* (Hottinger, 1960; Drobne, 1977; Schaub, 1981; Hottinger and Drobne, 1988; Hottinger et al., 1998), 20 shallow benthic zones (SBZ) have been established for the Paleogene, especially for the western Neo-Tethyan Ocean (Serra-Kiel et al., 1998).

In south Tibet, Paleocene LBF with the dominant genera of *Miscellanea*, *Daviesina*, *Lockhartia*, *Kathina*, *Ranikothalia* and *Operculina* and Early Eocene LBF like *Alveolina*, *Nummulites* and *Orbitolites* have been reported (e.g., Ho et al., 1976; Wan, 1991; Willems et al., 1996; Wan et al., 2002, 2010; Zhang et al., 2013) and SBZ were constructed based on thin section analyzes from Tingri and Gamba by Zhang et al. (2013). However, taxonomic studies on these LBF are still very poor, especially because of the large amount of described species.

Investigated sediments of this work were deposited within the eastern Neo-Tethyan Ocean. Based on the high diversity of endemic LBF belonging to the rotaliid subfamily Lockhartiinae (i.e., *Lockhartia*, *Dictyoconoides* and *Sakesaria*) in the Paleocene Ranikot Formation from India, the eastern Neo-Tethyan Ocean was also

called "Ranikot Sea" (Davies, 1937) or "Lockhartia Sea" (Hottinger, 1998), covering an area ranging from South Turkey in the west to Tibet and Pakistan in the east, and to Somalia and Egypt in the south (Hottinger, 2007, 2014b). Due to their high diversity, the foraminifera of the genus *Lockhartia* occupy certain chronostratigraphic positions in the Paleocene and therefore some species are accepted as index species (Hottinger, 2014a).

1.3.1 LBF of the genus *Lockhartia*

Belonging to the Family Rotaliidae Ehrenberg, 1839 the larger benthic foraminifera (LBF) *Lockhartia* shows a perforate-bilamellar calcareous test with a trochoid chamber arrangement. Within his monograph Hottinger (2014a) transferred the genus *Lockhartia* Davies, 1932, as well as the genera *Dictyoconoides* Nuttall, 1926, *Sakesaria* Davies, 1937 and the new described species *Rotalispira* n. gen., into a new subfamily named Lockhartiinae. This subfamily is characterized by its umbilical structure, showing umbilical cavities delimited by successive horizontal arranged foliar walls and numerous continuous and laminated umbilical piles (Fig. 1.4a). To distinguish the different species of *Lockhartia* the appearance of foliar walls and piles (Fig. 1.4b, c, f) are the most important morphological features (e.g., Davies, 1932; Smout, 1954). The spire of the test is sharply separated from the umbilicus by an umbilical plate (see Fig. 1.4e, g). Dorsal side of the test is stoutly lenticular to convex with no (see Fig. 1.4a, d) or different pattern (e.g., Fig. 1.4e) of ornamentation.

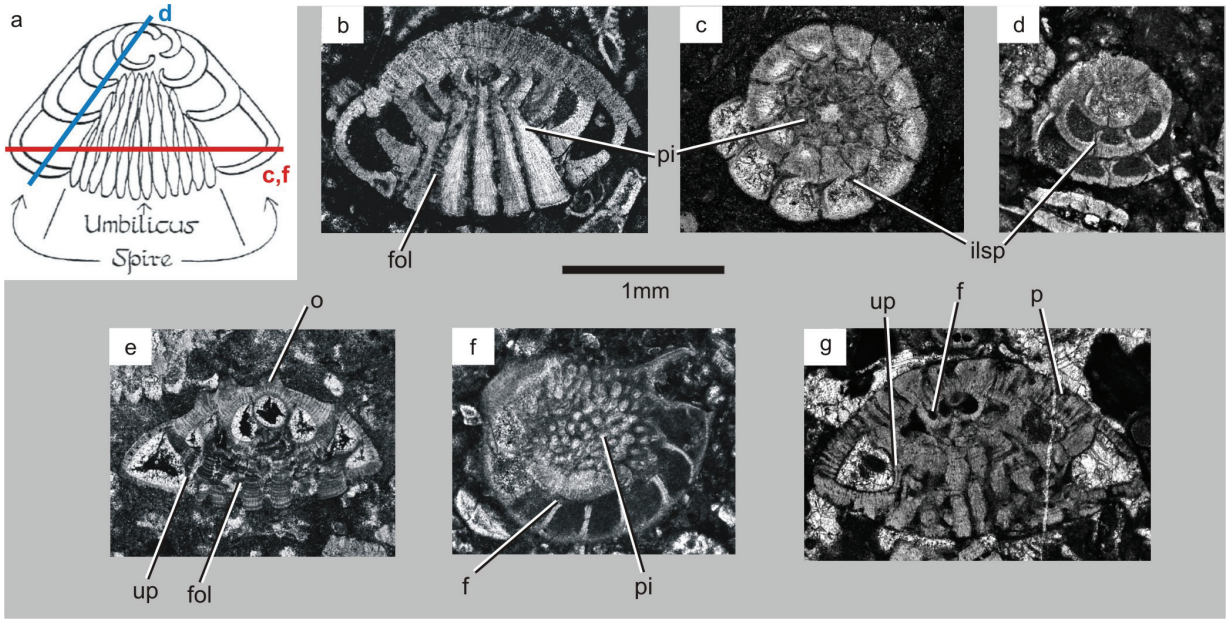

Figure 1.4: A Axial cutting showing the trochoid chamber arrangement of the genus *Lockhartia* Davies, 1926 leaving a wide umbilical area of complex structure (after Davies, 1932), not to scale. Coloured lines indicate different cuttings: e.g., oblique cutting (blue line) as seen in figure 1.4d and section perpendicular to the coiling axis (red line) as seen in figures 1.4c and 1.4f. **B-D** *Lockhartia conditi*, **E-F** *Lockhartia haimei* and **G** *Lockhartia praehaimei* of South Tibet (after Kahsnitz et al., 2016). The umbilical area of the perforate (p = pore) foraminifera is filled with continuous and laminated piles (pi) and horizontal arranged foliar walls (fol), which are the most important morphological features to distinguish between different species of *Lockhartia*. Other morphologic characteristics of *Lockhartia* are the occurrence and distribution of the foramen (f), the interseptal interlocular space (ilsp), the umbilical plate (up) or the smooth to heavy cancellate ornamentation (o).

Since the first description of *Lockhartia* in 1926 by Davies, a lot of research papers were published describing new species or mentioning the occurrence of the larger benthic foraminifera *Lockhartia* at different localities. Since then more than 30 described species and variations (var.) of the rotaliid LBF *Lockhartia* were published. Based on the high amount of described species, taxonomic work on the genus is highly hindered. During the years some of the species were revised and transferred into other genera of foraminifera. For example, *Lockhartia bermudezi*, described by Cole, 1942, was revised as *Kathina jamaicensis* by Brown and Bronnimann (1957). Nevertheless, *Lockhartia bermudezi* was used in literature published subsequently (e.g., Auboin and Neumann, 1959).

A summary of already revised and a critical review of *Lockhartia* species that belong to another species or even to other genera is given in the following paragraphs. It is important to reduce the number of *Lockhartia* species in order to simplify taxonomic work and to make it applicable and more convenient. Additionally, some important literature illustrating the occurrence of *Lockhartia* is given (Table 6.1) to complete the work.

***Lockhartia bermudezi* Cole, 1942 revised as *Kathina jamaicensis* (Cushmann and Jarvis, 1931)**

First described from Cuba by Cole (1942) as *Lockhartia bermudezi* was later shown as a junior synonym of *Eponides jamaicensis* (Cushmann and Jarvis, 1931). Smout (1954) noted that *L. bermudezi* Cole, 1942 has an axial plug without cavities and fissures and therefore named it *Kathina bermudezi*. This view was accepted by Brown and Bronnimann (1957, p. 36): ”This species is neither an *Eponides* nor a *Lockhartia*, and should be assigned to the genus *Kathina*, as noted by Smout (1954)” and renamed this species *Kathina jamaicensis* Cushmann and Jarvis, 1931. Cole accepted this in 1971, and noted that ”*Eponides jamaicensis* Cole (synonym: *Lockhartia bermudezi* Cole)” belongs to the genus *Kathina*.

***Lockhartia conica* Smout, 1954 revised as *Rotospirella conica* (Smout, 1954)**

Lockhartia conica was first described from the Paleocene of Qatar. The umbilical structure of this species is characterized by ”feebly developed” piles as well as a ”labyrinthine” arrangement of cavities (Smout, 1954, p. 53). This species was also described from Paleocene limestones of South Tibet where the morphological characteristics of the piles were also described as ”feebly developed” (Wan, 1991, p. 12). In his monograph, Hottinger (2014a) transferred *L. conica* Smout, 1954 into the newly described genus *Rotospirella conica* (Smout, 1954) and explained this approach by the lack of regular umbilical cavities, which would be morphological characteristic of *Lockhartia*.

***Lockhartia cushmani* Applin and Jordan, 1945 revised as *Rotalia cushmani* Applin and Jordan, 1945**

Another revised species of *Lockhartia* is *Lockhartia cushmani* Applin and Jordan, 1945 which was characterized by the authors as ”very similar to *Eponides gunteri* Cole, 1942” (Applin and Jordan, 1945, p. 143). Cole (1947) redescribed *L. cushmani* and assigned it to the species *Rotalia*. In 1950, Applin and Jordan explained, that the revision of *L. cushmani* to the genus *Rotalia* involved that it thereby became a homonymy of *Rotalia cushmani* Applin and Jordan, 1945 and proclaimed that they assigned this species as *Lockhartia* because they believed it was the morphologically most related genus (Applin and Jordan, 1950). According to Smout (1954), *L. cushmani* shows a structure intermediate between *Rotalia* and *Kathina*, because of the lack of umbilical cavities and the occurrence of slits which cut into the umbilical plug. Reiss and Merling (1958) stated that it was a typical *Rotalia* because of different characteristics like the clearly visible lips and the toothplates.

***Lockhartia hunti* var. *garoensis* Samanta, 1961 revised as *Lockhartia hunti* Ovey, 1947**

In literature the species *Lockhartia hunti* Ovey, 1947, as well as a variation *Lockhartia hunti* var. *pustulosa* Smout, 1954, is known. Another variation of *Lockhartia hunti* was described in 1961 by Samanta. It is noted that *Lockhartia hunti* var. *garoensis* differs from *Lockhartia hunti* by having a more conical dorsal side and a more convex base. In addition, the species shows a narrow umbilical pile with distinctive horizontal plates (Samanta, 1961). Here, I assume that the described morphologic differences between *L. hunti* and *L. hunti* var. *garoensis* are not sufficient enough to establish a separate taxon.

***Lockhartia luppovi* Bugrova, 1966**

First described by Bugrova in 1966 and 1967 from the Paleocene of southeast Turkmenistan (”Turkmenia”) and in 1997 from Southern Uzbekistan (Bugrova in Akhmetiev et al., 2012). Based on pictures given by Bugrova (1966) I assume that the described species does not belong to the genus *Lockhartia*. The foraminifera shown in these papers in contrast show more morphological features comparable to *Storrsella* Drooger, 1960b, or *Laffitteina* Marie, 1946.

***Lockhartia minuscula* Hofker, 1957 revised as *Daviesina minuscula* (Hofker, 1957)**

First described by Hofker (1957) as *Lockhartia minuscula* for the Late Cretaceous. In later publications Hofker (1958) noted similarities with the genus *Daviesina* and therefore used the term *Lockhartia* (*Daviesina*?) *minuscula* (Hofker, 1957). In subsequent publications the assignment *Daviesina minuscula* (Hofker, 1957) was used (Arbeitskreis deutscher Mikropaläontologen, 1962; Voigt, 1964; Norling, 1973).

***Lockhartia newboldi* (d´Archiac and Haime, 1853) revised as *Rotalia* cf. *newboldi* d´Archiac and Haime, 1853**

Rotalia newboldi d´Archiac and Haime, 1853, described from Pakistan was referred to the genus *Dictyoconoides newboldi* (d´Archiac and Haime, 1853) by Davies in 1927 firstly, afterwards to the genus *Lockhartia newboldi* (d´Archiac and Haime, 1853) by Davies in 1932. According to Gill (1953), the species *L. newboldi* is a morphological variation within the species *Rotalia trochidiformis* Lamarck, 1804. This was accepted by Smout in his monograph in 1954. In his work Hottinger transferred this species back to the first described genus and called it *Rotalia* cf. *newboldi* d´Archiac and Haime, 1853, but at the same time advised that the use of this species name was nevertheless tentative (Hottinger, 2014a).

***Lockhartia ramanae* Ten Dam, 1953**

In the Cretaceous of Turkey, a species named *Lockhartia ramanae* was described showing a few larger piles filling the umbilicus (Ten Dam, 1953). By looking at the published figures of *L. ramanae*, it seems that this species has got an axial plug instead of numerous piles and cavities, which is a morphological characteristic intermediate between *Rotalia* and *Kathina*. Because of the Late Cretaceous age and the umbilical plug, the described foraminifera may belong to the genus *Rotorbinella* Bandy, 1944. Therefore *L. ramanae* will be neglected in further discussions.

***Lockhartia reticulata* Silvestri, 1939 revised as "nomen nudum" Ten Dam (1953)**

The species *Lockhartia reticulata* Silvestri, 1939 was first mentioned from Eocene sediments of Somalia, unfortunately without giving any taxonomical descriptions. Therefore, *L. reticulata* was considered as "nomen nudum" by Ten Dam (1953).

***Lockhartia roestae* Visser, 1951 revised as *Eoconuloides roestae* (Visser, 1951)**

In 1951, Visser described the new foraminifera *Cibicides roestae* from the Maastrichtian of the Netherlands. Later Hofker (1955) revised this species as *Lockhartia roestae* (Visser, 1951), based on distinct morphological characteristics. In 1966, Hofker recognized that "the inner structure without any doubt excludes the genus *Cibicides*" and stated "that the species cannot belong to *Lockhartia* either" (Hofker, 1966, p. 24). Transverse sections of the tests show septal walls between the secondary chambers. These features were described by Brönnimann as typical for the genus *Tremastegina* (Brönnimann, 1950), and Hofker transferred it to the genus *Tremastegina roestae* (Visser, 1951) accordingly (Hofker, 1966). In his work from 1978, Gowda mentioned the type species *Cibicides roestae* (Visser, 1951) and revised it as *Praestorrsella roestae* (Visser, 1951). In 1988, Loeblich and Tappan described *Tremastegina* as a junior synonym of *Eoconuloides*. This was accepted by Leloux (2002) who transferred *Cibicides roestae*, *Lockhartia roestae* and *Tremastegina roestae* into the genus *Eoconuloides roestae* (Visser, 1951).

***Lockhartia schaubi* Hottinger, 1966 revised as *Calcarinella schaubi* (Hottinger, 1966)**

In 1966, Hottinger described a new species from the Pyrenees called *Pseudorotalia schaubi* which was later revised to the genus *Lockhartia schaubi*, realizing the morphological similarities with calcarenids: "In *Lockhartia schaubi* (Hottinger, 1966) the umbilical covers are two- or multi-layered and imperforate as in calcarinids." (Hottinger and Leutenegger, 1980, p.118). Butterlin and Fourcade (1989) recognized that the piles of the foraminifera were not continuous and rearranged it to the family Calcarinidae. Boix et al. (2009) transferred it into the genus *Calcarinella* and named it *Calcarinella schaubi* Hottinger, 1966, explaining that the structure was similar to that of *Lockhartia* but exhibiting evidences which were part of *Calcarinella* as well (e.g., folium with a retral foliar aperture, true umbilical plate).

***Lockhartia sijuensis* Samanta, 1961 revised as *Lockhartia conditi* (Nuttall, 1926)**

The species was first described from the Garo Hills (Assam) in eastern India by Samanta (1961). Morphologic characters like small test, rounded peripheral margin, smooth dorsal surface and semilunar shape of chambers in axial section are usually distinctive features of *Lockhartia conditi* Nuttall, 1926. Only the umbilical piles of *L. sijuensis*, which were described as narrow and discontinuous, make the difference from the huge and continuous piles typical for *L. conditi*. Possibly, the median axial section of *L. sijuensis* shown by Samanta (1961) was not an exact axial section traversing the umbilical piles so that they just appeared discontinuous. Here, I assume that the described *L. sijuensis* by Samanta (1961) belongs to the species *L. conditi* Nuttall, 1926.

Synonymy of *Lockhartia alveolata* Silvestri, 1942 and *Lockhartia hunti* Ovey, 1947

Silvestri (1942) first described the species *L. alveolata* from the Eocene of Somalia. In 1947, Ovey identified another new species of *Lockhartia* from Somalia and denominated it *L. hunti*. The author compared the images of *L. alveolata* (Silvestri, 1942) with the species *L. hunti* described from Somalia and recognized that

it had fewer and coarser piles and a more conical dorsal side (Ovey, 1947). In 1954 Smout pointed out, that *L. hunti* had got a higher cone, which coincides with the outer shape of *L. alveolata* tests. Because of this and the nearly same ratio of height/diameter, *L. hunti* was placed in synonymy with *L. alveolata* by Al-Hashimi (1974). As a consequence the variation of *L. hunti* was assigned as *L. alveolata* var. *pustulosa*.
The assumption of Al-Hashimi (1974), concerning the synonymy of *L. alveolata* and *L. hunti*, based on morphological features such as shape and size of the test, ignoring the fact that *L. alveolata* exhibits fewer and coarser piles than *L. hunti* as described by Ovey in 1974. As mentioned above, the appearance of plates and piles within the umbilical area is a very distinctive feature to distinguish between different species of *Lockhartia*. For this reason, it is questionable whether *L. alveolata* is a synonym of *L. hunti*. Additionally, in later publications the denominations *L. hunti* and *L. hunti* var. *pustulosa* were used instead of *L. alveolata* (e.g., Ho et al., 1976; Hasson, 1985; Wan, 1991; White, 1994; Willems et al., 1996; Pignatti et al., 1998).
Based on the occurrence of heavier beads, Smout (1954) distinguished between *L. hunti* Ovey, 1947 and *L. hunti* var. *pustulosa* Smout, 1954. In Hottingers work these differences were described being ”insufficient to distinguish a separate taxon” (Hottinger, 2014a, p. 81).
According to differences in morphology, *Lockhartia alveolata* Silvestri, 1942 and *Lockhartia hunti* Ovey, 1947 are possibly separate species, but the morphological variation described by Smout (1954) will be neglected.

Remaining *Lockhartia* species

According to the evaluation of bibliographic data the following species of *Lockhartia* should be removed: *L. bermudezi*, *L. conica*, *L. cushmani*, *L. hunti* var. *garoensis*, *L. hunti* var. *pustulosa*, *L. luppovi*, *L. minuscula*, *L. newboldi*, *L. ramanae*, *L. roestae*, *L. schaubi* and *L. sijuensis*. This reduces the number of described *Lockhartia* species down to 17 species and 4 variations ranging from Paleocene to lower Middle Eocene:

- *L. akbari* (Tambareau et al., 1997)
- *L. altispira* Smout, 1954
- *L. alveolata* Silvestri, 1942
- *L. conditi* (Nuttall, 1926)
- *L. daviesi* Ten Dam, 1953
- *L diversa* Smout, 1954
- *L. gyropapapulosa* Levin, 1957
- *L. haimei* (Davies, 1927)
- *L. haimei* var. *nudimarginata* Sander, 1962
- *L. haimei* var. *spirachordata* Sander, 1962
- *L. haimei* var. *suturadicata* Sander, 1962
- *L. haimei* var. *vermiculata* Sander, 1962
- *L. hunti* Ovey, 1947
- *L. lobulata* Sander, 1962
- *L. megapapulata* Hu, 1976
- *L. prealta* Levin, 1957
- *L. praehaimei* Smout, 1954
- *L. retiata* Sander, 1962
- *L. roeae* (Davies, 1930)
- *L. susuaensis* Pessagno, 1960
- *L. tipperi* (Davies, 1926)

Based on this literature review and for further taxonomic studies of *Lockhartia*, sediments were taken from the Paleocene to Lower Eocene limestones of South Tibet (China). Shallow-water limestones of the Tethyan Himalaya (Tingri, Gamba and Guru) stratigraphic distribution of seven species of *Lockhartia* (*L. conditi*, *L. haimei*, *L. hunti*, *L. praehaimei*, *L. retiata*, *L. roeae* and *L. tipperi*) were recognized whose stratigraphic distributions were used to establish five interval biozones for South Tibet. Characteristic for the stratigraphic distribution of *Lockhartia* was the high diversity of species (up to 5 species) in the Middle and Late Paleocene and the drastic reduction (down to 2 species) in the Lower Eocene in combination with a change from a rotaliid dominated assemblage to an alveolinid dominated assemblage (see chapter 3 ”Stratigraphic distribution of the larger benthic foraminifera *Lockhartia* in South Tibet (China)”, p. 57).

Changes in foraminiferal diversity and assemblage at the Paleocene-Eocene boundary were reported as larger-foraminifera turnover (LFT; high diversification of foraminifera at specific level, adult dimorphism, as well as larger shell sizes) and benthic extinction event (BEE; extinction of about 40 % of smaller benthic foraminifera) and interpreted to be the result of the climatic and geochemical changes described as Paleocene-Eocene Thermal Maximum (PETM) and carbon isotope excursion (CIE) characterizing the Paleocene-Eocene boundary (e.g., Kennet and Stott, 1991; Pak and Miller, 1992; Hottinger, 1998; Thomas, 1998; Dickens, 1999; Zachos et al., 2001; Speijer and Morsi, 2002). The Paleocene-Eocene Thermal Maximum (PETM) was first described by Kennet and Stott (1991) from sediment cores of the Ocean Drilling Project (ODP 690B) on the flank of Maud Rise, Weddel Sea, Antarctica (also known as Late Paleocene thermal maximum (LPTM) by Zachos et al. in 1993 and described as an event of global warming within a short period of 10.000 to 30.000 years, with increasing temperatures between 4 to 5 °C in the tropics and the deep ocean and 6 to 8 °C in high latitudes (e.g., Kennet and Stott, 1991; Thomas and Shackelton, 1996; Röhl et al., 2000; Tripati and Elderfield, 2004). Rising temperatures at the P-E boundary coincided with a sharp negative δ^{13}C excursion described as carbon isotope excursion (e.g., Dickens, 1999). In literature the carbon isotope excursion (CIE) was described from terrestrial (e.g., Koch et al., 1995, 2003; Wing et al., 2005), as well as from shallow-water (e.g., Dupuis et al., 2003) and deep-sea (e.g., Bains et al., 1999) sediments with different thicknesses (Table 1.1). In South Tibet, the negative CIE representative for the Paleocene-Eocene boundary is located in a nodular limestone bed of the Zhepure Shan Formation in Tingri (Zhang et al., 2013, 2017).

1.4 Nodular limestone

In South Tibet, nodular limestones of the Zhepure Shan Formation in Tingri exhibit the negative carbon isotope excursion (CIE) representative for the Paleocene-Eocene boundary (Zhang et al., 2013, 2017). The extraordinary thickness of the CIE here (about 11 m), compared to the CIE as described by Bains et al. (1999) from ODP690 (about 1 m) leads to the question whether those nodular limestones were formed due to autochthonous (e.g., carbonate diagenesis) or allochthonous (e.g., transport, reworking) processes and if the genesis of the formation may possibly be responsible for the extraordinary thickness of the CIE.

In literature, nodular limestones have been reported from different stratigraphic periods, on a global scale and due to large genetic process variabilities ranging from diagenetic (bioturbation, solution, cementation, nodule-growth within the sediment) to sedimentary (transportation, reworking) or tectonic (shearing) processes. Devonian nodular limestones from Southern France (”Griotte”) and Germany

locality	North America Bighorn basin	Egypt Dababiya	Antarctica Maud Rise	China Tibet (Tingri)
depositional environment	terrestrial	marine 150 m - 250 m	marine deep sea (ODP 690)	marine < 40 m - 80 m
lithology	sandstone shale claystone	limestone shale clay	carbonate	nodular limestone
thickness CIE	about 57 m	about 3.5 m	about 1 m	about 11 m
literature	after Wing et al. (2005)	after Dupuis et al. (2003)	after Bains et al. (1999)	after Zhang et al. (2013, 2017)

Table 1.1: Negative carbon isotope excursion (CIE) reported from terrestrial, shallow-water and deep-sea sediments, showing different thicknesses. In marine sediments the extraordinary thickness of the CIE in Tingri (Zhang et al., 2013, 2017) is conspicuous, compared to the CIE indicated in Egypt (e.g., Dupuis et al., 2003) and the Antarctic (e.g., Bains et al., 1999).

(”Cephalopodenkalk”), as well as the Liassic red limestone breccias from the Northern Calcareous Alps (”Adneter Scheck”) are well-known nodular limestones in literature, showing different generic processes. While the ”Griotte” and ”Cephalopodenkalk” are described as products of early lithification and formation of nodules around goniatite shells (Tucker, 1974; Tucker and Wright, 2008), the Adneter Scheck was formed by mass transport of early cemented and semiconsolidated sediments due to tectonic activities (Schlager, 1966; Hudson and Jenkyns, 1969; Bernoulli and Jenkyns, 1970; Böhm et al., 1995).

Other possible processes that resulted in the creation of limestone nodules include burrowing organisms (Abed and Schneider, 1980), submarine dissolution of carbonate on the sea-floor (Hollmann, 1962, 1964; Bjorlykke, 1973, 1974), bacterially induced nodule growth (Jeans, 1980), sedimentary boudinage (McCrossan, 1958), degradation of organic material (Schindewolf, 1921, 1923, 1925), pressure solution (Wanless, 1979) and early diagenetic concretionary/nodular precipitation and lithification (Illies, 1949; Jenkyns, 1974; Müller and Fabricius, 1974; Mullins et al., 1980; Noble and Howells, 1974; Möller and Kvingan, 1988), differential diagenesis (Reinhardt et al., 2000; Westphal et al., 2000) and even the combination of different processes like hydrodynamic reworking, bioturbation, selective early cementation, mechanical compaction and pressure dissolution as reported by Bathurst (1987).

At Tingri (South Tibet), shallow-water nodular limestones can be classified into five different types of nodular limestone categories (Stylonodular Rock I, Nodular Rock I, Nodular Rock II, Stylobedded Rock, Stylomottled Rock) and some transitional members (Stylobedded Rock transitional to Stylobedded Rock II), based on their appearance in field. Observations of those types of nodular limestones suggest that they were mostly formed due to autochthonous rather than allochthonous processes (see chapter 4 ”Genesis of Paleocene and Lower Eocene shallow-water nodular limestones of South Tibet (China)”, p. 79).

”We shall not cease from exploration
and the end of all our exploring
will be to arrive where we started
and know the place for the first time.”

T. S. Eliot, taken from the poem ”Little Gidding”

2 Paleocene and Lower Eocene shallow-water limestones of Tibet: microfacies analysis and correlation of the eastern Neo-Tethyan Ocean

Michaela M. Kahsnitz[1,3], **Helmut Willems**[1,2], **Hui Luo**[2], **Zhicheng Zhou**[2]

[1] Department of Geosciences, University of Bremen, 28359 Bremen, Germany

[2] Nanjing Institute of Geology and Palaeontology, Chinese Academy of Sciences, Nanjing 210008, China

[3] Correspondence author. Email: michaela.kahsnitz@uni-bremen.de

Submitted to Palaeoworld

Abstract

Microfacial investigations of Lower Paleogene sediments, based on four sections of the passive Indian (Zanskar, Tingri, Gamba and Guru) and one section of the active Asian continental margin (Cuojiangding). Eleven microfacies from the Tethyan Himalaya (prefixed with P for passive continental margin) and four microfacies from the Xigaze forearc basin (prefixed with A for active continental margin) were observed, based on the distribution of fossil assemblages, representing depositional environment ranging from the tidal flat and restricted lagoonal part of the inner carbonate ramp to the outer carbonate ramp: (P1) Green algae pack-/grainstone with small miliolids, (P2) Bioclast grainstone, (P3) Rotaliidae packstone, (P4) Miscellaneidae-Rotaliidae-Nummulitidae pack-/grainstone, (P5) Laminated and bioturbated mud- and grainstone, (P6) *Alveolina* wacke-/packstone with Soritidae, (P7) *Nummulites-Alveolina-Orbitolites* pack-/floatstone, (P8) Discocyclinidae-Nummulitidae pack-/floatstone, (P9) Rhodolith wacke-/packstone, (P10) Mudstone with anhydrite nodules, (P11) Planktonic foraminiferal wackestone, (A1) Molluskan float-/rudstone, (A2) Nummulitidae wacke-/packstone, (A3) Rodolith wacke-/packstone, (A4) Discocyclinidae-Nummulitidae float-/rudstone. The correlation of our observations provides a detailed overview of the paleoenvironmental development and the sedimentary history of the eastern Neo-Tethyan Ocean, showing a deepening from Lower Paleocene to Lower Eocene in two stages.

KEYWORDS: paleoenvironment, microfacies analysis, eastern Neo-Tethys, Tethyan Himalaya, Xigaze forearc strata, Paleogene, carbonate

2.1 Introduction

This paper is aiming for the reconstruction of the paleoenvironmental conditions and sedimentary evolution based on the analysis and regional correlation of microfacies from the active and passive continental margin of the eastern Neo-Tethyan Ocean. After several decades of research the discussion on the India-Asia continental collision as well as the basin development within the eastern Neo-Tethys Ocean is still ongoing. Different approaches like microfacies and sedimentary analysis, systematic description of foraminifera and biostratigraphy, as well as provenance analysis have been used to reconstruct the geodynamic evolution of the passive continental margin focused on the section areas of Tingri and Gamba in Tibet (e.g., Liu, 1992; Willems, 1993; Willems et al., 1996; Wan et al., 2002, 2010; Hu et al., 2012; Zhang et al., 2012, 2013; Li et al., 2015; Kahsnitz et al., 2016), and the area of Zanskar in Ladakh (e.g., Gaetani et al., 1983, 1986; Nicora et al., 1987; Fuchs, 1987; Fuchs and Willems, 1990; Gaetani et al., 1996; Mathur et al., 2009).
Time-equivalent strata of the active continental margin were studied in the vicinity of Cuojiangding and Dajin (e.g., Liu et al., 1988; Dürr, 1993; Wan et al., 2002; Ding et al., 2005; BouDagher-Fadel et al., 2015; Wang et al., 2015; Hu et al., 2016). Though rough correlations between sediments of the Tethyan Himalaya (e.g., Fuchs and Willems, 1990) as well as between sediments from the active and passive continental margin (e.g., BouDagher-Fadel et al., 2015) have been considered, a detailed correlation between microfacies distribution patterns and accordingly the basin evolution of the eastern Neo-Tethyan Ocean is not yet available.

Microfacial investigations of Lower Paleogene sediments, based on four sections of the passive Indian (Zanskar, Tingri, Gamba and Guru) and one section of the active Asian continental margin (Cuojiangding). Eleven microfacies of the Tethyan Himalaya and four microfacies of the Xigaze forearc basin were observed, based on the distribution of fossil assemblages. Correlation of our observations provides a detailed overview of the paleoenvironmental development and the sedimentary history of the eastern Neo-Tethyan Ocean, showing a deepening from Lower Paleocene to Lower Eocene in two stages.

2.2 Geological setting

Sample for paleoenvironmental and sedimentary reconstructions were taken from Paleocene to Lower Eocene limestones from South Tibet (China) and Zanskar (Ladakh, India). Sediments of western Zanskar (India: 29°55'N, 84°19'E), Tingri (South Tibet: 28°41'N, 86°42'E), Gamba (South Tibet: 28°17'N, 88°32'E) and Guru (South Tibet: 28°06'N, 89°12'E) are deposited on a carbonate ramp forming the northern passive continental margin of the Indian continent (Gaetani et al., 1986; Fuchs and Willems, 1990; Willems, 1993; Zhang et al., 2012) close to the equator (Fig. 2.1a). In contrast to this, the sedimentary history of the Cuojiangding section (South Tibet: 29°56'N, 84°19'E) shows the depositional environment of a forearc basin (called Xigaze forearc basin), formed at the southern active margin of the Asian continent at lower to middle latitudes (Qian et al., 1982; Liu et al., 1988; Ding et al., 2005).

Today, the investigated sections belong to the Himalayan orogenic belt covering an area from Zanskar (Chulung Chu) in northern India to South-Tibet (Cuojiangding, Tingri, Gamba and Guru) in China (Fig. 2.1b). The Himalayan orogenic belt can be subdivided from north to south (Fig. 2.1c) into different structural units (Gansser, 1964): the Lhasa Block (here the southern Lhasa Block is represented by Gangdese batholiths and Linzizong volcanic successions), the Xigaze forearc strata, the Tethyan Himalaya and the Himalaya (subdivided into Higher, Lesser and Sub-Himalaya). During Paleocene, the Lhasa Block and the Xigaze forearc strata were part of the southern active continental margin of the Asian plate, while the Tethyan Himalaya was part of the northern passive continental margin of the Indian plate.

At Tingri, Gamba and Guru, the Paleocene to Lower Eocene sediments of the Zongpu Formation were deposited within a shallow-marine environment of a carbonate ramp (e.g., Willems, 1993; Willems et al., 1996; Li et al., 2015; Kahsnitz et al., 2016). Additionally, we investigated the time-equivalent Lingshet Limestone of the Spanboth Group of Chulung valley (= Chulung Chu) east of the Spongtang Massif in West

Figure 2.1 ***(following page)*****:** Paleogeographic, geographic and geological overview of the section area. **A** Paleocene paleogeographic position of Cuojiangding on the southern active continental margin of Asia and the locations of Chulung Chu (Ladakh), Tingri, Gamba and Guru on the northern passive continental margin of India in the eastern Neo-Tethyan Ocean. Paleogeographic map is redrawn from Smith et al. (1994). **B** Location of the five studied sections in China (Tibet: marked in grey) and India (Zanskar, Ladakh). Abbreviations: Bhu - Bhutan, Kathman - Kathmandu. **C** Geological map of the Himalaya (after Hu et al., 2016). Studied sections in Zanskar, Tingri, Gamba and Guru are part of the Tethyan Himalaya (Indian-affinity), while the section in Cuojiangding represents the Xigaze forearc strata (Asian-affinity). Abbreviations: GCT - Great Counter Thrust, KF - Karakoram Fault, STDZ - South Tibet Detachment System, MBT - Main Boundary Thrust, MCT - Main Central Thrust, MFT - Main Frontal Thrust. **D** Simplified stratigraphic sections of Cuojiangding, Zanskar, Tingri, Gamba and Guru correlated on the stratigraphic level of the Paleocene-Eocene boundary (red dotted line). Lithological accordance between the sections is marked with black dotted lines. Abbreviations: Cr - Cretaceous

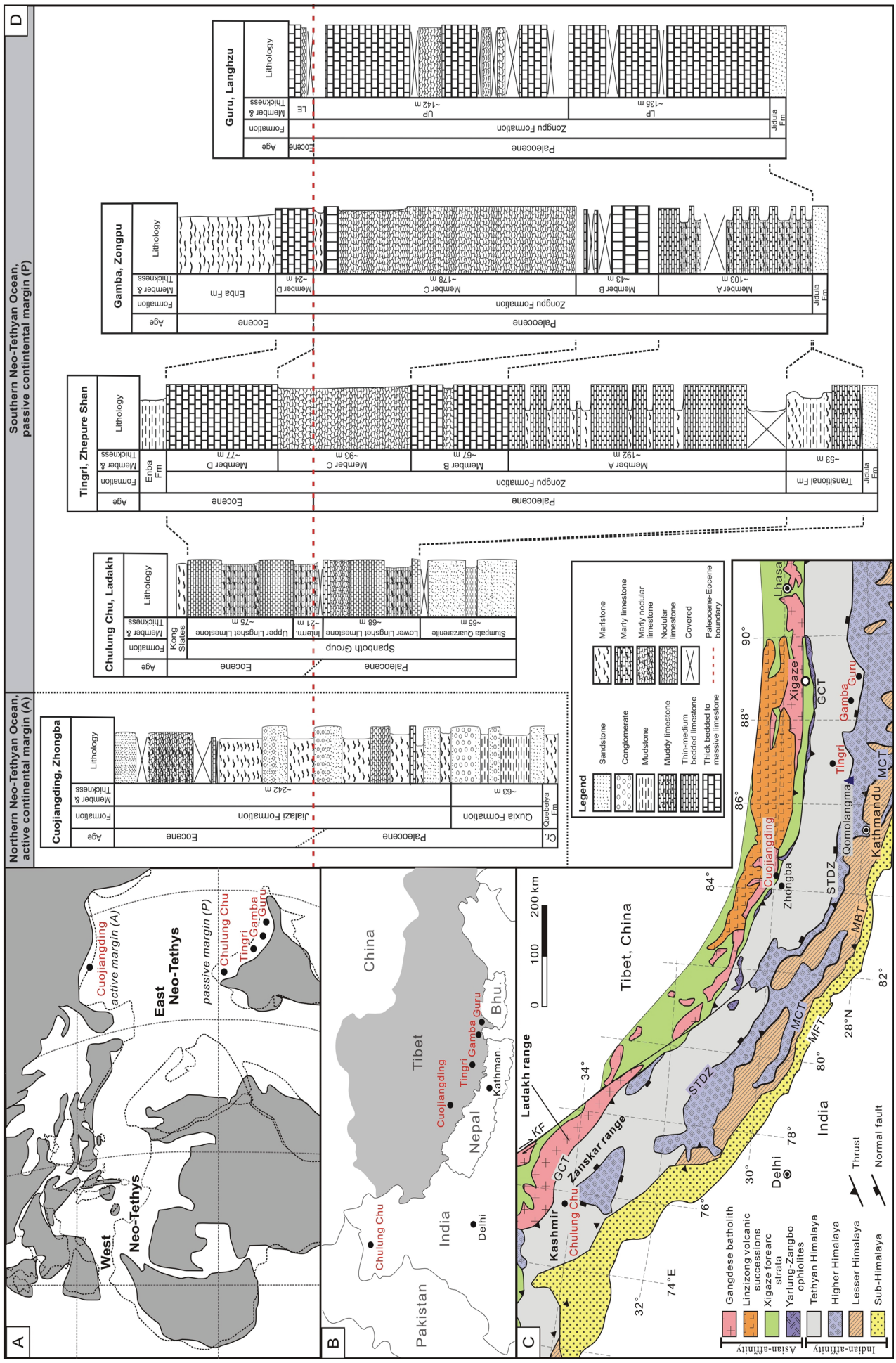
A
B
C
D
Northern Neo-Tethyan Ocean, active continental margin (A)
Southern Neo-Tethyan Ocean, passive continental margin (P)
East Neo-Tethys
West Neo-Tethys
active margin (A)
passive margin (P)
Cuojiangding
Chulung Chu
Tingri
Gamba
Guru
China
Tibet
Nepal
India
Pakistan
Bhu.
Kathman.
Delhi
Tibet, China
Ladakh range
Zanskar range
Kashmir
KF
GCT
STDZ
MCT
MFT
MBT
Lhasa
Xigaze
Zhongba
Qomolangma
Kathmandu
Thrust
Normal fault
Gangdese batholith
Linzizong volcanic successions
Xigaze forearc strata
Yarlung-Zangbo ophiolites
Tethyan Himalaya
Higher Himalaya
Lesser Himalaya
Sub-Himalaya
Asian-affinity
Indian-affinity
Legend
Sandstone
Conglomerate
Mudstone
Muddy limestone
Thin-medium bedded limestone
Thick bedded to massive limestone
Marlstone
Marly limestone
Marly nodular limestone
Nodular limestone
Covered
Paleocene-Eocene boundary
Cuojiangding, Zhongba
Chulung Chu, Ladakh
Tingri, Zhepure Shan
Gamba, Zongpu
Guru, Langhzu
Quxia Formation
Jidaizi Formation
Zongpu Formation
Paleocene
Eocene
Sparnotoh Group
Stumpata Quarzarenite
Lower Lungshet Limestone
Upper Lungshet Limestone
Kong Slates
Enba Fm
Transitional Fm
Jidula Fm
Quebeiya Fm
Lithology
Age
Formation
Member & Thickness

Zanskar (Ladakh). The depositional environment of the Dibling Limestone, correlating with the Lingshet Limestone of Zanskar (Fuchs, 1982), located within the Spanboth valley southwest of the Chulung Chu, was interpreted as a subtidal carbonate bay with terrigenous input. The base of the Dibling Limestone is indicated by a sharp deepening, followed by a regression leading to environmental conditions of a restricted lagoon (Gaetani et al., 1983, 1986; Nicora et al., 1987).

The Paleocene and Lower Eocene Quxia and Jialazi formations of Cuojiangding are described as being deposited in a fan-delta environment within the Xigaze forearc basin of the southern active continental margin of Asia (Hu et al., 2016).

2.3 Material and Methods

For microfacial analyses, about 1360 samples were taken from Paleocene to Lower Eocene strata of the following locations: Cuojiangding (Quxia Formation, Section: 10TS), Tingri (Zongpu Formation, Sections: 09ZS, 10/11TM), Gamba (Zongpu Formation, Sections: ZP, ZM, F, 11TMG), Guru (Zongpu Formation, Sections: GUR-LP/UP/LE) and Ladakh (Lingshet Limestone, Sections: ZL 1988/1990), with a sample density varying between 0.5 and 1.5 m. At Cuojiangding sample density varies strongly depending on lithologic variances, showing a sample gap of about 25 m in the middle part of the Jialazi Formation.
For better stratigraphic correlation, carbon isotope data are used from literature or measured to determine the Paleocene-Eocene boundary, which is characterized by a sharp negative carbon isotope excursion (Dickens, 1999). Carbon isotope data to determine the Paleocene-Eocene boundary in Tingri and Gamba were taken from Zhang et al. (Zhang et al., 2012, 2013). In order to define the position of the Paleocene-Eocene boundary in the sections of Chulung Chu (Ladakh), Cuojiangding and Guru, carbon isotopes were measured of bulk-samples ($\delta^{13}C_{bulk}$) using a Finnigan MAT 251 Spectrometer at the Center for Marine Environmental Sciences (MARUM, University of Bremen). Reproducibility of the internal laboratory standard (Solnhofen limestone) is $\pm$0.03 ‰ for δ^{13}C and $\pm$0.08 ‰ for δ^{18}O. Differences in lithology (interbedded limestone, sandstone and conglomerate) cause a high variability of carbonate contents, ranging from 0 % to 97 %, in the Cuojiangding section of the Xigaze forearc basin, bringing forth an incomplete carbon isotope curve when the carbonate content is too low. Therefore, samples from Cuojiangding were decarbonated first, using diluted hydrochloric acid (10 % HCl) for carbon isotope measurements at the total organic carbon ($\delta^{13}C_{TOC}$). Mass percentages of carbon isotopes were determined using a Thermo Finnigan Flash Elemental Analyzer 2000 with Delta V Plus Isotope Ratio Mass Spectrometer (IRMS) at the Center for Marine Environmental Sciences (MARUM, University of Bremen).

Thin section analysis was used to determine sedimentary and diagenetic features of the limestones. The determination of the microfacies was based on fossil assemblages and carbonate classification according to Dunham (1962) and the expanded classification of Embry and Klovan (1971). With regard to their deposition, either on the passive margin of the Indian continent or on the active margin of the Asian continent, microfacies types were prefixed P (e.g., P1) for passive and A (e.g., A1) for active margin. Samples investigated herein were stored at the working group Historical Geology/Paleontology of the Department of Geosciences (University of Bremen).

2.4 Litho- and (bio-)stratigraphy

A generalized lithological overview (Fig. 2.1d) of the investigated sections indicates that at all locations the underlying beds are characterized by the occurrence of a massive sandstone layer (Quxia Formation, Stumpata Quartzarenite and Jidula Formation). While on the passive margin (represented by the sections of Zanskar, Tingri, Gamba and Guru) these sandstone units are followed by Paleocene to Lower Eocene limestone beds (Lingshet Limestone/ Zongpu Formation), the active margin (section of Cuojiangding) shows a time-equivalent marl- and limestone deposition which is frequently intercalated by massive sandstone and conglomerate layers. The greenish and red marl- and mud-/claystones (Kong Slates, Enba Formation) from Zanskar, Tingri and Gamba lying on top of the limestone units represent the end of the marine sedimentary history during Lower Eocene.

2.4.1 The passive continental margin

Chulung Chu region, Zanskar - Spanboth Section

The Spanboth Group of Zanskar is subdivided into three lithological units from bottom to top called 'lower', 'middle' and 'upper Member' (Gaetani et al., 1983, 1986; Baud et al., 1984) or 'Marpo Limestone', 'Stumpata Quartzarenite' and 'Dibling Limestone' (Nicora et al., 1987), respectively. In the valley called Chulung Chu, the Spanboth Group is composed of the Stumpata Quartzarenite and the conformably overlying Lingshet Limestone, the latter merging laterally into the Dibling Limestone (Fuchs, 1982). The Stumpata Quartzarenite has a thickness of approx. 65 m (Fig. 2.1d) and consists of predominantly quarzitic sandstones, sometimes showing cross bedding (Nicora et al., 1987; Fuchs and Willems, 1990). The Quartzarenite comprises rare trace fossils (Skolithos) and is suggested to be of Lower Paleocene age (Nicora et al., 1987). The Lingshet Limestone can be subdivided into three parts: the Lower Lingshet Limestone at the base, an Intermediate Layer and the Upper Lingshet Limestone. Upper and Lower Lingshet Limestones show a thickness of approx. 68 m and approx. 75 m, respectively, and mainly consist of massive limestone beds as well as of marlstone, sometimes dolomitized limestones and nodular limestones. Additionally, the marl- and limestone sediments of the Lingshet Limestone are characterized by intercalated layers comprising numerous gypsum/anhydrite nodules. Upper and Lower Lingshet Limestones are separated by a so called 'intermediate layer', characterized by the occurrence of nodular and marly limestones retreating morphologically, showing a thickness of approximately 21 m. LBF such as *Daviesina*, *Alveolina*, *Nummulites* and *Discocyclina* indicate a Paleocene to Lower Eocene age of the Lingshet Limestone (Gaetani et al., 1983, 1986; Nicora et al., 1987; Mathur et al., 2009). In northern Zanskar, the end of marine sedimentation is characterized by the continental red beds of the Kong Slates on top of the Lingshet Limestone (Gaetani and Garzanti, 1991).

Tingri/Gamba/Guru region - Zhepure Shan/Zongpu/Langzhu Section

In southern Tibet, the Paleocene to Lower Eocene strata outcropped close to the villages of Tingri, Gamba and Guru. In Tingri, Gamba and Guru, the Zongpu Formation[1] shows a thickness ∼420 m, ∼350 m and ∼290 m,

[1] also known as Zhepure Shan Formation in Tingri (e.g., Willems, 1993; Zhang et al., 2013, 2017) and Langzhu Formation in Guru (Kahsnitz et al., 2016)

respectively, and is underlain by the Jidula Formation (Fig. 2.1d) and overlain by the Enba Formation[2] representing the end of the marine sedimentation (Willems, 1993; Zhu et al., 2005). In Tingri and Gamba the Zongpu Formation can be subdivided into four lithological units, which are from bottom to top: cyclic limestone (Member A), massive limestone (Member B), nodular limestone (Member C), massive limestone (Member D). In Guru the Zongpu Formation mainly consists of massive and nodular limestones but the general lithological successions fount at Tingri and Gamba are not fully developed. Larger benthic foraminifera such as *Lockhartia*, *Ranikothalia*, *Miscellanea*, *Alveolina* and *Nummulites* indicate a Paleocene to Lower Eocene age of the Zongpu Formation (Willems, 1993; Zhang et al., 2013).

2.4.2 The active continental margin

Zongba region - Cuojiangding Section

The Paleocene Quxia Formation in the vicinity of the village Cuojiangding of the Zongba region is unconformably overlying the Cretaceous Quebeiya Formation. It is composed of siliciclastic material, comprises a thickness of ∼63 m and consists of several fining upward sequences, starting with massive conglomerate at the base, passing over to sandstone and even to mudstone/shale at the top (Fig. 2.1d). The Quxia Formation is generally poor in fossils, providing no stratigraphic indications, therefore the age is suggested to be Danian (Wan et al., 2001). The Quxia Formation is conformably overlain by the lithologically very variable Jialazi Formation with a thickness of ∼242 m. It is composed of an alternating sequence of limestone, sandstone and conglomerate, and minor intercalations of volcanic tuff (Ding et al., 2005). The Jialazi Formation has a Paleocene to Lower Eocene age, as indicated by foraminifera (Liu et al., 1988; Ding et al., 2005; Hu et al., 2016).

2.5 Stratigraphic correlation based on isotope measurements

The Paleocene-Eocene boundary is characterized by a sharp negative carbon isotope excursion at the end of the Paleocene (Dickens, 1999). For better stratigraphic correlation of sediments observed in this study carbon isotope curves are either taken from literature (Zhang et al., 2012, 2013, for Tingri and Gamba) or have been measured (Zanskar, Cuojiangding and Guru).

Due to the high terrigenous input delivered from the Asian continent, the sedimentary sequence of Cuojiangding frequently alternates between limestone to sandstone and conglomerate. This results in a high variability of carbonate contents, ranging from 0 to 97 %, causing an incomplete carbon isotope curve from bulk sediments in cases where carbonate content is too low (see Fig. 2.2). Hence, carbon isotopes of the total organic carbon were measured as well, with the intention to gather more reliable data to clarify the stratigraphic position of the Paleocene-Eocene boundary in the Cuojiangding section. However, the carbon isotope data of total organic carbon seemed to be influenced by the lithological composition: sandstone and conglomerate display more negative, while limestone exhibits more positive carbonate isotope values. This could be explained by differences in the source area of the organic matter. Limestone mainly contains marine organic material, while organic material of sandstone and conglomerate certainly possess a more terrigenous

[2] also known as Youxia Formation in Tingri (e.g., Zhang et al., 2012, 2013) and Zongpubei Formation in Gamba (e.g., Willems, 1993; Zhang et al., 2012, 2013)

source area. Nevertheless, both carbon isotope curves ($\delta^{13}C_{bulk}$ and $\delta^{13}C_{TOC}$) are highly incomplete, especially in the middle part of the Jialazi Formation, just in a section part where the Paleocene-Eocene boundary is expected, due to remarkable changes in microfacies composition as well as a highly negative carbon isotope value of –10,10 ‰ measured in bulk carbonate. In Cuojiangding the Paleocene-Eocene boundary is therefore expected in the middle part of the Jialazi Formation in a thick sandstone to conglomerate layer below Microfacies A1.

Carbon isotope measurements from the Spanboth Group of Chulung Chu in Ladakh show a negative carbon isotope excursion at sample number 38 within the so called Intermediate Layer between the Lower and Upper Lingshet Limestone with an negative excursion of about –6 ‰ (see Fig. 2.3). Due to the high sample distance between sample 38 and 39, it is not possible to precisely indicate the Paleocene-Eocene boundary. Therefore the boundary is just roughly constrained.

At Tingri, the sedimentary sequence of the Zongpu Formation is nearly complete, showing a negative carbon isotope excursion in the nodular limestone section part (see Fig. 2.4), with an excursion of about –6 ‰ and a thickness of the sedimentary pile of ∼11 m (Zhang et al., 2013, 2017). At Gamba, the Paleocene-Eocene boundary of the Zongpu Formation is recorded directly at the boundary between nodular limestone of Member C and massive limestone of Member D (Zhang et al., 2012), indicating a hiatus between the two lithological units. The negative carbon isotope excursion is about –8 ‰ (see Fig. 2.5).

In the Zongpu Formation of Guru, the carbon isotope excursion is incomplete due to several sedimentary hiatuses, and thus doesn't provide any reliable information on the position of the CIE and consequently, the position of the Paleocene-Eocene boundary in the studied section is uncertain (see Fig. 2.6). Instead, the denomination of the Paleocene-Eocene boundary at Guru is drawn from investigations on the assemblage of larger benthic foraminifera carried out by Kahsnitz et al. (2016). Based upon their results, the Paleocene-Eocene boundary is roughly constrained in the upper part of the section, at the change from shallow benthic zone 5 to shallow benthic zone 7, where the microfacies changes from an algal-dominated assemblage with Rotaliidae LBF to an assemblage characterized by *Nummulites*, *Alveolina* and *Orbitolites*.

Figure 2.2 ***(following page)*:** Stratigraphic distribution of major fossils and allochems during Paleocene and Lower Eocene in the Quxia and Jialazi formations of Cuojiangding. Paleocene-Eocene boundary is roughly constrained, based on isotope analysis. Shallow benthic zones are taken from Hu et al. (2016). Due to a high variability of carbonate content ranging from 0 to 97 %, the carbon isotope excursion in Cuojiangding is highly incomplete. Paleocene-Eocene boundary is therefore roughly constrained (red area), where the carbon isotopes show one most negative value. See figure 2.11 for explanations of lithological symbols. Abbreviations: Cr - Cretaceous, PDB - Pee Dee Belemnite, Rotal - Rotaliidae, SBZ - Shallow benthic zones.

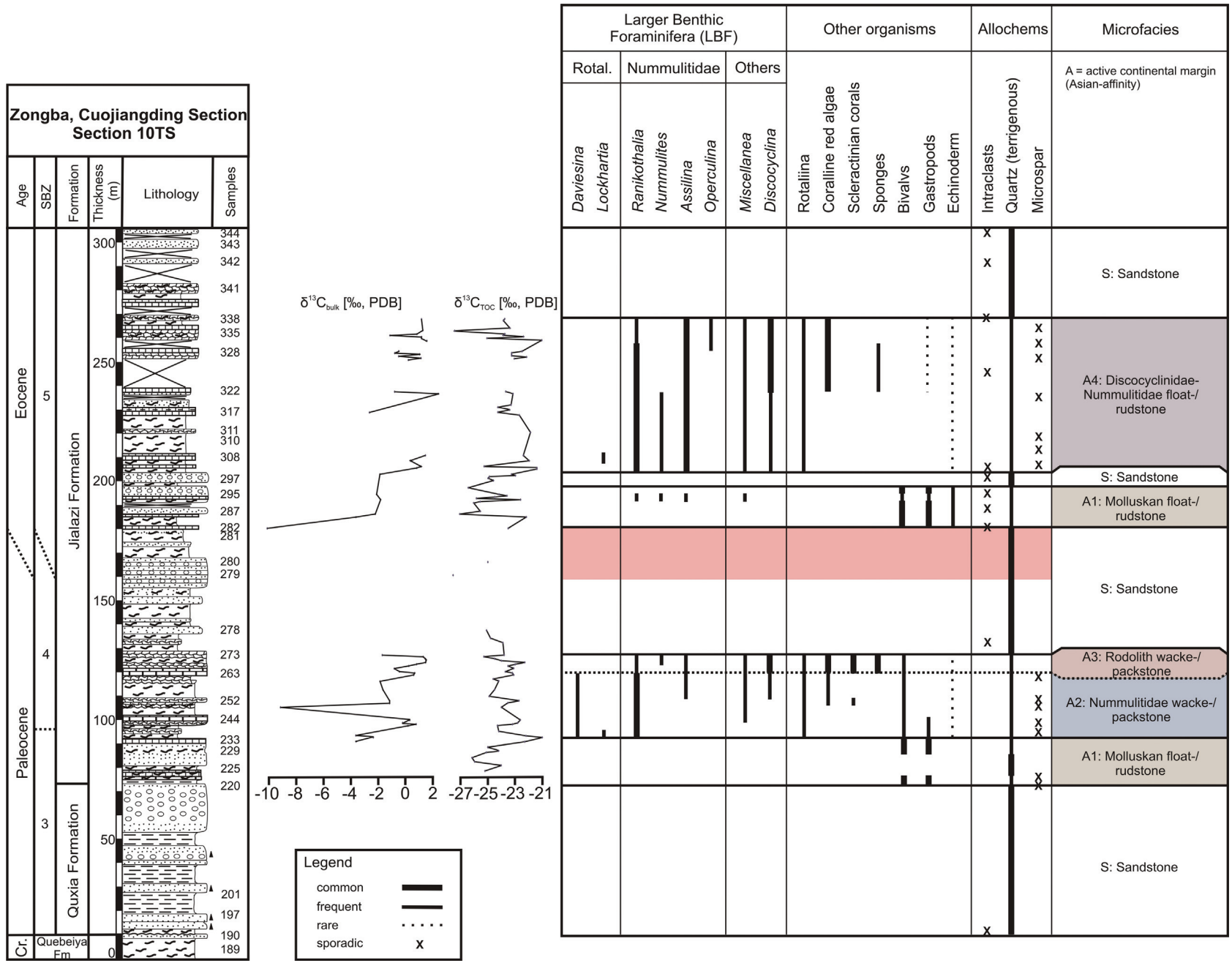
Zongba, Cuojiangding Section
Section 10TS
Age
SBZ
Formation
Thickness (m)
Lithology
Samples
Eocene
Paleocene
5
4
3
Jialazi Formation
Quxia Formation
Cr.
Quebeiya Fm
δ13Cbulk [‰, PDB]
δ13CTOC [‰, PDB]
-10 -8 -6 -4 -2 0 2
-27 -25 -23 -21
Legend
common
frequent
rare
sporadic
Larger Benthic Foraminifera (LBF)
Rotal.
Nummulitidae
Others
Daviesina
Lockhartia
Ranikothalia
Nummulites
Assilina
Operculina
Miscellanea
Discocyclina
Other organisms
Rotaliina
Coralline red algae
Scleractinian corals
Sponges
Bivalvs
Gastropods
Echinoderm
Allochems
Intraclasts
Quartz (terrigenous)
Microspar
Microfacies
A = active continental margin (Asian-affinity)
S: Sandstone
A4: Discocyclinidae-Nummulitidae float-/rudstone
S: Sandstone
A1: Molluskan float-/rudstone
S: Sandstone
A3: Rodolith wacke-/packstone
A2: Nummulitidae wacke-/packstone
A1: Molluskan float-/rudstone
S: Sandstone

Figure 2.3 ***(following page)*****:** Stratigraphic distribution of major fossils and allochems during Paleocene and Lower Eocene in the Spanboth Formation of the Chulung Chu section in Zanskar. Paleocene-Eocene boundary (red area) is roughly constrained, based on isotope data. Shallow benthic zones are taken from Mathur et al. (2009). See figure 2.11 for explanations of lithological symbols and figure 2.2 for quantitative symbols. Abbreviations: Num - Nummulitidae, PDB - Pee Dee Belemnite, SBZ - Shallow benthic zones.

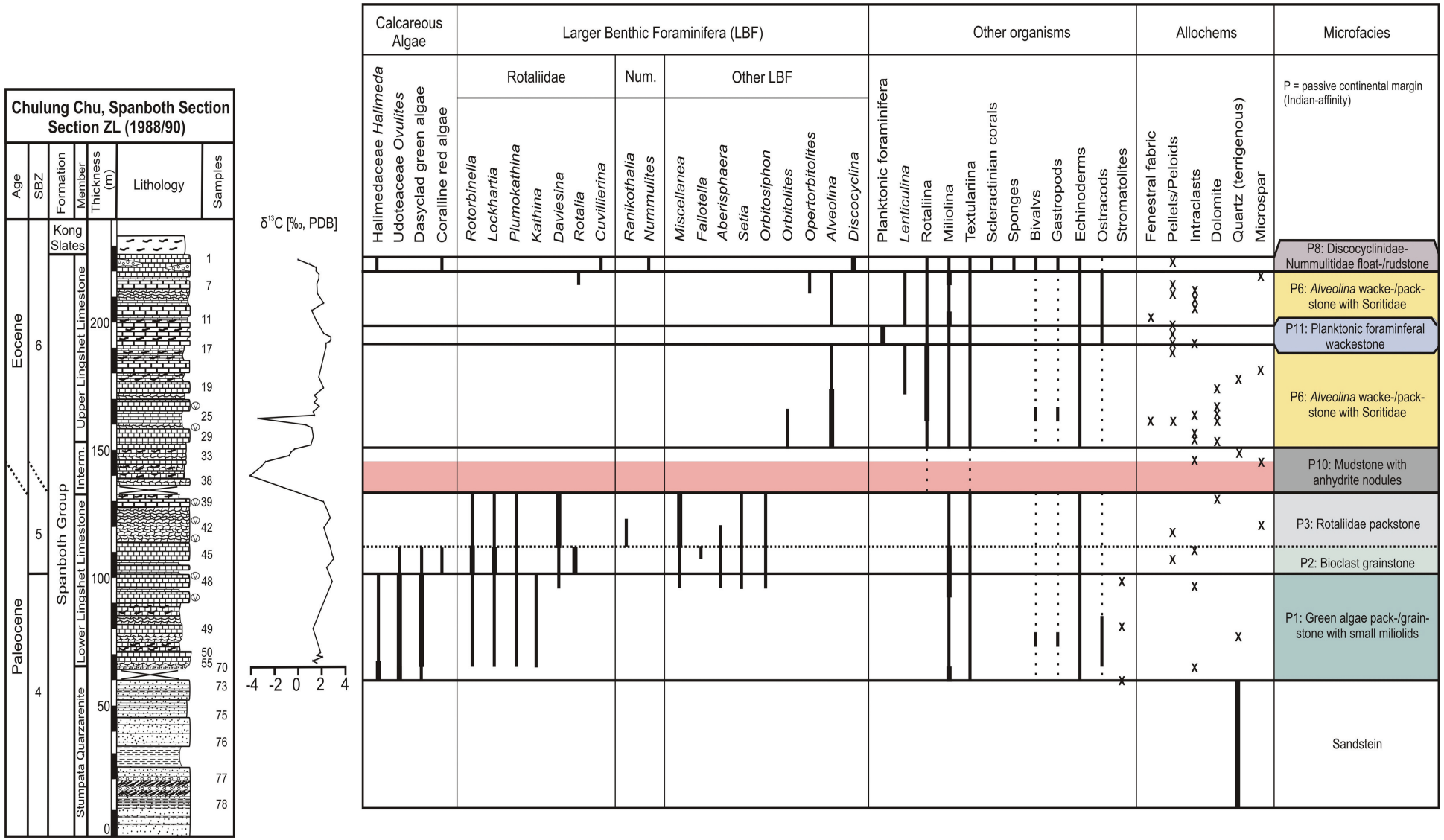
Chulung Chu, Spanboth Section
Section ZL (1988/90)
Age
SBZ
Formation
Member
Thickness (m)
Lithology
Samples
Eocene
Paleocene
6
5
4
Kong Slates
Spanboth Group
Upper Lingshet Limestone
Interm.
Lower Lingshet Limestone
Stumpata Quarzarenite
200
150
100
50
0
1
7
11
17
19
25
29
33
38
39
42
45
48
49
50
55
70
73
75
76
77
78
δ13C [‰, PDB]
-4 -2 0 2 4
Calcareous Algae
Halimedaceae Halimeda
Udoteaceae Ovulites
Dasyclad green algae
Coralline red algae
Larger Benthic Foraminifera (LBF)
Rotaliidae
Rotorbinella
Lockhartia
Plumokathina
Kathina
Daviesina
Rotalia
Cuvillierina
Num.
Ranikothalia
Nummulites
Other LBF
Miscellanea
Fallotella
Aberisphaera
Setia
Orbitosiphon
Orbitolites
Opertorbitolites
Alveolina
Discocyclina
Other organisms
Planktonic foraminifera
Lenticulina
Rotaliina
Miliolina
Textulariina
Scleractinian corals
Sponges
Bivalvs
Gastropods
Echinoderms
Ostracods
Stromatolites
Allochems
Fenestral fabric
Pellets/Peloids
Intraclasts
Dolomite
Quartz (terrigenous)
Microspar
Microfacies
P = passive continental margin (Indian-affinity)
P8: Discocyclinidae-Nummulitidae float-/rudstone
P6: Alveolina wacke-/packstone with Soritidae
P11: Planktonic foraminferal wackestone
P6: Alveolina wacke-/packstone with Soritidae
P10: Mudstone with anhydrite nodules
P3: Rotaliidae packstone
P2: Bioclast grainstone
P1: Green algae pack-/grainstone with small miliolids
Sandstein

Figure 2.4 *(following page)*: Stratigraphic distribution of major fossils and allochems during Paleocene and Lower Eocene in the Zongpu Formation of the Tingri. Paleocene-Eocene boundary (red line), carbon isotope curve and shallow benthic zones are taken from Zhang et al. (2013) for the Zhepure Section. See figure 2.11 for explanations of lithological symbols and figure 2.2 for quantitative symbols. Abbreviations: Keramosph. - *Keramosphaerinopsis*, PDB - Pee Dee Belemnite, SBZ - Shallow benthic zones.

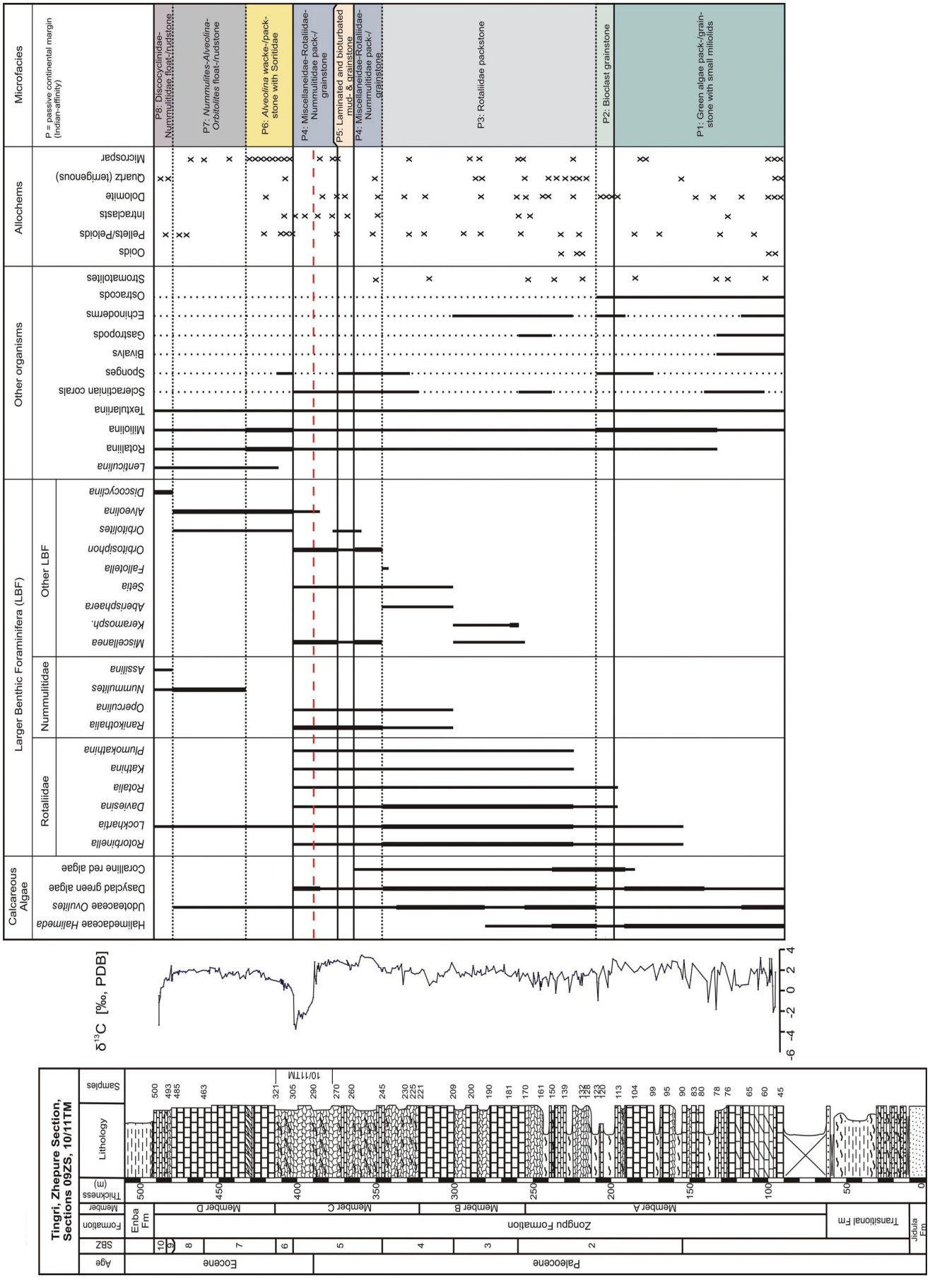
Tingri, Zhepure Section, Sections 09ZS, 10/11TM
Age
SBZ
Formation
Member
Thickness (m)
Lithology
Samples
Eocene
Paleocene
Enba Fm
Member D
Member C
Member B
Member A
Zongpu Formation
Transitional Fm
Jidula Fm
10/11TM
δ13C [‰, PDB]
Microfacies
Allochems
Other organisms
Larger Benthic Foraminifera (LBF)
Calcareous Algae
P = passive continental margin (Indian-affinity)
P8: Discocyclinidae-Nummulitidae float-/rudstone
P7: Nummulites-Alveolina-Orbitolites float-/rudstone
P6: Alveolina wacke-/packstone with Sortidae
P4: Miscellaneidae-Rotaliidae-Nummulitidae pack-/grainstone
P5: Laminated and bioturbated mud- & grainstone
P4: Miscellaneidae-Rotaliidae-Nummulitidae pack-/grainstone
P3: Rotaliidae packstone
P2: Bioclast grainstone
P1: Green algae pack-/grainstone with small miliolids
Microspar
Quartz (terrigenous)
Dolomite
Intraclasts
Pellets/Peloids
Ooids
Stromatolites
Ostracods
Echinoderms
Gastropods
Bivalvs
Sponges
Scleractinian corals
Textulariina
Miliolina
Rotaliina
Lenticulina
Discocyclina
Alveolina
Orbitolites
Orbitosiphon
Fallotella
Setia
Abenisphaera
Keramosph.
Miscellanea
Assilina
Nummulites
Operculina
Rankothalia
Pseudolockhartia
Kathina
Rotalia
Daviesina
Lockhartia
Rotorbinella
Corallina red algae
Dasycladacean green algae
Udoteacean Ovulites
Halimedacean Halimeda

Figure 2.5 ***(following page)*****:** Stratigraphic distribution of major fossils and allochems during Paleocene and Lower Eocene in the Zongpu Formation of Gamba. Paleocene-Eocene boundary (red line), carbon isotope curve and shallow benthic zonation are taken from Zhang et al. (2012, 2013). See figure 2.11 for explanations of lithological symbols and figure 2.2 for quantitative symbols. Abbreviations: Nummul - Nummulitidae, PDB - Pee Dee Belemnite, SBZ - Shallow benthic zones.

Gamba, Zongpu Section, Sections ZP, ZM, F, 11TMG
Age
SBZ
Formation
Member
Thickness (m)
Lithology
Samples
Microfacies
Allochems
Other organisms
Larger Benthic Foraminifera (LBF)
Calcareous Algae
Eocene
Paleocene
Enba Fm
Zongpu Formation
Member D
Member C
Member B
Member A
Jdula Fm
Section F (1983)
Section ZM (1992)
Section ZP (1992)
11TMG
P7: Nummulites-Alveolina-Orbitolites float-/rudstone
P6: Alveolina wacke-/packstone with Soritidae
P4: Miscellaneidae-Rotaliidae-Nummulitidae pack-/grainstone
P3: Rotaliidae packstone
P2: Bioclast grainstone
P1: Green algae pack-/grainstone with small miliolids
P = passive continental margin (Indian-affinity)
Microspar
Quartz (terrigenous)
Dolomite
Lithoclasts
Pellets/Peloids
Ooids
Stromatolites
Ostracods
Echinoderms
Gastropods
Bivalves
Sponges
Scleractinian corals
Textulariina
Miliolina
Rotaliina
Lenticulina
Orbitolites
Alveolina
Orbitosiphon
Setia
Miscellanea
Abertisphaera
Keramosph.
Nummulites
Operculina
Ranikothalia
Rotalia
Kathina
Daviesina
Plumokathina
Lockhartia
Rotorbinella
Rotaliidae
Nummul.
Other LBF
Udoteacean Uvuliites
Dasycladacean algae
Coralline red algae
δ13C [‰,PDB]

Figure 2.6 ***(following page)*****:** Stratigraphic distribution of major fossils and allochems during Paleocene and Lower Eocene in the Zongpu Formation of Guru. Due to the lack of information given by the carbon isotope data, the Paleocene-Eocene boundary (red line) and shallow benthic zonation based on isotope and foraminiferal analysis given by Zhang et al. (2012, 2013) and adopted according to Kahsnitz et al. (2016). See figure 2.11 for explanations of lithological symbols and figure 2.2 for quantitative symbols. Abbreviations: Nummul - Nummulitidae, PDB - Pee Dee Belemnite, SBZ - Shallow benthic zones.

Guru, Langzhu Section, Sections GUR-LP/UP/LE
Age
SBZ
Formation
Thickness (m)
Lithology
Samples
Paleocene
Eocene
Zongpu Formation
Jidula Fm
Microfacies
P = passive continental margin (Indian-affinity)
P6: Alveolina wacke-/packstone with Soritidae
P9: Rodolith wacke-/packstone
P4: Miscellaneidae-Rotaliidae-Nummulitidae pack-/grainstone
P3: Rotaliidae packstone
P2: Bioclast grainstone
P1: Green algae pack-/grainstone with small miliolids
Allochems
Pellets/Peloids
Intraclasts
Dolomite
Quartz (terrigenous)
Microspar
Other organisms
Stromatolites
Ostracods
Echinoderms
Gastropods
Bivalves
Sponges
Scleractinian corals
Textulariina
Miliolina
Rotaliina
Lenticulina
Larger Benthic Foraminifera (LBF)
Other LBF
Orbitolites
Alveolina
Orbitosiphon
Setia
Miscellanea
Abertisphaera
Keramosph.
Nummul.
Nummulites
Operculina
Ranikothalia
Rotaliidae
Daviesina
Kathina
Rotalia
Plumokathina
Lockhartia
Rotorbinella
Calcareous Algae
Coralline red algae
Dasycład green algae
Udoteacee Ovulites
Halimedacee Halimeda
δ13C [‰, PDB]
-2
0
2
4

2.6 Microfacies analysis

In this study, microfacies analysis of five stratigraphic sections in South Tibet and Ladakh (India) resulted in the definition of eleven microfacies types characterizing the passive continental margin of India (prefixed with P) and four microfacies types characterizing the active continental margin of Asia (prefixed with A, Table 2.1). Generally, the sediments from the active continental margin have a considerably higher content in siliciclastic material compared to those from the passive continental margin which are dominated by carbonates with low terrigenous input. In the frame of our microfacial investigation (see Figs. 2.3 to 2.6 for detailed biostratigraphy) of Paleocene and Eocene shallow-water limestone, larger benthic foraminifera (LBF) act as sensitive proxy for paleoenvironmental reconstructions, comprising important information of ancient water depth (e.g., Hallock and Glenn, 1986; Hottinger, 1973, 1997; Beavington-Penney and Racey, 2004). Occurrences of microfacies within the sediments are described in respect to the shallow benthic zones (SBZ) taken from Zhang et al. (2013) for Tingri and Gamba, from Kahsnitz et al. (2016) for Guru, from Mathur et al. (2009) for western Zanskar and from Hu et al. (2016) for Cuojiangding.

	Xigaze forearc basin	Tethys Himalaya			
MF-Type	Cuojiangding	Ladakh	Tingri	Gamba	Guru
A1	x				
A2	x				
A3	x				
A4	x				
P1		x	x	x	x
P2		x	x	x	x
P3		x	x	x	x
P4			x	x	x
P5			x		
P6		x	x	x	x
P7			x	x	x
P8		x	x		
P9					x
P10		x			
P11		x			

Table 2.1: Distribution of microfacies types (MF) in relation to the investigated areas of the Xigaze forearc basin and the Tethyan Himalaya. According their deposition within the eastern Neo-Tethyan Ocean the microfacies are prefixed with A for active continental margin of Asia (Xigaze forearc basin) and P for passice continental margin of India (Tethyan Himalaya).

2.6.1 The passive continental margin

Microfacies P1: Green algae Pack-/Grainstone with miliolids

Description: Characterized by a pack- to grainstone fabric with abundant occurrence of green algae *Halimeda* (Family Halimedaceae) and *Ovulites* (Family Udoteaceae) in Tingri and dasycladacean green algae in Gamba and Guru (Fig. 2.7a). In Ladakh, *Ovulites* and dasycladacean green algae are dominant. Small miliolid foraminifera, as well as gastropods and bivalves are common. First frequent occurrences of rotaliid foraminifera (e.g., *Lockhartia*, *Daviesina*, *Rotorbinella*) within the upper part of the microfacies. Further bioclasts are other benthic foraminifera, echinoderms, ostracods, scleractinian corals and sponges. Samples identified as packstone fabric are sometimes characterized by dolomite rhombs or microspar. Detrital quartz can be found sporadic, as well as ooids and pellets.

Occurrence: This microfacies forms the lowermost section part of the Lower Lingshet Limestone (upper part of SBZ4) in Ladakh and the Zongpu Formation of Tingri, Gamba and Guru (lower part of SBZ2).

Boundary and thickness: The transition with the overlying microfacies P2 is sharp in Ladakh, Tingri and Gamba and gradual with the overlying microfacies P9 in Guru, showing a thickness of ∼41 m, ∼108 m, ∼10 m and ∼50 m, respectively.

Depositional environment: The high amount of green algae indicates deposition within a shallow water environment with low energy. Especially, the udoteacean algae *Ovulites* is a good indicator for deposition in shallow lagoonal environments (Ghose, 1977; Wray, 1977). Therefore the depositional environment is regarded as a restricted shallow subtidal environment comparable to a lagoon or the restricted part of an inner carbonate ramp.

Microfacies P2: Bioclast grainstone

Description: Characterized by a grainstone fabric with dominant occurrence of Rotaliidae LBF, especially *Lockhartia*, *Daviesina* and *Rotorbinella* (Fig. 2.7b). Miliolids and echinoids with syntaxial rims are also common organisms. Red algae also characterizes this microfacies, while green algae occur frequently. Lithoclasts and fecal pellets are primary allochems of the microfacies.

Occurrence: Paleocene of the Lower Lingshet Limestone of Ladakh (lower part of SBZ5) and Zongpu Formation of Tingri (SBZ2), Gamba (upper part of SBZ2) and Guru (SBZ3).

Figure 2.7 ***(following page)*:** Microfacies types characteristic of the passive (P) Indian continental margin. **A** Microfacies P1: Green algae Pack-/Grainstone with miliolids (sample 09Z46). **B** Microfacies P2: Bioclast grainstone (sample ZP16). **C** Microfacies P3: Rotaliidae Pack-/Grainstone (sample 09ZS171). **D-E** Microfacies P4: Miscellaneidae-Rotaliidae-Nummulitidae Pack-/Grainstone (samples GUR-UP05 and 09ZS263). **F-G** Microfacies P5: Laminated and bioturbated Mud- and Grainstone (samples 09ZS264 and 09ZS265). **H** Microfacies P6: *Alveolina* Wacke-/Packstone with Soritidae (sample GUR-LE07). Abbreviations: Al - *Alveolina*, Ha - *Halimeda*, Ka - *Kathina*, Li - Lithoklast, Lo - *Lockhartia*, Mi - *Miscellanea*, Ml - miliolid foraminifera, Or - *Orbitolites*, Os - *Orbitosiphon*, Ov - *Ovulites*, Pl - *Plumokathina*, Ra - *Ranikothalia*.

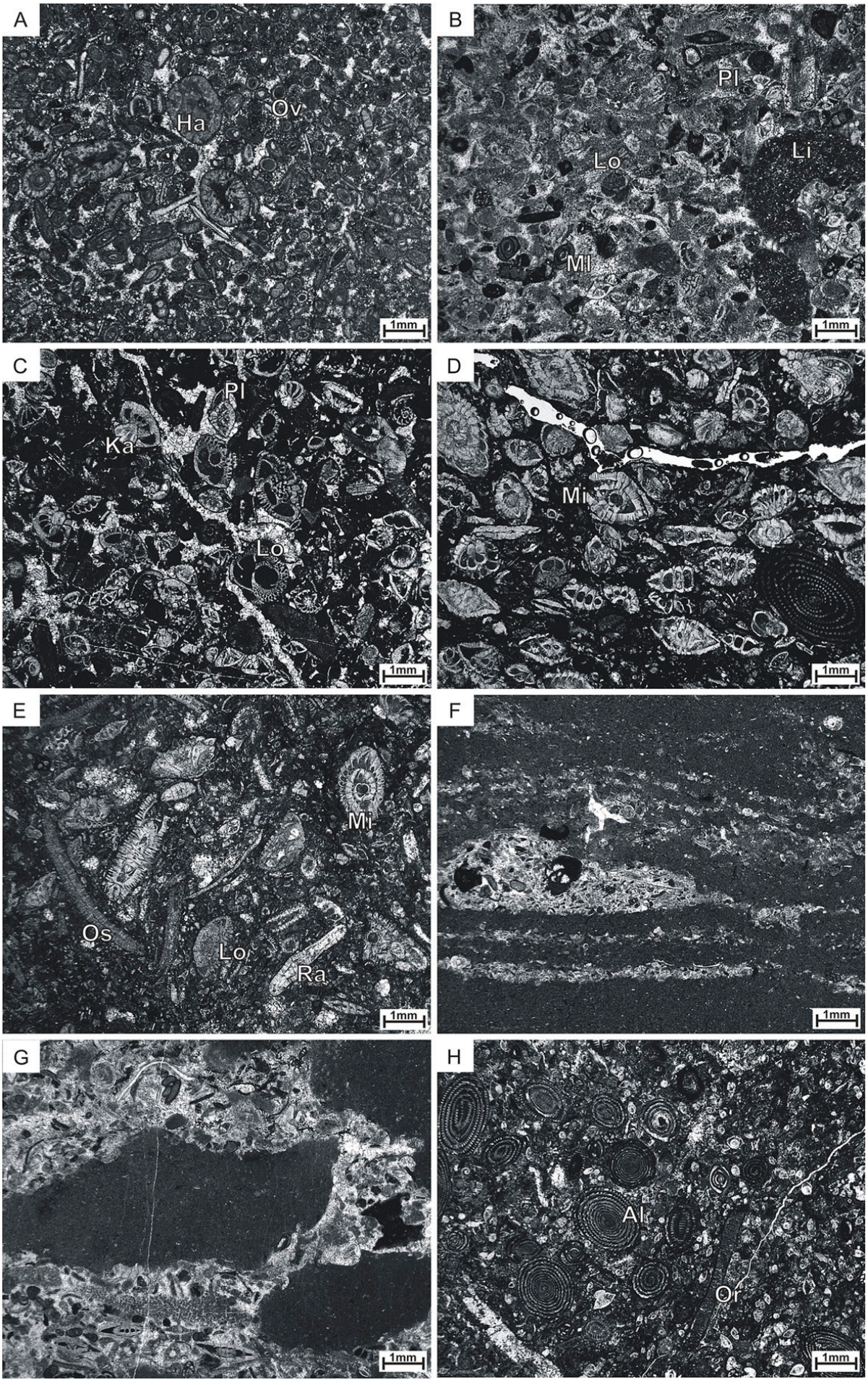
A
Ha
Ov
1mm
B
Pl
Lo
Li
Ml
1mm
C
Pl
Ka
Lo
1mm
D
Mi
1mm
E
Mi
Os
Lo
Ra
1mm
F
1mm
G
1mm
H
Al
Or
1mm

Boundary and thickness: The transition towards the underlying microfacies P1 at Zanskar, Tingri and Gamba is sharp, while the contact towards the overlying microfacies P3 is gradual. In Guru the transition to the underlying microfacies P1 and the overlying microfacies P9 is gradual. Thickness of P2 varies between ∼10 m in Ladakh, ∼12 m in Tingri, ∼36 m in Gamba and ∼20 m in Guru.

Depositional environment: This microfacies is described by Li et al. (2015) for the Zongpu Formation in Gamba and interpreted as deposited in shallow but open environments adjacent to shoal bars. Therefore we assume depositional environment on the inner carbonate ramp near shoal bars with very shallow water depths.

Microfacies P3: Rotaliidae Packstone

Description: Packstone samples of this microfacies comprise a dominant occurrence of Rotaliidae foraminifera, in particular *Lockhartia*, *Daviesina*, *Rotorbinella* (Fig. 2.7c). Further LBF are *Keramosphaerinopsis* and *Aberisphaera*, occasionally also *Fallotella* (Tingri and Ladakh). *Miscellanea*, *Ranikothalia*, *Setia* and *Orbitosiphon* appear frequently. At Tingri, green algae *Halimeda* (Family Halimedaceae) and *Ovulites* (Family Udoteaceae) are common, in Gamba dasycladacean green algae prevail. Small benthic as well as small miliolid foraminifera, red algae, ostracods, bivalves, gastropods, echinoids and corals appear rarely. Dolomite rhombs, microspar and terrigenous quartz are frequent. Additionally, fecal pellets may be part of the components.

Occurrence: Paleocene of the Lower Lingshet Limestone of Ladakh (upper part of SBZ5) and Zongpu Formation of Tingri (upper part of SBZ2 to SBZ4), Gamba (upper SBZ2 to SBZ4) and Guru (SBZ4).

Boundary and thickness: The transition towards the underlying microfacies P2 occurs gradually in Zanskar, Tingri and Gamba. At Guru, between microfacies P1, P2 and P3, intercalations of P9 can be recognized, showing gradual boundaries between the different microfacies. At Tingri, Gamba and Guru the transition towards the overlying microfacies P4 is gradual, while in Zanskar the transition to the overlying microfacies P10 is pronounced. The thickness of P3 varies between ∼20 m in Zanskar, ∼135 m in Tingri, ∼120 m in Gamba and ∼32 m in Guru.

Depositional environment: The dominant occurrence of rotaliids *Lockhartia* and *Daviesina* is characteristic for shallow subtidal environments with higher water agitation (Reiss and Hottinger, 1984; Hottinger, 1997). The occurrence of green algae is indicative for a good light penetration (Zhicheng et al., 1997). Therefore depositional environment is interpreted as open marine environment of the inner carbonate ramp.

Microfacies P4: Miscellaneidae-Rotaliidae-Nummulitidae Pack-/Grainstone

Description: The pack- and grainstone fabric is dominated by LBF Miscellanea, as well as Rotaliidae (e.g. *Daviesina*, *Lockhartia*, *Kathina*) and Nummulitidae (e.g., *Operculina*, *Ranikothalia*) foraminifera (Figs. 2.7d, 2.7e). Dasycladacean green algae and *Ovulites*, small miliolid foraminifera, echinoids, corals, and sponges are less frequent. Foraminifera *Orbitolites* and *Alveolina* act as accessory organisms. The matrix is micritic to microsparitic, sometimes selectively dolomitic. Terrigenous quartz as well as pellets are accessory particles.

Occurrence: Paleocene Zongpu Formation of Tingri, Gamba and Guru (SBZ5).

Boundary and thickness: The transition towards the underlying microfacies P3 at Tingri, Gamba and Guru is gradual. The contact to the overlying microfacies P6 at Tingri and Gamba is pronounced, while the transition into the overlying P9 in Guru is gradual. At Tingri, this microfacies is intercalated with pronounced boundaries by microfacies P5 and at Guru by microfacies P9 with gradual contacts. The thickness varies from ∼50 m at Tingri, ∼158 m at Gamba and ∼110 m at Guru.

Depositional environment: High amounts of well-preserved and abundant rotaliid and nummulitid foraminifera are indicative for open marine deposition. Additionally, the association of the LBF *Ranikothalia* with *Operculina* is described as indicative for low-energy environments with water depth ranging from 60 to 90 m (Hottinger, 1973; Reiss and Hottinger, 1984; Hottinger, 1997; Beavington-Penney and Racey, 2004). Therefore this microfacies is assumed to represent deposition on a mid-carbonate ramp.

Microfacies P5: Laminated and bioturbated Mud- and Grainstone

Description: Samples showing mud- and grainstone fabric arranged in a millimeter thick laminated (Fig. 2.7f) or strongly bioturbated way (Fig. 2.7g). Grainstone-type sediments are characterized by the occurrence of rotaliid (e.g. *Lockhartia*, *Daviesina*) and nummulitid (e.g. *Operculina*, *Ranikothalia*) LBF, as well as LBF *Orbitolites* and small miliolid foraminifera. Less frequent are dasycladacean algae, ostracods and sponges. The occurrence of a micritic matrix and the lack of fossils characterize those sediments described as mudstone-type.

Occurrence: Upper Paleocene Zongpu Formation (SBZ5) of Tingri.

Boundary and thickness: With a thickness of ∼10 m, the boundary to the underlying as well as the overlying microfacies P4, is pronounced.

Depositional environment: Described facies in sediment described as grainstone is similar to the associated organisms of microfacies P4 representative for a deposition on a mid-carbonate ramp. A similar microfacies is described from Spain (Bádenas and Aurell, 2010) suggesting deposition between the distal (low-energy) and proximal (high-energy) environment, where alternation of episodic storm-flows and accumulation of lime mud in quiet periods resulted in the formation of laminated mud- and grainstones. During quiet periods and the sedimentation of mud sediments bioturbation led to the noticed mixture of both sediment types.

Microfacies P6: *Alveolina* Wacke-/Packstone with Soritidae

Description: Wacke- and packstone fabrics, dominated and characterized by the abundant occurrence of *Alveolina* (Figs. 2.7h, 2.8a). At Tingri, Gamba and Guru Orbitolites occur as well, while at Ladakh the LBF *Opertorbitolites* are found. Small miliolid foraminifera and *Lenticulina* foraminifera are common in the upper part of the microfacies. In addition, small amounts of the rotaliid LBF *Lockhartia*, as well as ostracods, echinoids and fecal pellets occur. The matrix is frequently formed by microspar. Porcellaneous tests of *Alveolina* and miliolids often show a cloudy and indistinct appearance interpreted as ”the diffusely microsparitic preservation” of the porcellaneous foraminifera (Willems, 1993, p. 75) evident for the influence of freshwater diagenesis (Inden and Moore, 1983) within the Lower Eocene.

Occurrence: Lower Eocene of the Upper Lingshet Limestone of Ladakh (SBZ6), as well as the Zongpu Formation of Tingri (SBZ6 and lower part of SBZ7), Gamba (lower part of SBZ7) and Guru (SBZ7).

Boundary and thickness: The boundary with the underlying microfacies P5 at Tingri and Gamba and P9 at Guru is pronounced due to an outcrop gap. Demarcation with the overlying P7 at Tingri and Gamba is gradual. A distinct boundary exists to the underlying microfacies P10 and overlying P8, as well as the interfingering microfacies P11 at Ladakh. Thickness varies from ∼60 m at Ladakh, ∼30 m at Tingri, ∼20 m at Gamba to ∼15 m at Guru.

Depositional environment: The LBF *Alveolina* is described to live in an agitated environment with water depths down to about 60 m, while the LBF *Orbitolites* is indicative for restricted shallow environments (Hottinger, 1973; Reiss and Hottinger, 1984; Hottinger, 1997; Beavington-Penney and Racey, 2004). Therefore this microfacies is indicative for deposition in a restricted shallow water environment of the inner carbonate ramp with low-energy.

Microfacies P7: *Nummulites-Alveolina-Orbitolites* Pack-/Floatstone

Description: Pack- to floatstone fabrics are dominant, characterized by abundant occurrence of *Nummulites*, *Alveolina* and *Orbitolites* (Figs. 2.8b, 2.8c). Small miliolid foraminifera and *Lenticulina* are common. In small amounts the rotaliid LBF *Lockhartia*, as well as ostracods, echinoids, corals and sponges appear. Matrix is predominantly micritic.

Occurrence: Lower Eocene Zongpu Formation of Tingri (upper SBZ7 and SBZ8) and Gamba (upper part of SBZ7).

Boundary and thickness: With the underlying microfacies P6 the transition is gradual at Tingri and Gamba. With the overlying microfacies P7 in Tingri the transition is gradual as well. Thickness varies between ∼9 m in Gamba up to ∼48 m in Tingri.

Depositional environment: Thick-walled *Nummulites* accompanied by *Alveolina* and *Orbitolites* represent depositions in a mid-carbonate ramp environment with water depth ranging from 50 to 90 m (Reiss and Hottinger, 1984; Hottinger, 1997).

Microfacies P8: Discocyclinidae-Nummulitidae Pack-/Floatstone

Description: Pack- to floatstone fabrics which are characterized by abundant occurrence of the LBF *Discocyclina*, as well as by *Assilina* and *Nummulites* (Figs. 2.8d, 2.8e). Small miliolid foraminifera, bivalves, gastropods, echinoderms, corals and sponges are accessory components in the mainly micritic matrix.

Occurrence: Lower Eocene of the Upper Lingshet Limestone (SBZ6) and Zongpu Formation (SBZ9 and SBZ10) of Ladakh and Tingri.

Figure 2.8 ***(following page)*:** Microfacies types characteristic of the passive (P) Indian continental margin. **A** Microfacies P6: *Alveolina* Wacke-/Packstone with Soritidae (sample 11TM131). **B-C** Microfacies P7: *Nummulites-Alveolina-Orbitolites* Floatstone (samples 09ZS463 and 09ZS468). **D-E** Microfacies P8: Discocyclinidae-Nummulitidae Float-/Rudstone (samples 09ZS499 and 09ZS500). **F-G** Microfacies P9: Rodolith Wacke-/Packstone (samples GUR-LP47 and GUR-UP56). **H** Microfacies P10: Mudstone with anhydrite nodules (sample ZL35). Abbreviations: Al - *Alveolina*, Co - Corallinaceae, Di - *Discocyclina*, Gy - Gypsum, Nu - *Nummulites*, Or - *Orbitolites*, Py - Pyrite, Ra - *Ranikothalia*, Sc - Scleractinian coral.

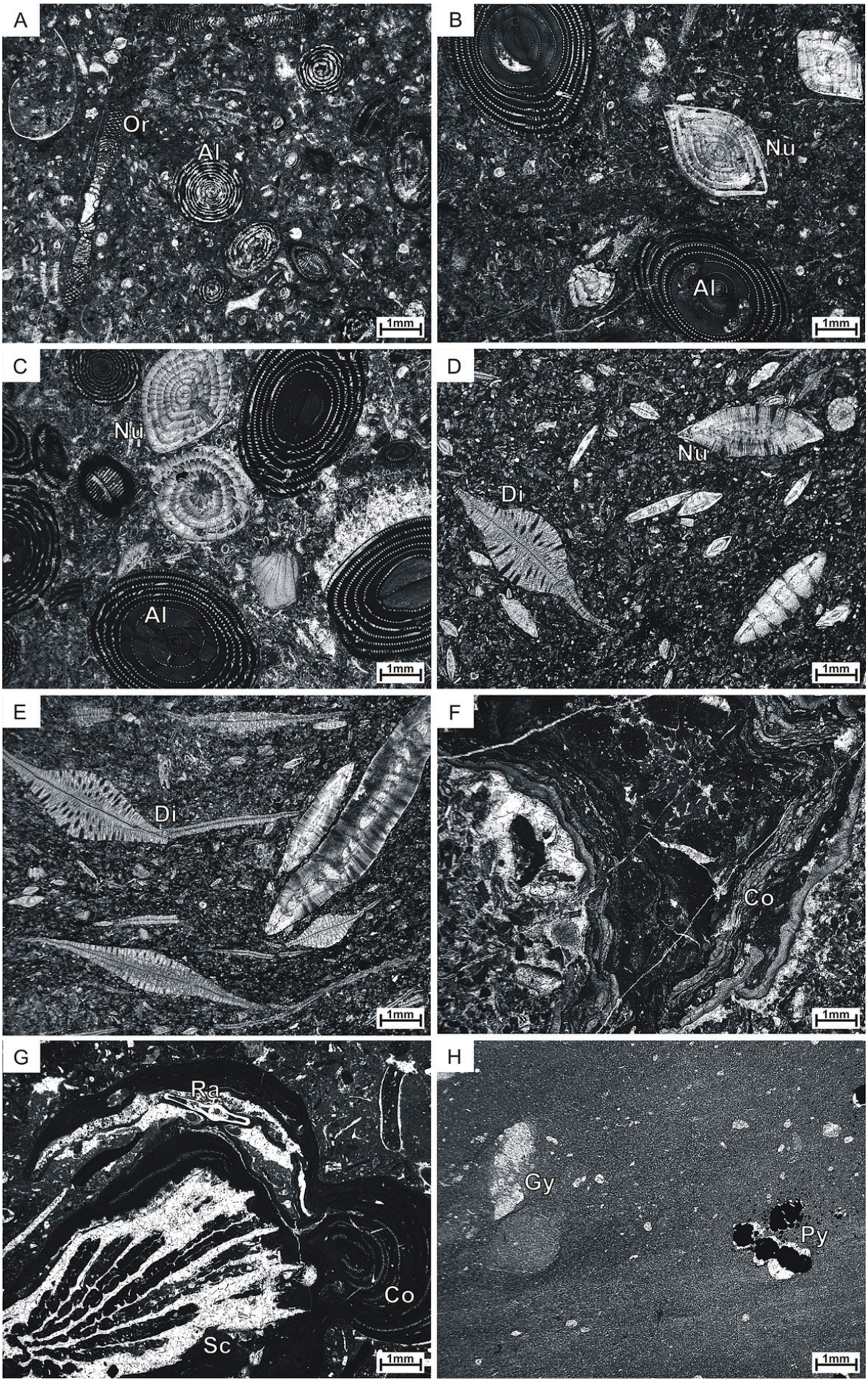
A
Or
Al
1mm
B
Nu
Al
1mm
C
Nu
Al
1mm
D
Nu
Di
1mm
E
Di
1mm
F
Co
1mm
G
Ra
Co
Sc
1mm
H
Gy
Py
1mm

Boundary and thickness: Boundaries with the underlying microfacies P6 and P7 in Ladakh and Tingri are gradual, exhibiting a comparable thickness of ∼9 m in Ladakh and ∼11 m in Tingri.

Depositional environment: Association of large and thin-walled *Nummulites* with similar shaped *Assilina* and *Discocyclina* represents environments with relatively deep water (Hottinger, 1997; Beavington-Penney and Racey, 2004). Therefore this microfacies represents a habitat within the lower photic zone of the outer carbonate ramp.

Microfacies P9: Rhodolith Wacke-/Packstone

Description: A characteristic feature is the high abundant occurrence of encrusting coralline red algae forming laminar rhodoids embedded in a wacke- to packstone fabric. Scleractinian corals and sponges often act as rhodoid nuclei (Figs. 2.8f, 2.8g). In most cases bivalves, gastropods and echinoids, as well as LBF like *Lockhartia*, *Ranikothalia* or *Miscellanea* occur frequently. Matrix is micritic to microsparitic.

Occurrence: Paleocene Zongpu Formation (boundary between SBZ2 and SBZ3, upper part of SBZ3 and upper part of SBZ5) of Guru.

Boundary and thickness: This microfacies appears as intercalations between microfacies P1, P2 and P3 and as intercalation within microfacies P4 in Guru, always exhibiting gradual transitions between the different facies. Thickness varies between ∼8 m and ∼17 m.

Depositional environment: In Tibet this type of microfacies is described to form rhodoids or small patch-reefs in shallow subtidal settings forming barriers between the open marine environment and the restricted lagoon of the inner carbonate ramp (Willems et al., 1996; Zhicheng et al., 1997).

Microfacies P10: Mudstone with anhydrite nodules

Description: The micritic, occasionally dolomitized matrix comprises no biota (Fig. 2.8h), except for some miliolid and agglutinating foraminifera. Scattered characteristic features are pyrite aggregates and especially anhydrite crystals.

Occurrence: At the Paleocene-Eocene boundary of the Spanboth Group and the Intermediate Layer between the Upper and the Lower Lingshet Limestone (boundary SBZ5 and SBZ6), both Ladakh.

Boundary and thickness: Distinct boundary with the underlying microfacies P2 and the overlying microfacies P6, showing a thickness of ∼19 m.

Depositional environment: Low biodiversity lime (dolo)mudstone, in combination with authigenic evaporite (here anhydrite) is representative for tidal flat environments or arid evaporitic coasts like sabkhas (Warren, 2006; Flügel, 2010). Authigenic pyrite documents the occurrence of organic material, replaced under reductive diagenetic conditions (Wilson, 1975; Flügel, 2010).

Microfacies P11: Planktonic foraminiferal Wackestone

Description: Characterized by planktonic foraminifera embedded in a micritic matrix producing a wackestone fabric (Fig. 2.9a). Further bioclasts like *Alveolina*, small benthic foraminifera, miliolid foraminifera, echinoderms and ostracods can be found frequently. Bivalves and gastropods are rare.

Occurrence: Lower Eocene part of the Upper Lingshet Limestone (SBZ6) of Ladakh.

Boundary and thickness: Distinct boundary to the underlying as well as overlying microfacies P5, showing a thickness of ∼10 m.

Depositional environment: Planktonic foraminifera within a micritic matrix indicate deposition in an open marine deep water environment of the outer carbonate ramp (Flügel, 2010).

2.6.2 The active continental margin

Microfacies A1: Molluskan Float-/Rudstone

Description: Fine-grained float- and rudstone with large-sized mollusks involving bivalves and gastropods with good shell preservation (Figs. 2.9b, 2.9c). LBF of the family Nummulitidae (*Ranikothalia*, *Nummulites* and *Assilina*), as well as some *Miscellanea* also occur frequently. Intraclasts are also common. Matrix is mostly micritic to microsparitic and characterized by the occurrence of poorly sorted, subangular to rounded detrital quartz grains.

Occurrence: Paleocene (upper SBZ3) and Lower Eocene (lower SBZ5) Jialazi Formation of Cuojiangding.

Boundary and thickness: Appears twice, once in the Upper Paleocene and once in the Lower Eocene, both showing a thickness of about 20 m. Microfacies A1 of Paleocene age shows sharp boundaries to the underlying sandstone layer as well as to the overlying microfacies A2. Lower Eocene microfacies A1 shows sharp contacts with the overlying and underlying sandstone layers.

Depositional environment: Dominant appearance of bivalve and gastropod shells, as well as the high amount of detrital quartz characterizes a very shallow tidal flat environment proximal to a terrestrial source area. This assumption is supported by other Cenozoic facies dominated by mollusks representing shallow and near-shore environments (e.g., Buxton and Pedley, 1989; Lukasik et al., 2000; Lukasik and James, 2006).

Microfacies A2: Nummulitidae Wacke-/Packstone

Description: Dominant appearance of *Ranikothalia* and some *Assilina* (Fig. 2.9d). Further foraminifera, such as *Daviesina*, *Lockhartia*, *Miscellanea* and *Discocyclina*, are less frequent. Additional bioclasts include small benthic foraminifera, fragments of coralline red algae, scleractinian corals, bivalves, gastropods and rare echinoderms. Sediment fabrics are dominated by wacke- and packstone. Matrix is mostly micritic to microsparitic with poorly sorted, subangular to rounded detrital quartz.

Occurrence: Paleocene (upper SBZ3 and lower SBZ4) Jialazi Formation of Cuojiangding.

Boundary and thickness: Thickness about 28 m with a sharp boundary to the underlying microfacies A1 and a transitional boundary to the overlying microfacies A3.

Figure 2.9 ***(following page)*****:** Microfacies types characteristic of the passive (P) Indian (Fig. a) and the active (A) Asian (Figs. b-h) continental margin. **A** Microfacies P11: Planktonic foraminiferal Wackestone (sample ZL18). **B-C** Microfacies A1: Molluskan Float-/Rudstone (samples 10TS282 and 10TS291). **D** Microfacies A2: Nummulitidae Wacke-/Packstone (sample 10TS241). **E-F** Microfacies A3: Rodolith Wacke-/Packstone (samples 10TS270 and 10TS270). **G-H** Microfacies A4: Discocyclinidae-Nummulitidae Float-/Rudstone (samples 10TS300 and 10TS331). Abbreviations: Bi - Bivalve, Co - Corallinaceae, Di - *Discocyclina*, Ga - Gastropod, Pf - Planktonic foraminifera, Py - Pyrite, Ra - *Ranikothalia*, Sp - Sponge.

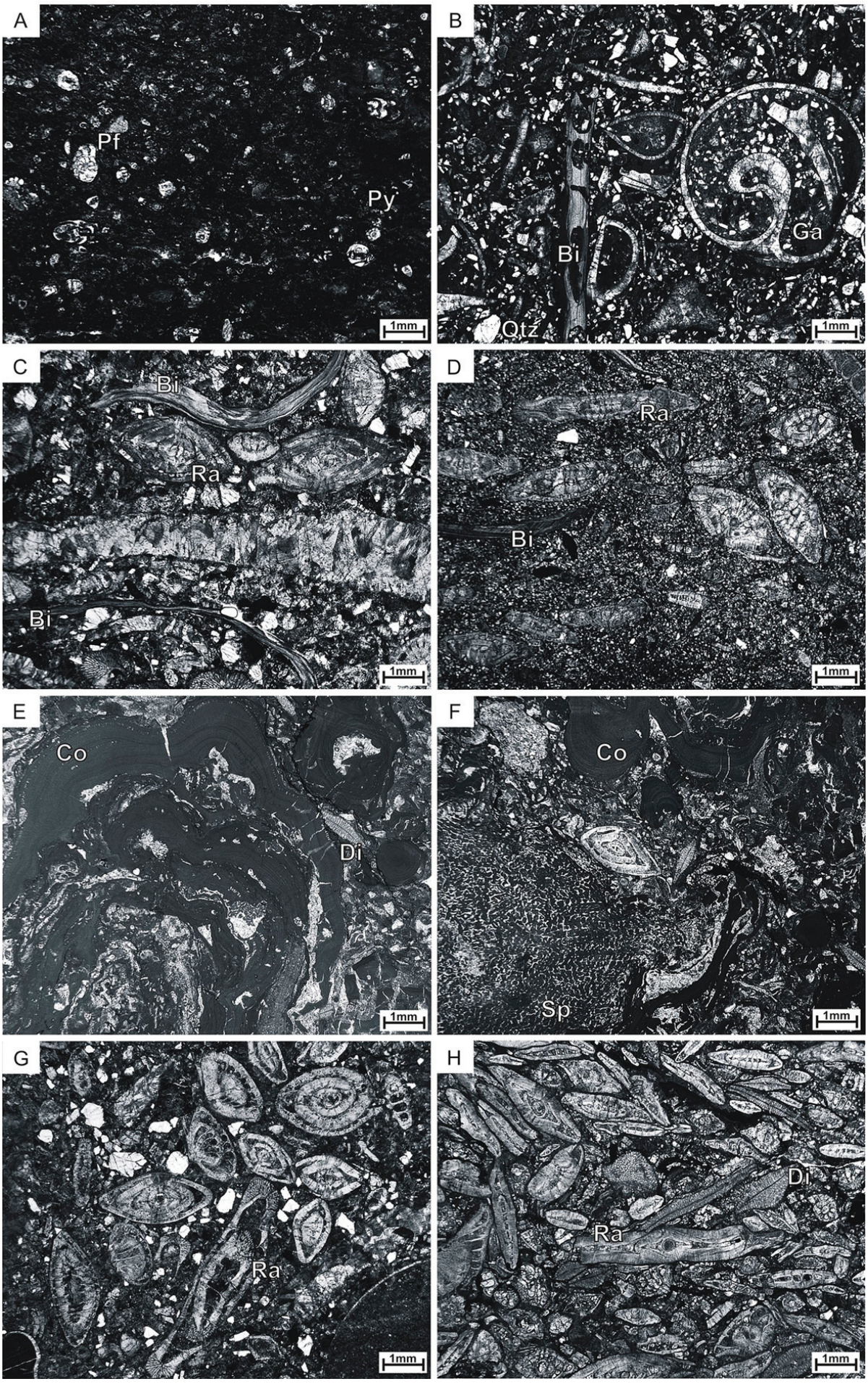
A
Pf
Py
1mm
B
Bi
Ga
Qtz
1mm
C
Bi
Ra
Bi
1mm
D
Ra
Bi
1mm
E
Co
Di
1mm
F
Co
Sp
1mm
G
Ra
1mm
H
Di
Ra
1mm

Depositional environment: The dominant appearance of nummulitid LBF, especially the association of *Ranikothalia* and *Operculina*, indicates deposition in a low-energy and open marine environment with water depth ranging from 60 to 90 m (Hottinger, 1973; Reiss and Hottinger, 1984; Hottinger, 1997; Beavington-Penney and Racey, 2004). Therefore we assume deposition below fair-weather-wave base of the Xigaze forearc basin. High amount of detrital quartz show deposition proximal to a terrestrial source area, placed on the Lhasa Block.

Microfacies A3: Rodolith Wacke-/Packstone

Description: High abundance of encrusting corralinacean red algae corals forming laminar rhodoids embedded in a wacke- to packstone fabric. Scleractinian corals and sponges often act as rhodoid nuclei (Figs. 2.9e, 2.9f). LBF like *Ranikothalia*, *Nummulites*, *Assilina*, *Miscellanea* and *Discocyclina*, as well as small benthic foraminifera and bivalves can be found frequently. Detrital quartz appears sporadically.

Occurrence: Paleocene (lower SBZ4) Jialazi Formation of Cuojiangding.

Boundary and thickness: Thickness of ∼9 m with a transitional boundary to the underlying microfacies A2 and a distinct boundary to the overlying sandstone layer.

Depositional environment: As described in microfacies P9, this microfacies is described to form rhodoids or small patch-reefs in shallow subtidal settings. Therefore it is assumed to form barriers between the open marine environment and the restricted lagoon of the inner carbonate ramp on the Indian passive continental margin (Willems et al., 1996; Zhicheng et al., 1997). For the Asian active continental margin we assume that the associated organisms form rhodoids or patch-reefs in a depositional environment above the fair-weather wave base within the Xigaze forearc basin.

Microfacies A4: Discocyclinidae-Nummulitidae Float-/Rudstone

Description: Common nummulitid LBF (*Ranikothalia*, *Nummulites*, *Assilina* and *Operculina*), as well as *Discocyclina* are the dominant biota (Figs. 2.9g, 2.9h) of these float- and rudstone. Further bioclasts are represented by *Miscellanea*, small benthic foraminifera, coralline red algae and sponges. Gastropods and echinoids are very rare. Matrix is predominantly micritic, sometimes microsparitic. Frequent occurrences of detrital quartz can be recognized.

Occurrence: Lower Eocene (SBZ5) of the Cuojiangding Formation.

Boundary and thickness: With a thickness of ∼65 m the facies exhibits a pronounced boundary with the underlying and overlying sandstone layer.

Depositional environment: Thin-walled *Assilina* and *Nummulites* are to be supposed representative of for depositional environments of the outer carbonate ramp with water depth ranging between 80 to 120 m (Hottinger, 1997). Therefore we assume a deposition below storm-wave base of the Xigaze forearc basin proximal to a terrestrial source area. Detrital quartz in this microfacies is possibly incorporated by aeolian transport or due to the erosion of the underlying sandstone layer.

2.7 Sedimentary model and regional correlation

Analysis and regional correlation of microfacies from stratigraphic sections of the passive Indian and active Asian continental margin were carried out to reconstruct the sedimentary and paleoenvironmental evolution of the eastern Neo-Tethyan Ocean and to demonstrate similarities and differences in the sedimentary history of both areas.

2.7.1 Sedimentary history of the passive continental margin

In literature the Cretaceous to Early Tertiary sedimentary evolution of the Indian passive continental margin is described as largely consistent, with strong similarities between the Chulung Chu area (Ladakh) and the studied sections in South Tibet (Gaetani et al., 1980; Fuchs and Willems, 1990; Zhang et al., 2012).

In the Tethyan Himalaya, the stratigraphically lowermost part of the Paleogene sequence is characterized by the occurrence of massive sandstone, the Stumpata Quartzarenite in Zanskar, and the Jidula Formation in south Tibet, representing marine shoreface sandstones. At Tingri, Gamba, Guru and Chulung Chu this sandstone is followed by Paleocene to Lower Eocene limestone beds (Lingshet Limestone, Zongpu Formation) and Lower Eocene marl and mudstone in some sections (Kong Slates, Enba Formation), indicating the final stage of marine sedimentary history.

At Gamba, a detailed microfacies analysis has been carried out by Li et al. (2015), showing two deepening-upward sequences separated by a disconformity. This transgressive trend evolves from shallow-water environments of inner parts of an open marine carbonate ramp to sediments deposited in a distal outer environment. This sedimentary tendency can be recognized all over the entire Tethyan Himalaya from Ladakh (Nicora et al., 1987) to Tingri and Gamba (Zhang et al., 2012).

Our investigations exhibit strong similarities in the stratigraphic succession of microfacies from the Tethyan Himalaya (Fig. 2.10), ranging from algal-dominated (P1, P2) to microfacies controlled by Rotaliidae and/or Nummulitidae LBF (P3, P4) and up to *Alveolina*-Soritidae and Nummulitidae dominated microfacies (P5, P6), showing an overall deepening process during Paleocene to Lower Eocene. Here, a first deepening event from Middle Paleocene to the end of Paleocene (microfacies P4 in Tingri, Gamba and Guru), can be recognized, followed by a shallowing event associated with uplift at or after the Paleocene-Eocene boundary (microfacies P6 in Ladakh, Tingri, Gamba and Guru) and a new transgression in the Early Eocene (microfacies P8 in Ladakh, Microfacies P7 in Tingri and Gamba). This two-stepped deepening event with a shallowing process at the Paleocene-Eocene boundary can be proved in nearly all sections of the Tethyan Himalaya (Fig. 2.10). At Ladakh the first deepening event from Middle Paleocene to the end of Paleocene is not well documented due to the occurrence of microfacies representing depositional environment only on the inner carbonate ramp. At Guru the second deepening event in the Early Eocene is not documented. At Tingri and Gamba, the shallowing tendency at the Paleocene-Eocene boundary, documented by distribution patterns of larger benthic foraminifera, is supposed to indicate a sedimentary environment of a forebulge (Zhang et al., 2012; Li et al., 2017).

At Tingri (Enba Formation) and Zanskar (Kong Formation) the Lower Eocene is characterized by the occurrence of Discocyclinidae and Nummulitidae, representing an outer ramp environment, shortly before the

end of the marine sedimentary history. This pronounced and rapid deepening period is supposed to indicate the transition from a forebulge to a foredeep environment as reported by Hu et al. (2012) and Zhang et al. (2012).

Besides strong similarities in the sedimentary history of the passive continental margin, some differences were observed as well. In literature, the area of Gamba is described as being located closer to the orogenic belt of the Asian continent, showing a shallower depositional environment at the Paleocene-Eocene boundary compared to Tingri and thus underwent earlier flexural subsidence due to the onset of the India-Asia continent-continent collision (Zhang et al., 2012). Those observations can also be expected for the area of Guru. Our analyzes show, that stratigraphic successions of microfacies found at Tingri and Gamba can also be observed in the Zongpu Formation of the Langzhu Section near Guru. Nevertheless, analyzes indicate that the depositional environment of Guru is highly influenced by intercalations of sediments observed as rhodolith fabrics (Microfacies P9), representative for shallower-water conditions. Due to the more marginal position of Guru and the more proximal position to the Indian continent, the depositional environment is generally shallower compared to Tingri and Gamba, which caused that minor sea level changes stand out more clearly at Guru.

At Tingri, microfacies P4 (Miscellaneidae-Rotaliidae-Nummulitidae pack-/grainstone with green algae) is intercalated by facies P5 (Laminated and bioturbated mud- and grainstone) both of a mid-carbonate ramp realm, indicating an alternation of a storm-generated deposit (grainstone fabric) and a deposition under quiet conditions (mudstone fabric), which cannot be recognized at other study sections of the Tethyan Himalaya, indicating deeper depositional environments in some parts of the sedimentary history.

Compared to this, sediments of the Chulung Chu area of Zanskar exhibit some unique strata, carrying nodules of gypsum and anhydrite as well as pyrite crystals within a fine-grained micritic matrix (microfacies P10: Mudstone with anhydrite nodules), providing evidence of temporarily restricted depositional settings comparable to a sabkha environment (Gaetani et al., 1986) close to the Paleocene-Eocene boundary. A further sedimentary difference at Zanskar, compared to sediments from Tingri, Gamba and Guru, is the occurrence of microfacies P11 (Planktonic foraminifera wackestone) of Lower Eocene age showing a short term deepening event followed by a shallowing process (microfacies P6). Discrepancies in facies patterns along the passive continental margin are interpreted as a matter of distance from a source area, a gentle northward dipping of the shelf, or slight variations in water depth (Fuchs and Willems, 1990) due to varying positions on the carbonate ramp.

Figure 2.10 ***(following page)*****:** Stratigraphic distribution and regional correlation of the eleven defined microfacies in the four studied sections (Zanskar, Tingri, Gamba and Guru) from the passive continental margin of the eastern Neo-Tethyan Ocean showing strong similarities of microfacies distribution patterns. Microfacial studies indicate a two-stepped deepening event from Middle Paleocene to Early Eocene: first deepening event from Middle Paleocene to the end of Paleocene (microfacies P4 in Tingri, Gamba and Guru; orange arrow), a shallowing event associated with uplift at or after the Paleocene-Eocene boundary (microfacies P6 in Ladakh, Tingri, Gamba and Guru; green arrow) and a new transgression in the Early Eocene (microfacies P8 in Ladakh, microfacies P7 in Tingri and Gamba; brown arrow). Stratigraphic position of the Paleocene-Eocene boundary in the Chulung Chu area (Zanskar) is roughly constrained, based on isotope analysis (see Fig. 2.3), while the boundary in Tingri and Gamba are based on isotope and foraminiferal analysis given by Zhang et al. (2012, 2013) and adopted for Guru according to Kahsnitz et al. (2016). Shallow benthic zones (SBZ) taken from Zhang et al. (2013) for Tingri and Gamba, from Kahsnitz et al. (2016) for Guru and from Mathur et al. (2009) for Zanskar. See figure 2.11 for explanations of lithological symbols as well as colors for microfacies and arrows.

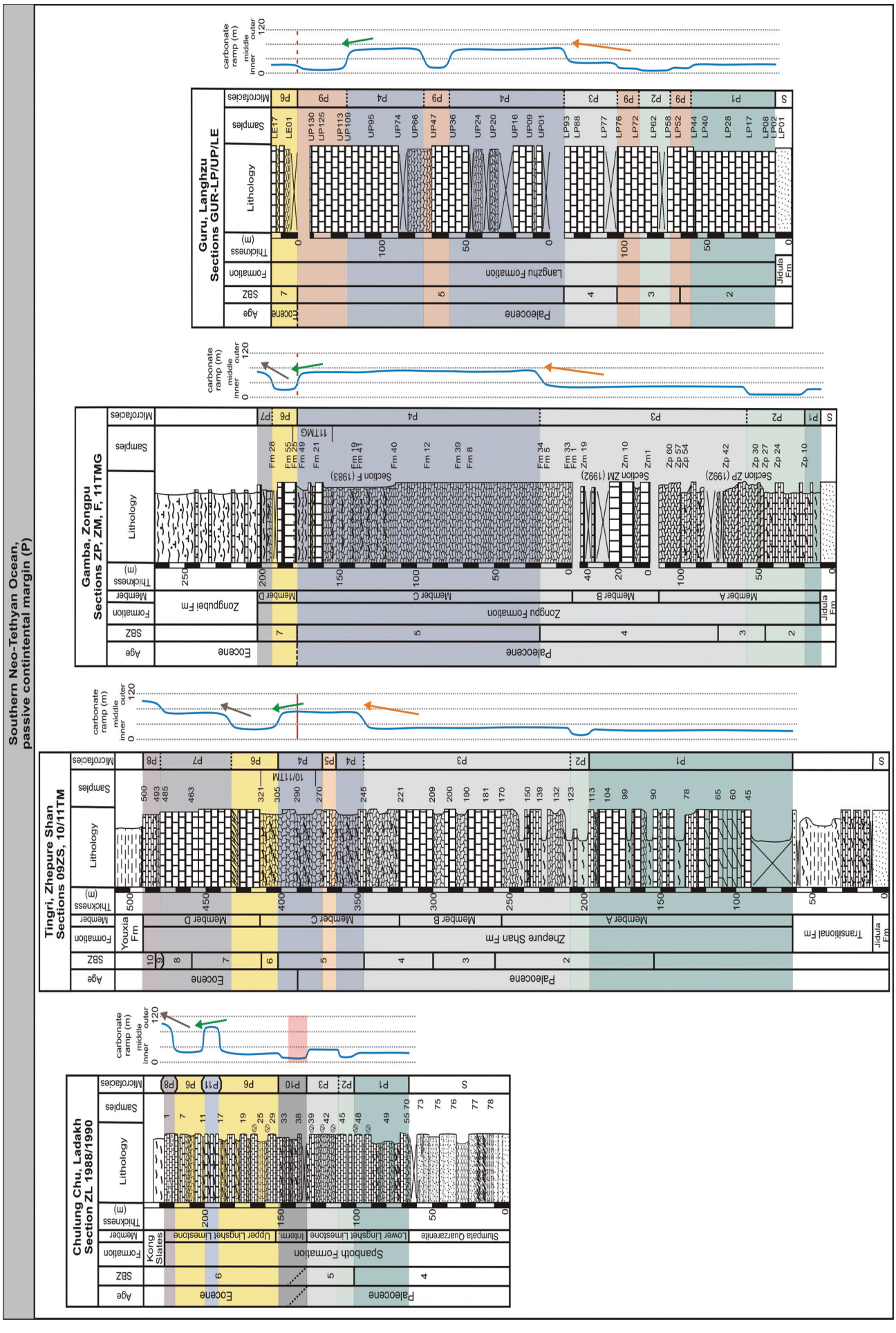
Southern Neo-Tethyan Ocean, passive continental margin (P)
Chulung Chu, Ladakh
Section ZL 1988/1990
Tingri, Zhepure Shan
Sections 09ZS, 10/11TM
Gamba, Zongpu
Sections ZP, ZM, F, 11TMG
Guru, Langhzu
Sections GUR-LP/UP/LE
Age
SBZ
Formation
Member
Thickness (m)
Lithology
Samples
Microfacies
Paleocene
Eocene
Sparboth Formation
Kong States
Stumpata Quarzarenite
Lower Lingshet Limestone
Interm.
Upper Lingshet Limestone
Zhepure Shan Fm
Youxia Fm
Member A
Member B
Member C
Member D
Transitional Fm
Zongpu Formation
Zongpubei Fm
Langzhu Formation
Jidula Fm
carbonate ramp (m)
inner
middle
outer

2.7.2 Sedimentary history of the active continental margin

Sediments in Cuojiangding of the Xigaze forearc basin are frequently intercalated by sandstone banks, characterized by mostly angular, poorly sorted, fine- to sand-sized detrital quartz. In literature, those sandstones are identified by the occurrence of andesitic and rhyolitic detritus derived from the volcanic arc (Gangdese arc) and therefore indicate a northern source area (Ding et al., 2005; Hu et al., 2016).

Lower Paleocene sediments of Cuojiangding show a stratigraphic succession of microfacies, ranging from a bivalve- and gastropod-dominated facies of the tidal flat (microfacies A1), to microfacies characterized by Nummulitidae LBF showing deposition below the fair-weather wave base (microfacies A2) and up to facies characterized by rhodolites in a wacke- to packstone fabric indicating deposition above the fair-weather wave base (microfacies A3). During Lower Eocene microfacies ranges from a bivalve- and gastropod-dominated (microfacies A1) to microfacies characterized by Nummulitidae (microfacies A4), showing a deepening base from a tidal flat of the forearc basin (microfacies A1) to deposition below the storm-wave base (Fig. 2.11).

2.7.3 Correlation of passive and active continental margin

In general, diversity of fossil assemblages is described as more diverse on the Indian Plate (BouDagher-Fadel et al., 2015). Our microfacial analyzes of sediments from Cuojiangding indicate similarities but also distinct differences from the sedimentary evolution of the Tethyan Himalaya.

During the Lower Paleocene, sediments of the passive continental margin of the Tethys Ocean are characterized by occurrence of a massive sandstone layer called Stumpata Quartzarenite, underlying the marine limestone in Zanskar and Jidula Formation in south Tibet. Even the lower Paleocene of the Xigaze forearc basin is characterized by sandstone and conglomerate layers, called Quxia Formation.

The first occurrence of green algae (microfacies P1) on top of the sandstone layers represents the beginning opening of the depositional environment in the Tethyan Himalaya from an lagoonal environment (microfacies P1) to open marine conditions during Lower/Middle Paleocene (microfacies P4). Compared to this, sediments of the active continental margin also show first marine sedimentation of tidal flat areas due to occurrence of gastropods and bivalves (microfacies A1).

From Lower to Upper Paleocene, sediments of the Tethyan Himalaya show a first deepening of the paleoenvironment (see Fig. 2.10, orange arrow) from a restricted lagoon of the inner carbonate (microfacies P1) ramp to the open marine environment of the inner carbonate ramp (microfacies P3) and the mid-carbonate ramp (microfacies 4). This first deepening event can also be recognized in sediments of the active continental margin (microfacies A1 to A2). Nevertheless, the dominant occurrence of detrital quartz and massive sandstone layers within the Jialazi Formation of Cuojiangding show, that sedimentation on the active continental margin is controlled by a high terrigenous material input, while on the passive continental margin a pelagic controlled sedimentation prevailed. The nearly similar microfacies P4 (Miscellaneidae-Rotaliidae-Nummulitidae pack-/grainstone) of the passive and microfacies A2 (Nummulitidae wacke-/packstone) of the active margin are represented by the high amount of LBF of the Family Nummulitidae (e.g., *Ranikothalia*). In Cuojiangding microfacies A2 is marked by minor occurrences of Rotaliidae (e.g., *Lockhartia*, *Daviesina*) as well as *Miscellanea*, while microfacies P4 of the Tethyan Himalaya is dominated by Rotaliidae solely.

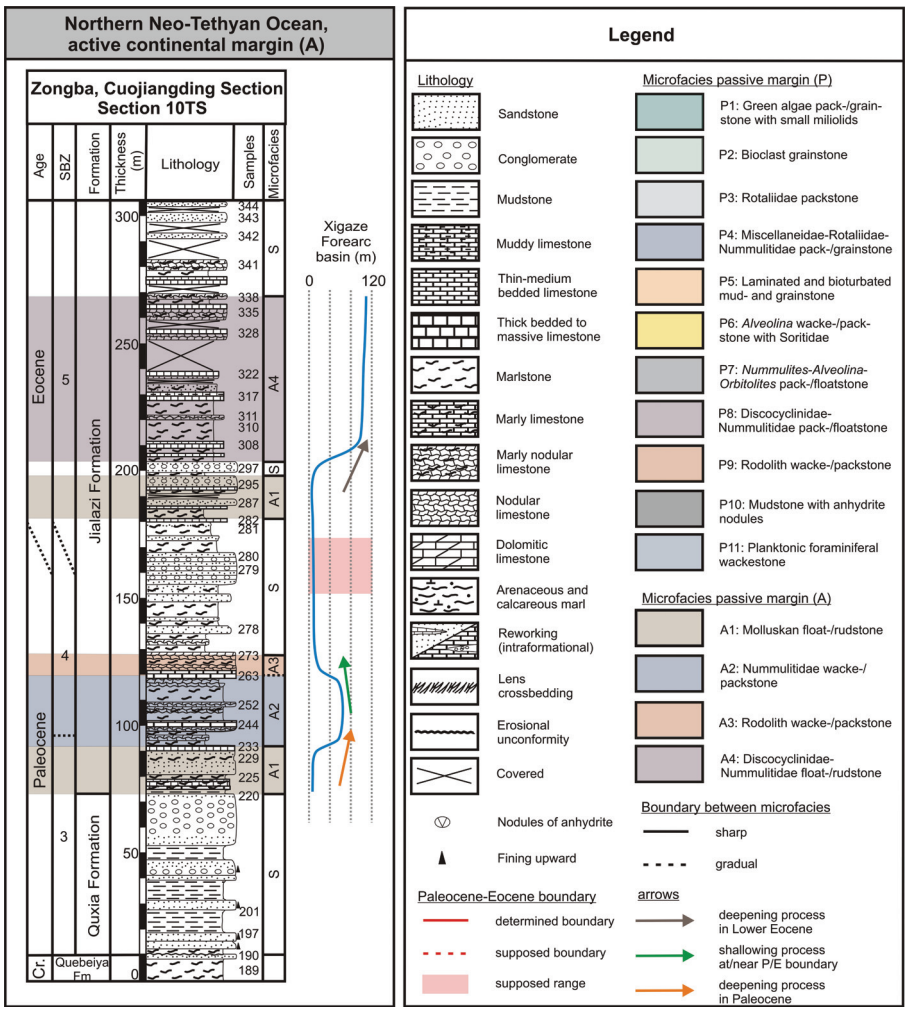

Figure 2.11: Stratigraphic distribution of the four defined microfacies in the studied section (Cuojiangding) from the active continental margin of the eastern Neo-Tethyan Ocean. The two-stepped deepening event recognized for sediments of the Tethyan Himalaya can also be observed in the section of the active continental margin: first deepening event in Middle Paleocene (microfacies A2; orange arrow), followed by a shallowing event (microfacies A3; green arrow) and a new transgression in the Early Eocene (microfacies A4; brown arrow). Stratigraphic position of the Paleocene-Eocene boundary is roughly constrained, based on isotope analysis (see Fig. 2.2). Shallow benthic zones (SBZ) are taken from Hu et al. (2016). Abbreviation: Cr - Cretaceous.

Additionally, the Paleocene sediments of Cuojiangding are characterized by the occurrence of *Discocyclina*, while within the Tethyan Himalaya the LBF *Orbitosiphon* and *Setia* appear. Green algae do not occur within Cuojiangding sediments, while they are representative for the sediments of the carbonate ramp of the passive continental margin of the eastern Neo-Tethyan Ocean. Those differences in microfacies possibly go along with differences in terrigenous input on the passive and active margin.

On the passive as well as the active continental margin a short-termed shallowing process occurred within the marine sediments (see Figs. 2.10 and 2.11, green arrow), interrupting the overall deepening process at or near the Paleocene-Eocene boundary, followed by a second overall deepening event showing water depths up to 120 m (see Figs. 2.10 and 2.11, brown arrow) within the Lower Eocene.

2.8 Conclusions

Lithostratigraphic and microfacial analyzes of sediments of the passive Indian continental margin (Tethyan Himalaya) and the active Asian continental margin (Xigaze forearc basin) reveal information on paleoenvironment and the geodynamic evolution of the eastern Neo-Tethyan Ocean:

1. All investigated stratigraphic sections exhibit the occurrence of a massive sandstone unit at the base, indicating strong terrigenous material input derived from the Indian continent in the Tethyan Himalaya (Chulung Chu, Tingri, Gamba and Guru) and from the Asian continent in the Xigaze forearc basin (Cuojiangding).
2. In the entire Tethyan Himalaya, a general trend from an algal-dominated facies (P1) at the base, to a facies dominated by Rotaliidae and/or Nummulitidae LBF (P3, P4), up to an *Alveolina*-Soritidae (and Nummulitidae) dominated facies (P6, P7) is evident, representing a general deepening tendency during Paleocene to Lower Eocene. This trend is observed on the active continental margin as well.
3. The overall deepening of the depositional setting of the carbonate ramp is interrupted by a short-term shallowing event at or close to the Paleocene-Eocene boundary, showing a two-stepped deepening lasting from Lower Paleocene to Lower Eocene. This happened at the passive as well as the active continental margin.
4. The shallowing upward event at the Paleocene-Eocene boundary is presumed to indicate a sedimentary environment of a forebulge, where porcellaneous foraminifera like *Alveolina* and miliolids are strongly influenced due to meteoric diagenesis.
5. Saline gypsum/anhydrite nodules and crystals are only observed at Zanskar, showing a temporarily and regionally restricted depositional setting of an inter- to supratidal environment close to the Paleocene-Eocene transition; comparable features cannot be recognized in other areas of the Tethyan Himalaya.
6. Sediments of Guru generally represent a shallower depositional environment compared to Tingri and Gamba, which is interpreted as the result of a more marginal position of the Guru area within the basin where minor changes in sea level stand out more distinctly.
7. Sediments of the active continental margin of Cuojiangding are influenced by a high terrigenous material input from the adjacent volcanic arc area of the Asian continent to the north, while the passive continental margin show a pelagic influenced sedimentation with only very low terrigenous input, resulting in distinct microfacial differences.

Acknowledgements

Dr. Qinghai Zhang, Christiane Schott, Elke Leipprand and Anne Hübner are thanked for their assistance in field and laboratory work. We want to thank Dr. Ines Wendler for constructive comments and critical discussions. Jenny Wendt and Dr. Henning Kuhnert (Center for Marine Environmental Sciences, MARUM, University of Bremen) are gratefully thanked for isotope measurements. Xiumian Hu (Nanjing University, China) and Edanjarlo Marquez (University of the Phillippines, Manila) are thanked for their critical remarks, which improved the paper. This project is supported by the Priority Program 1372 Tibetan Plateau: Formation - Climate - Ecosystem (TiP) and the Strategy Priority Research Program (B) of the Chinese Academy of Sciences (CAS, Grant No. XDB03010102) and is funded by the German Science Foundation (DFG Wi725/29) and the University of Bremen (Germany).

”Tibet, das Dach der Welt.
Es kommt mir vor,
als hätten wir eine mittelalterliche Felsenfestung erstürmt,
die sich im Herzen Asiens befindet.
Das ist das höchstgelegene Land der Erde.
Und das abgeschiedenste.”

7 Jahre in Tibet

3 Stratigraphic distribution of the larger benthic foraminifera *Lockhartia* in South Tibet (China)

Michaela M. Kahsnitz[1,3], **Qinghai Zhang**[1], **Helmut Willems**[1,2]

[1] Department of Geosciences, University of Bremen, 28359 Bremen, Germany

[2] Nanjing Institute of Geology and Palaeontology, Chinese Academy of Sciences, Nanjing 210008, China

[3] Correspondence author. Email: michaela.kahsnitz@uni-bremen.de

Journal of Foraminiferal Research (2016), 46:34-47

Received: 20th January 2015; Accepted: 1st May 2015

Abstract

This paper reveals the stratigraphic applicability of the larger benthic foraminifer (LBF) *Lockhartia* from the Paleocene to Lower Eocene of the eastern Neo-Tethyan Ocean outcropping in South Tibet. During the Paleocene, faunas of the western and eastern Neo-Tethys show distinct differences: The western area is dominated by coralgal assemblages, while in the east, LBF predominate the so-called "Lockhartia Sea". Shallow-water limestones of Tingri, Gamba and a completely new section close to the village of Guru in the eastern Neo-Tethyan Ocean reveal the stratigraphic ranges of seven species of *Lockhartia*: *L. conditi*, *L. haimei*, *L. hunti*, *L. praehaimei*, *L. retiata*, *L. roeae* and *L. tipperi*. Five interval biozones, called "*Lockhartia* biozones", are defined for the Paleocene to Lower Eocene based on the stratigraphic distribution of these species. The biozones are used to facilitate regional correlations of the three sections and to compare them with the well-established shallow benthic zones (SBZ) used for biostratigraphy of shallow-water environments. The stratigraphic distribution of *Lockhartia* suggests an earlier evolution of some species in the eastern Neo-Tethyan Ocean compared to the western region as a result of different latitudinal positions of the ocean basins.

3.1 Introduction

Larger benthic foraminifera (LBF) refer to a group of foraminifera with large test sizes and complicated internal structures. Biostratigraphic studies on Paleogene LBF such as *Alveolina* (Hottinger, 1960; Drobne, 1977), *Assilina* and *Nummulites* (Schaub, 1981), have been used to establish 20 shallow benthic zones (SBZ) in the western Neo-Tethyan Ocean (Serra-Kiel et al., 1998). However, LBF of the western and eastern Neo-Tethyan Ocean are described as similar but not identical (Hottinger, 1971). Within the Paleocene, the western Neo-Tethys is dominated by coralgal reefs (e.g., Accordi et al., 1998; Turnsek and Drobne, 1998; Baceta et al., 2005; Scheibner et al., 2007), while LBF predominate in the eastern Neo-Tethys Ocean (e.g., Wan et al., 2002, 2010; Afzal et al., 2011; Zhang et al., 2013). Based on the high diversity of the LBF genus *Lockhartia* in the Paleocene Ranikot Formation from India, the eastern Neo-Tethyan Ocean was also called "Ranikot Sea" (Davies, 1937) or "Lockhartia Sea" (Hottinger, 1998), covering an area ranging from South Turkey in the west to Tibet and Pakistan in the east, and to Somalia and Egypt in the south (Hottinger, 2007, 2014b). Another consequence of their high diversity is that *Lockhartia* occupy certain chronostratigraphic positions in the Paleocene, comparable to *Alveolina*, *Assilina* and *Nummulites* in the Eocene. For example, *L. retiata* Sander, 1962 and *L. praehaimei* Smout, 1954 are accepted as index species of SBZ3 (Hottinger, 2014a).

Paleocene and Lower Eocene shallow-water limestones cropping out in the proximity of Tingri, Gamba and Guru in South Tibet were deposited on the southern passive continental margin of the eastern Neo-Tethyan Ocean. Five interval biozones within the limestone sections of Tingri, Gamba and a new lithological section near the village of Guru are proposed, based on the stratigraphic distributions of *Lockhartia* spp., which increased in diversity during the Paleocene, peaking at the Paleocene-Eocene boundary, and then substantially decreasing within the Lower Eocene. Additionally, we document a generalized stratigraphic distribution pattern of *Lockhartia* for South Tibet and compare these data with the SBZ established by Zhang et al. (2013)

for Tingri and Gamba to transfer the local interval biozones to the eastern Neo-Tethys Ocean. Furthermore, we compare the stratigraphic distributions of some *Lockhartia* species through the entire Neo-Tethyan Ocean, which supports the early evolution of LBF within the eastern Neo-Tethyan Ocean (Scheibner and Speijer, 2008).

3.2 Geological setting and methods

For taxonomic studies of *Lockhartia*, samples were taken from Paleocene to Lower Eocene limestones of South Tibet (China). The sediments were deposited on a carbonate ramp at the northern passive margin of the Indian continent (Willems, 1993) within a shallow-marine environment of the eastern Neo-Tethyan Ocean close to the equator (Fig. 3.1a).

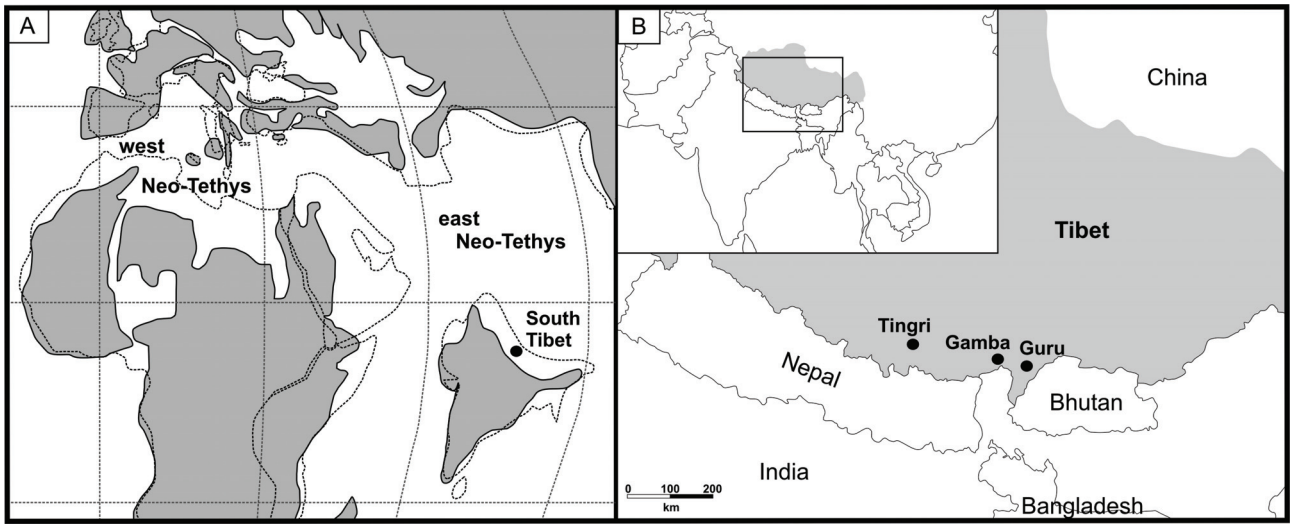

Figure 3.1: Position of the studied sections. **A** Paleogeographic position of South Tibet at the northern margin of the Indian continent within the eastern Neo-Tethyan Ocean during the Paleocene. Paleogeographic map is redrawn from Smith et al. (1994). **B** Location of the three study areas Tingri (28°41'N, 86°42'E), Gamba (28°17'N, 88°32'E) and Guru (28°06'N, 89°12'E) in Tibet (marked in grey).

In Tingri (Zhepure Shan Formation, 28°41'N, 86°42'E) and Gamba (Zongpu Formation, 28°17'N, 88°32'E), the limestones show a similar consecutive lithological sequence of four members from bottom to top (Zhang et al., 2013): cyclic limestones (Member A), massive limestones (Member B), nodular limestones (Member C) and massive limestones (Member D). The formations are overlying the Cretaceous and Lower Paleocene Jidula Sandstone Formation and underlying the green marls of the Youxia Formation in Tingri and the Zongpubei Formation in Gamba (Willems, 1993). Additionally, we introduce a new section from the Guru area. Here, the Langzhu Formation (28°06'N, 89°12'E), named after a mountain near the section, overlies the Jidula Formation as well. The Langzhu Formation mainly consists of massive and nodular limestones, but the generalized lithological successions of Tingri and Gamba (Zhang et al., 2013) are not fully developed.

Altogether 1076 samples, collected between 1983 and 2013, have been examined for the stratigraphic distribution of *Lockhartia* within the Zhepure Shan Formation of Tingri, the Zongpu Formation of Gamba, and the Langzhu Formation of Guru (Fig. 3.1b). The stratigraphic section in Tingri is more complete than those in Gamba and Guru. Samples and thin sections analyzed here are deposited in the Historical Geology/Palaeontology research group of the Department of Geosciences (University of Bremen). From the

Zhepure Shan Formation of Tingri, 420 m thick, 512 samples (Sections: 09ZS and 10/11TM) were studied. From the Zongpu Formation in Gamba, 350 m thick, we studied 324 samples (Sections: ZP, ZM, F and 11TMG). From the Langzhu Formation in Guru, ∼290 m thick, we studied 240 samples (Sections: GUR-LP, GUR-UP and GUR-LE). Taxonomic classifications are based on descriptions given by Nuttall (1926), Davies (1926, 1927, 1930), Ovey (1947), Smout (1954), Sander (1962) and Hottinger (2014a).

3.3 Stratigraphic distribution of *Lockhartia* in Tibet

In the Paleocene to Lower Eocene shallow-water limestones of Tingri, Gamba and Guru, seven species of *Lockhartia* are recognized: *L. conditi*, *L. haimei*, *L. hunti*, *L. praehaimei*, *L. retiata*, *L. roeae* and *L. tipperi*. Within the work of Zhang et al. (2013), *L. altispira* and *L. megapapulata* also are recorded in the sediments of South Tibet. The genus *Lockhartia* is described as "always low-trochospiral" (Hottinger, 2014a, p. 61), while the species described as *L. altispira* reported from South Tibet is characterized by a high-trochospiral shell, as found in *Sakesaria*. Furthermore, we assume that the reported *L. megapapulata* by Zhang et al. (2013) is a morphological variation of *L. haimei*.

Based on the stratigraphic distributions of the seven species of *Lockhartia*, five interval biozones have been established for the investigated sections in South Tibet (Fig. 3.2). The interval biozones are established by the first appearance datum (FAD) and last appearance datum (LAD) of species and are called '*Lockhartia* biozones' during further discussions.

Overlying the Jidula Sandstones and before the onset of *Lockhartia* biozone 1 in the Zhepure Shan Formation of Tingri, calcareous green algae and small miliolid foraminifera are abundant. In Gamba and Guru, *Lockhartia* biozone 1 directly overlies the Jidula Sandstones. The base of *Lockhartia* biozone 1 is defined by the FAD of *L. praehaimei* and *L. retiata*, while the boundary between biozones 1 and 2 is characterized by the FAD of *L. roeae*. *Lockhartia praehaimei* and *L. retiata* occur further up within this biozone. The FAD of *L. haimei* characterizes the boundary between biozones 2 and 3. In *Lockhartia* biozone 3, *L. haimei* dominates the assemblage and defines the base of the biozone. In Tingri and Gamba, *L. conditi* occurs at the base of biozone 3 as well, while in Guru, *L. conditi* shows its first occurrence higher in this zone. *Lockhartia roeae* shows a continuous occurrence within this biozone. The boundary between *Lockhartia* biozones 3 and 4 is defined by the FAD of *L. tipperi*. In Tingri and Gamba, *L. hunti* first appears within this biozone as well. *Lockhartia conditi*, *L. roeae* and *L. haimei* continue up section. Biozone 4 contains the highest diversity of *Lockhartia* species in South Tibet and is characterized by the occurrence of five species. The boundary between *Lockhartia* biozones 4 and 5 is defined by the sudden disappearance of most *Lockhartia* species. Only *L. hunti* and *L. tipperi* can be recognized within biozone 5, with lower abundance and smaller test sizes compared to the stratigraphically older biozones.

Figure 3.2 ***(following page)*:** Stratigraphic distribution of *Lockhartia* species detected in South Tibet. Paleocene-Eocene boundaries for Tingri and Gamba based on carbon isotope measurements and SBZ taken from Zhang et al. (2013). In some cases, SBZ are modified for Tingri (no SBZ1 and new position for SBZ2) and adopted for the Langzhu Formation of Guru. At Guru, the Paleocene-Eocene boundary is roughly constrained by the change from SBZ5 to SBZ7. Based on distribution patterns of seven *Lockhartia* species, five interval biozones could be established in South Tibet. Abbreviation: LBF = larger benthic foraminifera, PDB = Pee Dee Bee, SBZ = shallow benthic zone.

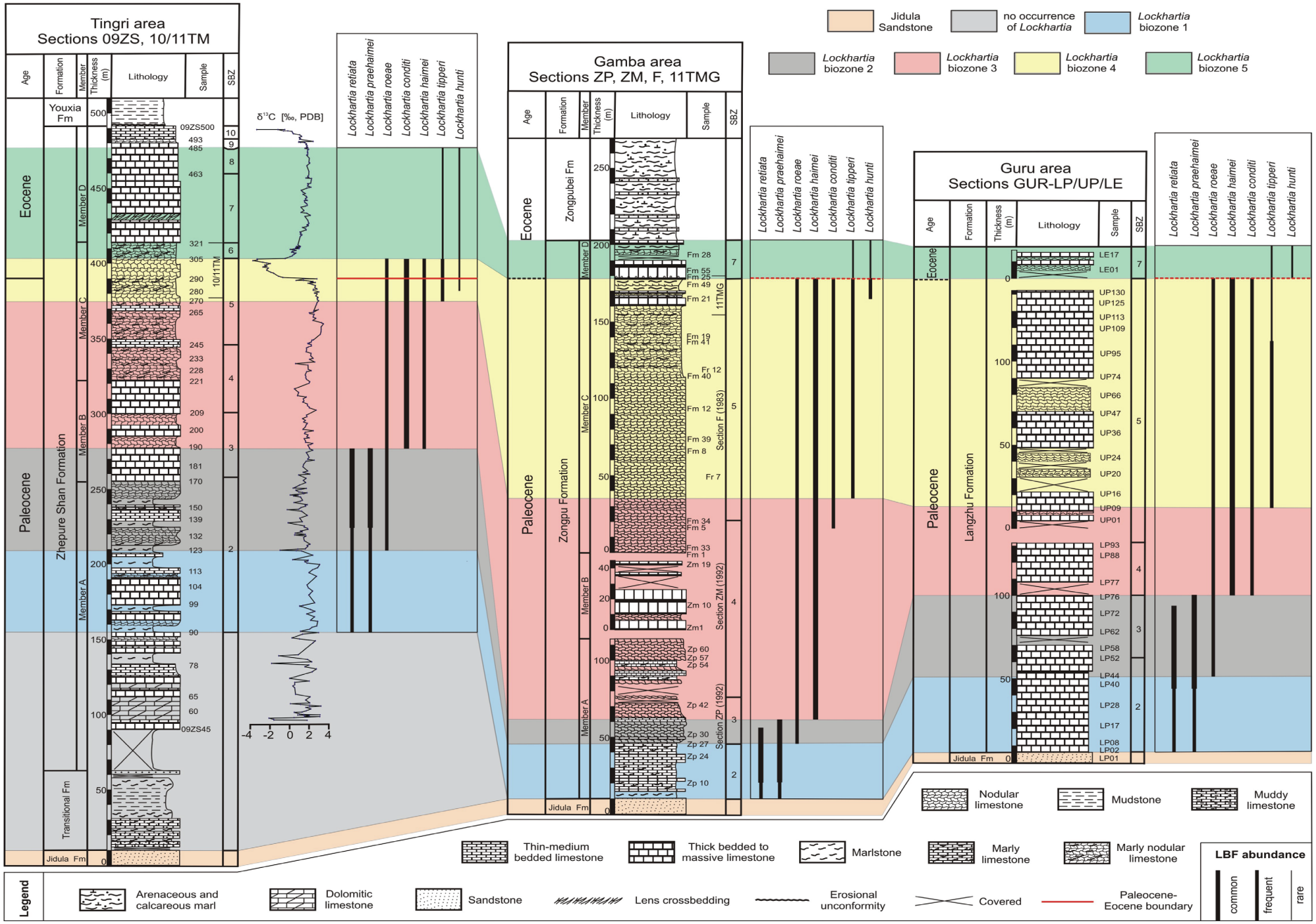
Tingri area
Sections 09ZS, 10/11TM
Gamba area
Sections ZP, ZM, F, 11TMG
Guru area
Sections GUR-LP/UP/LE
Jidula Sandstone
no occurrence of Lockhartia
Lockhartia biozone 1
Lockhartia biozone 2
Lockhartia biozone 3
Lockhartia biozone 4
Lockhartia biozone 5
Lockhartia retiata
Lockhartia praehaimei
Lockhartia roeae
Lockhartia conditi
Lockhartia haimei
Lockhartia tipperi
Lockhartia hunti
Eocene
Paleocene
Youxia Fm
Zhepure Shan Formation
Transitional Fm
Jidula Fm
Zongpubei Fm
Zongpu Formation
Langzhu Formation
Member A
Member B
Member C
Member D
δ13C [‰, PDB]
Section F (1983)
Section ZM (1992)
Section ZP (1992)
11TMG
10/11TM
Nodular limestone
Mudstone
Muddy limestone
Thin-medium bedded limestone
Thick bedded to massive limestone
Marlstone
Marly limestone
Marly nodular limestone
LBF abundance
common
frequent
rare
Legend
Arenaceous and calcareous marl
Dolomitic limestone
Sandstone
Lens crossbedding
Erosional unconformity
Covered
Paleocene-Eocene boundary

3.3.1 Regional correlation of *Lockhartia* biozones and shallow benthic zones

Shallow benthic zones (SBZ) defined for Tingri and Gamba (Zhang et al., 2013) are adopted for the Langzhu Formation of Guru (Fig. 3.2). Based on the stratigraphic distribution of rotaliid LBF (e.g., *Lockhartia*, *Daviesina*, *Rotorbinella*), in Tingri the beginning of SBZ2 is relocated earlier (sample 09ZS90) within the Zhepure Shan Formation, in comparison to the placement by Zhang et al. in 2013 (sample 09ZS113). Additionally, the extension of SBZ1 in Tingri is questionable because the lower section layers of the Zhepure Shan Formation lack LBF. Therefore it is not possible to exactly place the base of SBZ1 within the lower part of the Zhepure Shan Formation.

In Tingri, the Paleocene-Eocene boundary is clearly assigned by the beginning of the negative carbon isotope excursion described by Zhang et al. (2013). The change from the rotaliid LBF dominated assemblage of SBZ5 to the alveolinid LBF dominated assemblage of SBZ6 in Tingri is not coexistent with the Paleocene-Eocene boundary but postdates it. Instead *Lockhartia* biozone 4 includes the Paleocene-Eocene boundary. In comparison to Tingri, the Gamba section is not complete, as shown by the carbon isotopic curve in Zhang et al. (2012), as well as the absence of SBZ6, which indicates a sedimentary hiatus at the Paleocene-Eocene boundary (Zhang et al., 2013). In the Langzhu Formation of Guru, the generalized lithological succession (Member A to Member D), representative for Tingri and Gamba (Zhang et al., 2013), is not comparably developed. Additionally, the sedimentary sequence in Guru is stratigraphically not fully covered due to hiatuses within the formation. Thus the Paleocene-Eocene boundary in Guru is roughly constrained by the transition from SBZ5 to SBZ7. Accordingly, the boundary between *Lockhartia* biozone 4 and 5 seems to correlate with the P-E boundary at Gamba and Guru.

A regional distribution pattern of *Lockhartia* in South Tibet is provided by the correlation of the herein established biozones and the SBZ of Tingri, Gamba and Guru established by Zhang et al. in 2013 (Fig. 3.3). While the shallow benthic zones are based on the stratigraphic occurrence of LBF assemblages, the *Lockhartia* biozones established here are based upon the stratigraphic distribution (first and last occurrences) of species within the genus *Lockhartia* exclusively. The Lower Paleocene of South Tibet is characterized by the abundance of dasycladacean green algae, as well as the udoteacean green algae *Halimeda* and *Ovulites*. No LBF occur within the lower section, while *Lockhartia* biozone 1, correlating with the lower part of SBZ2, is revealed by the first occurrence of *L. praehaimei* and *L. retiata*. The dominance of calcareous green algae within the Lower Paleocene indicates protected or even restricted shallow-water environments of an inner carbonate ramp (Ghose, 1976; Wray, 1977).

Biozone 2 represents the upper part of SBZ2, as well as the lower part of SBZ3, marked by an increase in *L. praehaimei* and *L. retiata*, and the first occurrence of *L. roeae*. This biozone is characterized by the abundance of LBF of the family Rotaliidae (e.g., *Lockhartia*, *Daviesina*, *Rotorbinella*), as well as calcareous green algae, representing an open marine depositional environment of the inner carbonate ramp with water depths ∼40 m (Hottinger, 1997). *Lockhartia* biozone 3 is characterized by the FAD of *L. haimei* and *L. conditi*, coexisting with *L. roeae* of the previous biozone. Biozone 3 correlates with the upper part of SBZ3, as well as SBZ4 and the lower part of SBZ5. The correlation of *Lockhartia* biozone 3 with SBZ3 is still characterized by the dominance of rotaliid LBF (e.g., *Lockhartia*, *Daviesina*, *Rotorbinella*) and calcareous green algae. In correlation with SBZ4 and SBZ5, the *Lockhartia* biozone 3 furthermore shows abundant rotaliid LBF, accompanied by Nummulitidae (e.g., *Ranikothalia, Miscellanea*), representing deposition on a

mid-carbonate ramp with water depths between 40 and 80 m (Hottinger, 1997). Morphological similarities of the umbilical structure, as well as the early stratigraphic occurrence, led to the assumption that *L. praehaimei* is the predecessor of *L. haimei*.

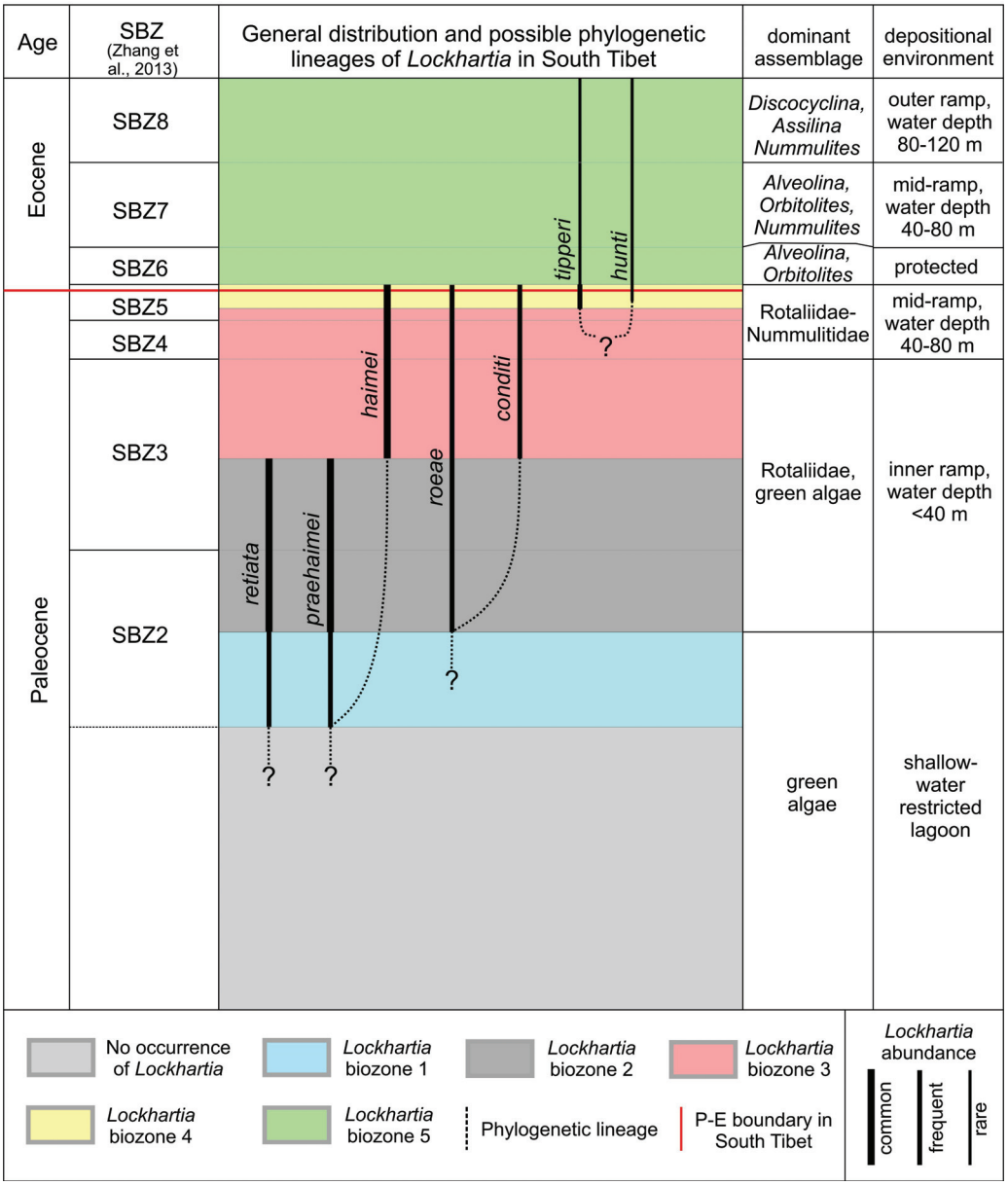

Figure 3.3: Generalized extend of *Lockhartia* biozones as defined in this paper compared with shallow benthic zones (SBZ) taken from Zhang et al. (2013) for South Tibet. For some species potential lineages are indicated. Dominant assemblages, as well as assumed depositional environment, are also indicated.

Hottinger (2014a) considered *L. roeae* to be the predecessor of *L. tipperi* based upon similarities in morphological features: chamber shape, high number of umbilical piles and small dyad embryos. In South Tibet, specimens of *L. roeae* show four to six piles within the umbilical area, while *L. tipperi* always show more than six piles. Also piles of *L. tipperi* are tall and thin, leaving big cavities between them and the foliar walls, while *L. roeae* show very thick piles leaving just a little space for the foliar walls. The umbilical structure of *L. roeae* bears more resemblance to the umbilical structure of *L. conditi*, leading to the assumption that either both have a common predecessor or one species emerged from the other.

Lockhartia biozone 4 correlates with the upper part of SBZ5 and is characterized by the first occurrence of *L. tipperi* and *L. hunti*, and their coexistence with *L. haimei*, *L. conditi* and *L. roeae*. At the same time, the assemblage of foraminifera in this biozone is dominated by rotaliid and nummulitid LBF (e.g., *Lockhartia*, *Ranikothalia*, *Miscellanea*), representing a depositional environment of a mid-carbonate ramp with water depths between 40 and 80 m (Hottinger, 1997). Because of the size, the high number and arrangement of piles and foliar walls within the umbilical area, we postulate that *L. hunti* and *L. tipperi* had a common predecessor or that one species emerged from the other. Hottinger considered *L. roeae* as the predecessor of *L. tipperi*, but at the same time he noted the difficulty in distinguishing between *L. hunti* and *L. tipperi* and describes some species of *Lockhartia* as "*Lockhartia* cf. *hunti* or young specimens of *L. tipperi*" (Hottinger, 2014a, p. 84, pl. 5.20, figs. 1-6). This statement supports the assumption that *L. hunti* and *L. tipperi* had a common predecessor.

Lockhartia biozone 5 correlates with SBZ6, SBZ7 and even with SBZ8, showing much fewer *L. tipperi* and *L. hunti*. The assemblage of foraminifera here is characterized by such LBF as: *Alveolina* and *Orbitolites* (e.g., *A. ellipsoidalis*, *A.* cf. *subtilis*, *A. agerensis*) within SBZ6; *Alveolina*, *Orbitolites* and *Nummulites* (e.g., *A. ellipsoidalis*, *A.* cf. *subtilis*, *A. mousoulensis*, *N.* cf. *subramondi*) within SBZ7; and *Discocyclina*, *Assilina* and *Nummulites* (e.g., *A. leymeriei*, *A. subspinosa*, *N. globolus*, *N.* cf. *subramondi*) in SBZ8 (Zhang et al., 2013). These taxa are characteristic of a shallow, protected environment of an inner carbonate ramp with water depths <40 m, as well as mid- to outer carbonate ramps with water depths between 40 to 80 m and 80 to 120 m, respectively (Hottinger, 1997).

3.4 Comparison of *Lockhartia* distributions in the western and eastern Neo-Tethyan Ocean

The distributions of the LBF assemblages of the western and eastern Neo-Tethyan Ocean are described as being similar, but not identical (Hottinger, 1971). Here, we compare the stratigraphic distributions of some *Lockhartia* species from the western and central Neo-Tethyan Ocean (Hottinger, 2014b), with those from Pakistan (Afzal et al., 2011) and South Tibet (this work), as representative for the eastern Neo-Tethyan Ocean (Fig. 3.4).

Lockhartia roeae appears in SBZ3 and SBZ4 of the western and central Neo-Tethyan Ocean (Hottinger, 2014a). In contrast, this species shows a stratigraphic distribution ranging from SBZ2/SBZ3 to the beginning of SBZ5 in the eastern Neo-Tethyan Ocean (Afzal et al., 2011; this work). *Lockhartia praehaimei* and *L. retiata* are described as index species of SBZ3, ranging from SBZ3 to SBZ4 and even up to SBZ5 for *L. praehaimei* (Hottinger, 2014a,b) within the western Neo-Tethys. In the eastern Neo-Tethys these species stratigraphically range from SBZ2 to SBZ3 (Afzal et al., 2011; this work).

Within the western and central Neo-Tethys, the stratigraphic distribution of *L. tipperi* extends from SBZ7 to SBZ9, while *L. hunti* ranges from SBZ12 to SBZ14 (Hottinger, 2014a). In the eastern Neo-Tethyan Ocean, *L. tipperi* and *L. hunti* both range from the upper part of SBZ5 to SBZ8 (this work).

Stratigraphic ranges of species in the Tethys Ocean indicate earlier evolution of *Lockhartia* in the eastern Neo-Tethys and a later development in the western part. Differences in evolution of LBF within the Neo-Tethys are hypothesized to be due to different latitudinal positions of the western and the eastern regions (Scheibner and Speijer, 2008). During the Paleocene, the western Neo-Tethyan Ocean was geographically

located at lower and middle latitudes, and was dominated by coralgal reefs (e.g., Accordi et al., 1998; Turnsek and Drobne, 1998; Baceta et al., 2005; Scheibner et al., 2007). In contrast, the eastern Neo-Tethys was located within low latitudes, closer to the equator, where the LBF predominated in carbonate depositional environments (Wan et al., 2002, 2010; Afzal et al., 2011; Zhang et al., 2013).

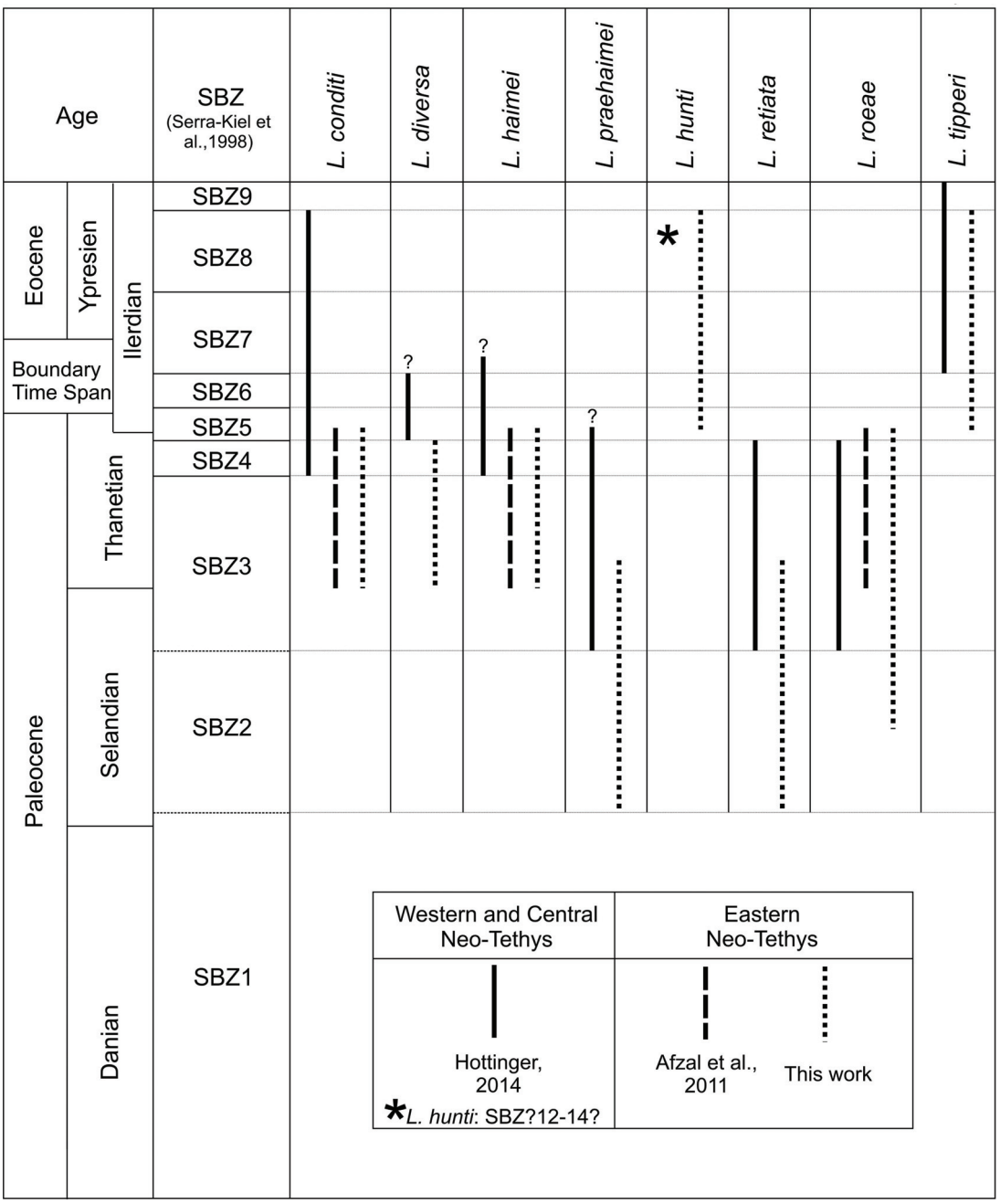

Figure 3.4: The stratigraphic distribution of *Lockhartia* from the entire Neo-Tethys suggests an earlier evolution of species within the eastern Neo-Tethys. The SBZ are based on Serra-Kiel et al. (1998).

3.5 Systematic Paleontology

Seven species of *Lockhartia* can be identified in the investigated sections of Tingri, Gamba and Guru in South Tibet. Based on the monograph of Smout (1954), a "Key to species" of *Lockhartia* for those species found in South Tibet has been established (Table 3.1). Here, species are arranged in groups with regard to morphological similarities in the appearance of piles and foliar walls filling the umbilical area. Species within the same group are assumed to have a common predecessor.

In the following systematic description of the genus *Lockhartia*, the species recognized in South Tibet are given. Terms for morphological descriptions are adopted from the "Illustrated glossary of terms used in foraminiferal research" (Hottinger, 2006). Biometric data found for *Lockhartia* species of South Tibet are compared to those from previous studies (Table 3.3).

Order ROTALIIDA Delage and Hérouard, 1896
Suborder ROTALIINA Delage and Hérouard, 1896
Superfamily ROTALIOIDEA Ehrenberg, 1839
Family ROTALIIDAE Ehrenberg, 1839
Subfamily LOCKHARTIINAE Hottinger, 2014a
Genus *Lockhartia* Davies, 1932
Type Species *Dictyoconoides haimei* Davies, 1927

Description. Test is calcareous and perforate-bilamellar, stoutly lenticular to convex on the dorsal side and flat to convex on the ventral side. The height of the test is generally not exceeding the diameter of the base. In axial section the chambers are nearly evolute dorsally. The trochospiral chamber arrangement leaves a wide umbilical area of complex structure, filled with vertically continuous and laminated piles, extending from the chambers to the base of the foraminifera test. Additional horizontal folia walls occur within the umbilical area. In axial section the appearance of plates and folia walls within the umbilical area is a very distinctive feature for the different species of *Lockhartia*. The spire is sharply separated from the umbilical region of the test by an umbilical plate.

Remarks. Previously, the genus *Lockhartia* was placed in the subfamily Rotaliinae Ehrenberg, 1839 (e.g., Al-Hashimi, 1974; Jauhri, 1985). Within his monograph, Hottinger (2014a) transferred the genus *Lockhartia* Davies, 1932, as well as the genera *Dictyoconoides* Nuttall, 1926, *Sakesaria* Davies, 1937 and *Rotalispira* n. gen., into a new subfamily named Lockhartiinae. The new subfamily can be distinguished from the previously used subfamily by the umbilical structure (umbilical cavities: piles and folia walls), low-trochospiral shells, and dorsal ornamentation.

Group	Umbilical region		Periphery	Perforation	Chambers in axial section	Ornamentation of the apex	Test	Proloculus	Species
1	piles and folia walls very distinct	numerous tall thin piles of uniform size	unkeeled	fine	semi-lunar, "longer in the direction of growth than their radial extension" (Hottinger, 2014a)	smooth	large, low conical, base slightly convex	small	*L. tipperi*
		five to eight thick piles of uniform size					small, conical with base generally slightly convex, relatively thin wall		*L. hunti*
2	piles and folia walls distinct	five to six tall thin piles of uniform size	keeled	coarse	wedge-shaped	coarse bars and pustules	convex dorsally, ventral side convex to flat	large, dyad, subequal	*L. haimei*
		six to eight piles of uniform size				fine bars	lenticular shells, very rounded dorsal surface		*L. praehaimei*
3	piles distinct, folia walls between being difficult to see	generally three to four heavy piles in the direction of growth	unkeeled	fine	semi-lunar, "longer in the direction of growth than their radial extension" (Hottinger, 2014a)	smooth	conical with slight convex base	small	*L. conditi*
		four to six piles of unequal size, central one slightly thicker					conical and straight sided, triangular shape, ventral side weakly convex	small, sometimes biconch	*L. roeae*
4	piles and folia walls confused	irregularly rounded piles	unkeeled	coarse	rounded to subsphearical	thick cancellate network	rounded dorsal contour, ventral face flat to weakly convex	large, dyad, first chamber almost globular	*L. retiata*

Table 3.1: Key to species of the LBF *Lockhartia* in South Tibet (based on Smout, 1954). Taxonomic groups based on the distribution of piles and folia walls within the umbilical region. Species within the same taxonomic groups may have similar predecessors.

L. conditi	**Reference**	**Nuttall, 1926**	**Davies, 1927**	**Smout, 1954**		**Hottinger, 2014a**	**This work**
	Location	Sind, Pakistan	Thal, Pakistan	Qatar		WNT	South Tibet
	Diameter (mm)	1.5–2.8	1.7	0.8–4.0 (1.1–3.2)		1.5	1.12–2.36 (1.55)
	Height (mm)	1.0–1.9	1.1	0.5–2.0 (0.7–1.9)		—	0.75–1.29 (1.00)
	Diameter/Height	—	—	1.25–1.67 (1.43)*		1.5–1.8	1.22–1.92
L. haimei	**Reference**	**Davies, 1927**	**Davies, 1937**	**Smout, 1954**	**Sander, 1962**	**Hottinger, 2014a**	**This work**
	Location	Sind, Pakistan	Thal, Pakistan	Qatar		WNT	South Tibet
	Diameter (mm)	1.64	2.5	0.8–3.6 (1.8–2.3)	1.19–1.61	—	1.07–2.12 (1.53)
	Height (mm)	0.97	1.0	0.6–3.0 (1.2–2.0)	0.82–0.90	—	0.54–1.31 (0.85)
	Diameter/Height	—	—	1.11–2.5 (1.43)*	1.79–1.81	2.0–3.0	1.45–2.66
L. hunti	**Reference**	**Ovey, 1947**		**Smout, 1954**			**This work**
	Location	Somalia		Qatar			South Tibet
	Diameter (mm)	1.57		1.4			0.94–1.73 (1.34)
	Height (mm)	2.00		0.7			0.56–1.12 (0.75)
	Diameter/Height	—		—			0.63–2.00
L. praehaimei	**Reference**			**Smout, 1954**		**Hottinger, 2014a**	**This work**
	Location			Qatar		WNT	South Tibet
	Diameter (mm)			0.5–2.5 (1.8)		—	1.16–2.65 (1.68)
	Height (mm)			0.3–1.9 (1.0)		—	0.68–1.24 (0.93)
	Diameter/Height			1.25–2.5 (2.0)*		1.8–2.2	1.48-2.33
L. retiata	**Reference**				**Sander, 1962**		**This work**
	Location				Saudi Arabia		South Tibet
	Diameter (mm)				1.1–1.9 (1.49)		0.77–1.39 (1.12)
	Height (mm)				0.8–1.7 (1.15)		0.56–1.02 (0.78)
	Diameter/Height				1.29		0.71–1.64
L. roeae	**Reference**	**Davies, 1930**				**Hottinger, 2014a**	**This work**
	Location	Kohat, Pakistan				WNT	South Tibet
	Diameter (mm)	1.4–2.5				—	1.21–1.82 (1.43)
	Height (mm)	0.8–1.35				—	0.72–1.08 (0.84)
	Diameter/Height	—				2.0–2.3	1.44–1.90
L. tipperi	**Reference**	**Nuttall and Brighton, 1931**	**Davies, 1937**	**Smout, 1954**	**Sander, 1962**	**Hottinger, 2014a**	**This work**
	Location	Somalia	Punjab, Pakistan	Qatar	Saudi Arabia	WNT	South Tibet
	Diameter (mm)	3.0	3.5	1.7–3.6 (2.3)	0.7–3.8	3.3	1.72–3.79 (2.79)
	Height (mm)	1.5	1.45	1.4–1.7 (1.5)	0.4–2.2	1.8	0.96–2.16 (1.55)
	Diameter/Height	—	2.0*	2.5–3.3(2.5)*	—	—	1.47–2.47

Table 3.3: Size of *Lockhartia* species in South Tibet compared to those described in literature. In some cases, average sizes of species are given in brackets after size ranges; * indicates the original ratio between diameter (D) and height (H) were given in H/D. Abbreviation: WNT = Western and Central Neo-Tethys.

3.5.1 *Lockhartia conditi* (Nuttall, 1926)

Figs. 3.5.1–3.55

Dictyoconoides conditi Nuttall, 1926, p. 119, pl. 6, figs. 7–8; Davies, 1927, p. 279, pl. 21, figs. 10–12, pl. 22, fig. 5; Davies, 1930, p. 76–77, pl. 10, fig. 9.

Lockhartia conditi Nuttall, 1926. Davies, 1932, p. 408, pl. 2, fig. 7, pl. 4, fig. 7; Davies and Pinfold, 1937, p. 47–48, pl. 5, fig. 24; Smout, 1954, p. 55, pl. 5, figs. 16–19; Zhang et al., 2013, p. 1434–1435, figs. 6.10–6.11; Hottinger, 2014a, p. 76–81, pl. 5.10, figs. 7–9, pl. 5.14, figs. 1–24, pl. 5.15, figs. 1–13.

Lockhartia aff. *conditi* Nuttall, 1926. Hottinger, 2014a, p. 76–81, pl. 5.12, figs. 10–16.

Description. Test is conical dorsally, slightly convex at the base. Perforation is fine and chambers are semi-lunar or ”longer in the direction of growth than their radial extension” (Hottinger, 2014a, p.81) in axial section. Periphery is unkeeled. The apex is smooth and shows no ornamentation. Axial sections generally show three to four piles, which are distinct and huge, the foliar walls between are difficult to see. *Lockhartia conditi* shows 3–4, rarely 5 whorls. Size varies between 1.12–2.36 mm in diameter and 0.75–1.29 mm in height. Specimens that occur during the Early Eocene are slightly smaller in diameter. Proloculus diameter ranges from 0.08–0.13 mm. The specimens of *L. conditi* in South Tibet are approximately the same size as those specimens described from Thal (Davies, 1927), but they are much smaller than those described from Sind (Nuttall, 1926) or Qatar (Smout, 1954).

Occurrence. In addition to the Tingri, Gamba and Guru locations in South Tibet, *L. conditi* has been recorded from the Ranikot of Sind and Thal by Nuttall (1926) and Davies (1927). It also has been reported from the Paleocene of Qatar by Smout (1954) and in Tingri and Gamba by Zhang et al. (2013).

Remarks. The ornamentation of *L. conditi* seems to vary at different localities. Nuttall (1926) described nearly smooth specimens from Sind, which show indistinct granules at the apex. In contrast, the specimens from Qatar (Smout, 1954) have a smooth apex. The specimens described from Tingri, Gamba and Guru show no ornamentation as well. Smout (1954) supposed that *L. conditi* exhibits some dimorphism, with smaller specimens exhibiting about four and larger ones about seven whorls, but with no significant difference in the size of the nucleoconch. Dimorphism could not be observed in South Tibet. *Lockhartia conditi* can be distinguished from *L. tipperi* by its small number of very large piles and from *L. roeae* and *L. hunti* by the shape of the test and the number and arrangement of piles.

3.5.2 *Lockhartia haimei* (Davies, 1927)

Figs. 3.5.6–3.5.10

Rotalia newboldi d´Archiac and Haime, 1853, p. 347.

Dictyoconoides haimei Davies, 1927, p. 280–281, pl. 11, figs. 13–15.

Lockhartia haimei Davies, 1927. Davies, 1930, p. 75–76, pl. 10, figs. 6–7; Davies, 1932, p. 407, pl. 2, figs. 4–6; Davies and Pinfold, 1937, p. 45–46, pl. 7, figs. 9–13, 15; Smout, 1954, p. 49, pl. 2, figs. 1–14; Sander, 1962, p. 19, pl. 5, figs. 1–37; Zhang et al., 2013, p. 1434, fig. 6.8; Hottinger, 2014a, p. 61-65, pl. 5.5, figs. 1–12, pl. 5.6, figs. 1–17, pl. 5.8, figs. 1–14.

Lockhartia megapapulata Hu, 1976. Zhang et al., 2013, p. 1434, fig. 6.14.

Description. Test is flat to convex on the ventral side and more convex on the dorsal side. Perforation is fine and chambers are wedge-shaped in axial section. The periphery is keeled. Ornamentation shows coarse bars and pustules on the dorsal side. Piles and foliar walls are distinct. Umbilical region is large and crowded with five to six tall thin piles of uniform size. Proloculus is double (dyad) and of great but unequal size. There are 2–3 whorls. Sizes of *L. haimei* in South Tibet range from 1.07–2.12 mm in diameter and 0.54–1.31 mm in height. The size of the proloculus ranges from 0.14–0.34 mm. Specimens from South Tibet are approximately the same size as those described from Thal (Davies, 1927) and Arabia (Sander, 1962), but are much smaller than those described from the Punjab Salt Range of Pakistan (Davies and Pinfold, 1937) or Qatar (Smout, 1954).

Occurrence. In addition to the Tingri, Gamba and Guru locations in South Tibet, *L. haimei* has been recorded from the Paleocene of an area of India that is now part of Pakistan by Davies (1927). It also was recorded from the Paleocene of Pakistan (Davies and Pinfold, 1937), Qatar (Smout, 1954) and in Tingri and Gamba by Zhang et al. (2013).

Remarks. Sander described four different variations of *L. haimei*, based on differences in ornamentation on the dorsal side (Sander, 1962): *L. haimei* var. *nudimarginata*, *L. haimei* var. *spirachordata*, *L. haimei* var. *suturadicata* and *L. haimei* var. *vermiculata*. Based on the taxonomic determination of *Lockhartia* in thin sections, no differences in the dorsal ornamentation could be recognized within *L. haimei* of South Tibet. Therefore, no variation of *L. haimei* could be defined. *Lockhartia haimei* can be distinguished from other species like *L. praehaimei* by its large and double protoconch as well as the distinct ornamentation.

3.5.3 *Lockhartia hunti* Ovey, 1947

Figs. 3.5.11–3.5.15

Lockhartia hunti Ovey, 1947, p. 573, pl. 10, figs. 1–6, pl. 11, fig. 1; Smout, 1954, p. 54, pl. 4, fig. 7; Zhang et al., 2013, p. 1435, fig. 6.5; Hottinger, 2014a, p. 81, pl. 5.16, figs. 1–15, pl. 5.17, fig. 1–16, pl. 5.18, figs. 16–27.

Lockhartia cf. *hunti* Ovey, 1947. Hottinger, 2014a, p. 81, pl. 5.20, figs. 1–6.

Description. Test is conical with the base generally slightly convex and shows 3–4 whorls. Perforation is fine and chambers are large and semi-lunar or ”longer in the direction of growth than their radial extension” (Hottinger, 2014a, p. 81) in axial section. The periphery is unkeeled and the dorsal surface is smooth. Piles and foliar walls are very distinct, with 5–8 thick piles of uniform size. The size of *L. hunti* of South Tibet ranges from 0.94–1.73 mm in diameter and 0.56–1.12 mm in height. Early Eocene species are slightly smaller. *Lockhartia hunti* of South Tibet is approximately the same size as *L. hunti* described from Qatar (Smout, 1954), but are smaller than those described from Somalia (Ovey, 1947) and larger than specimens described from India (Jauhri, 1985). Proloculus size ranges between 0.07–0.14 mm.

Occurrence. In addition to the Tingri, Gamba and Guru locations in South Tibet, *L. hunti* was recorded from the Early Eocene of Somalia by Ovey (1947). It was also described from the Early Eocene of Qatar (Smout, 1954). In South Tibet, it was previously recorded from the Late Paleocene and Lower Eocene of Tingri and Gamba by Zhang et al. (2013).

Remarks. Lockhartia hunti can be distinguished from other species of *Lockhartia* by the number and arrangement of piles and the external shape. Because of the size, along with the number and arrangement of

piles and foliar walls within the umbilical area, we postulate that *L. hunti* and *L. tipperi* have a common predecessor or one species emerged from the other. Even in Hottinger's monograph, the author indicates the difficulty in distinguishing between these species and describes some species of *Lockhartia* as "*Lockhartia* cf. *hunti* or young specimens of *L. tipperi*" (Hottinger, 2014a, p. 84, pl. 5.20, figs. 1-6). This statement supports the assumption of a common predecessor.

3.5.4 *Lockhartia praehaimei* Smout, 1954

Figs. 3.5.16–3.5.19

Lockhartia prehaimei Smout, 1954, p. 51, pl. 2, figs. 21–22, plate, 7, fig. 14; Zhang et al., 2013, p. 1434, fig. 6.5.

Lockhartia praehaimei Smout, 1954. Hottinger, 2014a, p. 61, pl. 5.3, figs. 1–16, pl. 5.4, figs. 1–17, pl. 5.10, figs. 16–18.

Description. Test is lenticular with 2–3 whorls. Perforation is fine and chambers are wedge-shaped in axial section. Periphery is keeled. Ornamentation on dorsal surface shows numerous fine bars. Piles and foliar walls are distinct. Umbilical region is crowded with 6–8 tall, thin piles of the same size. Size of *L. praehaimei* in South Tibet varies between 1.16–2.65 mm in diameter and 0.68–1.24 mm in height. Proloculus ranges between 0.10–0.17 mm in size. The specimens are similar in size to those described from Qatar (Smout, 1954).

Occurrence. In addition to the Tingri, Gamba and Guru locations in South Tibet, *L. praehaimei* has been recorded from the Paleocene of Qatar by Smout (1954), as well as from the Paleocene of Tingri and Gamba by Zhang et al. (2013).

Remarks. Smout (1954) noted some transitional specimens between the sedimentary strata where *L. praehaimei* occur and those where *L. haimei* occur. In South Tibet, no transitional specimens were observed. *Lockhartia praehaimei* can be distinguished from *L. haimei* by its smaller ornamentation and smaller proloculus. It can be distinguished from *L. conditi* by the higher numbers of very thin piles of uniform size. This species is considered to be the predecessor of *L. haimei* because of similarities within the umbilical structure.

3.5.5 *Lockhartia retiata* Sander, 1962

Figs. 3.6.1–3.6.5

Lockhartia haimei Davies, 1927. Drooger, 1960a, p. 458, pl. 2, figs. 4a–6a; Drooger, 1960b, p. 302, pl. 3, figs. 1–10.

Lockhartia retiata Sander, 1962, p. 22, pl. 4, figs, 1–21; Zhang et al., 2013, p. 1434, fig. 6.4; Hottinger, 2014a, p. 65, figs. 5.1A–G, figs. 5.2A–G, pl. 5.9, figs. 1–20, pl. 5.10, figs. 1–15.

Description. Rounded dorsal contour, ventral face is flat to weakly convex, showing 2 whorls within the test. Perforation is coarse and chambers exhibit a rounded to subsperical shape in axial section. Periphery is unkeeled. Ornamentation is described as cancellate. Piles are irregularly rounded, disabled and together with foliar walls indistinct. Size of the test varies between 0.77–1.39 mm in diameter and 0.56–1.02 mm in height. The proloculus is double (dyad) and large, the first chamber is almost globular and 0.12–0.34 mm in size.

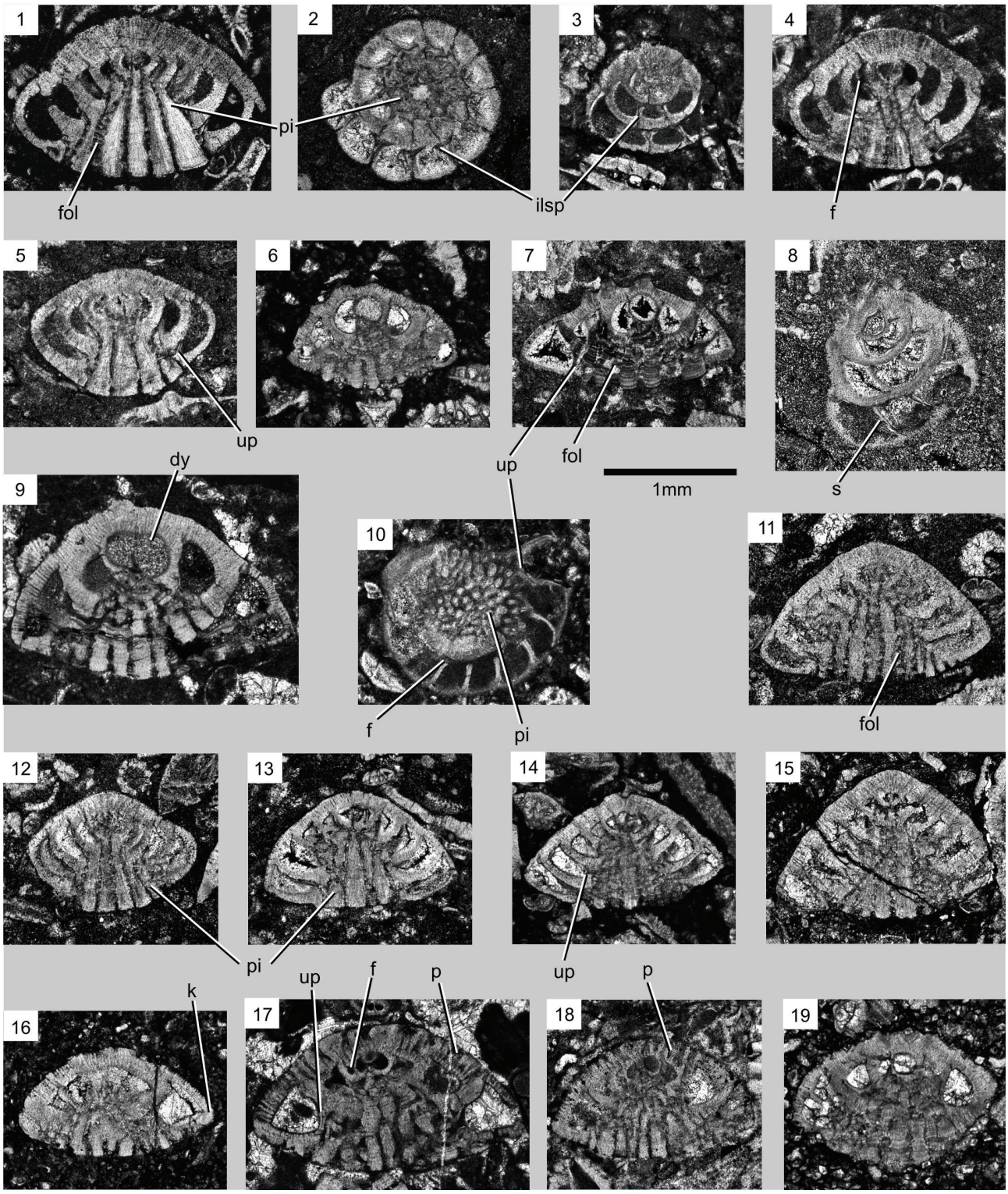

Figure 3.5: *Lockhartia conditi*, *L. haimei*, *L. hunti* and *L. praehaimei* from South Tibet. **1-5** *L. conditi* (Nuttall, 1926): **1** axial section; **2** section perpendicular to the coiling axis; **3** tangential section; **4** axial section; **5** adaxial section. **6-10** *L. haimei* (Davies, 1927): **6-7** axial sections; **8** equatorial section; **9** axial section, **10** section perpendicular to the coiling axis. **11-15** *L. hunti* Ovey, 1947, axial sections. **16-19** *L. praehaimei* Smout, 1954: **16** adaxial section; **17-18** axial sections; **19** adaxial section. Abbreviations: dy = dyad, f = foramen, fol = folia, ilsp = intraseptal interlocular space, k = keel, p = pore, pi = pile, s = septum, up = umbilical plate.

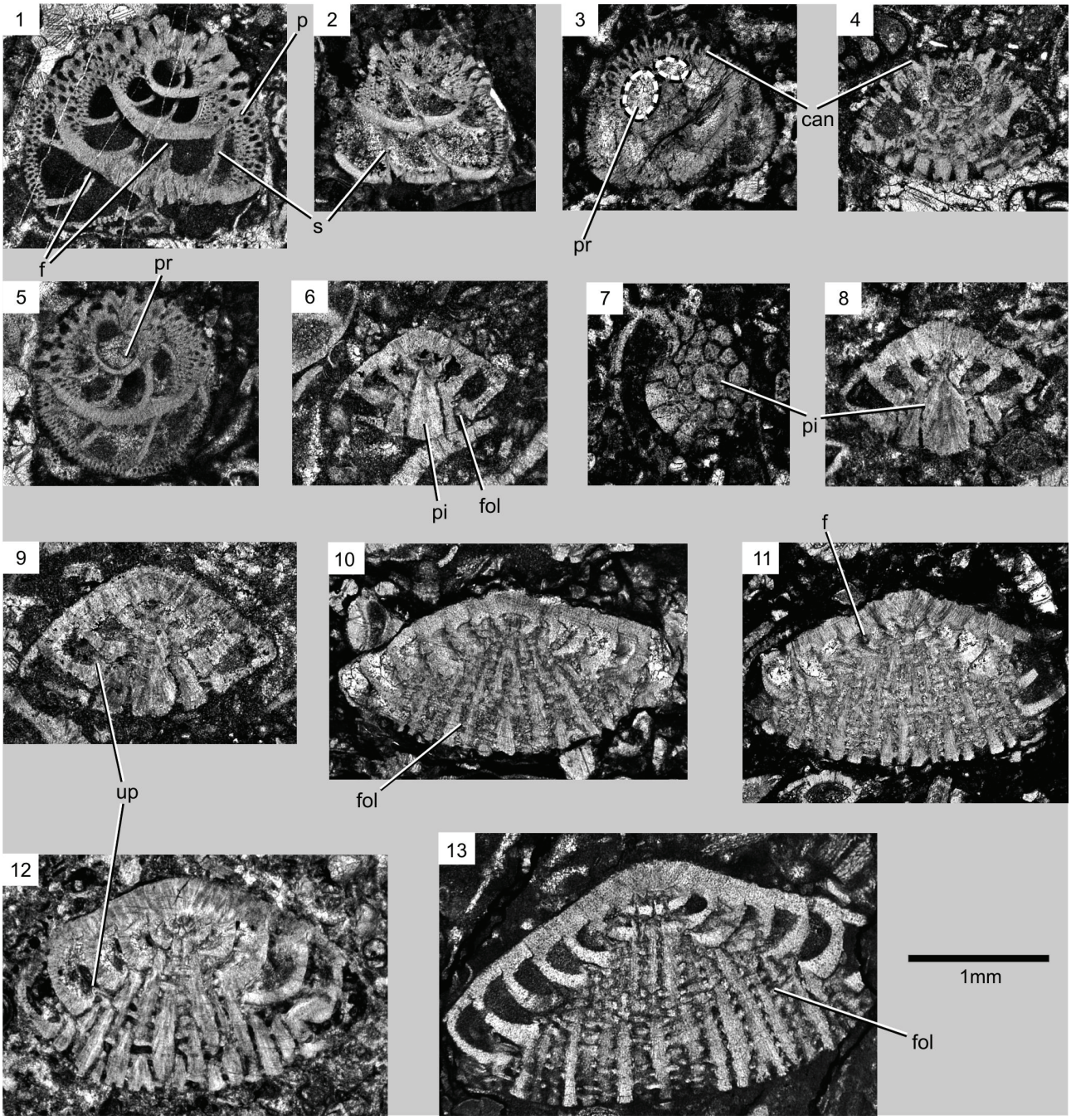

Figure 3.6: *Lockhartia retiata*, *L. roeae* and *L. tipperi* from South Tibet. **1-5** *L. retiata* Sander, 1962: **1-2** oblique sections; **3** oblique section, dyad embryonic chambers are redrawn for better identification; **4** adaxial section; **5** section perpendicular to the coiling axis. **6-9** *L. roeae* (Davies, 1930): **6** axial section; **7** section perpendicular to coiling axis; **8-9** axial sections. **10-13** *L. tipperi* (Davies, 1926): **10-11** axial sections; **12-13** adaxial sections. Abbreviations: can = cancellate, f = foramen, fol = folia, p = pore, pi = pile, pr = proloculus, s = septum, up = umbilical plate.

Occurrence. In addition to the Tingri, Gamba and Guru locations in South Tibet, *L. retiata* is recorded from the Lower Paleocene of East Saudi Arabia by Sander (1962), and also from the Paleocene of Tingri and Gamba by Zhang et al. (2013).

Remarks. In South Tibet, the thick cancellate network and the large proloculus of *L. retiata* are distinctive. The species can be distinguished from *L. diversa* in having a less rounded test and from *L. haimei* by its cancellate ornamentation.

3.5.6 *Lockhartia roeae* (Davies, 1930)

Figs. 3.6.6–3.6.9

Dictyoconoides conditi Nuttall, 1926, p. 119, pl. 6, figs. 7–8; Davies, 1927, p. 279, pl. 21, figs. 10–12, pl. 22, fig. 5.

Dictyoconoides conditi Nuttall var. *roeae* Davies, 1930, p. 76–77, pl. 10, fig. 9.

Lockhartia conditi Nuttall var. *roeae* Davies, 1930. Silvestri, 1938, p. 63 & 81, pl. 7, fig. 4.

Lockhartia roeae Davies, 1930. Zhang et al., 2013, p. 1434, figs. 6.6–6.7; Hottinger, 2014a, p. 67, pl. 5.12, figs. 1–6, pl. 5.13, figs. 1–16.

Description. Test is conical dorsally and straight sided in vertical section, showing 4–5 whorls. Perforation is fine. In axial section, chambers are semi-lunar in shape or ”longer in the direction of growth as compared to their radial extension” (Hottinger, 2014a, p. 76). Periphery is unkeeled. Smooth dorsal surface without ornamentation. Umbilical area is filled with 4–6 thin piles. Piles are distinct and have unequal size, the pile in the center of the test slightly thicker. Size of the test ranges from 1.21–1.82 mm in diameter and 0.72–1.08 mm in height. Specimens that occur in Early Eocene strata are slightly smaller. Specimens of South Tibet are slightly smaller than those described from Pakistan (Davies, 1930). Proloculus is small, sometimes biconch, ranging in size from 0.07–0.11 mm in diameter.

Occurrence. In addition to the Tingri, Gamba and Guru locations in South Tibet, *L. roeae* is recorded from the Paleocene of Pakistan by Davies (1930) and from Tingri and Gamba by Zhang et al. (2013).

Remarks. Davies (1930) distinguished forms found in the Samana Range from the species *L. conditi* described by Nuttall in 1926 because of the arrangement and size of piles, as well as the shape of chambers. *Lockhartia roeae* can be distinguished from other species of *Lockhartia* by the shape of the test and the unequal size of the piles, with one slightly thicker pile found towards the center.

3.5.7 *Lockhartia tipperi* (Davies, 1926)

Figs. 3.6.10–3.6.13

Conulites tipperi Davies, 1926, p. 247–248, pl. 18, fig. 8.

Dictyoconoides tipperi Davies, 1926. Nuttall and Brighton, 1931, p. 56–57, pl. 3, figs. 14–17.

Lockhartia tipperi Davies, 1926. Davies, 1932, p. 407; Davies and Pinfold, 1937, p. 48–49, pl. 6, figs. 14–16, pl. 7, fig. 17; Ovey, 1947, p. 574, pl. 10, fig. 13; Smout, 1954, p. 55, pl. 4, figs. 11–13; Sander, 1962, p. 24, pl. 4, figs. 25–26, 33–36; Zhang et al., 2013, p. 1435, fig. 6.13; Hottinger, 2014a, p. 81–85, pl. 5.19, figs. 1–14, pl. 5.20, figs. 7–13.

Lockhartia roeae Davies, 1930. Hottinger, 2014a, p. 67–76, pl. 5.13, figs. 2–4 (partly).

Description. Low conical test with a slightly convex base; *L. tipperi* is much larger than other species of *Lockhartia*, showing 5–7 whorls. Perforation is fine and chambers are semi-lunar or ”longer in the direction of growth in respect to their radial extension” (Hottinger, 2014a, p. 85). Periphery is unkeeled. Exterior is smooth. Piles and foliar walls are very distinct. The umbilical area is characterized by large and regular cavities because of the numerous very thin piles that fill the umbilical region. Test size ranges from 1.72–3.79 mm in diameter and 0.96–2.16 mm in height. Specimens of the Lower Eocene are slightly smaller. Specimens of *L. tipperi* of South Tibet are smaller than those described from Somalia (Nuttall and Brighton, 1931) and Pakistan (Davies and Pinfold, 1937), but are slightly bigger than those described from Qatar (Smout, 1954). Proloculus is small, ranging in size from 0.11–0.29 mm in diameter.

Occurrence. In addition to the Tingri, Gamba and Guru locations in South Tibet, *L. tipperi* is recorded from the Paleocene and Lower Eocene of India (now part of Pakistan) by Davies (1926), as well as from the Lower Eocene of Qatar (Smout, 1954) and Somalia (Nuttall and Brighton, 1931). The species *L. tipperi* is also described from the Paleocene and Eocene of Saudi Arabia (Sander, 1962) and from Tingri and Gamba by Zhang et al. (2013).

Remarks. Lockhartia tipperi shows differences in its dorsal ornamentation at different localities. Davies and Pinfold (1937) noted that the species known from Pakistan are smoother than those of Qatar as described by (Smout, 1954), which are ornamented with a considerable number of isolated pustules. In Tingri, Gamba and Guru, the tests of *L. tipperi* exhibit a smooth surface. This species can be distinguished from *L. conditi* and *L. hunti* by the large size of the test and number of very thin piles.

3.6 Summary and Conclusions

Based on the high diversity of *Lockhartia* species, we were able to establish a high-resolution biozonation pattern valuable for South Tibet. Seven *Lockhartia* species within five *Lockhartia* interval biozones were defined, showing that a regional stratigraphic correlation of Tingri, Gamba and a new profile of Guru is feasible. The biozones indicate an increasing diversification of *Lockhartia* from Middle Paleocene to Late Paleocene and a drastic reduction of diversity within Lower Eocene.

The comparison of stratigraphic ranges of *Lockhartia* suggests that some species exhibit an earlier evolution within the eastern Neo-Tethyan Ocean, also called Lockhartia Sea, compared to the western part of the Ocean. These differences are possibly due to latitudinal differences. During the Paleocene, the western Neo-Tethyan Ocean was located at lower to middle latitudes of the northern hemisphere, while the eastern part of the Ocean was located at equatorial latitudes.

Analysis of foraminifera assemblages and accompanying organisms within the limestones of South Tibet indicate a depositional environment ranging from a restricted shallow-water lagoon to the outer carbonate ramp with water depths ranging from very shallow to possibly as deep as 120 meters.

Acknowledgements

Anne Hübner, Elke Leipprand and Christiane Schott are gratefully thanked for their assistance in field and laboratory work. We also want to thank Dr. Ines Wendler and Dieter von Bargen for their careful and constructive comments on an earlier version of the manuscript. Esmeralda Caus (Universitat Autònoma de Barcelona, Spain) and Vicent Vicedo (Museu de Ciències Naturals de Barcelona, Spain) are thanked for their critical remarks, which improved the paper. Special thanks to the editor, Pamela Hallock, for the helpful suggestions on the manuscript. This project is part of the priority program 1372 Tibetan Plateau: Formation - Climate - Ecosystem (TiP), funded by the German Science Foundation (DFG Wi725/26) and the University of Bremen (Germany).

Appendix

Appendix 1. List of species mentioned in the text that are not included in the section on SYSTEMATIC PALEONTOLOGY.

- *Alveolina agerensis* (Gaemers, 1987)
- *Alveolina ellipsoidalis* Schwager, 1883
- *Alveolina mousoulensis* Hottinger, 1960
- *Alveolina* cf. *subtilis* Hottinger, 1960
- *Assilina leymeriei* (d'Archiac & Haime, 1853)
- *Assilina subspinosa* Davies, 1937
- *Lockhartia altispira* Smout, 1954
- *Lockhartia megapapulata* Hu, 1976
- *Nummulites globolus* Leymeriei, 1846
- *Nummulites* cf. *subramondi* de la Harpe, 1883

”Das Unerwartete ist für den Reisenden in Tibet das Alltägliche.”

Alexandra David-Néel (2012)
Mein Weg duch Himmel und Höllen - Das Abenteuer meines Lebens

4 Genesis of Paleocene and Lower Eocene shallow-water nodular limestones of South Tibet (China)

Michaela M. Kahsnitz[1,3], **Helmut Willems**[1,2]

[1] Department of Geosciences, University of Bremen, 28359 Bremen, Germany

[2] Nanjing Institute of Geology and Palaeontology, Chinese Academy of Sciences, Nanjing 210008, China

[3] Correspondence author. Email: michaela.kahsnitz@uni-bremen.de

Accepted for publication in Carbonates and Evaporites

Abstract

This paper examines the genesis of the Paleocene to Lower Eocene shallow-water nodular limestones in South Tibet. The negative carbon isotope excursion representative for the Paleocene-Eocene boundary is located in one nodular limestone bed of the Zhepure Shan Formation showing an extraordinary thickness of about 11 m, inspiring the question under which conditions these nodular limestones were formed. Based on field appearance, the shallow-water nodular limestones of Tingri and Gamba can be classified into five nodular limestone categories (Stylonodular Rock I, Nodular Rock I, Nodular Rock II, stylobedded rock and stylomottled rock) and some transitional members (stylobedded rock transitional to Stylobedded Rock II). Clay variations are assumed to be responsible for these various types of nodular limestones within the sediments. Observations of nodular limestones in South Tibet suggest that those sediments were mostly formed due to autochthonous rather than allochthonous processes. Differential diagenesis resulted in an early selective cementation of limestone nodules due to carbonate-supply, while the marls were not cemented but provide the carbonate for the nodule cementation. Additionally, cemented and carbonate-rich nodules are resistant to chemical compaction, while the uncemented and clay-rich marl layers affected by pressure solution processes due to an overburden of sediments. Additionally, a model is presented, illustrating the origin of different nodular limestones described here.

KEYWORDS: Nodular limestones, Differential diagenesis, South Tibet, Paleogene

4.1 Introduction

Paleocene and Lower Eocene carbonate rocks close to the village of Tingri (South Tibet) are deposited on the northern passive margin of the Indian continent in a shallow-water realm (Willems, 1993). The negative carbon isotope excursion (CIE) representative for the Paleocene-Eocene boundary is located in a nodular limestone bed of the Zhepure Shan Formation (Zhang et al., 2013, 2017). The extraordinary thickness of about 11 m of this isotope excursion at Tingri, compared to the CIE from ODP690 (about 1 m) described by Bains et al. (1999), requires thorough investigations in order to determine under which conditions these nodular limestones were formed.

In literature, the formation of nodular limestone is described as a result of diagenetic (solution, cementation, nodule-growth within the sediment), sedimentary (transport, reworking) or tectonic (shearing) processes (Flügel, 2010). They are discussed in a wide variety of potential formation conditions from different stratigraphic periods on a global scale.

For example, marine platform carbonates of Silurian, Carboniferous and Jurassic ages within the United Kingdom also exhibit nodular beds. Processes leading to the nodular texture are described as a combination of hydrodynamic reworking and bioturbation, selective early cementation of carbonate-rich areas, mechanical compaction and pressure dissolution (Bathurst, 1987).

Devonian nodular limestones from Southern France (”Griotte”) and Germany (”Cephalopodenkalk”) have been described as products of early lithification, and include the formation of nodules around goniatite shells.

Compaction and pressure dissolution result in the formation of stylolites and marly seams, emphasizing their nodular features (Tucker, 1974; Tucker and Wright, 2008).

Red limestone breccias of Liassic (Early Jurassic) age are found within the Northern Calcareous Alps, southeast of Salzburg, called Adneter Scheck. The formation of these breccias is described as being due to the mass transport of early cemented and semiconsolidated sediments via tectonic activities. Transport of the material on steep slopes and deposition on slightly inclined plains caused sediment brecciation (Schlager, 1966; Hudson and Jenkyns, 1969; Bernoulli and Jenkyns, 1970; Böhm et al., 1995).

The Upper Cretaceous nodular limestones of Jordan were formed due to burrowing organisms. The shapes and sizes of the nodules depend on the structure of the burrow system (Abed and Schneider, 1980).

Other possible processes that result in the creation of limestone nodules include submarine dissolution processes of carbonate on the seafloor (Hollmann, 1962, 1964; Bjorlykke, 1973, 1974; Müller and Fabricius, 1974), bacterially induced nodule growth (Jeans, 1980), sedimentary boudinage (McCrossan, 1958), degradation of organic material (Schindewolf, 1921, 1923, 1925), pressure solution (Wanless, 1979) and early diagenetic concretionary/nodular precipitation and lithification (Illies, 1949; Jenkyns, 1974; Noble and Howells, 1974; Möller and Kvingan, 1988).

Nodular limestones, like limestone-shale/chalk alternations and well-bedded limestones, are also variations of so called limestone-marl alternations (Munnecke and Samtleben, 1996; Westphal et al., 2000; Munnecke et al., 2001; Munnecke and Westphal, 2004), characterized by their pronounced ABAB rhythm of limestone beds and marly interbeds (Einsele et al., 1991). Limestone-marl alternations are described as results of orbital climatic changes (Milankovitch cycles) or variations in the sedimentary input of carbonate and clay. In this case, diagenesis will enhance primary differences of heterogeneous sediment layers (e.g., Ricken, 1986; Bathurst, 1987; Einsele et al., 1991; De Boer and Smith, 1994). On the other hand, an exclusively diagenetic origin from primarily homogenous sediments is discussed (Hallam, 1986; Munnecke and Samtleben, 1996). The interpretation based on different diagenetic processes influencing the limestone layers/nodules and the marly layers, called differential diagenesis is discussed controversially (Reinhardt et al., 2000; Westphal et al., 2000). While the limestone layers/nodules show early cementation before compaction, the marly layers show strong compaction due to overburden (e.g., Ricken, 1986; Munnecke and Samtleben, 1996; Westphal et al., 2000).

In this study and in respect to the extraordinary thickness of the carbon isotope excursion, Paleocene and Lower Eocene limestones of the Zhepure Shan Formation in Tingri (South Tibet) were examined. Here nodular limestones, as well as nodular beds within cyclic limestones, are observed with respect to their depositional environment, as well as their diagenetic features and isotopic signatures.

4.2 Geologic setting

Samples of Paleocene to Lower Eocene limestones from the Shenkeza section (N28°69', E086°71') NE of Tingri village, South Tibet in China (Fig. 4.1) were taken for this study. Here, sediments were deposited in a shallow marine environment at the northern passive margin of the Indian continent (Willems, 1993; Zhang et al., 2012). Today, the study area Tingri is part of the Tethyan Himalaya, which is bounded by the Gangdese batholiths of the Lhasa Terrane to the north and by the Crystalline sequences of the High Himalaya to the

south (Yin and Harrison, 2000; Zhang et al., 2012) and is generally subdivided into a northern and a southern zone (Gansser, 1964; Ratschbacher et al., 1994). The northern Tethyan Himalaya is characterized by Mesozoic to Paleogene deep-water outer shelf continental slope and rise deposits (e.g., Liu and Einsele, 1994; Li et al., 2005; Hu et al., 2008), while the southern zone is dominated by Paleozoic to Eocene shallow-water carbonates and terrigenous strata (e.g., Liu and Einsele, 1994; Willems, 1993; Willems et al., 1996). In the southern Tethyan Himalaya, Paleozoic to Cretaceous marine sediments are widely exposed, while nearly complete sections of the Paleocene and Early Eocene limestones are mainly exposed at Tingri, Gamba and Guru. Paleocene sediments of Gamba and Guru also show the occurrence of nodular limestones but are not fully discovered, especially at the Paleocene-Eocene boundary, compared to the Zhepure Shan Formation in Tingri (Zhang et al., 2013; Kahsnitz et al., 2016). Therefore observations on the genesis of nodular limestones in South Tibet are focused on sediments from Tingri.

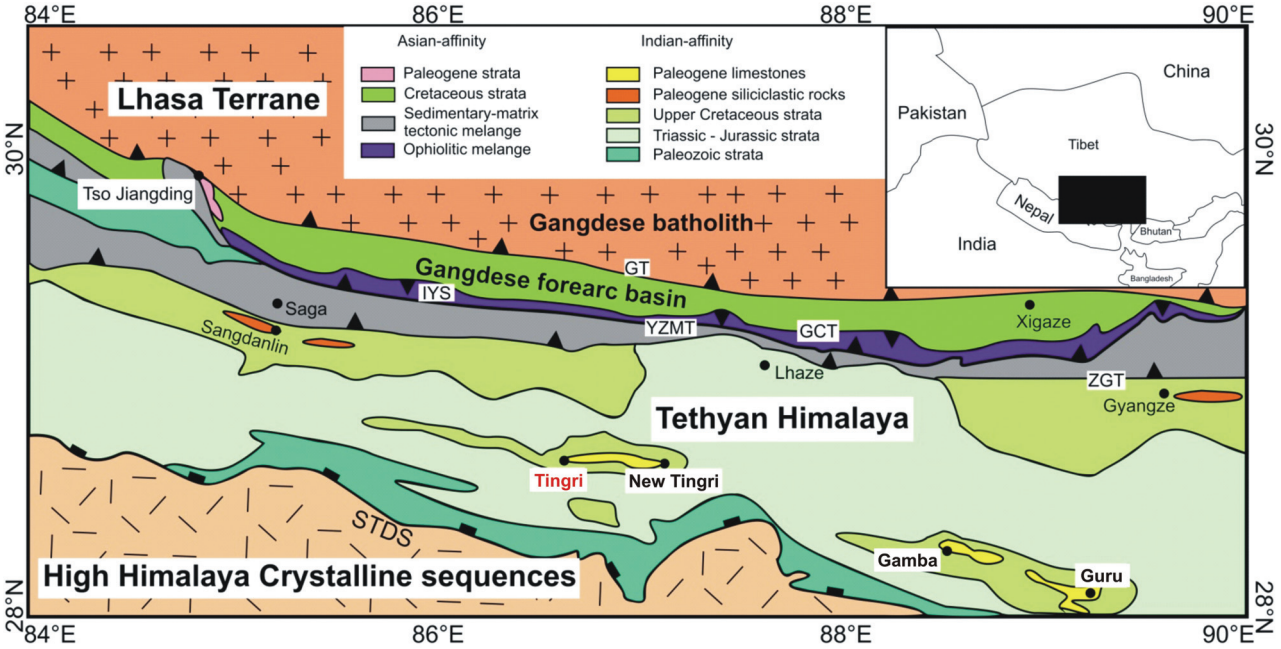

Figure 4.1: Geological map showing the location of the studied section in the vicinity of Tingri village in South Tibet (after Zhang et al., 2013). Abbreviations: GTC = Great Counter Thrust, IYS = Indus-Yarlung Zangbo Suture, STDS = South Tibet detachment system, YZMT = Yarlung Zangbo Mantle Thrust, ZGT = Zhongba-Gyangze Thrust.

4.3 Material and Methods

In Tingri, the limestone sequence, called Zhepure Shan Formation, can be subdivided into four members (Zhang et al., 2013) from bottom to top: cyclic limestones (Member A), massive limestones (Member B), nodular limestones (Member C) and massive limestones (Member D). The 90 m-thick Member C of the Zhepure Shan Formation is most suitable for investigations on the genesis of nodular limestone formations and thus is the focus of this study. Nodular beds of the 165 m-thick cyclic limestones (Member A) which are characterized by seven shallowing upward cycles, each consisting of marls, nodular limestones and thin-bedded limestones from bottom to top, were also considered.

Field observations: These observations were used for the determination of different types of well-developed nodular limestones. Lithological differences such as size, color, outer shape and fabric of limestone nodules, the spatial distribution of marls, as well as contacts between the two lithofacies were investigated. Terms used here to describe different sedimentary and diagenetic features based mainly on descriptions given by (Logan and Semeniuk, 1976).

Thin section analysis: This method is used to characterize microfacial, sedimentary and diagenetic fabrics, which yield information on processes leading to the formation of nodular limestones. The determination of microfacies was based on fossil assemblages and carbonate classification, following Dunham (1962) and the expanded classification according to Embry and Klovan (1971). The paleoenvironmental circumstances were discussed based on microfacies analysis.
Altogether, 442 samples from three sections (09ZS, 10/11TM, 11ZSC/NL) of Member A and Member C of the Zhepure Shan Formation were used for thin section analysis. Section 09ZS has got a sample density varying between 0.5 and 1 m per sample, covering Member A to Member C of the Zhepure Shan Formation, while section 10/11TM has got a sample density of about 0.2 m just covering the upper part of the nodular limestones (Member C) of the Zhepure Shan Formation. In addition, hand rock samples from Member C (ten samples, 11ZSNL) and Member A (five samples, 11ZSC) were taken especially for the observation of the genesis of nodular limestones in South Tibet. The samples investigated in the frame of this study are deposited at the working group Historical Geology/Paleontology of the Department of Geosciences (University of Bremen).

Isotope measurements and carbonate content: Ten samples of the nodular limestones (Member C, samples: 11ZSNL) and five samples of the cyclic limestones (Member A, samples: 11ZSC) were used for specific isotope measurements (δ^{13}C and δ^{18}O) and carbonate content. All measurements were conducted at limestone nodules, as well as the surrounding marls, to retrieve information on the genesis of the nodule generation. Isotopes were measured with a Finnigan MAT 251 Spectrometer at the Center for Marine Environmental Sciences (MARUM, University of Bremen). The reproducibility of the internal laboratory standard (Solnhofen limestone) was ± 0.03 for δ^{13}C and ± 0.08 for δ^{18}O.
Total organic carbon (TOC) and total carbon (TC) contents were measured with a LECO CS-200 Carbon Analyzer at the working group Sedimentology/Paleoceanography of the Department of Geosciences (University of Bremen). TC was measured directly from the pulverized bulk samples. For TOC measurements the inorganic carbon had to be removed first by a 12.5 % hydrochloride acid (HCl). TOC and TC contents were used to calculate the total inorganic carbon (TIC) and carbonate contents (CaCO3) of the samples using the following empirical formulas:

$$TIC(\%) = TC(\%) - TOC(\%)$$

$$CaCO3(\%) = TIC(\%) * \frac{(100)}{12}$$

Terminology	Context	Description	References
Chemical compaction	Compaction	In lithified limestones causing pressure solution (stylolites, dissolution seams)	Tucker and Wright (2008)
Condensed fabric	Fabric type	Contact of idens along their margins	Logan and Semeniuk (1976)
Dissolution seam	Pressure solution structure	Seam of insoluble residue around grains or particles, but not cutting them, similar to non-sutured seam solution of (Wanless, 1979)	Bathurst (1991)
Fitted fabric	Fabric type	Idens are in contact at their entire margins	Logan and Semeniuk (1976)
Iden	Fabric type	Body that behaves like a homogeneous object to stress; here: limestone nodule	Logan and Semeniuk (1976)
Iden-support	Fabric type	Idens are in contact at points	Logan and Semeniuk (1976)
Interidenic	Relationship to idens	Stylolites between idens (e.g., as described in the stylobedded rock of South Tibet)	Logan and Semeniuk (1976)
Mechanical compaction	Compaction	Fracturing and loss of porosity in uncemented sediments due to load of overlying sediments	Tucker and Wright (2008)
Non-sutured seam solution	Pressure solution structure	Microstylolites, microstylolite swarms and clay seams common within silty, clayey limestones; in or towards the margins of limestone units; characteristic product: nodular limestones; similar to dissolution seam of (Logan and Semeniuk, 1976)	Wanless (1979)
Reactate	Pressure solution residue	Mineral-crystallization at stylolite interfaces: e.g., dolomite, calcite, quartz	Logan and Semeniuk (1976)
Stylobedded	Rock type	Rocks with a bedded appearance due to stylolitic parting; stylobedding may be parallel to original layering, but also at low to high angles to original sediment layering	Logan and Semeniuk (1976)
Stylolaminated	Rock type	Set of planar to undulating and interidenic stylolites producing a lamination	Logan and Semeniuk (1976)
Stylolite	Pressure solution structure	Pressure-solution interface between two limestone units/masses of rocks; similar to sutured seam solution of (Wanless, 1979)	Logan and Semeniuk (1976); Bathurst (1987)
Stylomottled	Rock type	Rocks with irregular patches/mottles produced by pressure solution	Logan and Semeniuk (1976)
Stylonodular	Rock type	Idens separated and surrounded by stylolaminate	Logan and Semeniuk (1976)

Table 4.1: Terms used to characterize nodular limestones in the Paleocene and Lower Eocene of South Tibet.

Nodular type	**Fabric type**	**Limestone nodules**	**Marl layers / stylolites**	**Contact between lithofacies**	**Remarks**
Stylonodular Rock I	Iden supported to condensed	Large and lens-shaped nodules, sometimes broken and multilayered	Thick marl layers, highly stylolaminated	Sharp	Broken nodules possibly due to further compaction and shear motion
Nodular Rock I	Condensed to fitted fabric	Small and nearly spherical nodules	Reduced marls, untextured to slightly laminated	Gradual	Difficult to determine the boundary between the nodule and marl
Nodular Rock II	Iden supported fabric	Large, elongated and subrounded to angular nodules	Thick consolidated "marl" layers, slightly laminated	Gradual and sharp	Remarkable difference in color between the lithofacies; gray limestone fragments within the brown layers
Stylomottled rock	Condensed to fitted fabric	Large and irregular limestone lenses	Interidenic stylolite patches	Sharp	Stylolites as patches
Stylobedded rock	Iden supported	Large and angular lenses	Interidenic stylolites	Sharp	Sometimes very massive banks
Stylobedded rock (transitional to Stylonodular II)	Iden supported	large and very elongated lenses	Interidenic stylolite seams, further stylolamination of limestone bank	Gradual and sharp	Former stylobedded limestone bank with further compaction; gray nodules, brown solution seams

Table 4.2: Types of nodular limestones in the Paleocene and Lower Eocene of South Tibet and their characteristic features in field.

4.4 Results of field observations

Different types of nodular limestones were distinguished based on their lithological appearance in the field. Terms and references used to characterize distinct nodular limestone features are described in Table 4.1. Nodular limestones exhibited in Member C and as single or bundles of layers in the cyclic limestones of Member A are characterized by the occurrence of (1) nodules embedded in a marly matrix or (2) occurrence in massive limestone banks, surrounded by pressure solution seams, which create a nodular appearance. In addition, nodular limestone series are occasionally intercalated by massive limestone banks (Willems, 1993; Zhang et al., 2013).

Nodular limestones appear in five types, based on their textural features (Table 4.2). General distinguishing features of nodules are (1) size and shape, (2) amount and structural appearance of surrounding marls and (3) contacts between the limestones and marls. The textural appearance of the studied marls could be described either as untextured or as stylolaminated, due to the grade of compaction. The term stylonodular defines a pressure solution texture described by Logan and Semeniuk (1976), who characterized limestone nodules separated by marls with laminated stylolites. (Wanless, 1979) described this type of pressure solution texture as a non-sutured seam solution in argillaceous limestones.

4.4.1 Stylonodular Rock I

Stylonodular rock is characterized by occurrence of large, lens-shaped limestone nodules, varying from 3 to 15 cm in width and 12 to 25 cm in length. Limestone nodules occur at contact points, producing a condensed and often iden-supported frame (Fig. 4.2a). The marly matrix surrounding the nodules is characterized by a large amount of dissolution seams, producing a stylonodular fabric. The dissolution seams typically follow the outer shape of the limestone nodules, indicating nodular 'floating' in the matrix. Some nodules may be broken apart (Fig. 4.2b) or exhibit several limestone peelings (Fig. 4.2c) with this type of nodular limestone. The contact between limestone nodules and the matrix is distinct. This type of nodular limestone can be found in the lower section part of the nodular limestones of Member C.

Figure 4.2 ***(following page)*****:** Field observations of nodular limestones in South Tibet. **a-c** Stylonodular Rock I (Member C): large lens-shaped nodules (3–15 cm in width, 12–25 cm in length), producing an iden-supported fabric, with distinct contacts to the surrounding marly matrix. Pressure solution results in the occurrence of dissolution seams within the marls, producing a stylolaminated texture. Some of the nodules are fractured (Fig. 4.2b) and/or layered (Fig. 4.2c). **d, e** Nodular Rock I (Member C): nearly spherical limestone nodules (4-5 cm in diameter) with gradual contact to the surrounding marly matrix. Matrix is reduced, producing a condensed to fitted fabric of the nodular formation. The surrounding marls are untextured to slightly laminated. **f-h** Nodular Rock II (Member A): large, elongated and subrounded to angular nodules producing an iden-supported fabric. Marls are untextured to slightly laminated. The difference in color of the limestone nodules (gray) and the surrounding marl (brown) is remarkable. **i** Stylomottled rock (Member A): large and irregular limestone lenses with interidenic stylolite patches. Open caverns indicate areas where argillaceous marls have been washed out by erosion. **j** Stylobedded rock (Member A): large and angular limestone banks with interidenic stylolites producing large and angular lenses. **k, l** Stylobedded rock transitional to Stylonodular II (boulder within a valley): due to stylobedding (interidenic stylolites) of a former limestone bank large and angular lenses are produced. Further compaction and solution along the former stylolites produce elongated lenses surrounded by stylolamination.

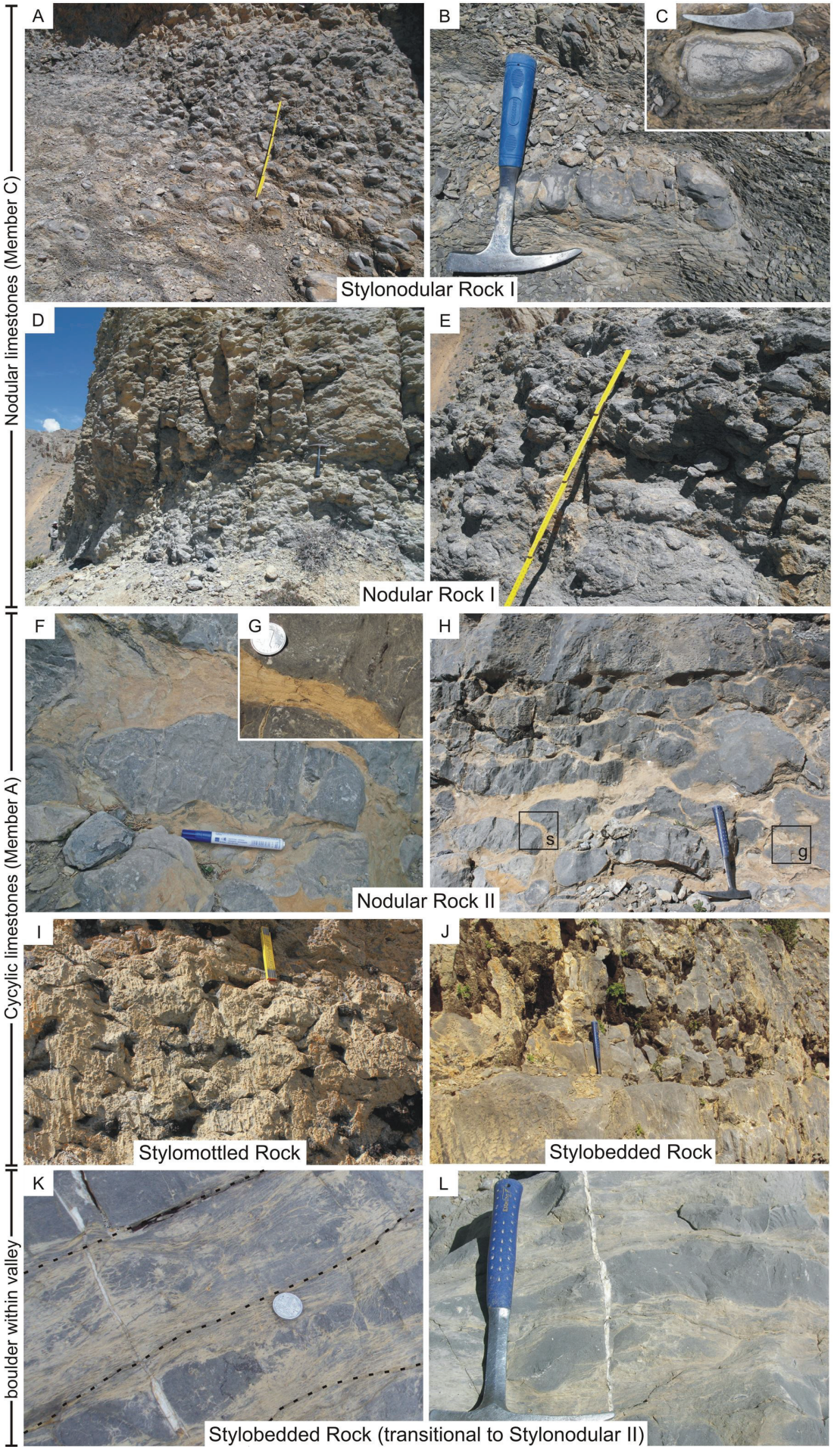
A
B
C
Stylonodular Rock I
D
E
Nodular Rock I
Nodular limestones (Member C)
F
G
H
s
g
Nodular Rock II
I
J
Stylomottled Rock
Stylobedded Rock
Cycylic limestones (Member A)
K
L
Stylobedded Rock (transitional to Stylonodular II)
boulder within valley

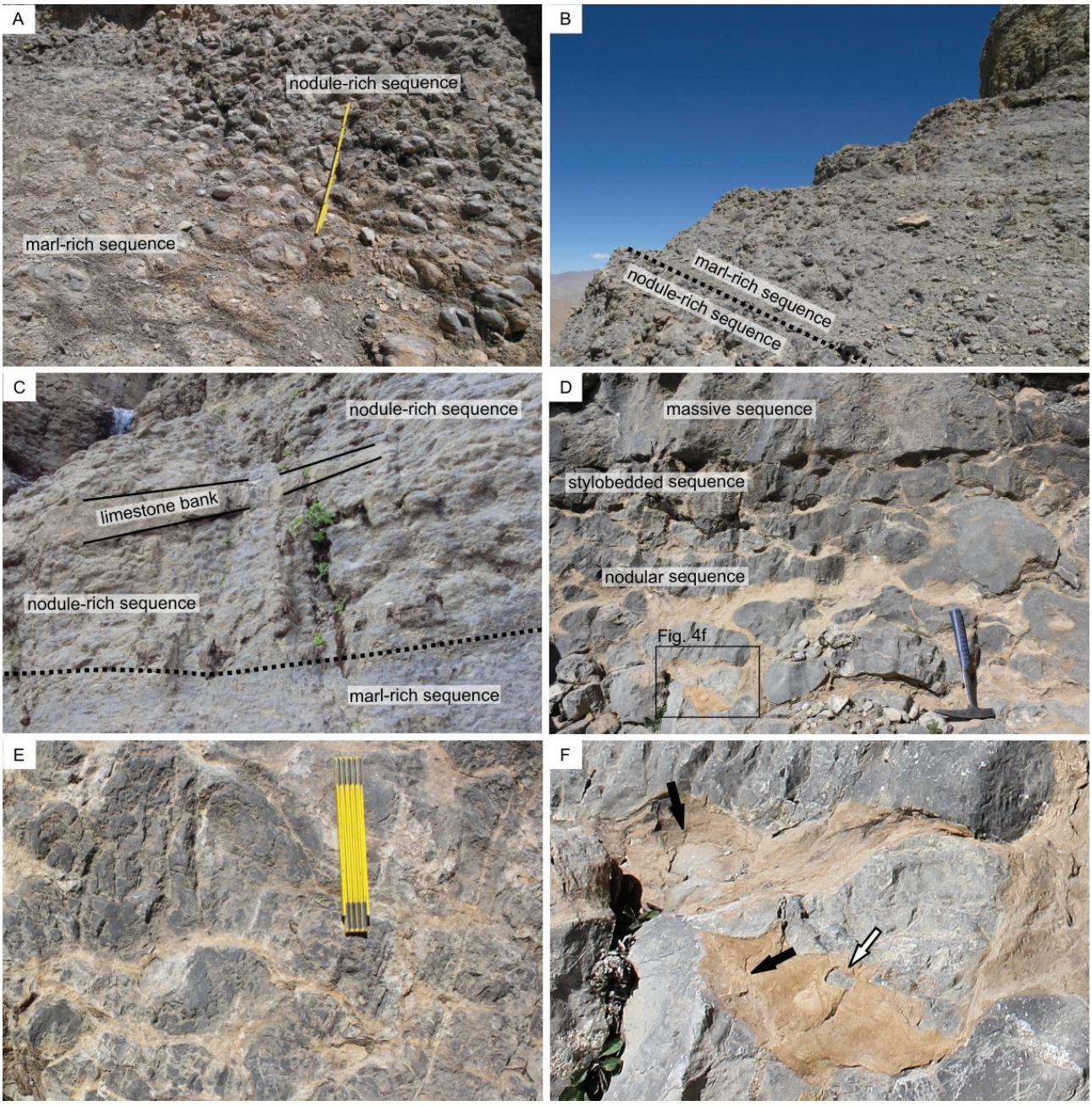

Figure 4.3: Field characteristics of nodular limestones. **a** Stylonodular Rock I of the nodular limestones (Member C) show gradual transitions from marl-rich to nodule-rich nodular limestones and sometimes even to slightly bedded sequences. **b** Nodular Rock I of the nodular limestones (Member C) showing alternations of marl-rich and nodule-rich sequences producing a cyclic appearance. **c** Nodular limestones (Nodular Rock I, Member C) are sometimes interrupted by well-bedded massive limestone banks. Those banks often taper out laterally, showing a gradual transition into the surrounding nodular-rich sediments. **d, e** Nodular Rock II (Member A) shows a gradual transition into the overlying stylobedded and massive limestones. Laterally, Nodular Rock II shows transitions into sediments described as stylobedded rock, transitional to stylonodular rock. **f** Within the brown layers of Nodular Rock II (Member A) the occurrence of small limestone fragments (white arrow) as well as grayish areas where the cemented sediments are partially dissolved (black arrows) is visible.

4.4.2 Nodular Rock I

In this category, the nodules are nearly spherical, with a size of 4–5 cm in diameter. The contact between the marly matrix and limestone nodules is gradual. Occasionally, a slight stylolaminated texture is visible, where marly layers are easily recognized. Typically the nodules produce a condensed to fitted fabric (Figs. 4.2d, 4.2e). Nodular Rock I occurs within the upper section part of Member C.

4.4.3 Nodular Rock II

This type of nodular limestone is characterized by occurrence of large-sized nodules with an elongated and subrounded to angular shape embedded in thick consolidated ”marl” layers (Fig. 4.2f). The difference in color of the nodules and the surrounding matrix is remarkable. While the limestone nodules appear dark gray, the marls are of brown color and exhibit a slight lamination (Fig. 4.2g). Nodules and surrounding marls produce an iden-supported fabric (Fig. 4.2h), characterized by sharp (s) and gradual (g) contacts. Nodular Rock II can be found in the fifth cycle of Member A, which is directly below the facies of Stylobedded Rock.

4.4.4 Stylomottled rock

Stylomottled rocks exhibit large angular limestone lenses, which produce a condensed to densely fitted fabric. Marls are restricted to pressure solution textures called interidenic stylolite patches in the carbonate rock, producing a stylomottled rock (Fig. 4.2i). This nodular rock type, which sometimes exhibits a cavernous appearance, is part of the third cycle of the cyclic limestones of Member A.

4.4.5 Stylobedded rock

Limestone nodules of this type of nodular limestone are large sized and angular. Marly interlayers are restricted to the interidenic stylolite seams between the nodules, producing an iden-supported fabric (Fig. 4.2j). Due to the occurrence of interidenic pressure solution structures, the rock is classified as stylobedded rock. Stylobedded rock appears in the upper part of the fifth cycle, as well as in the sixth and seventh cycle of Member A (cyclic limestones).

4.4.6 Other features/characteristic traits in field

In the field a transitional lithology between two of the above described nodule types was determined. This transitional nodular limestone type could be defined as stylobedded rock (transitional to Stylonodular II), which is characterized by large and very elongated, flattened nodules (Fig. 4.2k). Progressive sediment compaction generates additional clay seams alongside stylolites, creating a stylonodular texture. The stylobedded rock forms a condensed fabric, but due to stylolamination the limestone idens are separated, thus producing an iden-supported fabric (Fig. 4.2l). The nodules appear gray, while the pressure solution seams exhibit a brown color. This type of rock is a transitional member between stylobedded and stylonodular rocks

and can be classified as pre-nodular. Stylobedded rock (transitional to Stylonodular II) is not part of the investigated section part of the Zhepure Shan Formation, but appeared as an isolated boulder in the valley close to the cyclic limestones of Member A.

Another feature is the gradual transition from marl-rich to nodule-rich nodular limestones, intermittently to slightly bedded sequences, can be recognized within Stylonodular Rock I and Nodular Rock I (Fig. 4.3a). These transitional patterns frequently occur within the upper part of nodular limestones (Member C), originating in an alternation between the nodule-rich and marl-rich sequences, thus producing a cyclic sediment appearance (Fig. 4.3b). The nodular limestones of Member C are sporadically interrupted by occurrence of massive limestone banks, which can taper out laterally, exhibiting a gradual transition with the surrounding nodular limestones (Fig. 4.3c).

Similarly, Nodular Rock II exhibits a transition into overlying limestones, which is characterized by a massive but stylobedded appearance (Fig. 4.3d). Laterally, the limestones may also merge into sediments similar to those described as stylobedded rock transitional to Stylonodular Rock II (Fig. 4.3e). The very irregular and angular shaped limestone nodules of Nodular Rock II differ distinctly from the other nodular limestones described so far. In addition, small fragments of these nodules occur embedded in brown layers (Fig. 4.3f, white arrow) and within a grayish matrix where the cemented sediments are partially dissolved (Fig. 4.3f, black arrows).

4.5 Microfacial analysis and depositional environment

Based on the distribution and assemblages of marine organisms and sedimentary fabrics of the 442 investigated samples, six microfacies (MF) were established for the Zhepure Shan Formation at Tingri (Member A to Member C), (Fig. 4.4). Microfacies are described in an abrasive way. For detailed description of microfacies observed in Tingri and other localities of Tibet see Kahsnitz et al. (in prep.). Microfacies analysis is then used for the reconstruction of the depositional environment. In general, the cyclic limestones of Member A are mainly dominated by calcareous green algae, while the nodular limestones of Member C are dominated by larger benthic foraminifera (LBF).

Shallow benthic zones (SBZ) defined for Paleocene to Lower Eocene sediments of Tingri used within the following are taken from Zhang et al. (2013) and slightly modified by Kahsnitz et al. (2016).

Figure 4.4 ***(following page)*:** Lithologic section showing the stratigraphic distribution of defined nodular limestone types as well as microfacies (MF) in the Zhepure Shan Formation of Tingri. Shallow benthic zonation (SBZ) is taken from Zhang et al. (2013) and modified by Kahsnitz et al. (2016). Red lines indicate the four members of the formation, while the red dotted line represents the P-E boundary.
NRI Nodular Rock I, *NRII* Nodular Rock II, *SBR* stylobedded rock, *SMR* stylomottled rock, *SNRI* Stylonodular Rock I.

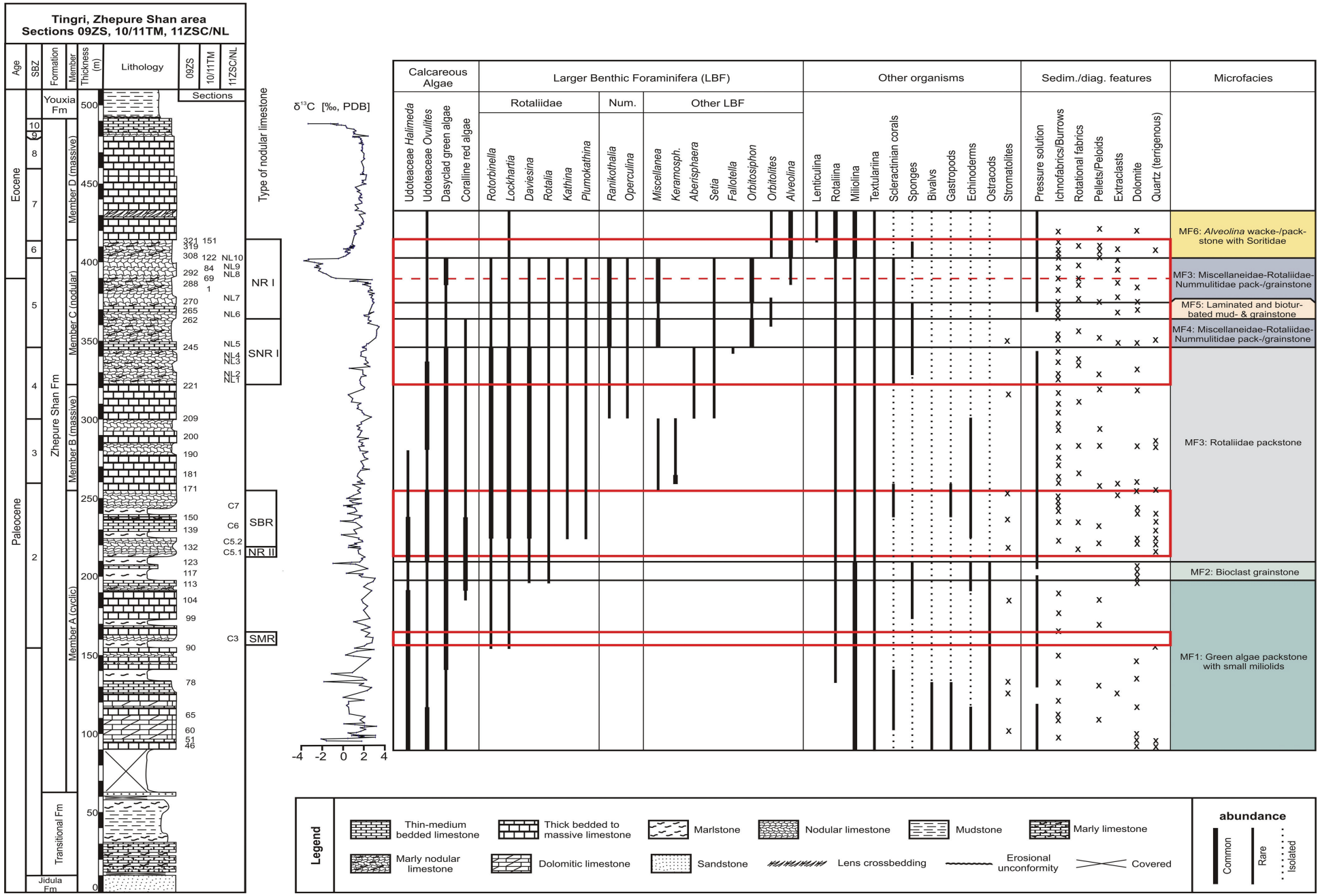
Tingri, Zhepure Shan area
Sections 09ZS, 10/11TM, 11ZSC/NL
Age
SBZ
Formation
Member
Thickness (m)
Lithology
09ZS
10/11TM
11ZSC/NL
Sections
Eocene
Paleocene
Youxia Fm
Zhepure Shan Fm
Transitional Fm
Jidula Fm
Member D (massive)
Member C (nodular)
Member B (massive)
Member A (cyclic)
Type of nodular limestone
NR I
SNR I
SBR
NR II
SMR
δ13C [‰, PDB]
-4 -2 0 2 4
Calcareous Algae
Udoteaceae Halimeda
Udoteaceae Ovulites
Dasyclad green algae
Coralline red algae
Larger Benthic Foraminifera (LBF)
Rotaliidae
Num.
Other LBF
Rotorbinella
Lockhartia
Daviesina
Rotalia
Kathina
Plumokathina
Ranikothalia
Operculina
Miscellanea
Keramosph.
Aberisphaera
Setia
Fallotella
Orbitosiphon
Orbitolites
Alveolina
Other organisms
Lenticulina
Rotaliina
Miliolina
Textulariina
Scleractinian corals
Sponges
Bivalvs
Gastropods
Echinoderms
Ostracods
Stromatolites
Sedim./diag. features
Pressure solution
Ichnofabrics/Burrows
Rotational fabrics
Pellets/Peloids
Extraclasts
Dolomite
Quartz (terrigenous)
Microfacies
MF6: Alveolina wacke-/packstone with Soritidae
MF3: Miscellaneidae-Rotaliidae-Nummulitidae pack-/grainstone
MF5: Laminated and bioturbated mud- & grainstone
MF4: Miscellaneidae-Rotaliidae-Nummulitidae pack-/grainstone
MF3: Rotaliidae packstone
MF2: Bioclast grainstone
MF1: Green algae packstone with small miliolids
Legend
Thin-medium bedded limestone
Thick bedded to massive limestone
Marlstone
Nodular limestone
Mudstone
Marly limestone
Marly nodular limestone
Dolomitic limestone
Sandstone
Lens crossbedding
Erosional unconformity
Covered
abundance
Common
Rare
Isolated

4.5.1 Microfacies 1: green algae packstone with miliolids

Fossil assemblage: Green algae *Halimeda* and *Ovulites* (Figs. 4.5a, 4.5b), miliolids, fragments of gastropods and bivalves.

Sedimentary/diagenetic features: Dolomite rhombs (Fig. 4.5c) or microspar, pressure solution seams, dissolved aragonite of green algae and gastropods/bivalves refilled with blocky calcite.

Depositional environment: Regarded as shallow lagoonal environment with low energy (Ghose, 1977; Wray, 1977).

Occurrence and type of nodular limestone: Cycle 1 to the lower part of cycle 4 of the cyclic limestones (Member A, lower part of SBZ2). Types of nodular limestones exhibiting MF1 are described as stylomottled rock.

4.5.2 Microfacies 2: bioclast grainstone

Fossil assemblage: Rotaliidae LBF (*Lockhartia*, *Daviesina*, *Rotorbinella*), miliolids, echinoids, corallinacean red algae (Fig. 4.5d).

Sedimentary/diagenetic features: Pressure solution structures, dolomite rhombs.

Depositional environment: In literature, this microfacies is described from the Zongpu section near Gamba by Li et al. (2015) and interpreted as deposited in shallow environments near shoal bars.

Occurrence and type of nodular limestone: Upper part of cycle 4 of the cyclic limestones (Member A, middle part of SBZ2). This microfacies covers the marly part of the fourth cycle and therefore is not part of a nodular sequence.

4.5.3 Microfacies 3: Rotaliidae pack-/grainstone

Fossil assemblage: Rotaliidae LBF, like *Lockhartia*, *Daviesina*, *Kathina* and *Plumokathina* (Fig. 4.5e) and green algae *Halimeda* and *Ovulites*. Locally, the LBF *Keramosphaerinopsis* and *Aberisphaera* occur.

Sedimentary/diagenetic features: Pressure solution seams, ichnofabrics, rotational fabrics, dolomite rhombs, microspar, dissolution and re-precipitation of aragonite shells.

Figure 4.5 ***(following page)*:** Microfacies (MF) 1–4 of the Zhepure Shan Formation of Tingri. **a, b** MF1: green algae packstone with miliolids, sample 09ZS46. **c** Dolomite rhombs forming the matrix of packstone fabrics, sample 09ZS51. **d** MF2: bioclast grainstone, sample 09ZS117. **e** Rotaliidae pack-/grainstone with green algae, sample 09ZS172. **f, g** MF3: Miscellaneidae-Rotaliidae-Nummulitidae pack-/grainstone, samples 09ZS262 and 09ZS292. **h** Burrow (ichnofabric) filled with algae debris and small benthic foraminifera, producing a circular swirl (arrows), indicative for bioturbation processes, sample 10TM7. *Al Alveolina*; *Co* Coralline red algae; *Ec* Echinoidea; *Ha Halimeda*; *Ka Kathina*; *Ke Keramosphaerinopsis*; *Lo Lockhartia*; *Mi Miscellanea*; *Os Orbitosiphon*; *Ov Ovulites*; *Pl Plumokathina*; *Ra Ranikothalia.*

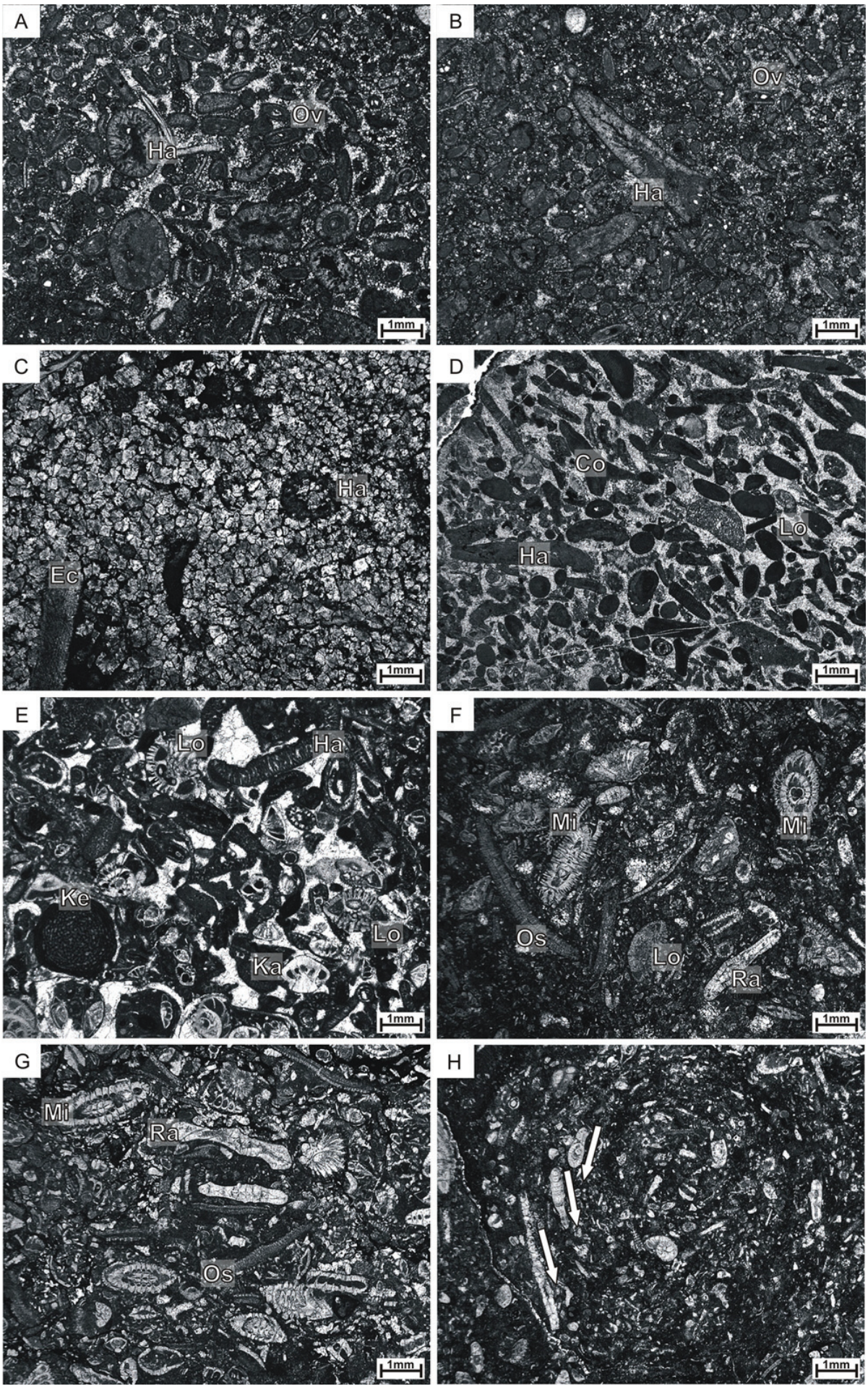
A
Ov
Ha
1mm
B
Ov
Ha
1mm
C
Ha
Ec
1mm
D
Co
Lo
Ha
1mm
E
Lo
Ha
Ke
Lo
Ka
1mm
F
Mi
Mi
Os
Lo
Ra
1mm
G
Mi
Ra
Os
1mm
H
1mm

Depositional environment: Representative for shallow subtidal and open marine environments with high water agitation (Reiss and Hottinger, 1984; Hottinger, 1997).

Occurrence and type of nodular limestone: MF3 can be found in the fifth to seventh cycle of cyclic limestones (Member A, upper part of SBZ2) showing nodular limestone types described as Nodular Rock II and stylobedded rock. Additionally, MF3 occurs within the lower part of the nodular limestones (Member C, upper part of SBZ4) described as Stylonodular Rock I.

4.5.4 Microfacies 4: Miscellaneidae-Rotaliidae-Nummulitidae pack-/grainstone

Fossil assemblage: LBF Miscellaneidae (Fig. 4.5f), Rotaliidae (e.g. *Lockhartia*, *Kathina*) and Nummulitidae (e.g., *Operculina*, *Ranikothalia*). Miliolid LBF, *Orbitolites* or *Alveolina* (Fig. 4.5g), act as accessory organisms.

Sedimentary/diagenetic features: Sometimes selectively dolomitic matrix, bioturbation (burrows and circular swirls filled with debris, Fig. 4.5h). Pressure solution structures (organisms, such as foraminifera, are often dissolved, especially in close contact with stylolites; Fig. 4.6a), rotational fabrics (Fig. 4.6b) and extraclasts (Fig. 4.6c).

Depositional environment: Representative for open marine depositions with low energy and water depths ranging from 60 to 90 m (Hottinger, 1973; Reiss and Hottinger, 1984; Hottinger, 1997; Beavington-Penney and Racey, 2004).

Occurrence and type of nodular limestone: Upper Paleocene of the nodular limestones (Member C, lower and upper part of SBZ5) of the Zhepure Shan Formation, described as Stylonodular Rock I and Nodular Rock I.

4.5.5 Microfacies 5: laminated and bioturbated mudstone and grainstone

Fossil assemblage: Rotaliid (e.g., *Lockhartia*) and nummulitid (e.g., *Operculina*, *Ranikothalia*) LBF in grainstone-type sediments. Miliolid LBF *Orbitolites* act as accessory organism. Mudstone-type sediments are poorly fossiliferous.

Sedimentary/diagenetic features: Mud- and grainstone-type sediments arranged in a laminated manner (Fig. 4.6d) are often strongly bioturbated (Fig. 4.6e).

Figure 4.6 ***(following page)*:** Microfacies (MF) 4–6 of the Zhepure Shan Formation of Tingri. **a, b** Organisms, such as foraminifera, are often partly dissolved along with to stylolite formation (**a**, sample 09ZS288) or show rotational fabrics (**b**, sample 10TM47). **c** Wackestone fabric of LBF, with rare fossil content and homogenous lithoclasts, sample 11TM122. **d, e** MF5: Laminated (**d**) and bioturbated (**e**) mudstone and grainstone, samples 09ZS264 and 09ZS265. **f** MF6: *Alveolina* wacke-/packstone with Soritidae, samples 11TM131. **g** *Alveolina* and miliolids often exhibiting strong recrystallization (white arrows) or borings (gray arrow), sample 09ZS319. **h** Ductile deformation (arrows) of *Alveolina* due to diagenesis, sample 09ZS308. *Al Alveolina*; *Le Lenticulina*; *Li* Lithoclast; *Mi* Miliolids; *Or Orbitolites*.

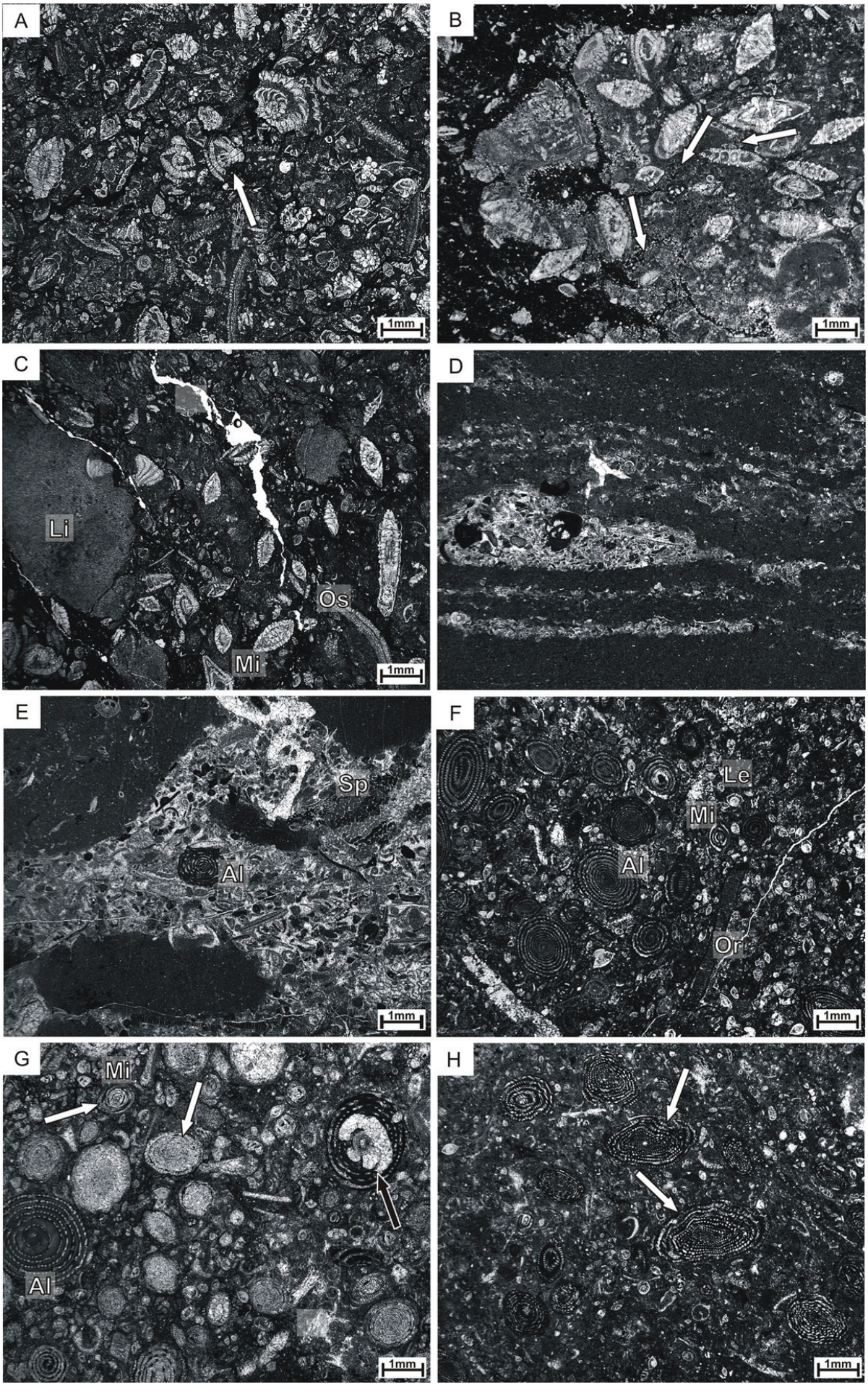
A
1mm
B
1mm
C
Li
Os
Mi
1mm
D
E
Sp
Al
1mm
F
Le
Mi
Al
Or
1mm
G
Mi
Al
1mm
H
1mm

Depositional environment: Suggesting deposition between a low-energy and high-energy environment resulting in an alternation of episodic storm-flows and quiet periods with deposition of lime mud sediments. Bioturbation is responsible for the characterized mixture of both sediments (Bádenas and Aurell, 2010).

Occurrence and type of nodular limestone: Within the middle part of the nodular limestones (Member C, middle part of SBZ5) described as Nodular Rock I.

4.5.6 Microfacies 6: *Alveolina* wacke-/packstone with Soritidae

Fossil assemblage: Alveolina and *Orbitolites* (Fig. 4.6f), small miliolids, benthic foraminifera *Lenticulina*.

Sedimentary/diagenetic features: Microspar and bioturbation. Sometimes the test of *Alveolina* and small miliolids show strong recrystallizations (Fig. 4.6g) described as ”diffusely microsparitic preservation” by Willems (1993, p. 75). Ductile deformation patterns of *Alveolina* due to diagenetic pressure solution can also be recognized (Fig. 4.6h).

Depositional environment: The occurrence of the LBF *Orbitolites* is indicative for restricted shallow environments with low energy (Hottinger, 1973; Reiss and Hottinger, 1984; Hottinger, 1997; Beavington-Penney and Racey, 2004). Cloudy and indistinct appearance of *Alveolina* and small miliolids is characteristic for freshwater diagenesis (Inden and Moore, 1983).

Occurrence and type of nodular limestone: MF6 appears within the upper part of the nodular limestones of Lower Eocene age (Member C, SBZ6), described as Nodular Rock I.

4.5.7 Interpretation of the depositional environment

The overall sedimentary evolution of the investigated section part of the Zhepure Shan Formation exhibits a transgressive phase within the Paleocene. It covers deposits of a restricted shallow-water lagoon of the inner carbonate ramp to the open marine outer carbonate ramp deposits, followed by a regressive phase within the Lower Eocene indicated by shallow-water deposits of the inner carbonate ramp.

The Lower Paleocene (lower SBZ2) cyclic limestones (Member A) at Tingri are dominated by green algae (MF1) representing a restricted shallow subtidal environment. Here from bottom to top, stylomottled rock as well as Nodular Rock II and stylobedded rock occur. The transition is from MF1 (green algae pack-/grainstone with small miliolids) over MF2 (bioclast grainstone) to MF3 (Rotaliidae packstone), and hence the change from a restricted to an open marine environment of the inner carbonate ramp does not effect the formation of a distinct type of nodular limestone. Additionally, the base of the nodular limestones of Member C is characterized by the occurrence of Stylonodular Rock I, exhibiting the same MF compared to the upper part of Member A, indicating an open marine environment.

Upper Paleocene and Lower Eocene (upper part of SBZ4 to SBZ6) nodular limestones are characterized by Stylonodular Rock I and Nodular Rock I, indicative of a depositional environment of a mid-carbonate ramp (MF4: Miscellaneidae-Rotaliidae-Nummulitidae pack-/grainstone; MF5: laminated and bioturbated mudstone and grainstone) to an inner carbonate ramp with shallow water, possibly interacting with a restricted open

marine lagoon environment and the influence of freshwater (MF6: *Alveolina* wacke-/packstone with Soritidae).

Although the cyclic limestones of Member A and nodular limestones of Member C show different types of nodular limestones, variations in microfacies and thus alterations in the depositional environment do not seem to effect the type of nodular limestone formations of the Zhepure Shan Formation.

4.6 Isotope and carbonate measurements

Isotope values (δ^{13}C, δ^{18}O), total organic carbon (TOC) and carbonate contents (CaCO3) were measured from ten specifically collected nodular limestone samples (Member C, samples 11ZSNL) and five samples from the cyclic limestone (Member A, 11ZSC) of the Zhepure Shan Formation. Limestone nodules and the surrounding marls were measured separately (Table 4.3) in order to retrieve more information on different lithofacies, hence the genesis of nodular limestone formation in South Tibet.

4.6.1 Isotope measurements

Oxygen isotopes of the nodular limestones (Member C) show a narrow range from –6.40 ‰ to –4.86 ‰ for the nodules itself, while the surrounding marly layers show more negative oxygen isotopes ranging from –12.65 ‰ to –6.31 ‰. Cyclic limestones (Member A) show a similar oxygen isotope pattern with higher δ^{18}O values for the limestone nodules ranging from –8.27 ‰ to –6.63 ‰ and –10.49 ‰ to –8.00 ‰ for the marls surrounding them. Limestone nodules of both, nodular and cyclic limestones are enriched in heavier oxygen isotopes compared to the marls (Fig. 4.7). The only exception was the cyclic limestone sample 11ZSC5.1, where the nodule was depleted in heavier oxygen isotopes (–11.46 ‰) compared to the marly layer (–9.35 ‰).

δ^{13}C values of the nodular limestones (Member C) vary between –2.55 ‰ and 2.88 ‰ for the nodules and –2.14 ‰ and 2.43 ‰ for the marly layers. Samples of cyclic limestones (Member A) exhibit a different carbon isotope pattern, where the nodules show lighter isotope values compared to the surrounding marly layers, ranging from 1.08 to 2.81 ‰ and 1.00 ‰ to 3.58 ‰, respectively.

In general, carbon isotope value variability is more profound in the nodular limestones than the cyclic limestones. This is mainly due to the fact that carbon isotopes in the cyclic limestones are only positive, while isotope values in the nodular limestones exhibit both, positive and negative values.

4.6.2 Interpretation of isotope values

Nodules of nodular and cyclic limestones are enriched in heavier oxygen isotopes compared to the marly layers showing average isotopic composition of –6.59 ‰ and –8.70 ‰, respectively. A similar trend is described from nodular limestones of the Vindhyan Basin (India) by Banerjee et al. (2006). Additionally, in Tingri some samples a characterized by very negative oxygen isotope values up to –12.65 ‰, suggesting the influence of subaerial exposure and the influence of isotopically light meteoric water, possibly leading to depleted δ^{18}O values (e.g., Heba et al., 2009; Swart, 2015). In thin sections feature characteristic for freshwater diagenesis like meniscus cements or bladed crystals (Flügel, 2010) could not be observed. Only

those samples from the upper part of the nodular limestones (Member C) show the influence of freshwater by the occurrence of strong recrystallized *Alveolina* and small miliolids. Sample 11ZSC5.1 determined as nodular rock show a different oxygen isotope pattern compared to other samples. Here the limestone nodule shows highly depleted oxygen isotope values in contrast to the surrounded consolidated ”marl” layers. This isotopic pattern may be described by the high amount of dolomite rhombs found in thin sections of this sample. Additionally, the brown color of the surrounding layer results from the presence of dolomite, effecting the isotopic composition of the sediments in a different way compared to the other samples of the cyclic limestones. Therefore isotope values of sample 11ZSC5.1 (Nodular Rock II, cyclic limestone) should be neglected.

Limestone nodules of the cyclic limestones (Member A) are depleted in carbon isotope values compared to the surrounding marls, but still exhibit positive values. Only, sample 11ZS5.1 exhibited a different pattern where the nodular portion is enriched in heavier carbon isotopes. A possible interpretation for the depletion of carbon isotope in the nodular portions could be an additional late phase of cementation, shifting carbon isotopes to lower values. This distinctive isotopic pattern is described in chalk sediments from Southern England and interpreted as a late phase of calcite cementation and marl seam formation due to pressure solution (Jeans, 1980). The marl seams are interpreted as ”the original bioclastic values of the chalk sediment unaffected by the addition of calcite cement, but modified by the selective loss of the finer calcite grains by pressure dissolution” (Jeans et al., 2012, p. 182). The interpretation of an additional late phase cementation, shifting the carbon isotopes to lower values is possibly inapplicable because sediments from Southern England are described as chalks, while sediments observed here are mainly limestones. Depletion of δ^{13}C is also described as a result of early cementation in the sulfate reduction zone, where the isotopically light dissolved inorganic carbon, normally accumulating ”in pore water of marine sediments as a consequence of bacterial oxidation of organic matter” (Küspert, 1982, p. 487), is bounded into the nodules.

Limestone nodules in the lower part of the nodular limestones (Member C, samples 11ZSNL1 to 11ZSNL7) exhibit positive δ^{13}C values and are enriched in heavier isotopes compared to the marls. In the literature, the heavier isotope enrichment in the limestone nodules of Member C is interpreted as a concentration of carbonate cements due to early diagenesis (Banerjee et al., 2006).

In the upper part of the nodular limestones (Member C, samples 11ZSNL8 to 11ZSNL10) the marly layers are also enriched in heavier carbon isotopes but show negative values compared to the cyclic limestones in the lower part of the Zhepure Shan section. In literature the Paleocene-Eocene boundary is described as being characterized by a short and abrupt episode of global warming, called Paleocene-Eocene Thermal Maximum (PETM), as well as a negative drop in carbon isotope composition, known as the carbon isotope excursion reflecting input of large amounts of carbon into the atmosphere (Bains et al., 1999; Dickens, 1999; Zachos et al., 2001; Aubry and Ouda, 2003). In Tingri the negative carbon isotope excursion (CIE) is described from one bed of nodular limestones (Member C) of the Zhepure Shan Formation showing a pronounced thickness and a large drop of carbon isotopes down to about –5 ‰ Zhang et al. (2013, 2017). Therefore negative carbon isotope values in the upper part of the nodular limestones (samples 11ZSNL8 to 11ZSNL10) are interpreted as being due to the beginning of the negative carbon isotope excursion (CIE) at the end of the Paleocene. Additionally, organisms like *Alveolina* and small miliolids show a cloudy and indistinct appearance indicative for the influence of freshwater diagenesis (Inden and Moore, 1983) shifting carbon isotopes to more negative values.

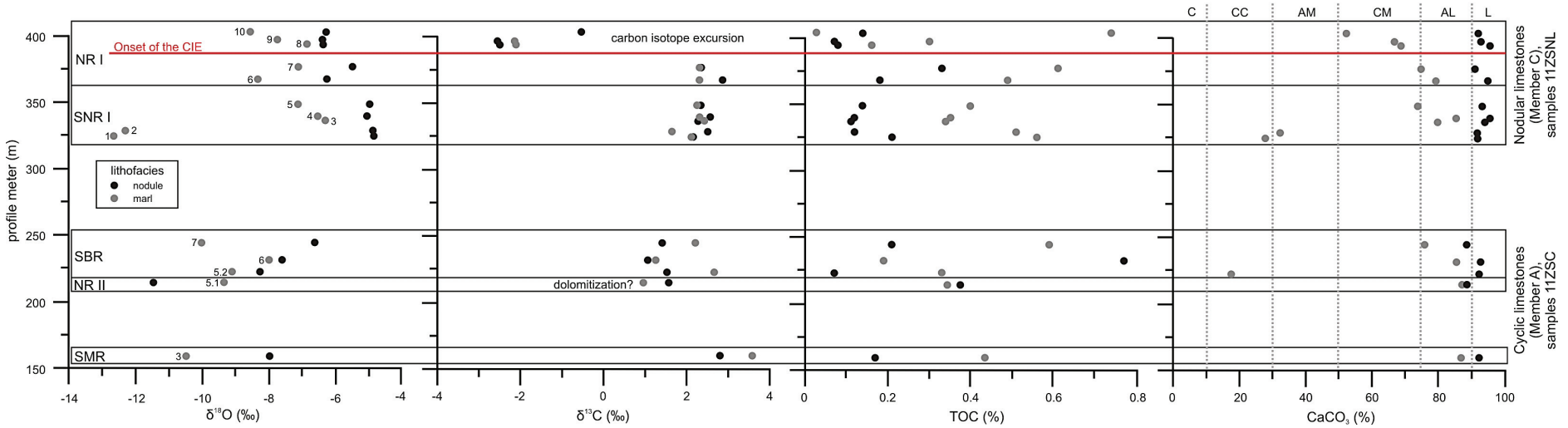

Figure 4.7: Isotopes values (δ^{18}O and δ^{13}C) and carbonate content (TOC and CaCO3) drawn against section meter for the different lithofacies (limestone nodules: black symbols; surrounding marls: gray symbols) of the nodular (Member C) and cyclic limestones (Member A). Sample numbers are marked in the diagram showing the δ^{18}O isotope values. *AL* argillaceous lime; *AM* argillaceous marl; *C* clay; *CC* calcareous clay; *CM* calcareous marl; *L* limestone.

Member	Type	sample	meter within formation	isotope data				carbonate data			
				δ^{18}O values (‰)		δ^{13}C values (‰)		TOC (%)		CaCO3 (%)	
				nodule	marl	nodule	marl	nodule	marl	nodule	marl
nodular limestones	Nodular Rock I	11ZSNL10	399	–6.29	–8.56	–0.53	–0.20	0.7	0.1	92.6	53.0
(Member C)		11ZSNL9	394	–6.40	–7.74	–2.55	–2.14	0.3	0.1	93.5	67.4
		11ZSNL8	391	–6.39	–6.86	–2.50	–2.11	0.2	0.1	96.3	69.5
		11ZSNL7	377	–5.50	–7.12	2.33	2.32	0.6	0.3	91.7	75.5
		11ZSNL6	368	–6.27	–8.33	2.88	2.31	0.5	0.2	95.5	79.9
	Stylonodular Rock I	11ZSNL5	349	–4.98	–7.13	2.34	2.25	0.4	0.1	93.9	74.4
		11ZSNL4	340	–5.07	–6.54	2.57	2.32	0.4	0.1	96.3	86.1
		11ZSNL3	337	–6.31	–6.31	2.28	2.43	0.3	0.1	94.7	80.4
		11ZSNL2	329	–4.89	–12.31	2.51	1.65	0.5	0.1	92.4	33.1
		11ZSNL1	325	–4.86	–12.65	2.15	2.12	0.6	0.2	92.6	28.5
cyclic limestones	Stylobedded rock	11ZSC7	245	–6.63	–10.02	1.41	2.21	0.6	0.2	89.4	76.4
(Member A)		11ZSC6	232	–7.61	–8.00	1.08	1.26	0.2	0.8	93.5	86.6
		11ZSC5.2	223	–8.27	–9.10	1.52	2.67	0.3	0.1	92.6	18.7
	Nodular Rock II	11ZSC5.1	215	–11.46	–9.35	1.58	1.00	0.3	0.4	89.1	88.1
	Stylomottled rock	11ZSC3	160	–7.97	–10.49	2.81	3.58	0.4	0.2	92.7	87.3
Limestone nodules and surrounding marly enveloping are measured separately											

Table 4.3: Isotope and carbonate data of nodular (Member C, section 11ZSNL) and cyclic (Member A, section 11ZSC) limestones of the Zhepure Shan Formation NE of Tingri.

4.6.3 Total organic carbon and carbonate content

In Member C of the nodular limestones the total organic carbon (TOC) is lower in the lithified limestone nodules than in the surrounding marly layers, ranging from 0.2 % to 0.7 % and 0.1 to 0.3 %, respectively (Fig. 4.7). Compared to this, cyclic limestones (Member A) show a highly disordered pattern, where TOC is enriched within the nodule or the marly layer, alternately. Here total organic carbon ranges from 0.2 % to 0.6 % for limestone nodules and 0.1 % to 0.8 % for marly layers.

Nodular limestone (Member C) and cyclic limestone (Member A) carbonate content measurements indicate higher carbonate contents in the limestone nodules than the surrounding marls or sediments from stylolites. The carbonate contents of the nodules in Member C vary between 91.7 % and 96.3 %, while the surrounding marls exhibit carbonate contents ranging from 28.5 % to 86.1 %. Limestone nodules of the cyclic limestones of Member A exhibit carbonate contents ranging from 89.1 % to 93.5 %, whereas in the adjacent marls and sediments from stylolites, they vary between 76.4 % and 88.1 %. In general, the limestone nodules are enriched in carbonate, with values consistently above 89 %, while the marls and sediments from stylolites vary between ∼19 % and ∼88 %.

4.6.4 Interpretation of carbonate content

Differences in carbonate content between the nodules and the encircling marls can be explained by differential diagenesis (Reinhardt et al., 2000; Westphal et al., 2000). This process is described by limestone-marl alternations, where limestone layers experience different diagenetic processes (e.g., cementation) in contrast to the marly layers (e.g., compaction phenomena). In the marly layers, where a combination of compaction and dissolution happens, the released carbonate migrates to the adjacent limestone layers or nodules where it is absorbed and re-precipitated (e.g., Bathurst, 1975; Eder, 1982; Ricken, 1986, 1987; Möller and Kvingan, 1988; Munnecke and Samtleben, 1996). Therefore, the limestone nodules, which act as ”receptor limestones”, are diagenetically further enriched by carbonate compared to the surrounding marls, which act as ”donor limestones” and therefore lose their carbonate content through diagenesis (Bathurst, 1975).

Based on the carbonate content sediments can be classified from clay (carbonate content 0–10 %) and calcareous clay (carbonate content 10–25 %), via argillaceous marl (carbonate content 25–50 %) and calcareous marl (50–75 %), to argillaceous lime (carbonate content 75–90 %) and limestone (90-100 %), (after Füchtbauer, 1988). Marls and sediments from stylolites of nodular limestones in South Tibet show carbonate contents varying between ∼19 % and ∼88 % or, based on the terms used before, ranges from calcareous clay to argillaceous lime. Cyclic limestones (stylomottled rock, Stylonodular Rock II and stylobedded rock) show high carbonate content (75–88 %) in nearly every ”marl” or sediment from stylolites and therefore are called argillaceous lime. Compared to this the carbonate contents of marly layers from nodular limestones (Nodular Rock I and Stylonodular Rock I) mostly vary between ∼53 and ∼86 %, classified as calcareous marl and argillaceous lime.

4.7 Origin of nodular limestones

The investigated Zhepure Shan Formation shows five different types of nodular limestones (Nodular Rock I, Nodular Rock II, Stylobedded Rock, stylomottled rock, Stylonodular Rock I, stylomottled rock) and several transitional textures in between these types, recognized based on their appearance in the field.

In most cases the Paleocene to Lower Eocene nodular limestones of the Zhepure Shan Formation show regularly formed, rounded to subrounded limestone nodules with weak bedding features indicating an early diagenetic genesis in a shallow-marine environment (Fig. 4.8). In literature nodular limestones are described as being deposited in intratidal to supratidal settings with evaporative conditions (Boggs, 2009; Patra and Singh, 2015). Features characteristic for evaporative environments (e.g., authigenic evaporite like anhydrite) could not be observed in Tingri. Other possibilities for the genesis of nodular limestones are storm activities on platforms and ramps (Burchette and Wright, 1992; Bádenas and Aurell, 2010) or even tectonic origin (Böhm et al., 1995). Nodular limestones formed due to storm or tectonic activities mostly show sharp boundaries, angular limestone nodules and are not bed-parallel arranged (e.g., Banerjee et al., 2006; Flügel, 2010). In Tingri, some types of nodular limestones show sharp boundaries between limestone nodules and ”marly” layers and/or sediments in stylolites (e.g, Stylonodular Rock I or stylobedded rock) or even angular limestone lenses (e.g., Nodular Rock II). Nevertheless storm or tectonic activities are ruled out as the limestone nodules often show a bed-parallel arrangement and the sharp and angular boundaries seem to be the result of pressure-solution and the formation of transitional types of nodular limestones.

In general, differences in the depositional environment, based on observations of microfacial assemblages, do not coexist with the changes in nodular limestone textures. Nevertheless, investigations showed, that cyclic limestones (Member A) tend to produce stylomottled rock, stylobedded rock (and stylobedded rock transitional to Stylonodular Rock II) and Nodular Rock II, where marly layers and/or sediments from stylolites seem to be more consolidated and the number of nodules was less compared to those from Nodular Rock I and Stylonodular Rock I of the nodular limestones (Member C). High carbonate content of more than 80 % in most of the ”marly” layers (rather: argillaceous lime) and/or sediments from stylolites support those field observations.

In literature, variations in the intensity of nodule formation are described by Jenkyns (1974, p. 254): ”The degree of nodularity–i.e., the degree of differentiation between nodule and matrix–is roughly proportional to the clay content of the whole rock. If the total clay content is high, the nodules can often be prized out with a finger...” (see also Lucas, 1955; Fabricius, 1966). Therefore, we assume that during deposition, primary sedimentary processes may produce slight compositional differences in organic matter, carbonate sediment (mixture of calcite and aragonite) and terrigenous clay, forcing the genesis of different types of nodularity in limestones. Differences like nodule-rich and marl-rich sequences within one type of nodular limestones as defined earlier in this paper, as well as the disruption of nodular limestone formation due to intercalated limestone banks support the assumption of a primary heterogenic sediment composition.

Marly layers are dominated by dissolution seams, sometimes producing a stylolaminated fabric and therefore represent the preferred site of chemical compaction (Bathurst, 1987; Munnecke and Westphal, 2004; Banerjee et al., 2006; Banerjee and Jeevankumar, 2007). Compared to this, limestone nodules exhibit only few compaction features like stylolites, indicating that first carbonate cementation started just before the compaction of sediments due to overburden (pre-compactional sedimentation). Bioturbation features

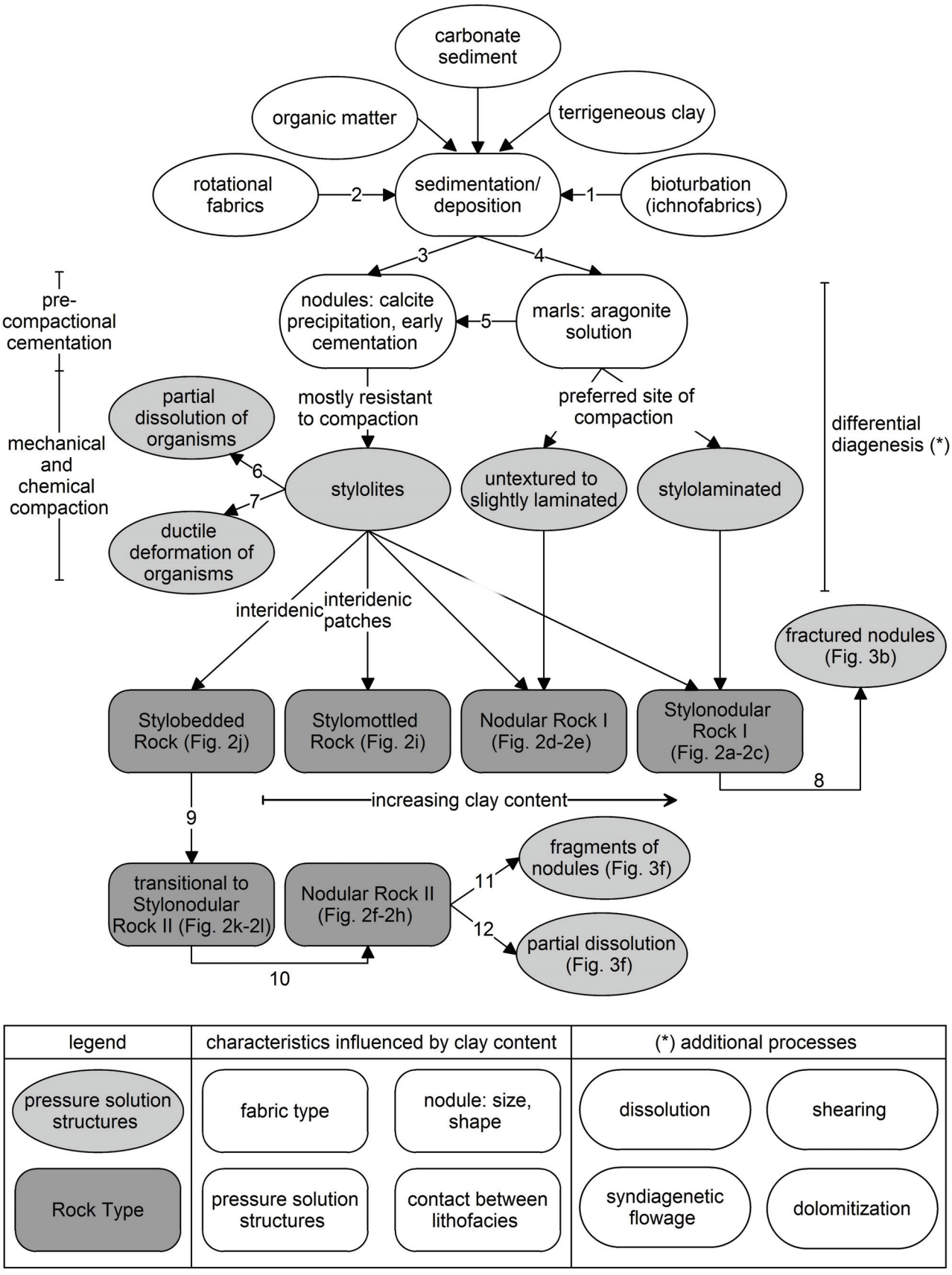

Figure 4.8: General model showing the diagenetic processes leading to the formation of the different types of nodular limestones (Stylonodular Rock I, Nodular Rock I and Nodular Rock II, stylomottled rock, stylobedded rock and stylobedded rock transitional to Stylonodular Rock II limestones) typical for the Zhepure Shan Formation. Numbers at arrows are described in text.

identified in the limestone nodules due to the occurrence of ichnofabrics (burrows, circular swirls) took place before the first phase of cementation as well (Fig. 4.8, arrow 1). The concentric arrangement of organisms, typically larger benthic foraminifera here is described as rotational fabrics (Fig. 4.8, arrow 2). In South Tibet this phenomenon is also described as ”convolute structures” by Willems (1993, p. 76). Deposition of sediments on an inclined carbonate ramp, as expected for sediments at passive continental margins and the overburden due to further sedimentation may result in the motion of the unconsolidated sediments (before cementation), ”if the components of gravity exceed the frictional or plastic flow limits of the sediment” (von Engelhardt, 1973, p. 93). Semiconsolidated sediments with high clay contents are preferred to begin movement, which is due to the thixotropic behavior of clay minerals. Dissolution seams, filled with clay minerals, therefore act as glide surfaces, reducing stress (overburden due to further sedimentation) via lateral shearing (von Engelhardt, 1973; Wanless, 1979; Heim, 1990). Therefore, the occurrences of rotational fabrics in South Tibet are interpreted as syndiagenetic flowage and shearing processes (Willems 1993). These allochthonous processes are assumed to act on small scales, without destroying the entire sedimentary unit. Variations in clay content of just a few percent (Zankl, 1969; Kennedy and Garrison, 1975) can result in a selective cementation, where sediments with high carbonate contents prefer early cementation (Fig. 4.8, arrow 3). Delayed cementation (Fig. 4.8, arrow 4) took place in sediments with lower carbonate and higher clay contents (Hallam, 1964; Ricken, 1986; Einsele et al., 1991; Banerjee et al., 2006).

In carbonate sedimentology, the source of carbonate cement to lithify sediments without compaction is discussed heavily (Bathurst, 1975; Raiswell, 1988; Ricken and Eder, 1991; Westphal et al., 2000). Because first cementation takes place before the mechanical compaction, pressure solution is not responsible for the cement to firstly lithify the limestone nodules. Therefore, we assume aragonite dissolution as the calcite donor within the aragonite dissolution zone (ASZ) and re-precipitation as calcite cement (microspar) within the limestone nodules (Westphal et al., 2000) which then produces a rigid framework to withstand subsequent mechanical compaction. Vertical gradients are described being trigger for aragonite dissolution in pore-water geochemistry, possibly due to microbial decomposition of organic matter in shallow-burial environments, resulting in vertical geochemical gradients (Canfield and Raiswell, 1991; Munnecke and Samtleben, 1996). Due to overburden sediments, further carbonate is dissolved within still unconsolidated portions of the sediment (marls) and subsequently re-precipitated within limestone layers (Fig. 4.8, arrow 5) due to differential diagenesis (e.g., Bathurst, 1975; Eder, 1982; Ricken, 1986, 1987; Möller and Kvingan, 1988; Munnecke and Samtleben, 1996).

In thin sections, chemical compaction can be recognized by the occurrence of stylolites (single or sets), as well as the dissolution (Fig. 4.8, arrow 6) and ductile deformation (Fig. 4.8, arrow 7) of tests of organisms affected by pressure solution. At times, reactate minerals (e.g., dolomite) can be found inside or close to the solution interfaces.

Non-sutured seam solutions (similar to stylolamination as described by Logan and Semeniuk (1976)) are being formed in sediments that contain a significant amount of clay, typically producing nodular limestones (Wanless, 1979). Because of the occurrence of highly stylolaminated marls surrounding the nodules as well as the fact that the nodules can easily be sampled, Stylonodular Rock I sediments in the Zhepure Shan Formation are assumed to comprise a higher amount of clay compared to other nodular types. This is supported by lower carbonate contents declaring most of the surrounding layers as calcareous marls, while marls and sediments from stylolites and other types of nodular limestones are classified as argillaceous lime. The ongoing

compaction processes, which are due to overburden, as well as shearing processes, are responsible for the formation of fractured nodules in the group of Stylonodular Rock I (Fig. 4.8, arrow 8).

Sediments of the Nodular Rock I type are assumed to contain a significant content of clay because the limestone nodules are embedded in very soft marly layers of minor carbonate cementation showing an untextured to slightly laminated appearance. The carbonate contents of Stylonodular Rock I and Nodular Rock I of nodular limestones support this by showing generally lower carbonate values for the marls compared to the marly layers of the cyclic limestones.
In contrast to this, the sediments classified as stylomottled and stylobedded contain interidenic patches of stylolites as well as interidenic stylolites, forming big limestone nodules creating a condensed fabric, which makes it difficult to sample single limestone nodules from here. Therefore, the clay content is assumed to be lower compared to Nodular Rock I and Stylonodular Rock I as described earlier. High carbonate content in the surrounding layers and sediments from stylolites called argillaceous lime support this.

Sediments defined as Nodular Rock II show gray subrounded to angular shaped limestone nodules within brown marl layers. The contact between the two lithofacies is described as typically sharp, although some gradual portions may exist. The vertical transition into the stylobedded rocks type and the lateral transition into the defined stylobedded rock transitional to Stylonodular Rock II as described above indicate that the genetic transitions of those types of nodular limestones are merging. Here it is assumed that compaction of massive limestone banks will result in limestones described as stylobedded rock by producing interidenic stylolites and a condensed fabric of nodules. Compaction and shearing processes in stylobedded rock sediments will merge with stylonodular sediments (transitional to Stylonodular Rock II; Fig. 4.8, arrow 9). Further overburden, compaction and shearing may result in sediments characterized as Nodular Rock II (Fig. 4.8, arrow 10). The occurrence of limestone fragments (Fig. 4.8, arrow 11) and partially dissolved limestone nodules (Fig. 4.8, arrow 12) within the brown ”marls” (argillaceous lime) of Nodular Rock II, as well as the gradual transition into stylobedded and stylonodular sediments, support this assumption.
Nodular Rock II is part of the cyclic limestone (Member A) and represented by the sample 11ZSC5.1. This sample exhibits a different isotopic composition in the gray limestone nodules and the surrounding brown marl layers compared to the other samples of Member A. Different degrees of dolomitization within these sediments are responsible for the remarkable color and isotopic differences.

Limestone nodules from the cyclic limestones are depleted in heavy carbon isotopes compared to marls. Therefore, we assume that a late cementation process affected the isotopic composition of the nodules.

4.8 Conclusions

Microfacial and geochemical analyzes of Paleocene to Lower Eocene sediments reveal information on the genesis of nodular limestones in Tingri (South Tibet):

1. Variable clay contents in carbonate rocks are responsible for the genesis of five different types of nodule fabrics of the Zhepure Shan Formation (Tingri, South Tibet): Stylonodular Rock I, Nodular Rock I, Nodular Rock II, stylomottled rock, stylobedded rock.

2. The surrounding layers and sediments from stylolites of cyclic limestones (Member A) contain higher carbonate content compared to those from nodular limestones (Member C).

3. Observations of nodular limestones in Zhepure Shan Formation, with regard to the carbon isotope excursion (CIE) at the Paleocene-Eocene boundary, suggest that sediments are formed in-situ due to autochthonous processes: pre-compactional cementation followed by mechanical and chemical compaction.
4. Still, other processes like shearing and syndiagenetic flowage can be observed (e.g., fractured nodules, rotational fabrics), representing allochthonous processes without destroying the entire sedimentary unit.

Acknowledgements

We thank Dr. Q. Zhang, F. Wieseler, A. Hübner and C. Schott for their assistance with field and laboratory work. We gratefully thank the reviewers for their critical remarks and thorough review of the manuscript. This project is part of the priority program 1372 Tibetan Plateau: Formation - Climate - Ecosystem (TiP) and is funded by the German Science Foundation (DFG Wi725/29) and the University of Bremen (Germany).

5 Conclusions and future perspectives

5.1 Conclusions

Biostratigraphic, microfacial, sedimentary and isotope analyses of sections from the passive Indian (Tethyan Himalaya, sections at Chulung Chu, Tingri, Gamba and Guru) and active Asian continental margin (Xigaze forearc strata, section at Cuojiangding) reveal several results concerning the general biostratigraphical, paleoenvironmental and geodynamic evolution in the eastern Neo-Tethyan Ocean. The following conclusions were drawn from the observations of this work:

1. Sediments of the eastern Neo-Tethyan Ocean show a two-stepped deepening event from Paleocene to Lower Eocene (Chapter 2).

Investigations of sediments from the eastern Neo-Tethyan Ocean exhibit strong similarities in the stratigraphic succession of eleven microfacies from the passive Indian continental margin (microfacies P1 to P11; sections from Chulung Chu, Tingri, Gamba and Guru) and four microfacies of the active Asian continental margin (microfacies A1 to A4; section from Cuojiangding). Correlation of observed microfacies provides a detailed overview of the paleoenvironmental development and the sedimentary history showing an overall deepening process during Paleocene to Lower Eocene from the shallow-water restricted/lagoonal part up to an open marine environment with water depths up to 80 m. This deepening trend is interrupted by a short-term shallowing event at or close to the Paleocene-Eocene boundary, resulting in a two-stepped deepening event lasting from Lower Paleocene to Lower Eocene in all observed sections.

Detailed microfacies analysis at Gamba, showing the two-stepped deepening event has been carried out by Li et al. (2015). Our work shows, that the occurrence of this event can be recognized in sediments from the passive Indian, as well as the active Asian continental margin and therefore can be found in the entire eastern Neo-Tethyan Ocean.

2. Similar stratigraphic distribution pattern of the larger benthic foraminifera (LBF) *Lockhartia* in the Tethyan Himalaya of South Tibet (Chapter 3).

Paleocene to Lower Eocene shallow-water limestones of Tingri, Gamba and Guru in the Tethyan Himalaya of South Tibet show the stratigraphic ranges of seven species of the LBF genus *Lockhartia* (*L. conditi*, *L. haimei*, *L. hunti*, *L. praehaimei*, *L. retiata*, *L. roeae* and *L. tipperi*). Based on the stratigraphic distribution of these species five interval biozones (called ”*Lockhartia*” biozones) were defined with a similar pattern in all three observed profiles, showing that a regional stratigraphic correlation of South Tibet is possible.

Indicative is the increasing diversification of *Lockhartia* from Middle to Late Paleocene (up to 5 species) and a reduction of diversity within the Lower Eocene (down to 2 species).

3. Early evolution of the genus *Lockhartia* in the eastern Neo-Tethyan Ocean, called Lockhartia Sea, compared to the western Neo-Tethys (Chapter 3).

Based on the great diversity of the LBF genus *Lockhartia* in the Paleocene Ranikot Formation from India, the eastern Neo-Tethyan Ocean was also called "Ranikot Sea" (Davies, 1937) or "Lockhartia Sea" (Hottinger, 1998). The detailed biostratigraphic studies on the distribution of *Lockhartia* in the different sections were used to generate a generalized stratigraphic distribution pattern of *Lockhartia* in South Tibet. Comparison of the stratigraphic distributions of some *Lockhartia* through the entire Neo-Tethyan Ocean exhibit an earlier evolution in the eastern Neo-Tethyan Ocean compared to the western region as a result of different latitudinal positions of the ocean basins. During the Paleocene, the western Neo-Tethyan Ocean was located at lower to middle latitudes of the northern hemisphere characterized by coralgal assemblages, while the eastern part was located at equatorial latitudes where LBF predominate as reported by Scheibner and Speijer (2008).

4. Genesis of 5 different types of nodular limestones in Tingri due to variations in clay and carbonate content (Chapter 4).

Five types of nodular limestones (Stylonodular Rock I, Nodular Rock I, Nodular Rock II, stylobedded rock, stylomottled rock) and some transitional textures between them (stylobedded rock transitional to Stylobedded Rock II) could be recognized in the sediments of Tingri (South Tibet), based on their appearance in field. Those different types of nodular limestones are described to be the result of differences in the primary composition (organic matter, carbonate sediment and terrigenous clay) during sedimentation. Primary differences of sediment composition then results in different diagenetic behaviors, where sediments with high carbonate and low clay contents prefer early cementation, while low carbonate and high clay contents obtain delayed cementation (differential diagenesis). Ongoing diagenetic processes resulted in the formation of different types of nodular limestones.

5. Autochthonous formation of nodular limestones in Tingri (Chapter 4).

Autochtonous diagenetic processes like pre-compactional cementation, mechanical and chemical compaction (including dissolution and reprecipitation of carbonate), resulted in the genesis of nodular limestones in South Tibet. The occurrence of rotational fabrics and fractured limestone nodules are indicative for a syndiagenetic flowage of the deposited sediments due to the inclination of the carbonate ramp of the passive continental margin, the increasing pressure due to overburden sediments and the thixotrophic behavior of clay minerals. In South Tibet those allochthonous processes just show minor occurrences without destroying the entire sedimentary unit. Therefore it is suggested, that the sediments are formed in-situ due to autochthonous processes.

5.2 Future perspectives

The knowledge obtained from biostratigraphic, microfacial, sedimentary and geochemical analyzes of Paleocene to Lower Eocene sediments deposited in the eastern Neo-Tethyan Ocean can be improved by further research on following aspects:

1. Further studies on selected larger benthic foraminifera of the Tethyan Himalaya

Paleocene sediments of Tingri and Gamba show a short but considerable and consecutive appearance of two larger benthic foraminifera (LBF) described as *Keramospherinopsis haydeni* and *Aberisphaera gambanica*. Due to their high abundances and limited biostratigraphic ranges they are taken as index fossils for SBZ3 and SBZ4, respectively (Zhang et al., 2013). In this work we observe a complete new section close to the village of Guru. Microfacies analysis of the Langzhu Formation of Guru show a similar but not identical stratigraphic distribution pattern for these two LBF.

In the lower part of the Langzhu Formation *Keramosphaerinopsis* and *Aberisphaera* show the same short-term and consecutive distribution similar to the distribution in Tingri and Gamba representing SBZ3 and SBZ4, respectively. Unlike at Tingri and Gamba, at Guru a second short-termed and consecutive appearance but inverse succession of both LBF can be recognized within SBZ5 (Kahsnitz and Willems, in press).
Additionally, the occurrence of *Aberisphaera* in the Zhepure Shan Formation in Tingri is accompanied by a short-term occurrence of the LBF *Fallotella* within the upper part of SBZ4 (Zhang et al., 2013), unverifiable in sediments of Gamba and Guru.
Further studies on the selected larger benthic foraminifera *Keramosphaerinopsis*, *Aberisphaera* and *Fallotella* in the Tethyan Himalaya may help to understand the paleoenvironmental and/or paleoecological differences along the northern passive Indian continental margin.

2. Carbon isotope excursion (CIE)

The Paleocene-Eocene boundary in sediments is characterized by the occurrence of a sharp negative trend in the δ^{13}C isotope-curve, called the carbon isotope excursion (CIE), described from terrestrial, as well as from shallow-water and deep-sea sediments with different thicknesses (e.g., Koch et al., 1995; Bains et al., 1999; Dupuis et al., 2003; Koch et al., 2003; Wing et al., 2005). In South Tibet the CIE is located in shallow-water nodular limestones of the Zhepure Shan Formation, showing an extraordinary thickness (Zhang et al., 2013, 2017), compared to other marine depositions like sediments from the Ocean Drilling Program site 690 (Bains et al., 1999) or from Egypt (Dupuis et al., 2003). In respect to the extraordinary thickness of the isotope excursion, sedimentary and geochemical investigations of this work suggest that those nodular limestones in Tingri (South Tibet) are formed in-situ due to autochthonous processes. Therefore also the extraordinary thickness of the CIE in Tingri is supposed to be of primary origin.

Investigations of Paleocene larger benthic foraminifera show no changes to the onset of the CIE as described from other shallow-marine sediments. In Tingri the change in foraminiferal assemblage is recognized within the Lower Eocene, where the initial recovery of the CIE starts (Zhang et al., 2013 and this work).

Additional paleontological, sedimentological and geochemical studies of the sediments in Tingri may help to understand the extraordinary thickness of the CIE, as well as the distribution of shallow-marine organisms and the diagenesis of sediments with respect to the geochemical and climatic changes of the CIE-PETM interval.

3. Clay mineral analysis

Investigations on nodular limestones showed, that variations in primary composition of the sediments resulted in the genesis of five different types of nodule fabrics in Tingri (South Tibet). Here we assume, that especially the amount of clay in the sediment is responsible for differences in size and shape of nodules, the amount and structural appearance of the surrounding marls, as well as the contact between the two lithofacies. An important aspect in respect to the genesis of nodular limestones could be the thixotropic behavior of some clay minerals according to the water content incorporated in their crystal lattice.

Thixotropy described the variation of viscosity of certain gels or fluids, from high-viscous to a low-viscous gel/fluid, due to mechanical stress (e.g., shearing). When the stresses were reduced the medium went back into its original viscosity (Heim, 1990). It is suggested, that the thixotropic behavior of clay minerals possibly facilitate the genesis of nodules due to processes like overburden and shearing. Therefore further observation and analysis on the clay minerals via X-ray powder diffraction (XRPD) will help to get more information about the genesis of nodular limestones in Tingri.

References

Abed, A. M. and Schneider, W. (1980). A General Aspect in the Genesis of Nodular Limestones Documented by the Upper Cretaceous Limestones of Jordan. *Sedimentary Geology*, 26:329–335.

Accordi, G., Carbone, F., and Pignatti, J. (1998). Depositional history of a Paleogene carbonate ramp (West Cephalonia, Ionian Islands, Greece). *Geological Romana*, 34:131–205.

Afzal, J., Khan, F. R., Khan, S. N., Alam, S., and Jalal, M. (2005). Foraminiferal Biostratigraphy and Paleoenvironments of the Paleocene Lockhart Limestone from Kotal Pass, Kohat, Northern Pakistan. *Pakistan Journal of Hydrocarbon Research*, 15:9–23.

Afzal, J., Williams, M., and Aldridge, R. J. (2009). Revised stratigraphy of the lower Cenozoic succession of the Greater Indus Basin in Pakistan. *Journal of Micropaleontology*, 28:7–23.

Afzal, J., Williams, M., Leng, M. J., Aldridge, R. J., and Stephenson, M. H. (2011). Evolution of Paleocene to Early Eocene larger benthic foraminifer assemblages of the Indus Basin, Pakistan. *Lethaia*, 44:299–320.

Aitchison, J. C., Ali, J. R., and Davies, A. M. (2007). When and where did India and Asia collide? *Journal of Geophysical Research*, 112:1–19.

Al-Hashimi, H. A. J. (1974). Alveolinidae and Rotaliidae from the Eocene Dammam Formation. *Journal of the Geological Society of Iraq*, 8:51–74.

Ali, J. R. and Aitchison, J. C. (2005). Greater India. *Earth-Science Reviews*, 72:169–188.

Applin, E. R. and Jordan, L. (1945). Diagnostic Foraminifera from Subsurface Formation in Florida. *Journal of Paleontology*, 19:129–148.

Applin, E. R. and Jordan, L. (1950). "*Lockhartia*" *cushmani* Applin and Jordan and Notes on Two Previously Described Foraminifera from the Tertiary Rocks in Florida. *Journal of Paleontology*, 24:474–478.

Arbeitskreis deutscher Mikropaläontologen (1962). *Leitfossilien der Mikropaläontologie.* Bornträger.

Auboin, J. and Neumann, M. (1959). Contribution a l'étude stratigraphique et micropaléontologique de l'Eocène en Grèce. *Revue de Micropaléontologie*, 2:31–49.

Aubry, M.-P. and Ouda, K. (2003). Introduction to the Upper Paleocene-Lower Eocene of the Upper Nile valley. *Micropaleontology*, 49:2–4.

Babazadeh, S. A. (2008). Lower Eocene transgressive successions of Sahlabad province, eastern Iran, implication of biostratigaphy and microfacies analysis. *Revue de Paléobiologie, Géneve*, 27:449–459.

Baceta, J. I., Pujalte, V., and Bernaola, G. (2005). Paleocene coralgal reefs of the western Pyrenean basin, northern Spain: new evidence supporting an earliest Paleogene recovery of the reefal systems. *Palaeogeography, Palaeoclimatology, Palaeoecology*, 224:117–143.

Baig, M. S. and Munir, M. H. (2007). Foraminiferal biostratigraphy of Yadgar area, Muzaffarabad Azad Kashmir, Pakistan. *Journal of Himalayan Earth Science*, 40:33–43.

Bains, S., Corfield, R. M., and Norris, R. D. (1999). Mechanisms of Climate Warming at the End of the Paleocene. *Science*, 285:724–727.

Bandy, O. L. (1944). Eocene Foraminifera from Cape Blanco, Oregon. *Journal of Paleontology*, 18:366–377.

Banerjee, S. and Jeevankumar, S. (2007). Facies and depositional sequence of the Mesoproterozoic Rohtas Limestone: Eastern Son valley, Vindhyan basin. *Journal of Asian Earth Sciences*, 30:82–92.

Banerjee, S., Jeevankumar, S., Panyal, P., and Bhattacharyya, S. K. (2006). Stable isotope ratios and nodular limestone of the Proterozoic Rothas limestone: Vindhyan Basin, India. *Carbonates and Evaporites*, 31(2):133–143.

Bathurst, R. G. C. (1975). *Carbonate sediments and their diagenesis.* Developments in Sedimentology 12, Elsevier.

Bathurst, R. G. C. (1987). Diagenetically enhanced bedding in argillaceous platform limestones: stratified cementation and selective compaction. *Sedimentology*, 34:749–778.

Bathurst, R. G. C. (1991). Pressure-Dissolution and Limestone Bedding: the Influence of Stratified Cementation. In Einsele, G., Ricken, W., and Seilacher, A., editors, *Cycles and Events in Stratigraphy*, pages 451–463. Springer.

Baud, A., Gaetani, M., Garzanti, E., Fois, E., Nicora, A., and Tintori, A. (1984). Geological observations in southeastern Zanskar and adjacent Lahul area (northwestern Himalaya). *Eclogae Geologicae Helvetiae*, 77:171–197.

Bádenas, B. and Aurell, M. (2010). Facies model of a shallow-water carbonate ramp based on distribution of non-skeletal grains (Kimmeridgian, Spain). *Facies*, 56:89–110.

Beavington-Penney, S. J. and Racey, A. (2004). Ecology of extant nummulitids and other larger benthic foraminifera: applications in palaeoenvironmental analysis. *Earth-Science Reviews*, 67:219–265.

Bernoulli, D. and Jenkyns, H. C. (1970). A Jurassic Basin: The Glasenbach Gorge, Salzburg, Austria. *Verhandlungen der Geologischen Bundesanstalt*, 4:504–531.

Bjorlykke, K. A. (1973). Origin of limestone nodules in the Lower Palaeozoic of the Oslo Region. *Norsk Geologisk Tidsskrift*, 53:419–431.

Bjorlykke, K. A. (1974). Geochemical and mineralogical influence of Ordovician Island Arcs on epicontinental clastic sedimentation. A study of Lower Palaeozoic sedimentation in the Oslo Region, Norway. *Sedimentology*, 21:251–272.

Boggs, S. J. (2009). *Petrology of Sedimentary Rocks.* Number 2nd. Cambridge University Press, Cambridge.

Böhm, F., Dommergues, J.-L., and Meister, C. (1995). Breccias of the Adnet Formation: indicators of a Mid-Liassic tectonic event in the Northern Calcareous Alps (Salzburg/Austria). *Geologische Rundschau*, 84:272–286.

Boix, C., Villalonga, R., Caus, E., and Hottinger, L. (2009). Late Cretaceous rotaliids (Foraminiferida) from the Western Tethys. *Neues Jahrbuch für Geologie und Paläontologie - Abhandlungen*, 253:197–227.

BouDagher-Fadel, M. K., Price, G. D., Hu, X., and Li, J. (2015). Late Cretaceous to early Paleogene foraminiferal biozones in the Tibetan Himalayas, and a pan-Tethyan foraminiferal correlation scheme. *Stratigraphy*, 12:67–91.

Brönnimann, P. (1950). *Tremastegina*, ein neues Genus der Familie Asterigerinidae d'Orbigny. *Eclogae geolociae Helvetiae*, 43:255–265.

Brown, N. K. and Bronnimann, P. (1957). Some Upper Cretaceous Rotaliids from the Caribbean Region. *Micropaleontology*, 3:29–38.

Bugrova, E. M. (1966). Occurence of the foraminiferal genus *Lockhartia* in the Paleocene of the USSR. *Paleontologicheskii Zhurnal*, 2:122–125.

Bugrova, E. M. (1967). Occurence of the foraminiferal genus *Lockhartia* in the Paleocene of the USSR. *International Geology Review*, 9(3):278–281.

Burchette, T. P. and Wright, V. P. (1992). Carbonate ramp depositional systems. *Sedimentary Geology*, 79:3–57.

Butt, A. A. (1991). *Ranikothalia sindens* Zone in Late Paleocene Biostratigraphy. *Micropaleontology*, 37:77–85.

Butterlin, J. and Fourcade, E. (1989). Stratigraphic Range and Geographic Distribution of the Genus *Lockhartia* Davies, 1932 (Foraminifera, Rotaliidae). *Revue de Micropaléontologie*, 31(4):225–242.

Buxton, M. W. N. and Pedley, H. M. (1989). Short Paper: A standard model for Tethyan Tertiary carbonate ramps. *Journal of the Geological Society, London*, 146:746–748.

Cai, F., Ding, L., Leary, R. J., Wang, H., Xu, Q., Zhang, L., and Yue, Y. (2012). Tectonostratigraphy and provenance of an accretionary complex within the Yarlung-Zangpo suture zone, southern Tibet: insights into subduction-accretion processes in the Neo-Tethys. *Tectonophysics*, 574-575:181–192.

Canfield, D. E. and Raiswell, R. (1991). Carbonate precipitation and dissolution - its relevance to fossil preservation. In Allison, A. and Briggs, D. E. G., editors, *Taphonomy - Releasing the Data Locked in Fossils*, pages 411–453. Plenum Press.

Chung, S. L., Chu, M. F., Zhang, Y. Q., Xie, Y. W., Lo, C. H., Lee, T. Y., Lan, C. Y., Li, X. H., Zhang, Q., and Wang, Y. Z. (2005). Tibetan tectonic evolution inferred from spatial and temporal variations in post-collisional magmatism. *Earth-Science Reviews*, 68:173–196.

Cole, W. S. (1942). *Lockhartia* in Cuba. *Journal of Paleontology*, 16:640–642.

Cole, W. S. (1947). Internal Structure of some Floridian Foraminifera. *Bulletins of American Paleontology*, 31:227–255.

Cole, W. S. (1971). Internal structure of three American species of Rotaliina (Foraminifera). *Journal of Foraminiferal Research*, 1:29–38.

Cotton, L. J. and Pearson, P. N. (2012). Larger Benthic Foraminifera from the Middle Eocene to Oligocene of Tanzania. *Austrian Journal of Earth Sciences*, 105(1):189–199.

Cushmann, J. A. and Jarvis, P. W. (1931). Some new Eocene Foraminifera from Jamaica. *Contribution Cushman Foundation for Foraminiferal Research*, 7:75–78.

d´Archiac, A. and Haime, J. (1853). *Description des animaux fossiles du groupe nummulitique de l'Inde, précédée d'un résumé géologique et d'une monographie des Nummulites.* Gide et J. Baudry, Paris.

Datta, A. K. and Banerji, R. K. (1966). Palaeocene species of *Dictyoconoides*, *Lockhartia* and *Dictyokathina* from the Subathu subgroup in Simla and Nahan-Dadahu areas. *Bulletin of the Oil and Natural Gas Commission*, 3(2):61–66.

Davies, L. M. (1926). Remarks on Carter's Genus *Conulites* (=*Dictyoconoides* Nuttall), with descriptions of some new species from the Eocene of North-West India. *Records of the Geological Survey of India, Calcutta*, 59:237–253.

Davies, L. M. (1927). The Ranikot Beds at Thal (North-West Frontier Provinces of India). *Quarterly Journal of the Geological Society of London*, 83:260–290.

Davies, L. M. (1930). *Memoirs of the Geological Survey of India.* Palaeontologica India, India.

Davies, L. M. (1932). XIII. – The Genera *Dictyoconoides* Nuttall, *Lockhartia* nov., and *Rotalia* Lamarck: Their Type Species, Generic Differences, and Fundamental Distinction from the *Dictyoconus* Group of Forms. *Transactions of the Royal Society of Edinburgh*, 57:397–428.

Davies, L. M. (1937). Extent of the Ranikot Sea. *Nature*, 135:188.

Davies, L. M. and Pinfold, E. S. (1937). *The Eocene Beds of the Punjab Salt Range.* Memoirs of The Geological Survey of India.

De Boer, P. L. and Smith, D. G. (1994). *Orbital forcing and cyclic sequences*, volume 19. International Association of Sedimentologists Special Publication, Oxford.

Delage, Y. and Hérouard, E. (1896). *Traité de Zoologie Concrète. 1. La Cellule et les Protozoaires.* Schleicher Frères.

Dickens, G. R. (1999). The blast in the past. *Nature*, 401:752–755.

Ding, L., Kapp, P., and Wan, X. (2005). Paleocene-Eocene record of ophiolithe obduction and initial India-Asia collision, south central Tibet. *Tectonics*, 24:1–18.

Drobne, K. (1977). Alvéolines paléogènes de la Slovénie et de l'Istrie. *Schweizerische Paläontologische Abhandlungen*, 99:1–132.

Drooger, C. W. (1960a). Some early rotaliid Foraminifera. I. *Paleontology*, 63:287–301.

Drooger, C. W. (1960b). Some early rotaliid Foraminifera. II. *Proceedings of the Koninklijke Nederlandse Academie van Wetenschappen (B)*, 63(3):302–318.

Dunham, R. J. (1962). Classification of carbonate rocks according to depostitional texture. In Ham, W. E., editor, *Classification of carbonate rocks*, pages 108–121. American Association of Petroleum Geologist Memoir.

Dupuis, C., Aubry, M.-P., Steurbaut, E., Berggren, W. A., Ouda, K., Magioncalda, R., Cramer, B. S., Kent, D. V., Speijer, R. P., and Heilmann-Clausen, C. (2003). The Dababiya Quarry Section: Lithostratigraphy, clay mineralogy, geochemistry and paleontology. *Micropaleontology*, 49(1):41–59.

Dürr, S. (1993). *The mid- to early Late Cretaceous Xigaze forearc basin (South Tibet): sedimentary evolution and provenance of clastic sediments.* Tübinger Geowissenschaftliche Arbeiten (TGA), Reihe A.

Eder, W. (1982). Diagenetic redistribution of carbonate, a process in forming limestone-marl alternations (Devonian and Carboniferous, Rheinisches Schiefergebirge, W. Germany). In Einsele, G. and Seilacher, A., editors, *Cyclic and Events Stratifications*, pages 98–112. Springer, Berlin.

Ehrenberg, C. G. (1839). Über die Bildung der Kreidefelsen und des Kreidemergels durch unsichtbare Organismen. *Physikalische Abhandlungen der Königlich-Bayerischen Akademie der Wissenschaften*, 1838:59–148.

Einsele, G., Ricken, W., and Seilacher, A. (1991). Basic Concept and Terms. In Einsele, G., Ricken, W., and Seilacher, A., editors, *Cycles and Events in Stratigraphy*, pages 1–19. Springer, Heidelberg.

Embry, A. F. and Klovan, J. E. (1971). A late Devonian reef tract on northeastern Banks Island. N. W. T. *Bulletin of Canadian Petroleum Geology*, 19:730–781.

Fabricius, F. H. (1966). *Beckensedimentation und Riffbildung an der Wende Trias/Jura in den Bayerisch-Tiroler Kalkalpen.* International Sedimentary Petrographical Series 9, Leiden.

Flügel, E. (2010). *Microfacies of Carbonate Rocks - Analysis, Interpretation and Application.* Springer, Berlin.

Fuchs, G. (1982). The geology of Western Zanskar. *Jahrbuch der Geologischen Bundesanstalt*, 125:1–50.

Fuchs, G. (1987). The Geology of Southern Zanskar (Ladakh) - Evidence for the Autochthony of the Tethys Zone of the Himalaya. *Jahrbuch der Geologischen Bundesanstalt*, 130:465–491.

Fuchs, G. and Willems, H. (1990). The Final Stages of Sedimentation in the Tethyan Zone of Zanskar and their Geodynamic Significance (Ladakh - Himalaya). *Jahrbuch der Geologischen Bundesanstalt*, 133:159–173.

Füchtbauer, H. (1988). *Sediment und Sedimentgesteine.* Schweizerbart Science Publishers, Stuttgart.

Gaetani, E., Critelli, S., and Ingersoll, R. (1996). Paleogeographic and paleotectonic evolution of the Himalayan Range as reflected by detrital modes of Tertiary sandstones and modern sands (Indus transect, India and Pakistan). *Geological Society of America Bulletin*, 108:631–642.

Gaetani, M., Casnedi, R., Fois, E., Garzanti, E., Jadoul, F., Nicora, A., and Tintori, A. (1986). Stratigraphy of the Tethys Himalaya in Zanskar, Ladakh. Initial Report. *Rivista Italiana di Paleontologia e Stratigrafia*, 91:443–478.

Gaetani, M. and Garzanti, E. (1991). Multicyclic history of the Northern India continental margin (Northwest Himalaya). *AAPG Bull*, 75:1427–1446.

Gaetani, M., Nicora, A., and Premoli Silva, I. (1980). Uppermost Cretaceous and Paleocene in the Zanskar Range (Ladakh-Himalaya). *Rivista Italiana di Paleontologia e Stratigrafia*, 86(1):127–166.

Gaetani, M., Nicora, A., Premoli Silva, I., Fois, E., Garzanti, E., and Tintori, A. (1983). Upper Cretaceous and Paleocene in Zanskar Range (NW Himalaya). *Rivista Italiana di Paleontologia e Stratigrafia*, 89:81–118.

Gansser, A. (1964). *Geology of the Himalayas.* Interscience Publishers.

Garzanti, E., Baud, A., and Mascle, G. (1987). Sedimentary record of the northward flight of India and its collision with Eurasia (Ladakh-Himalaya, India). *Geodinamica Acta*, 1:197–312.

Ghose, B. K. (1976). Paleogene reef-rock complex of the meghalaya and its oil potentialities. *Science and Culture*, 42:248–253.

Ghose, B. K. (1977). Paleoecology of the Cenozoic reefal foraminifera and algae - a brief review. *Palaeogeography, Palaeoclimatology, Palaeoecology*, 22:231–256.

Gill, W. D. (1953). Facies and Fauna in the Bhadrar Beds of the Punjab Salt Range, Pakistan. *Journal of Paleontology*, 27:824–844.

Hallam, A. (1964). Origin of the limestone-shale rhythms in the Blue Lias of England: a composite theory. *The Journal of Geology*, 72:157–168.

Hallam, A. (1986). Origin of minor limestone-shale cycles: climatically induced or diagenetic? *Geology*, 14:609–612.

Hallock, P. (1984). Distribution of selected species of living algal symbiont-bearing foraminifera on two Pacific coral reefs. *Journal of Foraminiferal Research*, 14:250–261.

Hallock, P. (1985). Why are Larger Foraminifera Large? *Paleobiology*, 11:195–208.

Hallock, P. (1999). Symbiont-bearing foraminifera. In Gupta, B. K. S., editor, *Modern Foraminifera*, pages 123–139, Dordrecht. Kluwer Academic.

Hallock, P. and Glenn, E. C. (1986). Larger Foraminifera: A Tool for Paleoenvironmental Analysis of Cenozoic Carbonate Deositional Facies. *PALAIOS*, 1:55–64.

Hasson, P. F. (1985). New Observations on the Biostratigraphy of the Saudi Arabian Umm er Radhuma Formation (Paleogene) and Its Correlation with Neighboring Regions. *Micropaleontology*, 31:335–364.

Haynes, J. R. (1965). Symbiosis, wall structure and habitat in foraminifera. *Special Publication-Cushman Foundation for Foraminiferal Research*, 16:40–43.

Heba, G., Prichonnet, G., and El Albani, A. (2009). Meteoric diagenesis of Upper Cretaceous and Paleocene-Eocene shallow-water carbonates in the Kruja Platform (Albania): geochemical evidence. *Geologica Carpathica*, 60:165–179.

Heim, D. (1990). *Tone und Tonminerale: Grundlagen der Sedimentologie und Mineralogie.* Ferdinand Enke Verlag, Stuttgart.

Ho, Y., Zhang, P.-K., Hu, L.-Y., and Sheng, J.-C. (1976). Mesozoic and Cenozoic foraminifera from the

Mount Jolmo Lungma Region. In Sinica, T. S. E. T. A., editor, *A report of the Scientific Expedition in the Mount Jolmo Lungma Region (1966-1986)*, volume 2, pages 1–124. Science Press.

Hofker, J. (1955). Foraminifera of Southern Limburg, Netherlands. 1. *Lockhartia roestae* (Visser). *Natuurhistorisch Maandblad*, 44(1):4–5.

Hofker, J. (1957). Foraminiferen der Oberkreide von Nordwestdeutschland und Holland.

Hofker, J. (1958). *Daviesina voigti* n. sp., eine gesteinsbildende Foraminifere aus dem Campan der subherzynen Kreide. *Mitteilungen aus dem Geologischen Staatsinstitut in Hamburg*, 27:69–73.

Hofker, J. (1966). Foraminifera from the Upper Cretaceous of South-Limburg, Netherlands LXXXIII. *Natuurhistorisch Maandblad*, 55:24–26.

Hollmann, R. (1962). Über Subsolution und die Knollenkalke des calcare Ammonitico Rosso Superiore im Monte Baldo (Malm; Norditalien). *Neues Jahrbuch für Geologie und Paläontologie - Monatshefte*, 1962:163–174.

Hollmann, R. (1964). Subsolutions-Fragmente (Zur Biostratinomie der Ammonoidea im Malm des Monte Baldo (Malm; Norditalien). *Neues Jahrbuch für Geologie und Paläontologie - Abhandlungen*, 119:163–174.

Hottinger, L. (1960). Über Eocäne und Paleozäne *Alveolinen*. *Eclogae geologicae Helvetiae*, 53:265–283.

Hottinger, L. (1966). Foraminiféres rotaliformes et Orbitoides du Sénonien inférieur pyrénéen. *Eclogae Geologicae Helvetiae*, 59:277–301.

Hottinger, L. (1971). Larger foraminifera common to Mediterranean and Indian Paleocene and Eocene formations. *Annales Instituti Geologici Publici Hungarici*, 54:145–151.

Hottinger, L. (1973). Selected Paleogene larger foraminifera. In Hallem, A., editor, *Paläontologische Kursbücher*, pages 443–452, Amsterdam. Elsevier.

Hottinger, L. (1981). Répartition comparée des grandes foraminifères de la Mer Rouge et de l'Océan Indien. *Annals of the University Ferrara*, NS IX/6 supplement:1–13.

Hottinger, L. (1983). Processes determining the distribution of larger foraminifera in space and time. *Utrecht Micropaleontological Bulletins*, 30:239–253.

Hottinger, L. (1997). Shallow benthic foraminiferal assemblages as signals for depth of their deposition and their limitations. *Bulletin Societe geologique de France*, 168:491–505.

Hottinger, L. (1998). Shallow benthic foraminifera at the Paleocene-Eocene boundary. *Strata*, 9:61–64.

Hottinger, L. (2006). Illustrated glossary of terms used in foraminiferal research. *Carnets de Geologie / Notebooks on Geology, Brest, Memoir 2006/02 (CG2006_M02)*, pages 1–43.

Hottinger, L. (2007). Revision on the foraminiferal genus *Globoreticulina* Rahaghi, 1978, and of its associated fauna of larger foraminifera from the late Middle Eocene of Iran. *Carnets de Géologie / Notebooks on Geology, Brest, Article 2007/07 (CG2997_A06)*, 06:1–53.

Hottinger, L. (2009). The Paleocene and earliest Eocene foraminiferal Family Miscellaneidae: neither nummulitids nor rotaliids. *Carnets de Geologie / Notebooks on Geology*, 06:1–41.

Hottinger, L. (2014a). New Subfamily Lockhartiinae. In Bassi, D., editor, *Paleogene larger Rotaliid foraminifera from the Western and Central Neotethys*, pages 57–97. Springer International Publishing, Switzerland.

Hottinger, L. (2014b). Rotaliid Shell Architecture and the Palaeodiversity of the Lockhartia Sea. In Bassi, D., editor, *Paleogene larger Rotaliid foraminifera from the Western and Central Neotethys*, pages 3–12. Springer International Publishing, Switzerland.

Hottinger, L. and Drobne, K. (1988). Alvéolines tertiarires: Quelques problèmes liés à la conconcept de l'espèce. *Revue de Palaeobiology*, 2:665–685.

Hottinger, L. and Leutenegger, S. (1980). The structure of calcarinid foraminifera. In Hottinger, L., editor, *Schweizerische Paläontologische Abhandlungen*, pages 115–154. Birkhäuser Verlag Basel.

Hottinger, L., Sameeni, S. J., and Butt, A. A. (1998). Emendation of *Alveolina vredenburgi* Davies and Pinfold, 1937 from the Surghar range, Pakistan. In Hottinger, L. and Drobne, K., editors, *Paleogene shallow benthos of the Tethys*, volume 34/2, pages 155–163. Dela-Opera SAZU 4, Razprave, Slovenian Academy of Science and Arts, Ljubljana.

Hu, X., Sinclair, H. D., Wang, J., Jiang, H., and Wu, F. (2012). Late Cretaceous-Palaeogene stratigraphic and basin evolution in the Zhepure Mountain of southern Tibet: implications for the timing of India-Asia initial collision. *Basin Research*, 24:520–543.

Hu, X., Wang, J., BouDagher-Fadel, M. K., Garzanti, E., and An, W. (2016). New insights into the timing of the India-Asia collision from the Paleogene Quxia and Jialazi formations of the Xigaze forearc basin, South Tibet. *Gondwana Research*, 32:76–92.

Hu, X. M., Jansa, L., and Wang, C. S. (2008). Upper Jurassic-Lower Cretaceous stratigraphy in south-eastern Tibet: a comparison with the western Himalayas. *Cretaceous Research*, 29:301–305.

Hudson, J. D. and Jenkyns, H. C. (1969). Conglomerates in the Adnet Limestones of the Adnet (Austria) and the origin of the "Scheck". *Neues Jahrbuch für Geologie und Paläontologie - Abhandlungen*, 1969:552–558.

Illies, H. (1949). Die Lithogenese des Untereozäns in Nordwestdeutschland. *Mitteilungen aus dem Geologischen Staatsinstitut in Hamburg*, 18:7–46.

Inden, R. F. and Moore, C. H. (1983). *Carbonate Depositional Environments*, volume 33, chapter Beach environments, pages 211–265. AAPG Memoir.

Ismail, Ahmed, A. and Boukhary, M. (2008). Larger foraminifera from the Early Eocene of Shabwa area, Southeastern Yemen. *Revue de Palaeobiology*, 27(1):89–97.

Jadoul, F., Berra, F., and Garzanti, E. (1998). The Tethys Himalayan passive margin from late Triassic to early Cretaceous (South Tibet). *Journal of Asian Earth Sciences*, 16:173–194.

Jauhri, A. K. (1985). On the Foraminifer *Lockhartia alveolata* Silvestri. *Journal of the Palaeontological Society of India*, 30:30–34.

Jeans, C., Hu, X., and Mortimore, R. (2012). Calcite cements and the stratigraphical significance of the

marine δ^{13}C carbonate reference curve for Upper Cretaceous Chalk of England. *Acta Geologica Polonica*, 62:173–196.

Jeans, C. V. (1980). Early submarine lithification in the red chalk and lower chalk of eastern England: a bacterial control model and its implications. *Proceedings of the Yorkshire Geological Society*, 43:81–157.

Jenkyns, H. C. (1974). Origin of red nodular limestones (Ammonitico Rosso, Knollenkalke) in the Mediterranean Jurassic: a diagenetic model. In Hsü, K. J. and Jenkyns, H. C., editors, *Pelagic Sediments: on Land and under the Sea*, pages 249–271. Special Publication of the International Association of Sedimentologists.

Ji, J. C., Wu, F.-Y., Chung, S.-L., Li, L.-X., and Liu, C.-Z. (2009). Zircon U-Pb geochronology and Hf isotopic constraints on petrogenesis of the Gangdese batholith, southern Tibet. *Chemical Geology*, 262:229–245.

Jiang, T., Aitchison, J. C., and Wan, X. (2016). The youngest marine deposits preserved in southern Tibet and disappearance of the Tethyan Ocean. *Gondwana Research*, 32:64–75.

Kaever, M. (1970). *Die alttertiären Großforaminiferen Südost-Afghanistans unter besonderer Berücksichtigung der Nummulitiden — Morphologie, Taxonomie und Biostratigraphie —*, volume 16/17. Münstersche Forschungen zur Geologie und Paläontologie.

Kahsnitz, M. M., Zhang, Q., and Willems, H. (2016). Stratigraphic distribution of the larger benthic foraminifera *Lockhartia* in South Tibet (China). *Journal of Foraminferal Research*, 46(1):34–47.

Kennedy, W. J. and Garrison, R. E. (1975). Morphology and genesis of nodular chalks and hardgrounds in the Upper Cretaceous of southern England. *Sedimentology*, 22:311–386.

Kennet, J. P. and Stott, L. D. (1991). Abrupt deep-sea warming, palaeoceanographic changes and benthic extinctions at the end of the Paleocene. *Nature*, 353.

Koch, P. L., Clyde, W. C., Hepple, R. P., Fogel, M. L., Wing, S. L., and Zachos, J. C. (2003). Carbon and oxygen isotope records from paleosols spanning the Paleocene-Eocene boundary, Bighorn Basin, Wyoming. *Geological Society of America*, 369.

Koch, P. L., Zachos, J. C., and Dettman, D. L. (1995). Stable isotope stratigraphy and paleoclimatology of the Paleogene Bighorn Basin (Wyoming, USA). *Palaeogeography, Palaeoclimatology, Palaeoecology*, 115:61–89.

Küspert, W. (1982). Environmental changes during oil shale deposition as deduced from stable isotope ratios. In Einsele, G. and Seilacher, A., editors, *Cyclic and Event Stratification*, pages 482–503. Springer.

Lamarck, J. B. (1804). Suite des mémoires sur les fossiles des environs de Paris. *Annales du Muséum national d'histoire naturelle*, pages 429–436.

Lee, J. J. (1998). "Living sands" - Larger foraminifera and their endosymbiotic algae. *Symbiosis*, 25:71–100.

Leloux, J. (2002). Type specimens of Maastrichtian fossils in the National Museum of Natural History, Leiden. *Nationaal Natuurhistorisch Museum Technical Bulletin*, 4:1–40.

Leutenegger, S. (1984). Symbiosis in Benthic Foraminifera: Specificity and Host Adaptions. *Journal of Foraminiferal Research*, 14:16–35.

Levin, H. L. (1957). Micropaleontology of the Oldsmar Limestone (Eocene) of Florida. *Micropaleontology*, 3:137–154.

Li, J., Hu, X., Garzanti, E., An, W., and Wang, J. (2015). Paleogene carbonate microfacies and sandstone provenance (Gamba area, South Tibet): Stratigraphic response to initial India-Asia continental collision. *Journal of Asian Earth Sciences*, 104:39–54.

Li, J., Hu, X., Garzanti, E., and BouDagher-Fadel, M. K. (2017). Shallow-water carbonate response to the Paleocene-Eocene thermal maximum in the Tethyan Himalaya (southern Tibet): Tectonic and climatic implications. *Palaeogeography, Palaeoclimatology, Palaeoecology*.

Li, X. H., Wang, C. S., and Hue, X. M. (2005). Stratigraphy of deep-water Cretaceous deposits in Gyangze, southern Tibet, China. *Cretaceous Research*, 26:33–41.

Liu, C., Yin, J., Shun, X., and Sun, Y. (1988). Marine Late Cretaceous-early Tertiary sequences - The non-flysch deposits of the Xigaze forearc basin in South Xizang. *Memoirs of Institute of Geology, Academia Sinica*, 3:130–157.

Liu, G. (1992). *Permian to Eocene Sediments and Indian Passive Margin Evolution in the Tibetian Himalayas.* Number 13. Tübinger Geowissenschaftliche Arbeiten (TGA), Reihe A.

Liu, G. and Einsele, G. (1994). Sedimentary history of the Tethyan basin in the Tibetan Himalayas. *Geologische Rundschau*, 83:32–61.

Loeblich, A. R. J. and Tappan, H. (1988). *Foraminiferal Genera And Their Classification*. Van Nostrand Reinhold Company.

Logan, B. and Semeniuk, V. (1976). *Dynamic metamorphism; processes and products in Devonian carbonate rocks, Canning Basin, Western Australia*, volume 6. Special Publications geological Society of Australia, Sydney.

Lucas, G. (1955). Caractères pétrographiques de calcaires noduleux, à faciès ammonitico-rosso, de la region méditerranéenne. *Comptes rendus hebdomadaires des séances de l'Académie des sciences*, 240:1909–1911.

Lukasik, J. and James, N. P. (2006). Carbonate sedimentation, climate change and stratigraphic completeness on a Miocene cool-water epeiric ramp, Murray Basin, South Australia. In Pedley, H. M. and Carannante, G., editors, *Cool-water carbonates: depositional systems and palaeoenvironmental controls*, pages 217–244. Geological Society Special Publication No 225, London.

Lukasik, J. J., James, N. P., McGowran, B., and Bone, Y. B. (2000). An epeiric ramp: low-energy, cool-water carbonate facies in a Tertiary inland sea, Murray Basin, South Australia. *Sedimentology*, 47:851–881.

Marie, P. (1946). Sur *Laffitteina bibensis* et *Laffitteina monodi*, nouveau genre et nouvelles espéces de Foraminifères du Montien. *Bulletin Societe geologique de France*, 15:419–434.

Mathur, N. S., Juyal, K. P., and Kumar, K. (2009). Larger foraminiferal biostratigraphy of lower Paleogene successions of Zanskar Tethyan and Indus-Tsangpo Suture Zones, Ladakh, India in the light of additional data. *Himalayan Geology*, 30:45–68.

Matsumaru, K., Sari, B., and Özer, S. (2010). Larger foraminiferal biostratigraphy of the middle Tertiary of Bey Daglari Autochton, Menderes-Taurus Platform, Turkey. *Micropaleontology*, 56:439–463.

McCrossan, R. G. (1958). Sedimentary ”boudinage” structure in the Upper Devonian Ireton Formation of Alberta. *Journal of Sedimentary Petrology*, 28:316–320.

Müller-Merz, E. (1980). *Schweizerische Paläontologische Abhandlungen*, volume 101, chapter Strukturanalyse ausgewählter rotaloider Foraminiferen (Structural Analysis of selected Rotaliid Foraminifera), pages 5–70. Birkhäuser Verlag Basel.

Mo, X. X., Niu, Y. L., Dong, G. C., Zhao, Z. D., Hou, Z. Q., Zhou, S., and Ke, S. (2008). Contribution of syncollisional felsic magmatism to continental crust growth: a case study of the Paleogene Linzizong volcaniv Succession in southern Tibet. *Chemical Geology*, 250:49–67.

Möller, N. K. and Kvingan, K. (1988). The genesis of nodular limestones in the Ordovician and Silurian of the Oslo Region (Norway). *Sedimentology*, 35:405–420.

Müller, J. and Fabricius, F. (1974). Magnesian-calcite nodules in the ionian deep sea: an actualistic model for the formation of some nodular limestones. In Hsü, K. J. and Jenkyns, H. C., editors, *Pelagic Sediments: on Land and under the Sea*, pages 235–247. Special Publication of the International Association of Sedimentologists.

Mullins, H. T., Neumann, A. C., Wilber, R. J., and Boardman, M. R. (1980). Nodular Carbonate Sediment on Bahamian Slopes: Possible Precursors to Nodular Limestones. *Journal of Sedimentary Petrology*, 50:0117–0131.

Munnecke, A. and Samtleben, C. (1996). The Formation of Micritic Limestones and the Development of Limestone-Marl Alternations in the Silurian of Gotland, Sweden. *Facies*, 34:159–176.

Munnecke, A. and Westphal, H. (2004). Schwankende Umweltbedingungen des südwestdeutschen Oberjura dokumentiert in Kalk-Mergel-Wechselfolgen. *Jahreshefte der Gesellschaft für Naturkunde in Württemberg*, 160:33–48.

Munnecke, A., Westphal, H., Elrich, M., and Reijmer, J. J. G. (2001). The mineralogical composition of precursor sediments of calcareous rhythmites: a new approach. *International Journal of Earth Sciences (Geologische Rundschau)*, 40:795–812.

Nicora, A., Garzanti, E., and Fois, E. (1987). Evolution of the Tethys Himalaya continental shelf during Maastrichtian to Paleocene (Zanskar, India). *Rivista Italiana di Paleontologia e Stratigrafia*, 92:439–496.

Noble, J. P. A. and Howells, K. D. M. (1974). Early marine lithification of the nodular limestones in the Silurian of New Brunswick. *Sedimentology*, 21:597–609.

Norling, E. (1973). The Foraminiferal Fauna. In Bergström, R. and Johansson, C., editors, *The Geology at Särdal*, pages 97–112. Bulletin of the Geological Society of Denmark.

Nuttall, W. L. F. (1926). The Larger Foraminifera of the Upper Ranikot Series (Lower Eocene) of Sind, India. *The Geological Magazine*, 63:112–123.

Nuttall, W. L. F. and Brighton, A. G. (1931). Larger Foraminifera from the Tertiary of Somalialand. *The Geological Magazine*, 68:49–65.

Ovey, C. D. (1947). A new Eocene Species of *Lockhartia* Davies, from British Somalia, with Note on other Species of the Genus. *The Annals and Magazine of Natural History*, 13:571–578.

Pak, D. J. and Miller, K. G. (1992). Paleocene to Eocene benthic foraminiferal isotopes and assemblages: implications for deep water circulation. *Paleoceanography*, 7:405–422.

Patra, A. and Singh, N. P. (2015). Facies characteristics and depositional environments of the Paleocene-Eocene strata of the Jaisalmer basin, western India. *Carbonates and Evaporites*, 30:331–346.

Pessagno, Emile A., J. (1960). Stratigraphy and Micropaleontology of the Cretaceous and Lower Tertiary of the Puerto Rico. *Micropaleontology*, 6:87–110.

Pignatti, J., Matteucci, R., Parlow, T., and Fantozzi, P. L. (1998). Larger foraminiferal biostratigraphy of the Maastrichtian-Ypresian Wadi Mashib succession (South Hadramawt Arch, SE Yemen). *Zeitschrift für Geologische Wissenschaften*, 26:609–635.

Qian, D. Y., Zhang, S. M., and Gu, Q. G. (1982). Some new data on the age of the Ngamring Formation of the Xigaze group in the southern Xizang (Tibet), China. *Scientia Geologica Sinica*, 3:329–332.

Raiswell, R. (1988). Chemical model for the origin of minor limestone-shale cycles by anaerobic methane oxidation. *Geology*, 16:641–644.

Ratschbacher, L., Frisch, W., Liu, G., and Chen, G. (1994). Distributed deformation in southern and western Tibet during and after the India-Asia collision. *Journal of Geophysical Research*, 99:19917–19945.

Reinhardt, E. G., Cavazza, W., Patterson, R. T., and Blenkinsop, J. (2000). Differential diagenesis of sedimentary components and the implication for strontium isotope analysis of carbonate rocks. *Chemical Geology*, 164:331–343.

Reiss, Z. and Hottinger, L. (1984). *The Gulf of Aqaba. - Ecological Micropaleontology.* Springer Verlag.

Reiss, Z. and Merling, P. (1958). Structure of Some Rotaliidea. *Geological Survey of Israel, Paleontolology Division, Jerusalem*, 21:1–19.

Renema, W. (2002). *Larger foraminifera as marine environmental indicators.* Scripta Geologica.

Ricken, W. (1986). *Diagenetic Bedding: A Model for Marl-Limestone Alternations.* Lecture Notes in Earth Sciences, Springer Verlag.

Ricken, W. (1987). The carbonate compaction law: a new tool. *Sedimentology*, 34:571–584.

Ricken, W. and Eder, W. (1991). Diagenetic Modification of Calcareous Beds - an Overview. In Einsele, G., Ricken, W., and Seilacher, A., editors, *Cycles and Events in Stratigraphy*, pages 430–449. Springer.

Röhl, U., Bralower, T. J., Norris, R. D., and Wefer, G. (2000). New chronology for the late Paleocene thermal maximum and its environmental implications. *Geology*, 28:927–930.

Ross, C. A. (1974). Evolutionary and ecological significance of large, calcareous Foraminiferifa (Protozoa), Great Barrier Reef. *Proceedings of the 2nd International Coral Reef Symposium, Brisbane, Australia*, 1:327–333.

Samanta, B. K. (1961). *Lockhartia* from Siju Limestone Formation, Garo Hills, Assam. *Quarterly Journal of the Geological, Mining and Metallurgical Society of India*, 33:39–41.

Sameeni, S. J., Nazir, N., Abdul-Karim, A., and Naz, H. (2009). Foraminiferal Biostratigraphy and Reconnaissance Microfacies of Paleocene Lockhart Limestone of Jabri Area, Hazara, Northern Pakistan. *Geological Bulletin of the Punjab University*, 44:85–96.

Sander, N. J. (1962). Apercu paléontologique et stratigraphique du Paléogène en Arabic Séoudite orientale. *Revue de Micropaléontologie*, 5:3–40.

Sander, N. J. (2012). Paleontologic and stratigraphic overview of the Paleogene in eastern Saudi Arabia. *Carnets de Geologie / Notebooks on Geology*, 4:53–92.

Schaub, H. (1981). Nummulites et Assilines de la Téthys Paléogène: taxonomie, phylogenèse et biostratigraphie. *Schweizer Palöntologische Abhandlungen*, 104:1–236.

Scheibner, C., Rasser, M. W., and Mutti, M. (2007). The Campo section (Pyrenees, Spain) revisited: Implications for changing benthic carbonate assemblages across the Paleocene-Eocene boundary. *Palaeogeography, Palaeoclimatology, Palaeoecology*, 248:145–168.

Scheibner, C. and Speijer, R. P. (2008). Late Paleocene-early Eocene Tethyan carbonate platform evolution - A response to long- and short-term paleoclimatic change. *Earth-Science Reviews*, 90:71–102.

Schindewolf, O. H. (1921). Beiträge zur Kenntnis der Kramenzelkalke und ihrer Entstehung. *Geologische Rundschau*, 12:20–35.

Schindewolf, O. H. (1923). Nochmals zur Kramenzelfrage. *Geologische Rundschau*, 14:151–154.

Schindewolf, O. H. (1925). Einige Bemerkungen zur Entstehung der oberdevonischen Kramenzelgesteine. *Zentralblatt für Mineralogie, Geologie und Paläontologie*, 16:405–411.

Schlager, M. (1966). Bericht 1965 über geologische Arbeiten auf den Blättern Berchtesgaden (93) und Hallein (94). *Verhandlungen der Geologischen Bundesanstalt*, 1966:A50–A54.

Scotese, C. R. (2011). *The PALEOMAP Project PaleoAtlas for ArcGIS, Vol. 1, Cenozoic Paleogeographic and Plate Tectonic Reconstructions.* PALEOMAP Project, Arlington, Texas.

Serra-Kiel, J., Hottinger, L., Caus, E., Drobne, K., Ferrandez, C., Jauhri, A. K., Less, G., Pavlovec, R., Pignatti, J., Samso, J. M., Schaub, H., Sirel, E., Strougo, A., Tambareau, Y., Tosquella, J., and Zakrevskaya, E. (1998). Larger foraminiferal biostratigraphy of the Tethyan Paleocene and Eocene. *Bulletin de la Société Géologique de France*, 169:281–299.

Silvestri, A. (1938). Foraminiferi dell'Eocene della Somalia. In *Foraminiferi dell'Eocene della Somalia. Parte I. Paleontologia della Somalia. IV Fossili dell'Eocene*, volume XXXII, supplement 3, pages 49–89. Palaentographia Italica.

Silvestri, A. (1939). Foraminiferi dell'Eocene della Somalia. In *Foraminiferi dell'Eocene della Somalia. Parte II. Paleontologia della Somalia. IV Fossili dell'Eocene*, volume XXXII, supplement 4, pages 79–180. Palaentographia Italica.

Silvestri, A. (1942). Foraminiferi dell'Eocene della Somalia. In *Foraminiferi dell'Eocene della Somalia. Parte III. Paleontologia della Somalia. IV Fossili dell'Eocene*, volume XXXII, supplement 5, pages 1–94. Palaentographia Italica.

Smith, A. G., Smith, D. G., and Funnell, B. M. (1994). *Atlas of Mesozoic and Cenozoic Coastlines.* Cambridge University Press, Cambridge.

Smout, A. H. (1954). *Lower Tertiary Foraminifera of the Qatar Peninsula.* British Museum, London.

Smout, A. H. and Haque, A. F. M. M. (1956). *Shorter contributions to the Geology of Pakistan*, volume 8, chapter A note on larger foraminifera and ostracoda in the Ranikot from the Nammal Gorge, Salt Range, Pakistan, pages 49–60. Records of the Geological Survey of Pakistan, Karachi.v.

Speijer, R. P. and Morsi, A. M. M. (2002). Ostracode turnover and sea-level changes associated with the Paleocene-Eocene Thermal Maximum. *Geology*, 30:23–26.

Swart, P. K. (2015). The geochemistry of carbonate diagenesis: The past, present and future. *Sedimentology*, 62:1233–1304.

Tambareau, Y., Hottinger, L., Rodriguez-Lazaro, J., Villate, J., Babinot, J.-F., Colin, J.-P., Garcia-Zarraga, E., Rocchia, R., and Guerrero, N. (1997). Communautes fossils benthiques aux alentours de la limite Cretace/Tertiaire dans les Pyrenees. *Bulletin de la Société Géologique de France*, 168:795–804.

Ten Dam, A. (1953). Two New Species of the Foraminiferal Genus *Lockhartia* from Turkey. *Bulletin of the Geological Society of Turkey*, 4:84–94.

Thomas, E. (1998). Biogeography of the late paleocene benthic foraminiferal extinction. In Aubry, M. P., Lucas, S., and Berggren, W. A., editors, *Late Paleocene-Early Eocene Climatic and Biotic Events in the Marine and Terrestrial Records*, pages 214–243, New York. Columbia University Press.

Thomas, E. and Shackelton, N. J. (1996). The Paleocene-Eocene Benthic Foraminiferal Extinction and Stable Isotope Anomalies. *Division III Faculty Publications*, 101:401–441.

Tripati, A. and Elderfield, H. (2004). Abrupt hydrographic changes in the equatorial Pacific and subtropical Atlantic from foraminiferal Mg/Ca indicate greenhouse origin for the thermal maximum at the Paleocene-Eocene Boundary. *Geosystems*, 5:1–11.

Tucker, M. E. (1974). Sedimentology of Paleozoic pelagic limestones: the Devonian Griotte (Southern France) and Cephalopodenkalk (Germany). In Hsü, K. J. and Jenkyns, H. C., editors, *Pelagic Sediments: on Land and under the Sea*, pages 71–92. Special Publication of the International Association of Sedimentologists.

Tucker, M. E. and Wright, V. P. (2008). *Carbonate Sedimentology.* Blackwell Science.

Turnsek, D. and Drobne, K. (1998). Paleocene corals from the northern Adriatic platform. In Hottinger, L. and Drobne, K., editors, *Paleogene Shallow Benthos of the Tethys 2*, pages 129–154. Dela-Opera SAZU 4, Razprave, Slovenian Academy of Science and Arts, Ljubljana.

van Hinsbergen, D. J. J., Lippert, P. C., Dupont-Nivet, G., McQuarrie, N., Doubrovine, P. V., Spakman, W., and Torsvik, T. H. (2012). Greater India Basin hypothesis and a two-stage Cenozoic collusion between India and Asia. *Proceedings of the National Academy of Sciences*, 109:7659–7664.

Visser, A. M. (1951). Monography on the foraminifera of the type-locality of the Maestrichtian (South Limburg, Netherlands). *Leidse Geologische Mededelingen*, 16:197–359.

Voigt, E. (1964). Zur Temperatur-Kurve der oberen Kreide in Europa. *Geologische Rundschau*, 54:270–317.

von Engelhardt, W. (1973). *Sediment-Petrologie Teil III - Die Bildung von Sedimenten und Sedimentgesteinen.* Nägele u. Obermiller, Stuttgart.

Wan, X. (1991). Palaeocene Larger Foraminifera from Southern Tibet. *Revista Española de Micropaleontologia*, 23:7–28.

Wan, X., Ding, L., Li, J., and Cai, H. (2001). Late Cretaceous to early Eocene marine strata in the Zhongba region, Tibet. *Journal of Stratigraphy*, 25:267–272.

Wan, X., Jansa, L. F., and Sarti, M. (2002). Cretaceous and Paleogene boundary strata in southern Tibet and their implication for the India-Eurasia collision. *Lethaia*, 35:131–146.

Wan, X., Jiang, T., Zhang, Y., Xi, D., and Li, G. (2014). Palaeogene marine stratigraphy in China. *Lethaia Review*, 47:297–308.

Wan, X., Wang, X., and Jansa, L. F. (2010). Biostratigraphy of a Paleocene-Eocene Foreland Basin boundary in southern Tibet. *Geoscience Frontiers*, 1:69–79.

Wang, J.-G., Hu, X.-M., BouDagher-Fadel, M. K., Wu, F.-Y., and Sun, G.-Y. (2015). Early Eocene sedimentary recycling in the Kailas area, southwesouth Tibet: Implications for the initial India-Asia collision. *Sedimentary Geology*.

Wanless, H. R. (1979). Limestone Response to Stress: Pressure Solution and Dolomitization. *Journal of Sedimentary Petrology*, 49:0437–0462.

Warren, J. K. (2006). *Evaporites - Sediments, Resources and Hydrocarbons.* Springer, Berlin.

Weiss, W. (1993). Age Assignments of Larger Foraminiferal Assemblages of Maastrichtian to Eocene Age in Northern Pakistan. *Zitteliana*, 20:223–252.

Westphal, H., Head, M. J., and Munnecke, A. (2000). Differential Diagenesis of Rhythmic Limestone Alternations Supported by Palynological Evidence. *Journal of Sedimentary Research*, 70:715–725.

White, M. R. (1994). Foraminiferal biozonation of the northern Oman Tertiary carbonate succession. In Simmons, M. D., editor, *Micropalaeontology and Hydrocarbon Exploration in the Middle East*, pages 309–341, London. British Micropaleontological Society, Chapman & Hall.

Willems, H. (1993). *Geoscientific investigations in the Tethyan Himalayas.* Berichte aus dem Fachbereich Geowissenschaften, Universität Bremen.

Willems, H., Zhou, Z., Zhang, B., and Gräfe, K.-U. (1996). Stratigraphy of the Upper Cretaceous and Lower Tertiary strata in the Tethyan Himalayas of Tibet (Tingri area, China). *Geologische Rundschau*, 85:723–754.

Wilson, J. L. (1975). *Carbonate Facies in Geologic History*. Springer Verlag.

Wing, S. L., Harrington, G. J., Smith, F. A., Bloch, J. I., Boyer, D. M., and Freeman, K. H. (2005). Transient Floral Change and Rapid Global Warming at the Paleocene - Eocene Boundary. *Science*, 310:993–996.

Wray, J. L. (1977). *Calcareous Algae.* Elsevier Scientific Publishing Company, Amsterdam.

Xu, Z.-Q., Dilek, Y., Yang, J.-S., Liang, F.-H., Liu, F., Ba, D.-Z., Cai, Z.-H., Li, G.-W., Dong, H.-W., and Ji, S.-C. (2015). Crustal structure of the Indus-Tsangpo suture zone and its oophiolite in southern Tibet: a new border for Paleo-Tethys? *Journal of Asian Earth Sciences*, 34:76–89.

Yin, A. and Harrison, T. M. (2000). Geologic Evolution of the Himalayan-Tibetan Orogen. *Annual Review of Earth and Planetary Sciences*, 28:211–280.

Zachos, J., Pagani, M., Sloan, L., Thomas, E., and Billups, K. (2001). Trends, Rhythms, and Aberrations in Global Climate 65 Ma to Present. *Science*, 292:686–693.

Zachos, J. C., Lohmann, K. C., Walker, J. C. G., and Wise, S. W. (1993). Abrupt climate change and transient climates during the Paleogene: a marine perspective. *The Journal of Geology*, 101:191–213.

Zankl, H. (1969). Structural and Textural evidence of early lithification in fine grained carbonate rock. *Sedimentology*, 12:241–256.

Zhang, Q., Wendler, I., Xu, X., Willems, H., and Ding, L. (2017). Structure and magnitude of the carbon isotope excursion during the Paleocene-Eocene thermal maximum. *Gondwana Research*, 46:114–123.

Zhang, Q., Willems, H., and Ding, L. (2013). Evolution of the Paleocene-early Eocene larger benthic foraminifera in the Tethyan Himalaya of Tibet, China. *International Jounal of Earth Sciences (Geologische Rundschau)*, 102:1427–1445.

Zhang, Q., Willems, H., Ding, L., Gräfe, K.-U., and Appel, E. (2012). Initial India-Asia Continental Collision and Foreland Basin Evolution in the Tethyan Himalaya of Tibet: Evidence from Stratigraphy and Paleontology. *The Journal of Geology*, 120(2):175–189.

Zhang, Z., Dong, X., Santosh, N., and Zhao, G. (2014). Metamorphism and tectonic evolution of the Lhasa terrane, Central Tibet. *Gondwana Research*, 25:70–189.

Zhicheng, Z., Willems, H., and Binggao, Z. (1997). Marine Cretaceous-Paleogene biofacies and ichnofacies in southern Tibet, China, and their sedimentary significance. *Marine Micropaleontology*, 32:3–29.

Zhu, B., Kidd, W. S. F., Rowley, D. B., Currie, B. S., and Shafique, N. (2005). Age of initiation of the India-Asia collision in the east-central Himalaya. *The Journal of Geology*, 113:265–285.

Zhu, D. C., Zhao, Z. D., Niu, Y. L., Dilek, Y., Hou, Z. Q., and Mo, X. X. (2013). The origin and pre-Cenozoic evolution of the Tibetan Plateau. *Gondwana Research*, 23:1429–1454.

Zhu, D. C., Zhao, Z. D., Niu, Y. L., Mo, X. X., Chung, S. L., Hou, Z. Q., Wang, L. Q., and Wu, F. Y. (2011). The Lhasa Terrane: record of a microcontinent and its histories of drift and growth. *Earth and Planetary Science Letters*, 301:241–255.

6 Appendix

6.1 *Lockhartia*-based literature

Since the first description of *Lockhartia* in 1926 by Davies, more than 30 described species and variations were published, making taxonomic work highly difficult. In chapter 3 ”Stratigraphic distribution of the larger benthic foraminifera *Lockhartia* in South Tibet (China)” (p. 57) a summary of revised and a critical review of *Lockhartia* species is given to simplify taxonomic work and to reduce the number of described species down to 17 species and 4 variations ranging from Paleocene to lower Middle Eocene. Important literature illustrating the occurrence of *Lockhartia* is given here and also listed in the reference list to complete the work.

Continent/Locality		Area	Formation	Age	Species	References	Notes/Illustrations (Plates/Figures)
America	Florida	Levy County	Oldsmar Lm	Eocene	*L. gyropapulosa* n. sp., *L. prealta* n. sp.	Levin, 1957	*L. gyropapulosa*: pl. 3, figs. 5-8, *L. prealta*: pl. 3, figs. 9-11
	Puerto Rico	Mayaguez-Yaouco District		Paleocene to Eocene	*L. susuaensis* n. sp.	Pessagno, 1960	*L. susuaensis*: pl. 4, figs. 1-6
Europe	France	Southwest		Paleocene: Selandian (SBZ2)	*L. akbari* nom. nud.	Tambareau et al., 1997	after Hottinger & Tambareau in Serra-Kiel et al. (1998)
	Turkey	Southeast	Germav Fm	Cretaceous: Maastrichtian	(*L. ramanae* n. sp.)	Ten Dam, 1953	*L. ramanae* may belong to the genus *Rotorbinella* Bandy, 1944 (this work): pl. 2, figs. 3-4
				Paleocene	*L. daviesi* n. sp.		*L. daviesi*: pl. 2, figs. 1-2
		Menderes-Taurus		Paleocene	*L. conditi*	Matsumaru et al., 2010	*L. conditi*: pl. 6, fig. 5; reworked into Oligocene sediments
Africa	Somaliland			Eocene	*L. alveolata* n. sp., *L. conditi* var. *roeae*, *L. haimei*	Silvestri, 1938	*L. alveolata*: pl. XI, fig. 4, *L. conditi* var. *roeae* = *L. roeae* Hottinger (2014a): pl. VII, fig. 4, *L. haimei*: pl. III, fig. 6
			Allakajid Beds	Early Eocene	*L. hunti* n. sp.	Ovey, 1947	*L. hunti*: pl. 10, figs. 1-13, pl. 11 and additional photos
		South		Eocene	*L.* sp.	Cotton and Pearson, 2012	*L.* sp.: pl. 1, fig. H; may be *L. conditi*
Asia	Afghanistan	Southeast	Miscellaneakalk, unterer Nummulitenkalk	Upper Paleocene	*L. conditi*, *L. haimei*	Kaever, 1970	*L. conditi*: pl. 8, figs. 7-11, *L. haimei*: pl. 8, figs. 1-4 (more like *L. hunti* and *L. conditi*), *L. tipperi*: pl. 7, figs. 5-6
				Lower Eocene	*L. conditi*, *L. tipperi*		
	India	Assam	Siju Lm	Eocene: Lutetian	*L. hunti*, (*L. hunti* var. *garoensis* n. sp.,) (*L. sijuensis* n. sp.)	Samanta, 1961	*L. hunti*: figs. 6-10, *L. sijuensis* = *L. conditi* (this work): figs. 1-3, *L. hunti* var. *garoensis* = *L. hunti* (this work)
		Simla and Nahan-Dadahu	Subathu subgroup	Paleocene	*L. haimei*, *L. tipperi*	Datta and Banerji, 1966	*L. haimei*: pl. 1, figs. 1.2, 4, *L. tipperi*: pl. 1, figs. 3, 5
		Zanskar, Ladakh	Spanboth Fm	Paleocene	*L.* sp.	Gaetani et al., 1980	*L.* sp.: pl. 16, fig. 5
					L. sp., *L. haimei*	Gaetani et al., 1983	*L.* sp.: pl. 10, fig. 3, *L. haimei*: pl. 10, fig. 1
		Salabad province	Hassanabad section	Early Eocene	*L. conditi*, *L. haimei*	Babazadeh, 2008	*L. haimei*: fig. 4H (more like *L. conditi* or *L. hunti*)

Continent/Locality		Area	Formation	Age	Species	References	Notes/Illustrations (Plates/Figures)
Asia	Iraq	SE	Dammam Fm	Early Eocene: Cuisian, Lutetian	*L. alveolata*, (*L. alveolata* var. *pustulosa*)	Al-Hashimi, 1974	here *L. hunti* is placed in synonymy with *L. alveolata*; variations are neglected (this work); pl. 2, figs. 9-13
	Oman		Jafnayn Lm	Paleocene: Thanetian	*L. conditi* var. *roeae*, *L. diversa*	White, 1994	*L. diversa*: pl. 14; fig. 5, *L. conditi* var. *roeae* = *L. roeae* (Hottinger, 2014a)
	Pakistan	Sind*		Eocene	*L. conditi* n. sp.	Nuttall, 1926	*L. conditi*: first described as *Dictyoconides*, pl. 6, figs. 7-8
		near Kotri, Sind*		Eocene: Ypresian	*L. tipperi* n. sp.	Davies, 1926	*L. tipperi*: first described as *Conulites*, pl. 18, figs. 8
		Sind*	Ranikot Beds	Lower Eocene	*L. conditi*, *L. haimei* n. sp., (*L. newboldi*)	Davies, 1927	first described as *Dictyoconides*, *L. conditi*: pl. 21, figs. 10-12, *L. haimei*: pl. 21, figs. 13-15, *L. newboldi* = *Rotalia trochidiformis* (Davies, 1932)
		Samana Range		Paleocene	*L. conditi*, *L. conditi* var. *roeae*, *L. haimei*, (*L. newboldi*)	Davies, 1930	*L. conditi* var. *roeae* = *L. roeae* (Hottinger, 2014a): pl. 10, fig. 9, *L. haimei*: pl. 10, figs. 6-7, *L. newboldi* = *Rotalia trochidiformis* (Davies, 1932)
		Punjab Salt Range	Dak Pass beds, Khairabad Lm, Patala shales	Paleocene: Ranikot	*L. conditi*, *L. haimei*, *L. tipperi*	Davies and Pinfold, 1937	*L. conditi*: pl. 5, fig. 24, *L. haimei*: pl. 7, figs. 9-13, 15, *L. tipperi*: pl. 6; figs. 14-16, pl. 7, fig. 17, *L. newboldi* = *Rotalia trochidiformis* (Davies, 1932)
			Sakesar Lm	Eocene: Ypresien	(*L. newboldi*,) *L. tipperi*		
		Yadgar area		Eocene	*L. conditi*, *L. haimei*, *L. tipperi*	Baig and Munir, 2007	*L. conditi*: pl. 1, figs. b-c, e, *L. haimei*: pl. 1, figs. a, f, *L. tipperi*: pl. 1, fig. d
		Salt Range	Dhak Pass beds, Khairabad Lm	Paleocene: Thanetian, Eocene: Ilerdian	*L. conditi*, *L. haimei*	Smout and Haque, 1956	*L. conditi*: pl. 11, figs. 5a-b, *L.* aff. *diversa*: pl. 11, figs. 4a-b, *L. haimei*: pl. 11, figs. 3a-b
			Patala shale		*L.* aff. *diversa*, *L. haimei*		
		Punjab Salt Range	Ranikot Fm	Paleocene	*L. conditi*, *L. conditi* var. *roeae*, *L. haimei*, *L. tipperi*	Müller-Merz, 1980	*L. conditi*: pl. 10, figs. 4, 6 *L. conditi* var. *roeae* = *L. roeae* (Hottinger, 2014a): pl. 10, figs. 2, 5, *L. haimei*: fig. 19, pl. 9, figs. 5-6, pl. 10, fig. 7, *L. tipperi*: pl. 10, figs. 1, 3
		North	Hangu Fm, Lockhart Lm, Chorfali Fm	Paleocene	*L. conditi*, *L. haimei*, *L. tipperi*	Butt, 1991	*L. conditi*: pl. 3, fig. h, pl. 4, figs. a-b, *L. haimei*: pl. 2, fig. h

Continent/Locality		Area	Formation	Age	Species	References	Notes/Illustrations (Plates/Figures)
Asia	Pakistan	North	Margala Hill Lm, Chorgali Fm	Early Eocene	*L. conditi*, *L. tipperi*	Butt, 1991	*L. conditi*: pl. 3, fig. h, pl. 4, figs. a-b
		Salt Range, Punjab	Patala shales, Lockhart Lm, Khairabad Lm	Paleocene	*L. conditi*, *L. haimei*, *L. tipperi*	Weiss, 1993	*L.* aff. *conditi*: pl. 1, fig. 4, *L. conditi*: pl. 5, fig. 3 (rather *L. haimei*), *L.* aff. *haimei*: pl. 3, fig. 4 (rather *L. hunti*), *L. haimei*: pl. 1, fig. 2, pl. 2, fig. 1 (rather *L. conditi* or *L. hunti*), pl. 7, fig. 6, *L. conica* = *Rotorspirella conica* (Hottinger, 2014a), *L. hunti* var. *pustulosa* = *L. hunti* (this work)
		Sulaiman Range	Brewery Lm	Paleocene	*L. haimei*		
			Kirthar Fm	Eocene	*L. altispira*, (*L. conica*,) *L. hunti*, (*L. hunti* var. *pustulosa*,) *L. tipperi*		
		Jabri area	Lockhart Lm	Late Paleocene	*L. conditi*, *L. haimei*, *L. tipperi*	Sameeni et al., 2009	*L. conditi*: pl. 2, figs. B, D, *L. haimei*: pl. 2, fig. A (questionable), *L. tipperi*: pl. 1, fig. E, pl. 3, fig. D
		Kohat-Kotal Pass	Lockhart Lm	Middle to Late Paleocene	*L. conditi*, (*L. conica*,) *L. diversa*, *L. haimei*, *L. tipperi*	Afzal et al., 2005	*L. conditi*: pl. 1, fig. 2, *L. diversa*: pl. 1, fig. 7 (rather *L. retiata*), *L. haimei*: pl. 1, fig. 1, *L. tipperi*: pl. 1, fig. 4, *L. conica* = *Rotorspirella conica* (Hottinger, 2014a)
		Kohat area	Lockhart Lm	Paleocene	*L. conditi*, *L. haimei*	Afzal et al., 2009	*L. conditi*: pl. 1, figs. 2, 4, *L. haimei*: pl. 1, figs. 7, 9
		Upper Indus Basin	Kotal Pass section	Paleocene: Thanetian (SBZ3, SBZ4)	*L. conditi*, (*L. conica*,) *L. diversa*, *L. haimei*	Afzal et al., 2011	*L. conditi*: fig. 8D, *L. haimei*: fig. 8F, *L. conica* = *Rotorspirella conica* (Hottinger, 2014a)
			Shakardara Well-1				
	Qatar			Paleocene	*L. altispira*, *L. conditi*, (*L. conica* n. sp.,) *L. diversa* n. sp., *L. haimei*, *L. prehaimei* n. sp.	Smout, 1954	*L. altispira*: pl. 4, figs. 4-6, *L. conditi*: pl. 5, figs. 16-19, *L. diversa*: pl. 3, figs. 1-20, *L. haimei*: pl. 2, figs. 13-15, *L. prehaimei* = *L. praehaimei* (Hottinger, 2014a): pl. 2, figs. 21-22, pl. 7, fig. 14, *L. hunti*: pl. 4, fig. 7, *L. hunti* var. *pustulosa* = *L. hunti* (this work): pl. 4, fig. 8-10, *L. tipperi*: pl. 4, figs. 11, *L. conica* = *Rotorspirella conica* (Hottinger, 2014a)
				Eocene	*L. hunti*, (*L. hunti* var. *pustulosa*,) *L. tipperi*		

Continent/Locality		Area	Formation	Age	Species	References	Notes/Illustrations (Plates/Figures)
Asia	Pakistan	Rub'al Khali Basin	Umm er Radhuma	Eocene	*L. altispira*, *L. conditi*, (*L. conica*,) *L. diversa*, *L. haimei*, (*L. hunti* var. *pustulosa*,) *L. tipperi*	Hasson, 1985	*L. diversa*: pl. 4, figs. 11a-b, *L. conica* = *Rotorspirella conica* (Hottinger, 2014a), *L. hunti* var. *pustulosa* = *L. hunti* (this work)
		eastern	Um er Radhuma Fm	Paleocene	*L. conditi*, *L. haimei*, *L. haimei* variations n. sp., *L. lobulata* n. sp., *L. retiata* n. sp., *L. tipperi*	Sander, 1962, 2012	*L. conditi*: pl. 4, figs. 37-39, *L. haimei*: pl. 5, figs. 1-8, 31-34, *L. haimei* variations *nudimarginata*/*spiracordata*/*suturadicata*/*vermiculata*: pl. 5, figs. 16-21, 35-36, pl. 5, figs. 25-30, pl. 5, figs. 22-24, 27, pl. 5, figs. 10-15, *L. lobulata*: pl. 3, figs. 21-27, *L. retiata*: pl. 4, figs. 1-21, *L. tipperi*: pl. 4, figs. 25-36
				Lower Eocene	*L. tipperi*		
	Tibet			Paleocene	*L.* sp., *L. conditi*, *L. haimei*, *L. hunti*, *L. megapapulata* n. sp., *L. tipperi*	Ho et al., 1976	*L.* sp.: pl. 33, fig. 10, *L. conditi*: pl. 27, fig. 2, pl. 34, fig. 9, *L. haimei*: pl. 22, figs. 1-2, pl. 27, figs. 1, 4, 9-11, *L. hunti*: pl. 27, figs. 5-8, pl. 34, figs. 6, 10, *L. megapapulata*: pl. 26, figs. 3, 6, pl. 27, fig. 3, *L. tipperi*: pl. 27, fig. 12
		Gamba	Zongpu Fm	Paleocene	*L. conditi*, (*L. conica*,) *L. diversa*, *L. haimei*, *L. hunti*, *L. megapapulata*, *L. tipperi*	Wan, 1991	*L. conditi*: pl. 1, figs. 26-27, *L. diversa*: pl. 1, figs. 30-32, *L. haimei*: pl. 2, figs. 1-2, *L. hunti*: pl. 2, figs. 3-4, *L. megapapulata*: pl. 2, figs. 5-7, *L. tipperi*: pl. 2, fig. 8, *L. conica* = *Rotorspirella conica* (Hottinger, 2014a)
		Tingri, Gamba	Zhepure Shan Fm, Zongpu Fm	Paleocene to Middle Eocene	*L.* sp., *L. haimei*	Willems, 1993	*L. haimei*: pl. 13, fig. 3, 5
		Tingri	Zhepure Shan Fm	Paleocene	*L. haimei*, *L. hunti*	Willems et al., 1996	*L. haimei*: pl. 14, figs. 3, 5, pl. 15, fig. 2
		Gamba	Jidula, Zongpu Fm	Paleocene	*L. altispira*, *L. conditi*, (*L. cushmani*,) *L. diversa*, *L. haimei*	Wan et al., 2002	*L.* sp.: fig. 7M, *L. diversa*: fig. 7I, *L. haimei*: figs. 7F, 7H, *L. cushmani* = *Rotalia cushmani* (Cole, 1947)

Continent/Locality		Area	Formation	Age	Species	References	Notes/Illustrations (Plates/Figures)
Asia	Tibet	Tingri	Zongpu Fm	Paleocene	*L. conditi*, (*L. cushmani*)	Wan et al., 2002	*L. cushmani* = *Rotalia cushmani* (Cole, 1947)
		Gamba	Jidula, Zongpu Fm	Paleocene	*L. altispira*, *L. conditi*, (*L. cushmani*,) *L. diversa*, *L. haimei*, *L. megapapulata*, *L. tipperi*	Wan et al., 2010	*L. cushmani Rotalia cushmani* (Cole, 1947)
				Early Eocene	*L. conditi*, *L. megapapulata*, *L. tipperi*		
		Tingri, Gamba	Zhepure Shan Fm, Zongpu Fm	Paleocene	(*L. altispira*,) *L. conditi*, *L. conditi* var. *roeae*, *L. haimei*, (*L. megapapulata*,) *L. prehaimei*, *L. retiata*, *L. tipperi*	Zhang et al., 2013	*L.* sp: fig. 6.12, *L. altispira*: fig. 6.9, *L. conditi*: fig. 6.10-6.11, *L. conditi* var. *roeae* = *L. roeae* (Hottinger, 2014a): fig. 6.6-6.7, *L. haimei*: fig. 6.8, *L. prehaimei* = *L. praehaimei* (Hottinger, 2014a): fig. 6.5, *L. retiata*: fig. 6.4, *L. tipperi*: fig. 6.13, *L. altispira* = *Sakesaria* (Kahsnitz et al., 2016), *L. megapapulata* = *L. haimei* (Kahsnitz et al., 2016)
				Eocene	*L. conditi*, *L. hunti*, *L. tipperi*		
		Tingri, Gamba, Guru	Zhepure Shan Fm, Zongpu Fm, Langhzhu Fm	Paleocene to Lower Eocene: SBZ2 to lower part of SBZ5	*L. conditi*, *L. haimei*, *L. hunti*, *L. praeheimei*, *L. retiata*, *L. roeae*, *L. tipperi*	Kahsnitz et al., 2016	*L. conditi*: fig. 5.1-5.5, *L. haimei*: fig. 5.6-5.10, *L. hunti*: fig. 5.11-5.15, *L. praeheimei*: fig. 5.16-5.19, *L. retiata*: fig. 6.1-6.5, *L. roeae*: fig. 6.6-6.9, *L. tipperi*: fig. 6.10-6.13
				Eocene: upper part of SBZ5 to SBZ8	*L. hunti*, *L. tipperi*		
	Yemen	South Hadramawt Arch	Wadi Mashib succession	Paleocene	*L.* cf. *altispira*, *L. diversa*, *L.* cf. *haimei*, *L.* cf. *prehaimei*	Pignatti et al., 1998	*L. prehaimei* = *L. praehaimei* (Hottinger, 2014a)

Continent/Locality		Area	Formation	Age	Species	References	Notes/Illustrations (Plates/Figures)
Asia	Yemen	South Hadramawt Arch	Wadi Mashib succession	Eocene	(*L. hunti* var. *pustulosa*,) *L. tipperi*	Pignatti et al., 1998	*L. hunti* var. *pustulosa* = *L. hunti* (this work): pl. 4, fig. 3, *L. tipperi* (described as *Dictyoconides*): pl. 4, fig. 1
		Ataq	Umm er Radhuma	Early Eocene	*L.* cf. *conditi*, *L. diversa*	Ismail and Boukhary, 2008	*L. conditi*: pl. 2, figs. 4-5, *L. diversa*: pl. 2, fig. 6
Western & Central Neotethys Ocean				Paleogene	*L. conditi*, *L. diversa*, *L. haimei*, *L. hunti*, *L. praehaimei*, *L. retiata*, *L. roeae*, *L. tipperi*	Hottinger, 2014a	*L. conditi*: pl. 5.12, figs. 7-16, pl. 5.14, figs. 1-24, *L. diversa*:pl. 5.11, figs. 1-19, *L. haimei* and variations: pl.5.5, figs. 1-12, pl. 5.6, figs. 1-17, pl. 5.7, figs. 1-12, pl. 5.8, figs. 1-13, *L. hunti*: pl. 5.17, figs. 1-16, pl. 5.18, figs. 16-27, *L. praehaimei*: pl. 5.3, figs. 1-17, pl. 5.4, figs. 1-17, pl. 5.10, figs. 16-18, *L. retiata*: figs. 5.1-5.2, pl. 5.9, figs. 1-20, pl. 5.10, figs. 1-15, *L. roeae*: pl. 5.12, figs. 1-6, pl. 5.13, fig. 1-16, *L. tipperi*: pl. 5.19, figs. 1-11, pl. 5.20, figs. 7-13, *L.* cf. *hunti* or young specimen of *tipperi*: pl. 5.20, figs. 1-6

Table 6.1: Important literature illustrating the occurrence of *Lockhartia* used for taxonomic work (see chapter 3 "Stratigraphic distribution of the larger benthic foraminifera *Lockhartia* in South Tibet (China)"). *Lockhartia* of the Locality Sind* formerly belonged to India (as reported by Davies, 1926; Nuttall, 1926; Davies, 1927), today this part belongs to Pakistan. Abbreviations: cf. = confer, compare with (used when the author is not sure about the species), Fm = Formation, L = *Lockhartia*, Lm = Limestone, n. sp. = new described species, SBZ = shallow benthic zone, sp. = species, var. = variation.

6.2 Glossary of terms

Extract of used terms for morphological descriptions of larger benthic foraminifera (LBF) in this work, as well as some additional terms for the sake of completeness. Taken from the ”Illustrated glossary of terms used in foraminiferal research” (Hottinger, 2006). Terms in descriptions listed within this glossary are underlined.

adaxial - directed towards or positioned near the shell axis.

agamont - specimen grown from the zygote, producing either gamonts or schizonts in an asexual process involving apogamous nuclear divisions and/or meiosis. Foraminiferal agamonts, produced by a sexual reproduction, are called microspheric (B - form).

aperture - the primary opening of the foraminiferal shell cavity towards the ambient environment. May be covered by subsequent chambers and thus transformed into a foramen. May be single or multiple.

apex - initial portion of trochospiral or conical test.

axial section - a slice bisecting the test in a plane coinciding with the axis of coiling and intersecting the proloculus.

bead - a small, rounded to hemispherical protuberance on the surface of lamellar shells, forming strings along septal, septular or hemiseptular sutures. Usually imperforate or poorly perforate.

biconch - protoconch and deuteroconch together, if separated by a straight septum, thus differing in shape from later, curved ones. The straight septal wall suggests that hydrostatic pressure in protoconch and deuteroconch was equal as a morphogenetic control before the wall was calcified. Thus, the two first chambers were formed together and represent a single growth stage similar to an embryonic apparatus.

bilamellar wall - in perforate foraminifera a chamber wall formed primarily by two mineralized layers (outer and inner lamellae) on either side of a primary organic sheet, the median layer.

canaliculate [canaliferous] **spine** - a spine- or club-shaped to arborescent radial structure composed of consecutive outer lamellae enclosing canals (supplemental skeleton). May contain spikes.

cancellate - having honeycomb-like surface ridges as ornament.

carina [keel] - a peripheral thickening of the shell. May be doubled in Cretaceous planktic foraminifera. In bilamellar foraminifera formed exclusively by the outer lamella and therefore imperforate.

chamber [loculus] - the space and its enclosing biomineralized walls formed at one instar.

cosmopolitan - Occurring all over the world where ever there is a suitable habitat, the contrary of endemic.

deuteroconch - the second chamber in an embryonic apparatus.

dimorphism - coexistence of two discrete morphotypes representing different generations in the life cycle of a single species. They are expressed in the adult growth stages and/or in the protoconch and in the following nepionic chambers. The protoconch diameter is large (megalospheric = A - form) when the agamont’s protoplasm is distributed (including eventual symbionts) among the cloned offspring. The protoconch diameter is small (microspheric = B - form) when the gamont’s gametes fuse pairwise to form a zygote whith no protoplasm or symbionts from the mother. If there is dimorphism in the adult shell, the B - form

becomes larger than the A - form. The compartments of the microspheric initial phases are small. It takes many growth steps to reach the initial shell size of the megalospheric generation. Reaching the adult oversize of the microspheric generation demands numerous additional instars. Consequently, the dimorphism of foraminiferal generations reflects different life times and thus different strategies of life within the same species: the microspheric generation is adapted to the permanent basic low-level carrying capacity of an oligotrophic and warm environment, while the megalospheric generation with its short life time adapts to both spring and eventual autumn seasonal peaks of carrying capacity.

dorsal - the side of a free, flattened organism turned away from its substrate, as opposed to ventral.

embryo(n) [embryonic apparatus] - the group of chambers including protoconch and deuteroconch (nucleoconch), and in some genera a flexostyle, that differs in size, shape and arrangement from subsequent chambers.

embryonic - the earliest growth stage in foraminiferal ontogeny, usually distinguished from later stages by an abrupt change in shell architecture, commonly with thickened walls indicating a longer period of cessation in growth as frequent in the megalospheric generation of larger K-strategists.

endemic - occurring in restricted geographic areas; the contrary of cosmopolitan.

flagella - a tubular extension of the cell, reinforced with microtubuli and anchored by centrioles deep inside the protoplast of dinophycean symbionts. The short flagellae are used for locomotion in the lacunar system of the host as a device for regulating irradiation intensity in order to avoid photoinhibition.

folium - (lip; tenon; umbilical flap; astral lobe, pars auct.) - in spiral lamellar foraminifera an axial-umbilical portion of the lateral chamber wall, generally triangular in outline and often texturally differentiated (porosity). The limit between the main lateral chamber wall and the folium may be marked by a short, posterior indentation or ”notch” and/or by an umbilical plate-suture. An opening (foliar aperture) is always present between the anterior margin of a folium and the adjacent previous coil. In addition, umbilical and/or posterior openings may be present, depending upon whether the folia are free or attached by their tips or along their posterior margin. In some genera such as *Asterorotalia*, the folia may extend onto the preceding chamber and be attached to it, partially covering intraseptal interlocular spaces wherever present. A folium is composed of the same layers as those forming the wall of the main chamber.

foramen [intercameral foramen] (plural: foramina) - the opening or openings that allow communication between the lumina of consecutive chambers and provide passage for functional endoplasm. May be primary, hence formed by an initial cameral aperture, or secondary, i.e. formed by resorption of masks or other parts of the septum (tunnel). Cameral apertures converted into intercameral foramina may be modified in shape by resorption or through restriction by attachment of a toothplate, foramenal plate or umbilical plate.

foramenal plate - (toothplate; paries proximus, pars auct.) - basically a primary infold or ”inpush” in the direction of growth of the posterio-lateral chamber wall at a sutural notch, and attached to a single intercameral foramen. A foramenal plate is a detached continuation of a septal flap that may or may not be connected with a cover plate in the previous chamber. A foramenal plate separates to some degree the main chamber lumen from the lumen of the foliar chamberlet and the chamber plasm from the ectoplasm in the interlocular spaces.

gamont - a specimen producing gametes in the process of reproduction irrespective of its involvment in meiosis (diploid gamonts) or not (haploid gamonts). Foraminiferal gamonts, produced by asexual reproduction are megalospheric (A - form).

granule - see bead, papilla.

imperforate - lacking pores or parapores.

instar - a single step in the discontinuous growth process of most foraminifera. It is reflected by the formation of one chamber of the shell (or of a cycle of chamberlets).

interlocular space (lacuna, pars auct.) - a space formed as a consequence of a deeply sunken suture between consecutive chamber walls or between consecutive coils.

interseptal pillars [pillars] (lamelliform buttresses) - in porcelaneous and agglutinated species: the multiple columnar projections between consecutive septa and parallel to protoplasmic flow. Pillars are part of the endoskeleton. To be distinguished from piles of lamellae.

intraseptal interlocular space - the interlocular space formed between the posterior bilamellar wall of a chamber and the distal bilamellar wall of the preceding chamber, as a result of a deeply sunken suture. Intraseptal spaces may be open to the exterior along their margins either continuously or through openings between points of marginal adherence of consecutive lateral chamber walls.

megalospheric - the large proloculus in di- or trimorphic species; a defining characteristic for gamonts and schizonts in contrast to the microsphere of the agamont.

microspheric - in dimorphic species: a test having a small proloculus or microsphere; commonly an agamont.

nepionic - the juvenile stage immediately after an embryonic and preceding an ephebic stage.

nucleoconch - see embryonic apparatus.

papilla [pl. papillae] - a small, rounded, poorly or non-perforate protuberance, single or multiple, on the outer surface of perforate chamber or chamberlet walls, produced by local inflation of outer lamellae and linked to a conical outward spreading of the pores.

perforate - referring usually to walls possessing true pores. Where the term is applied to walls possessing parapores it should be replaced by ”paraporous”.

plug [umbilical plug] - an expanding pile of thickened lamellae in axial position in an umbilicus or in an umbilical bowl. May be single, compound and/or canaliculate.

pore - a minute tubular perforation traversing a lamellar chamber wall, coated internally by an organic sheathe. Subdivided by organic discs (”pore plate” auct.) and closed off internally by the inner organic lining. The latter may fuse with the basal disc corresponding to the median layer and form an organic pore plug. The size and shape of the external and internal pore openings may be identical (rounded to elongated) or dissimilar, when symbionts are positioned in egg-holders below the pore mouths for gas exchange.

proloculus - the initial chamber of a foraminiferal test without nepionic differentiation. Usually, a proloculus has a spherical outline and a single aperture.

protoconch - the first chamber of a test with an embryonic apparatus or in which a deuteroconch is differentiated. In most dimorphic larger foraminifera, the microspheric generation has a proloculus, the megalospheric generation a protoconch or megalosphere.

protoplasm - the living matter comprising the cell-body.

pustules [tubercle; papilla] - a hemispherical to subconical inflational protuberance of the outer lamella.

schizont - apogamic offspring of an agamont reproducing either by another apogamous nuclear division and cytotomy (i.e. by distributing the mother protoplasm among the offspring) or undergoing meiosis. Because the foraminiferal schizonts are produced by cytotomy, they are megalospheric (A - forms).

septum (French: cloison) - a wall separating two consecutive main chamber lumina, i.e. the portion of the free chamber wall that is covered by subsequent chambers and thus incorporated in the architecture of the shell as a partition between successive main chamber lumina. The connection between them is assured by one or many openings in the septum (intercameral foramina, stolon systems) that are in most cases converted primary apertures. When multiple chamberlets form simultaneously the septum may consist of many discrete parts acting as partitions between the lumina of successive chamberlet cycles (not of neighbouring chamberlets).

suture - the line of adhesion of chamber wall(s) to the previously formed test.

symbiont - an organism living together with or within an other organism to the benefit of both.

symbiosis - in foraminifera: algal cells living (as symbionts) within the foraminiferal cytoplasm in a mutualistic relationship with their host. The symbionts actively photosythesize and reproduce asexually in the host cell. They are engaged in recycling nutrients. They live either in vacuoles of the host cytoplasm and are displaced passively by the host's protoplasmic streaming, or are found in the lacunar system of the host cell within which they may move actively using their shortened flagella to regulate the amount of their irradiation by sunlight so as to avoid photoinhibition. During the asexual reproduction of the host, each offspring inherits a small number of symbionts from the mother cell. But after sexual reproduction, the foraminiferal zygote must take up symbionts from its ambient environment.

test - the shell or skeletal components of a foraminifer. The test may be composed of a variety of materials: secreted, agglutinated or in combination.

toothplate - (sipho; central pillar, pars auct.) - a contorted plate running from an intercameral foramen to an aperture, and attached to both. It may be shaped to form a single, double or spiral fold (or "tongue") with a free, often serrated distal end and distally protruding into the aperture. A toothplate separates partly or completely the main chamber lumen from an axial space (adapertural depression) in post-embryonic stages. It protrudes with a free edge distally and adaxially into the aperture. Interconnected toothplates in low-trochospiral umbilicate shells may produce a primary spiral canal. A toothplate is never associated with a foliar or stellar chamberlet.

trochospiral arrangement - chamber arrangement in whorls or coils where the rate of translation (net rate of movement along the growth axis to the net rate of movement away from the axis) is more than zero. Spiral and umbilical sides are dissimilar. May be involute or evolute on either the spiral or the umbilical side.

umbilical cavity - the axial complex of interconnected passageways delimited by axial chamber walls, inner umbilical walls, folia, foramenal plates, and cover plates. Includes thus the umbilical canal systems. May be restricted by piles or plugs and communicates with the exterior through foliar apertures or vertical canals.

umbilical plate (foramenal plate; umbilical flap; murus reflectus; toothplate; paries proximus, pars auct.) - a more or less contorted plate-like test element, extending between distal and proximal chamber walls and joined to both, attached to the intercameral foramen and to the main aperture, but not protruding into the latter. Separates the main chamber lumen from a primary umbilical-spiral canal. Between plate and adjacent coil or within the plate itself an opening provides connection between chamber and foliar chamberlet, wherever present. This opening may remain open in all chambers or it may be closed in all but the ultimate chamber by a sealing plate. An umbilical plate may be single or composed of two symmetrical branches in some planispiral genera, thereby producing one or two umbilical-spiral canals between plate and adjacent coil.

umbilicus - the axial space in spiral foraminifera communicating directly through apertures with surrounding main chamber lumina or foliar chamberlets. May be open or restricted by an umbilical plug.

ventral - the side of a flattened organism turned to its substrate, as opposed to dorsal. Secondarily flattened, almost planispiral or slightly reversed-spiral, involute shells like *Daviesina salsa* (Davies and Pinfold) or *D. langhami* (Smout) reveal their trochospiral phyletic origin by an asymmetric, ventral position of the main cameral foramen and of the umbilical plate.

whorl [coil] - in a spiral test, a single turn or volution through 360°.

zygote - a diploid cell resulting from fusion of two (haploid) gametes in sexual reproduction. The biomineralized envelope of the zygote is called a microsphere.